

Process-based simulation of the European terrestrial biosphere

An evaluation of present-day and future terrestrial carbon balance estimates and their uncertainty

Sönke Zaehle

Institut für Geoökologie
und
Potsdam Institut für Klimafolgenforschung e.V.

Process-based simulation of the European terrestrial biosphere

An evaluation of present-day and future terrestrial carbon balance estimates and their
uncertainty

Sönke Zaehle

Dissertation zur Erlangung des akademischen Grades
“doctor rerum naturalium”
(Dr. rer. nat.)
in der Wissenschaftsdisziplin “Geoökologie”

eingereicht an der
Mathematisch-Naturwissenschaftlichen Fakultät
der Universität Potsdam

Potsdam, den 4. April 2005

Institut für Geoökologie
und
Potsdam Institut für Klimafolgenforschung e.V.

Models are undeniably beautiful, and a man may justly be proud to be seen in their company. But they may have their hidden vices. The question is, after all, not only whether they are good to look at, but whether we can live happily with them.

(A. Kaplan)

ACKNOWLEDGEMENTS

First of all, said Bilbo, to tell you that I am immensely fond of you all, and that eleventy-one years is too short a time to live amongst such excellent and admirable hobbits. I don't know half of you half as well as I should like; and I like less than half of you half as well as you deserve.

(J.R.R. Tolkien, The Lord of the Rings)

- Prof. Dr. Wolfgang Cramer is gratefully acknowledged for supporting this thesis and giving me the opportunity to work in two international research projects (ATEAM and CarboEurope-IP). I greatly appreciated the freedom that I had, as well as his confidence in me. Thanks to his support I was able to meet, interact and learn from many fellow researchers.
- I am very grateful to Prof. Dr. Colin Prentice for giving me the chance to pick his brain on several occasions and learn a lot about various aspects of plant ecology. I am also very grateful for his preparedness to be a referee of this thesis.
- I am highly indebted to Stephen Sitch, who took me under his wings, and without whom this thesis would never have been completed. I've learnt a lot about the ways of both science and life from him. He's been a great support, especially in the last months. What's more, he always found the right, encouraging words, even if the results looked pretty disastrous.
- Many thanks also go to Markus Erhard, who's tried to help me sorting out my mind on several occasions, solving the 'famous Sönke's paradox', as well as giving advice and support on any question I had (and be it on how to climb a snowy mountain...).
- I am grateful to Ben Smith and Jari Liski for the many many fruitful discussions, helpful (subtle) hints, possibility for a visit, and encouragement I got from them, as well as to Dagmar Schröter, for never giving up on co-ordinating a confused PhD-student.
- I really appreciated the many discussions I had with the members of the LPJ consortium, especially with Thomas Hickler, who introduced me to plants and the problems they have with water. Alberte Bondeau and Prof. Dr. Martin Sykes are acknowledged for their helpful collaboration in the ATEAM project, as well as their moral support.
- Jeanette Meyer and Thies Eggers have been very helpful in explaining the various subtleties of *growth and* yield tables, and lot of other things relates to 'trees', as well as kindly taking care of me, be it in Potsdam or Finland...

- Thanks to Christoph Müller's enthusiasm, teaching has not only been a strain on my nerves, but has actually been quite a lot of fun...
- The 'Land Brandenburg' funded the first two years of this work with a scholarship of the Hochschulprogramm Brandenburg (AZ: 24-04/323; 200). The European Union funded the second half through the 6th framework project CarboEurope-IP (GOCE-CT2001-00125). My many travel bills were paid for by the ATEAM-project (EVK2-2000-00075), and the European Forest Institute supported a two-and-a-half months research stay in Joensuu. The 'Studienstiftung des deutschen Volkes' is acknowledged for moral support.
- I am indebted also to Torsten Grothmann, who had to bear my – bad – temper for the last three years, and with whom I had quite a lot of fun despite all the work – maybe the synchronisation will persist?
- Science is not all in life, or at least Cornelia, Matthias, Meggie, and Pascalle have tried to persuade me of that — not always unsuccessfully... Many thanks also go to my (former and present) flatmates, particularly to Gundolf and Melanie, who patiently bore my presence (or perhaps even more mental absence)...

My love goes to Kathrin, who has been a relentless port of encouragement and help over the last years. I'm deeply indebted to her for accepting my strange ways of being, but much more for sharing thoughts and feelings through all the ups and downs. Last but not least, I thank my parents for their support and encouragement over the last – well – it's decades now...

ABSTRACT

At present, carbon sequestration in terrestrial ecosystems slows the growth rate of atmospheric CO₂ concentrations, and thereby reduces the impact of anthropogenic fossil fuel emissions on the climate system. Changes in climate and land use affect terrestrial biosphere structure and functioning at present, and will likely impact on the terrestrial carbon balance during the coming decades – potentially providing a positive feedback to the climate system due to soil carbon releases under a warmer climate. Quantifying changes, and the associated uncertainties, in regional terrestrial carbon budgets resulting from these effects is relevant for the scientific understanding of the Earth system and for long-term climate mitigation strategies.

A model describing the relevant processes that govern the terrestrial carbon cycle is a necessary tool to project regional carbon budgets into the future. This study

- provides an extensive evaluation of the parameter-based uncertainty in model results of a leading terrestrial biosphere model, the Lund-Potsdam-Jena Dynamic Global Vegetation Model (LPJ-DGVM), against a range of observations and under climate change, thereby complementing existing studies on other aspects of model uncertainty.
- evaluates different hypotheses to explain the age-related decline in forest growth, both from theoretical and experimental evidence, and introduces the most promising hypothesis into the model.
- demonstrates how forest statistics can be successfully integrated with process-based modelling to provide long-term constraints on regional-scale forest carbon budget estimates for a European forest case-study.
- elucidates the combined effects of land-use and climate changes on the present-day and future terrestrial carbon balance over Europe for four illustrative scenarios – implemented by four general circulation models – using a comprehensive description of different land-use types within the framework of LPJ-DGVM.

The results of this study demonstrate that simulated present-day land-atmosphere carbon fluxes are relatively well constrained, despite considerable uncertainty in modelled net primary production mainly propagating from uncertainty in parameters controlling assimilation rate, plant respiration and plant water balance. Long-term trends in land-atmosphere fluxes of a suitably constrained model are consistently modelled. The projected global biospheric carbon uptake at the end of the 21st century is estimated at 3.35 ± 1.45 PgC yr⁻¹ for the specific scenario used, with the uncertainty range resulting almost equally from uncertainty in soil and vegetation carbon stock changes.

Evidence supports the hypothesis that hydraulic path length affects plant growth. It is shown that incorporating hydraulic acclimation to increased path length into the model improves the simulated changes in forest growth rate with stand age. Application of the advanced model for 77 European provinces shows that model-based estimates of biomass development with stand age compare favourably with forest inventory-based estimates for different tree species. Driven by historic changes in climate, atmospheric CO₂ concentration, forest area and wood demand between 1948 and 2000, the model predicts European-scale, present-day age structure of forests, ratio of biomass removals to increment, and vegetation carbon sequestration rates that are consistent with inventory-based estimates.

The combined effects of climate and land-use changes – projected under four alternative scenarios (2000 to 2100) – lead to average carbon uptake rates in Europe’s terrestrial biosphere corresponding to 18-68% of Europe’s present Kyoto emission reduction target. Carbon sequestration resulting from decreases in agricultural areas and afforestation correspond to one fifth of this emission reduction target. Accounting for the effect of forest age structure, net carbon uptake rates due to land-use changes may be even more pronounced. Under all scenarios, soil carbon losses resulting from climate warming counteract carbon uptake due to land-use change and growth enhancement from climate change and increasing atmospheric CO₂ concentrations in the second half of the 21st century. Uncertainty in the future European terrestrial carbon balance associated with uncertainty in the rate and spatial pattern of climate change among different climate models for a particular emission scenario is larger than the differences between alternative scenarios of consistent land-use and climate changes derived from one particular climate model.

This study presents a way to assess and reduce uncertainty in process-based terrestrial carbon estimates on a regional scale. Process-based terrestrial modelling and forest statistics are successfully combined to improve model-based estimates of vegetation carbon stocks and their change over time. Alternative scenarios of climate and land-use change in the 21st century suggest carbon sequestration in the European terrestrial biosphere during the coming decades will likely be on magnitudes relevant to climate mitigation strategies. However, the uptake rates are small in comparison to the European emissions from fossil fuel combustion, and will likely decline towards the end of the century. Uncertainty in climate change projections is a key driver for uncertainty in simulated land-atmosphere carbon fluxes and needs to be accounted for in mitigation studies of the terrestrial biosphere.

ZUSAMMENFASSUNG

Kohlenstoffspeicherung in terrestrischen Ökosystemen reduziert derzeit die Wirkung anthropogener CO₂-Emissionen auf das Klimasystem, indem sie die Wachstumsrate der atmosphärischer CO₂-Konzentration verlangsamt. Die heutige terrestrische Kohlenstoffbilanz wird wesentlich von Klima- und Landnutzungsänderungen beeinflusst. Diese Einflussfaktoren werden sich auch in den kommenden Dekaden auf die terrestrische Biosphäre auswirken, und dabei möglicherweise zu einer positiven Rückkopplung zwischen Biosphäre und Klimasystem aufgrund von starken Bodenkohlenstoffverlusten in einem wärmeren Klima führen. Quantitative Abschätzungen der Wirkung dieser Einflussfaktoren - sowie der mit ihnen verbundenen Unsicherheit - auf die terrestrische Kohlenstoffbilanz sind daher sowohl für das Verständnis des Erdsystems, als auch für eine langfristig angelegte Klimaschutzpolitik relevant.

Um regionale Kohlenstoffbilanzen in die Zukunft zu projizieren, sind Modelle erforderlich, die die wesentlichen Prozesse des terrestrischen Kohlenstoffkreislaufes beschreiben. Die vorliegende Arbeit

- analysiert die parameterbasierte Unsicherheit in Modellergebnissen eines der führenden globalen terrestrischen Ökosystemmodelle (LPJ-DGVM) im Vergleich mit unterschiedlichen ökosystemaren Messgrößen, sowie unter Klimawandelprojektionen, und erweitert damit bereits vorliegende Studien zu anderen Aspekten der Modelunsicherheit.
- diskutiert unter theoretischen und experimentellen Aspekten verschiedene Hypothesen über die altersbedingte Abnahme des Waldwachstums, und implementiert die vielversprechendste Hypothese in das Modell.
- zeigt für eine europäische Fallstudie, wie Waldbestandsstatistiken erfolgreich für eine verbesserte Abschätzung von regionalen Kohlenstoffbilanzen in Wäldern durch prozessbasierten Modelle angewandt werden können.
- untersucht die Auswirkung möglicher zukünftiger Klima- und Landnutzungsänderungen auf die europäische Kohlenstoffbilanz anhand von vier verschiedenen illustrativen Szenarien, jeweils unter Berücksichtigung von Klimawandelprojektionen vier verschiedener Klimamodelle. Eine erweiterte Version von LPJ-DGVM findet hierfür Anwendung, die eine umfassende Beschreibung der Hauptlandnutzungstypen beinhaltet.

Die Ergebnisse dieser Arbeit zeigen, dass der Nettokohlenstoffaustausch zwischen terrestrischer Biosphäre und Atmosphäre unter heutigen klimatischen Bedingungen relativ sicher abgeschätzt werden kann, obwohl erhebliche Unsicherheit über die modelbasierte terrestrische Nettoprimärproduktion existiert. Diese Unsicherheit entsteht hauptsächlich durch alternative Parameterwerte für die Assimilationsrate, die autotrophen Atmungsverluste, sowie die Wasserbilanz der Pflanzen. Langfristige Trends des terrestrischen Nettokohlenstoffaustausches werden - unter geeigneten Randbedingungen - mit alternativen

Parametrisierungen ebenfalls übereinstimmend simuliert. Die projizierte Kohlenstoffaufnahme der globalen terrestrischen Biosphäre am Ende des 21. Jahrhunderts kann für das untersuchte Klimaszenario mit einer Genauigkeit von $3,35 \pm 1,45 \text{ PgC } a^{-1}$ abgeschätzt werden, wobei die Unsicherheit zu etwa gleichen Teilen aus Unsicherheit über die Änderungen in der Kohlenstoffspeicherung von Böden und Vegetation entsteht.

Pflanzenphysiologische Studien legen nahe, dass sich die Länge des hydraulischen Transportweges innerhalb der Pflanze auf das Baumwachstum auswirkt. Es wird gezeigt, dass die prozessbasierte Simulation der altersbedingten Abnahme der Waldwachstumsrate durch die Berücksichtigung von hydraulischer Architektur und ihrer Änderung mit der Auswuchshöhe der Bäume verbessert wird. Die Anwendung des angepassten Modells in 77 europäischen Regionen zeigt, dass modellbasierte Abschätzungen des Biomasseaufwuchses in Wäldern weitgehend mit inventarbasierten Abschätzungen für verschiedene Baumarten übereinstimmen. Unter Berücksichtigung von historischen Änderungen in Klima, atmosphärischem CO_2 -Gehalt, Waldfläche und Holzernte (1948-2000) reproduziert das Modell auf europäischer Ebene die heutigen, auf Bestandsstatistiken beruhenden, Abschätzungen von Waldaltersstruktur, das Verhältnis von Zuwachs und Entnahme von Biomasse, sowie die Speicherungsraten im Kohlenstoffspeicher der Vegetation.

Abschätzungen der Auswirkung zukünftiger Klima- und Landnutzungsveränderungen auf die europäische Kohlenstoffbilanz – untersucht am Beispiel von vier alternativen Szenarien (2001-2100) – weisen eine mittlere Kohlenstoffspeicherungsrate im 21. Jahrhundert in der Größenordnung von 18-68% des momentanen europäischen Kyoto-Emissionsreduktionszieles auf. Die Auswirkungen der Verringerung landwirtschaftlich genutzter Fläche sowie von Aufforstungen entsprechen dabei etwa 20% des Emissionsreduktionszieles. Unter Berücksichtigung der Altersstruktur europäischer Wälder mit dem verbesserten Modelansatz dieser Arbeit anstelle der ursprünglichen Modelformulierung wirkt der Landnutzungseffekt auf die terrestrische Kohlenstoffaufnahme noch weiter verstärkt. In der zweiten Hälfte des 21. Jahrhunderts reduzieren erhöhte Bodenkohlenstoffverluste aufgrund der Klimaerwärmung unter allen Szenarien die durch Landnutzungsänderungen und Wachstumsstimulation bedingte terrestrische Kohlenstoffspeicherung. Die Unsicherheit der Abschätzung zukünftiger terrestrischer Kohlenstoffbilanzen durch unterschiedliche Raten und räumliche Muster der Klimaänderungen, basierend auf unterschiedlichen Klimamodellen für das gleiche Emissionsszenario, sind größer als die Unterschiede zwischen Projektionen alternativer Szenarien basierend auf einem Klimamodell.

Die vorliegende Arbeit stellt einen Ansatz vor, um Unsicherheiten in der prozessbasierten Abschätzung von terrestrischen Kohlenstoffbilanzen auf regionaler Skala zu untersuchen und zu reduzieren. Prozessbasierte Modellierung und Waldbestandsstatistiken wurden erfolgreich kombiniert, um verbesserte Abschätzungen von regionalen Kohlenstoffvorräten und ihrer Änderung mit der Zeit zu ermöglichen. Alternative Szenarien von zukünftigen Landnutzungs- und Klimaänderungen legen nahe, dass die Kohlenstoffaufnahme der europäischen terrestrischen Biosphäre von relevanter Größenordnung für Klimaschutzstrategien sind. Die Speicherungsraten sind jedoch klein im Vergleich zu den absoluten europäischen CO_2 -Emissionen, und nehmen zudem sehr wahrscheinlich gegen Ende des 21. Jahrhunderts ab. Unsicherheiten in Klimaprojektionen sind eine Hauptursache für die Unsicherheiten in den modellbasierten Abschätzungen des zukünftigen Nettokohlenstoffaustausches und müssen daher in Klimaschutzanalysen der terrestrischen Biosphäre berücksichtigt werden.

CONTENTS

1. Process-based simulation of the terrestrial biosphere	1
1.1 Background	1
1.2 Objectives of this thesis	3
1.3 Present understanding and methods	4
1.3.1 Methods to infer terrestrial carbon budgets	6
1.3.2 Bottom-up modelling approaches to estimate forest carbon balances	12
1.4 Research questions	14
1.5 Results	15
1.5.1 Parameter-based model uncertainty	15
1.5.2 Age-related decline in forest growth	17
1.5.3 Evaluation of regional forest growth and carbon balances	18
1.5.4 Analysis of Europe's present-day and future terrestrial carbon balances	21
1.5.5 Contrasting two alternative formulations of vegetation dynamics . .	23
1.6 Discussion	25
1.7 Conclusions	28
1.8 The author's contribution to the individual papers of this thesis	31
2. Parameter-based uncertainty of a DGVM	33
2.1 Introduction	34
2.2 Methods	36
2.2.1 LPJ-DGVM	36
2.2.2 Parameter values and sampling procedure	37
2.2.3 Data-sets	38
2.2.4 Modelling protocol	41
2.2.5 Parameter constraints and global benchmarking	42
2.3 Results	43
2.3.1 Parameter importance	43
2.3.2 Constraints to the parameter space	48
2.3.3 Parameter-based uncertainty in modelling the present-day carbon cycle	49

2.3.4	Model projections to 2100	55
2.4	Discussion	58
2.5	Conclusions	63
2.6	Appendix	65
3.	Tapering compensates height effect incompletely	67
3.1	Introduction	68
3.2	Review of theory and experimental evidence	69
3.3	Concluding remarks	73
3.4	Appendix	75
4.	Hydraulic acclimation and regional carbon balances	77
4.1	Introduction	78
4.2	Methods	80
4.2.1	LPJ	81
4.2.2	Data	84
4.2.3	Modelling protocol	86
4.3	Results	88
4.3.1	Stand-level model evaluation	88
4.3.2	Regional evaluation of modelled growth patterns	89
4.3.3	Regional application of the model to infer the forest carbon balance	94
4.4	Discussion	97
4.4.1	Tree growth in LPJ	97
4.4.2	Evaluation of simulated growth patterns using inventory data	98
4.4.3	European forest C balance	100
4.5	Conclusions	101
4.6	Appendix	103
4.6.1	Hydraulic acclimation theory	103
4.6.2	Plant water uptake considering hydraulic architecture	105
4.6.3	Forest management in LPJ	105
4.6.4	Gridded forest area, 1948-2000	110
5.	Europe's terrestrial carbon balance under climate and land-use change	113
5.1	Introduction	114
5.2	Material and Methods	115
5.2.1	Overview	115
5.2.2	Data	117

5.2.3	Model	122
5.3	Results	125
5.3.1	Present-day European carbon balance	125
5.3.2	Effects of land-use change	126
5.3.3	Effects of climate and atmospheric [CO ₂] change	129
5.3.4	Cumulative land-atmosphere flux between 1990 and 2100	132
5.4	Discussion	134
5.4.1	Land-use change	135
5.4.2	Climate change and increasing atmospheric [CO ₂]	136
5.4.3	General remarks	137
5.5	Conclusions	137
6.	Bibliography	139
	Appendix	163

LIST OF FIGURES

1.1	Historic and projected variations in atmospheric CO ₂ concentrations and annual mean air temperature between 1600-2100.	2
1.2	Main components of the global carbon cycle and fluxes due to the human perturbation	5
1.3	Parameter-based uncertainty in global land-atmosphere flux under the IS92a HadCM2-SUL climate change scenario simulated with LPJ-DGVM	16
1.4	Vegetation carbon and net increment with stand-age from a yield-table compared to estimates modelled with LPJ using two contrasting hypotheses about carbon allocation to plant tissues	18
1.5	Cumulative land-atmosphere flux over Europe between 1990 and 2100 under a range of SRES scenarios	22
1.6	Cumulative carbon uptake in forest vegetation due to land-use change after 1990 with two contrasting approaches of vegetation dynamics	24
2.1	The main processes, state variables and driving data for LPJ-DGVM	36
2.2	Spatial pattern of parameter importance for α_{C3} , α_a and g_m	45
2.3	Parameter combinations of α_{C3} and α_a and resulting global A and NPP	48
2.4	NPP at different EMDI sites	49
2.5	NEE at six sites of the EUROFLUX network	51
2.6	Average seasonal cycle of CO ₂ at three CO ₂ monitoring stations	52
2.7	Average annual global land-atmosphere flux for the 1980s and 1990s	54
2.8	Average annual NBE for 5° latitudinal bands in 1991-2000, 2041-2050 and 2091-2100 under the IS92a HadCM2-SUL climate change scenario.	55
2.9	Change in A , NPP and water-use efficiency between 1991-2000 and 2091-2100 under the IS92a HadCM2-SUL climate change scenario	56
2.10	Global land-atmosphere flux under the IS92a HadCM2-SUL climate change scenario	57
2.11	Change in foliage projective coverage between 2000 and 2100 under the IS92a HadCM2-SUL climate change scenario	58
3.1	Total plant hydraulic resistance as a function of total path length	70
4.1	Changes in allometric ratios with tree height	83
4.2	Forest area of deciduous and evergreen trees in Europe	85

4.3	Development of vegetation biomass and net increment with stand age . . .	88
4.4	Model and inventory-based biomass densities for a boreal, temperate, and mediterranean province.	90
4.5	Biomass densities in European forests by country	91
4.6	Average relative error of biomass estimates by LPJ	92
4.7	Average growth rate along a gradient in annual mean temperature	93
4.8	Effect of historic climate, atm. CO ₂ concentration, forest area and wood demand changes in forest age structure and growth rate	95
5.1	Overview of the simulation protocol implemented in this study	117
5.2	Changing land cover fractions for arable land, grassland, and forests under the four land-use change scenarios	119
5.3	Anomaly in annual mean temperature and annual precipitation over Europe projected by four different GCMs	121
5.4	Constituent fluxes of the net land-atmosphere carbon flux considering climate, atmospheric CO ₂ concentration and land-use change for 1901-2100 .	126
5.5	Land-atmosphere fluxes in the ATEAM-domain, 1901-2100	127
5.6	Land-atmosphere fluxes associated with the effects of land-use change . . .	128
5.7	Land-atmosphere fluxes associated with climate change and CO ₂ -fertilisation	131
5.8	Cumulative land-atmosphere fluxes between 1990 and 2100	133

LIST OF TABLES

1.1	Different methods to estimate terrestrial carbon budgets	8
1.2	Bottom-up modelling approaches to estimate forest carbon storage	13
1.3	Modelled and observed changes in forest ecosystem carbon pools of Europe in the 1990s	20
2.1	Key LPJ-DGVM parameters: Standard value, literature range, parameter description and literature sources	39
2.2	Overview over the experimental setup used in this study	41
2.3	Parameter importance for C fluxes	44
2.4	Parameter importance for C pools	46
2.5	Parameter importance for foliage projective cover	47
2.6	Root mean square error and coefficient of determination between measured and modelled monthly <i>NEE</i> for six eddy-covariance sites	50
2.7	NMSD between measured and modelled mean seasonal cycle of CO ₂ and parameter importance determining NMSD	52
2.8	Standard results, median and 90% confidence interval of present-day global carbon fluxes, H ₂ O fluxes and terrestrial carbon storage	53
3.1	Allometric scaling of hydraulic conductivity	73
4.1	Parameter values for the size dependent allocation scheme and the forest management module	83
4.2	Conversion factors for standing volume data to total vegetation biomass	86
4.3	Country average root mean square error of LPJ's biomass estimates	91
4.4	Modelled and observed changes in terrestrial C pools in the 1990s	96
4.5	Parameters and variables used of the size-dependent allocation module and plant hydraulics.	111
4.6	Parameters and variables of the forest management module.	112
5.1	Key characteristics of the climate change scenarios used.	120
5.2	The fate of carbon upon conversion and ecosystem management for different terrestrial ecosystems	124
5.3	Cumulative changes in terrestrial vegetation and soil carbon pools	132

1. PROCESS-BASED SIMULATION OF THE EUROPEAN TERRESTRIAL BIOSPHERE

AN EVALUATION OF PRESENT-DAY AND FUTURE TERRESTRIAL CARBON BALANCE ESTIMATES AND THEIR UNCERTAINTY

And this is what we meant by science. That both the question and the answer are tied up with uncertainty, and that they are painful. But that there is no way around them. And that you hide nothing; instead, everything is brought out into the open.

(P. Høeg, The Borderliners)

1.1 Background

Atmospheric carbon dioxide concentrations, $[\text{CO}_2]$, have reached absolute levels and rates of change that are unprecedented within the last 420,000 years (Petit *et al.*, 1999; Falkowski *et al.*, 2000). Fossil fuel burning and related industrial activities, as well as terrestrial carbon (C) losses from land-use change are the causes for the rise in atmospheric $[\text{CO}_2]$ from ~ 280 ppmv in pre-industrial times to about 370 ppmv in 2000 (Houghton, 1999; Marland *et al.*, 2000; McGuire *et al.*, 2001, Fig. 1.1). However, the observed growth rate of atmospheric $[\text{CO}_2]$ is significantly lower than expected from these emissions, implying a net uptake by oceans and/or land (Broecker *et al.*, 1979; Prentice *et al.*, 2001). Partitioning of the terrestrial and ocean fluxes based on simultaneous measurements of CO_2 and O_2 suggest that the terrestrial biosphere sequesters up to 30% of the fossil-fuel emissions (Ciais *et al.*, 1995; Prentice *et al.*, 2001; House *et al.*, 2003). The likely mechanisms for this net uptake include changes in land-use and more subtle changes in land-management or disturbance regimes, fertilising effects from increased atmospheric $[\text{CO}_2]$ and reactive nitrogen deposition, effects of natural climate variability and climatic change (Schimel *et al.*, 2001). The net flux is the sum of several poorly quantified fluxes, leaving their relative contribution uncertain (House *et al.*, 2003). Nevertheless, global terrestrial carbon fluxes have a substantial effect on the current growth rate of atmospheric $[\text{CO}_2]$.

CO_2 plays a key role in the climate system, contributing to about 50% of the total greenhouse gas forcing at present (Arrhenius, 1896; Ramaswamy *et al.*, 2001). The rise in atmospheric greenhouse gas concentrations since the beginning of the industrialisation in the 19th century is the most likely cause of the observed increase in global mean land

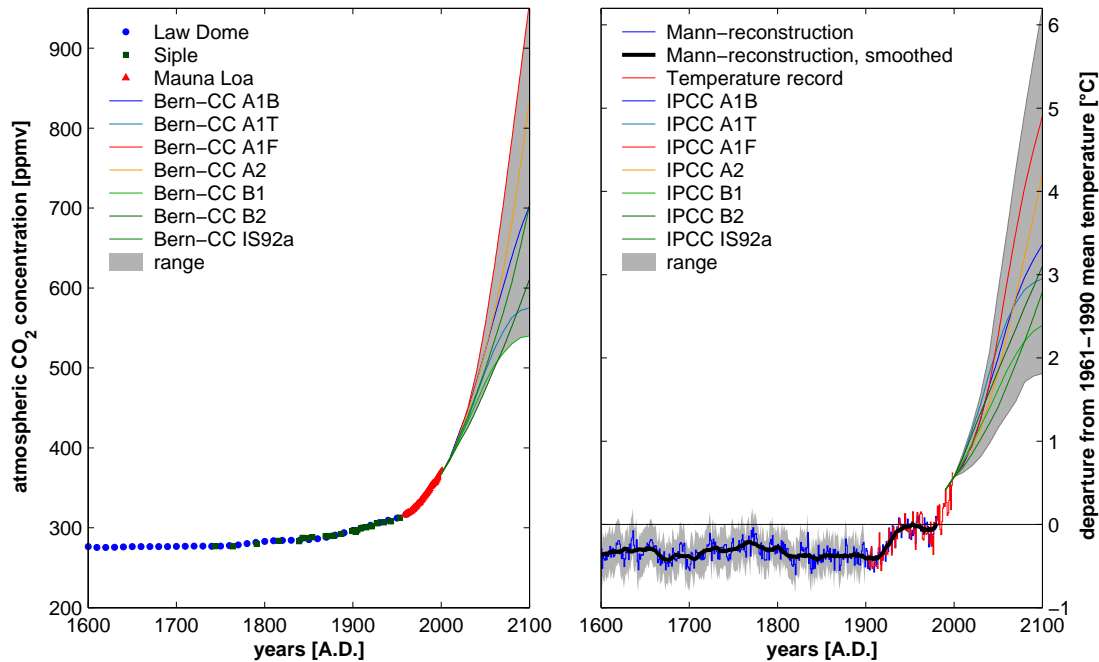


Fig. 1.1: **Left:** Variations in atmospheric [CO₂] between 1600 and 2000 (observations from Law Dome, Siple and Mauna Loa), as well as projections of future atmospheric [CO₂] for 2000 to 2100 of the Bern-CC model (redrawn from Prentice *et al.*, 2001). **Right:** Northern-hemisphere temperature anomaly relative to 1961-1990, based on proxy-data (1600-1980) and thermometer records (1900-2000) taken from Mann and Bradley (1999), as well as projections of global annual air temperature for 2000-2100 derived from several IPCC climate change scenarios, based on Houghton *et al.* (2001).

surface temperature by $0.6 (\pm 0.2)$ K over the 20th century (Houghton *et al.*, 2001, Fig. 1.1). Atmospheric concentrations of CO₂ and other greenhouse gases are expected to continue to rise in the 21st century mainly as a consequence of increasing anthropogenic fossil fuel use under a wide range of plausible scenarios of socio-economic development (Nakicenovic *et al.*, 2000). The contribution of CO₂ to the total radiative forcing of the atmosphere is likely to increase to up to 70-80% (Ramaswamy *et al.*, 2001). Climate change calculations based on such scenarios utilising general circulation models (GCMs) suggest that the global mean temperature may rise by up to 6 K relative to pre-industrial levels (Houghton *et al.*, 2001, Fig. 1.1).

Climate change already affects terrestrial ecosystems in various ways – including for instance phenology (*e.g.* bud break of trees, spring arrival of migratory birds), plant production, environmental envelopes of potential species distribution of plants and animals, and thereby the composition and dynamics of ecological communities (Walther *et al.*, 2002; Bakken *et al.*, 2002) – and will continue to do so in the future (Gitay *et al.*, 2001). Global warming may reduce the capacity of the terrestrial biosphere to sequester C, or lead to net carbon losses from the terrestrial biosphere thereby providing a positive feed-back to the climate system (Cox *et al.*, 2000; Cramer *et al.*, 2001; Friedlingstein *et al.*, 2003). Climate change will impact the functioning of terrestrial ecosystems adding to existing pressures

from human land-use and land-management (Gitay *et al.*, 2001). The functioning of the terrestrial biosphere, on the other hand, is central to the human system to which it provides a range of goods and services such as food production and freshwater supply (Daily, 1997; Watson *et al.*, 1998). Depending on the capacity of the affected human sectors to cope with changes in these services, potential decreases in service provision due to climate change may in turn impact on the human sectors, making humans themselves vulnerable to climate change (Schröter *et al.*, in press).

Recognising the threat of climate change, member states of the United Nation’s Framework Convention on Climate Change (UNFCCC, 1992) adopted the Kyoto Protocol in 1997 (UNFCCC, 1998). The protocol includes legally binding greenhouse gas emission reduction targets for signatory states with the aim to prevent any “dangerous anthropogenic interference with the climate system”, and entered into force in February 2005. Because of the tight interactions of terrestrial carbon budgets and the climate system, carbon sequestration in the terrestrial biosphere resulting from direct human actions – *i.e.* either related to land-use or land-management changes – after 1990 may be accounted for to offset a limited amount of the emission reduction target (Art. 3.3 and 3.4). Climate mitigation policies beyond the first Kyoto commitment period (2008-2012) need to consider the joint impact of land-use and climate changes on terrestrial carbon budgets on time-scales at which the components of the global carbon cycle and the climate system respond to changing environmental conditions to evaluate the effectiveness of climate protection strategies. In this context, estimation of regional terrestrial carbon budgets, their change over time, as well as an identification of the key driving processes become relevant not only for the scientific understanding of the Earth system, but also for mitigation policies.

1.2 Objectives of this thesis

The aim of this study is to integrate present-day understanding of the European terrestrial carbon balance into scenario analyses of climate mitigation and vulnerability assessments for the 21st century. Special emphasis is placed on the carbon dynamics in forests, since these account for a substantial part of the present-day terrestrial carbon uptake in Europe (Janssens *et al.*, 2003; Lindner *et al.*, 2004). Data-based approaches that document past and present changes of the terrestrial carbon balance are limited in their capacity to estimate terrestrial carbon balances under rapidly changing environmental conditions (see Section 1.3). Generalised ecosystem models that dynamically simulate growth changes under varying environmental conditions are a necessary tool for such a task, providing estimates of carbon fluxes at adequate temporal and spatial resolution. However, past, present and future land-use and land-management changes, which are of particular importance on a European scale, are only insufficiently represented in these models. This study therefore integrates forest statistics and ecophysiological understanding obtained from detailed field studies to improve regional-scale terrestrial carbon estimates under multiple environmental change scenarios.

Specifically, this study

1. assesses the parameter-based uncertainty in estimates of terrestrial carbon stocks and fluxes based on terrestrial biosphere modelling, and evaluates the consequences of this uncertainty on the ability of terrestrial biosphere models to project land-atmosphere fluxes under future environmental conditions (Chapter 2).
2. evaluates and improves the representation of forest dynamics, especially with respect to the representation of forest growth with age, and the influence of forest management on forest C stock development on a regional scale (Chapters 3 and 4).
3. provides an assessment of the effects of multiple scenarios of land-use and climate changes on the European terrestrial carbon balance for the period 1990-2100 (Chapter 5).

The present study contributes to the integration of different methods to estimate the contemporary terrestrial carbon balance at the European scale. The results are furthermore part of a comprehensive assessment of potential future changes in European ecosystem goods and services, such as agricultural and forest productivity, biodiversity, carbon storage and freshwater availability, under a range of plausible climate and land-use change scenarios. The simulated changes in ecosystem services, based on a suite of ecosystem models, form the basis of a spatially explicit assessment of the global change related vulnerability of human sectors, for instance forestry, but also more abstract ‘sectors’ as the societal interest in terrestrial C storage for climate mitigation. These changes have been assessed within the 5th EU framework research project ATEAM (Advanced Terrestrial Ecosystem Assessment and Modelling, Schröter *et al.*, 2004). The present-day terrestrial C balance of Europe is the research focus of the ongoing 6th EU framework integrated project CarboEurope-IP.

Section 1.3 gives an overview of the contemporary terrestrial carbon cycle and methods to infer terrestrial carbon balances. The specific research questions are presented in Section 1.4. Results of the individual papers of this thesis (Chapters 2-5) are summarised in Section 1.5. Section 1.6 discusses the findings of the study, leading to the conclusions in Section 1.7. Finally, Section 1.8 summarises the author’s contributions to the individual papers of this thesis.

1.3 Present understanding and methods

Contemporary C stocks in the terrestrial biosphere are estimated at about 2,000 PgC (Atjay *et al.*, 1979; Dixon, 1994; Mooney *et al.*, 2001), which is nearly three times the C stored in the atmosphere (730 PgC, Prentice *et al.*, 2001, Fig. 1.2a). Of the terrestrial C storage, about three quarters are estimated to be stored in soils, and the remainder mostly in the biomass of the world’s forests, which occupy about 30% of the land surface.

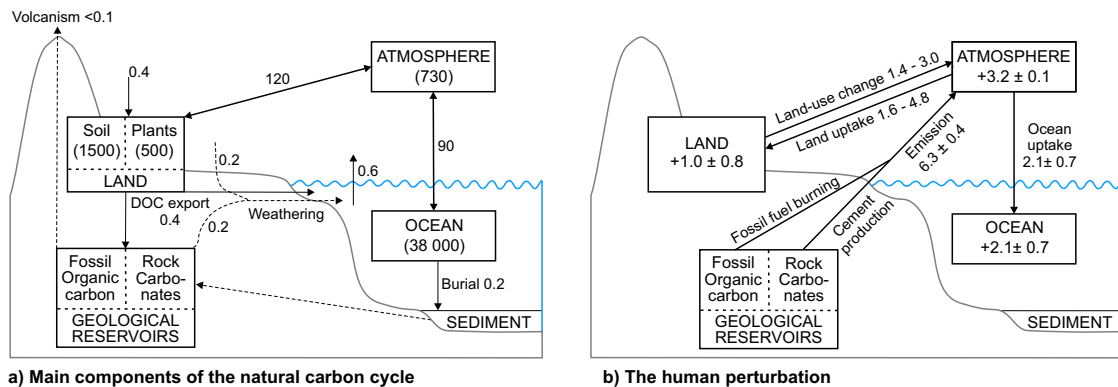


Fig. 1.2: **a)** The main components of the natural global carbon cycle and the fluxes between them in an undisturbed state, **b)** fluxes in contemporary cycle (1990s), redrawn from Prentice *et al.* (2001) and House *et al.* (2003).

More than one-third of the C in the atmosphere is cycled through leaves of higher plants every year (Farquhar *et al.*, 1993; Ciais *et al.*, 1997a,b). Some 120 PgC are actually ‘fixed’ by land plants through photosynthesis (Ciais *et al.*, 1997a, see Fig. 1.2a). Roughly one half of this gross primary production (*GPP*) is lost to the atmosphere via autotrophic respiration (R_a) from plant tissues (Lloyd and Farquhar, 1996; Waring *et al.*, 1998), the remaining ~ 60 PgC are incorporated into plant tissue as terrestrial net primary production (*NPP*, Atjay *et al.*, 1979; Ruimy *et al.*, 1994; Knorr and Heimann, 1995; Saugier and Roy, 2001, Fig. 1.2a). The small difference between the two large fluxes from *NPP* and C losses due to heterotrophic respiration (R_h), as well as (smaller) C losses from ecosystem disturbance and lateral transport determines the terrestrial carbon balance, the so called net biome exchange (*NBE*). Natural fluctuations in *NBE* result from the differential response of plant production, respiration and disturbance to climate variability (Peylin *et al.*, 2005). Box 1.1 describes the constituent fluxes of the *NBE*.

In the 1990s, only 3.2 ± 0.1 PgC yr⁻¹ of the 6.3 ± 0.4 PgC yr⁻¹ emitted from fossil fuel burning and cement production remained in the atmosphere (Prentice *et al.*, 2001, Fig. 1.2b). 2.1 ± 0.7 PgC yr⁻¹ were taken up by oceans (Bopp *et al.*, 2002; Le Quéré *et al.*, 2003). A terrestrial net C uptake of 1.0 ± 0.8 PgC yr⁻¹ has to be assumed to close this balance (House *et al.*, 2003). Estimates of terrestrial C losses due to deforestation range between 1.4 and 3.0 PgC yr⁻¹. A residual terrestrial C uptake of 1.6 to 4.6 PgC yr⁻¹ is required to close the terrestrial carbon budget when accounting for the C release from deforestation (House *et al.*, 2003).

The depletion of atmospheric [CO₂], relative to theoretically expected values (Tans *et al.*, 1990; Bousquet *et al.*, 1999; Gurney *et al.*, 2002), as well as ¹³C/¹²C ratios in the atmosphere (Ciais *et al.*, 1995) suggest a net carbon uptake in the mid-latitudes of the Northern Hemisphere. Such an uptake would be consistent with observations from remote sensing, which suggest increased vegetation activity in Northern mid- and high-latitudes (Myneni *et al.*, 2001; Lucht *et al.*, 2002; Slayback *et al.*, 2003). Several lines of

Box 1.1: Definition of terms describing the land-atmosphere flux

The net ecosystem exchange of carbon (NEE) on a patch-level is determined by the difference between the two large but opposing carbon fluxes of net primary production (NPP) and carbon losses due to heterotrophic respiration (R_h). Measurements of NEE do not account for the effect of disturbance that remove C from the ecosystem (such as fire or harvest) in a way that is representative for the larger region around the measurement site. The large-scale land-atmosphere flux, net biome exchange (NBE), is the difference between net primary production and regional-scale losses of C due to heterotrophic respiration, disturbance, either natural such as fire (Andreae and Merlet, 2001) or by harvest (Bolin *et al.*, 2000), as well as losses due to the transport of dissolved organic matter (Schlesinger and Melack, 1981; Sarmiento and Sundquist, 1992). Thus,

$$NEE = R_h - NPP \quad \text{and} \quad NBE = NEE + Disturbance$$

where negative NEE and NBE denote a net flux from the atmosphere to the land, *i.e.* an increased C storage in the biosphere, and *vice versa*.

evidence point to forests as the major land-use type of C uptake (Kauppi *et al.*, 1992; Friedlingstein *et al.*, 1995; Spieker *et al.*, 1996; Schimel *et al.*, 2001; McGuire *et al.*, 2001; Myneni *et al.*, 2001; Janssens *et al.*, 2003). The causes for this enhanced uptake are a combination of growth stimulation due to CO₂-fertilisation (Schimel, 1995; Amthor, 1995) and deposition of reactive nitrogen (Spieker *et al.*, 1996), as well as land-use history, and past forest management (Kohlmaier *et al.*, 1995; Karjalainen *et al.*, 1999; Nabuurs, 2004). Compilation of recent forest statistics (see Section 1.3.1) suggests that increasing vegetation C storage in temperate and boreal forests alone may account for half of the gap in the global carbon budget (Liski *et al.*, 2003). The share of biomass storage in European forests, as well as contribution to the total C uptake estimate of 0.88 PgC yr⁻¹ in temperate and boreal forests is relatively small (0.11 PgC yr⁻¹), because of their small contribution to the total forest area. Nevertheless, C uptake per unit area is largest in Europe (and the US), partly because forest vegetation in Europe is in a rebound phase, with an age-structure shifted towards young and fast growing stands that typically strongly sequester carbon (Nabuurs *et al.*, 2003).

1.3.1 Methods to infer terrestrial carbon budgets

Table 1.1 (page 8) summarises the different techniques that are available to estimate regional scale land-atmosphere fluxes. These include

- the inversion of atmospheric [CO₂] to biospheric fluxes using atmospheric transport models,
- the application of remotely sensed data to infer vegetation activity,
- small-scale field studies that measure changes in ecosystem carbon stocks over time

and/or directly the ecosystem-atmosphere carbon flux with the eddy-covariance technique,

- forest inventories and book-keeping methods, and
- terrestrial biosphere models.

Top-down methodologies

Atmospheric inversions: Measurements of atmospheric $[\text{CO}_2]$ at monitoring stations around the globe give estimates of the absolute concentration as well as the seasonal cycle of CO_2 within the footprint area of each station (Conway *et al.*, 1994). By inverting atmospheric wind fields, these data can be used to infer the sign and magnitude of C fluxes of predefined regions of the globe (Bousquet *et al.*, 2000; Rödenbeck *et al.*, 2003). Inversions are well capable of resolving latitudinal gradients in land-atmosphere carbon fluxes. However, the location of fluxes within a latitude band is less well constrained, so that presently only continental scale regions such as Northern America or Eurasia can be discerned (Peylin *et al.*, 2002). Inverting atmospheric fluxes poses an ill-constrained problem. The sparse data network (particularly on land), as well as uncertainty in the co-occurring fluxes from fossil fuel and ocean compound the identification of the land-atmosphere flux. 20 years of measurements that are available for the construction of an inversion-based land-atmosphere flux record suggest that the interannual variability in this flux is better constrained than the associated net fluxes (Peylin *et al.*, 2005; Rayner *et al.*, 2005).

Remote sensing: Remotely sensed data allow to detect seasonal and interannual variations in vegetation activity with high spatial and temporal resolution. In particular, the normalised difference vegetation index (NDVI) can be used to deduce global maps of leaf area index or the fraction of absorbed photosynthetically active radiation of vegetation (Myneni *et al.*, 1997). These quantities may in turn be used to diagnose C exchanges of the vegetation with the help of models, ranging from light-use efficiency approaches to more complex biogeochemical models (Fischer *et al.*, 1997). Recently, attempts have been made to correlate satellite-derived trends in vegetation greenness to variations in the terrestrial C cycle and its driving forces (Lucht *et al.*, 2002; Nemani *et al.*, 2003). First attempts to quantify the terrestrial carbon cycle have involved the assimilation of eddy-covariance data into simple satellite-based light-use efficiency models (Veroustraete *et al.*, 2002; Reichstein *et al.*, 2004), or assimilation of satellite data into more complex ecosystem models (Knorr and Heimann, 2001a; Potter *et al.*, 2003; Knorr *et al.*, 2004). Large-scale estimation of above-ground carbon stocks from satellite is still under development (Le Toan *et al.*, 2004; Hese *et al.*, 2005). However, satellite-derived data cannot account for soil C storage or its change over time.

	<i>'Top-down' approaches</i>		<i>'Bottom-up' approaches</i>		
	<i>Atmospheric inversion models</i>	<i>Remote sensing</i>	<i>Forest inventory/statistical bookkeeping</i>	<i>Eddy-covariance measurements</i>	<i>Terrestrial Biosphere Models</i>
Spatial coverage	complete	complete	complete ^a	discrete points	complete
Spatial resolution	continental	~10m to ~10km	regional	<1 km ²	~0.5° × 0.5°
Temporal resolution	daily-monthly	<monthly ^b	~10 years	hourly	daily-monthly
Temporal coverage	~20 years	~20 years ^c	>40 years	<10 years	~100 years
Property measured	<i>NBE</i>	vegetation reflectance	terrestrial C stock change ^d	<i>NEE</i>	<i>NBE</i>
Process identification	no	no	limited ^e	no	yes
<i>Processes included in flux estimates</i>					
Land-use change	✓	✓	✓	×	✓ ^f
Land management	✓	limited	✓	only locally	×
Disturbance	✓	limited	× ^g	only locally	limited ^h
Climate variability	✓	✓	×	✓	✓

^a Forest inventories only account for vegetation in forests. Bookkeeping methods theoretically cover all land, *e.g.* Houghton (1999).

^b depends on the product used, between 8 day and monthly composites.

^c AHVRR data available since 1982, newer and improved sensors such as MODIS have shorter temporal coverage (since 2000).

^d Forest inventories do not account for soil C; Houghton's book-keeping method relies on characteristic C densities for different land-use types instead of tracking inventoried C stocks.

^e Forest management change is implicit in forest statistics; land-use change effects can be obtained from book-keeping.

^f Representation of the replacement of natural vegetation with croplands and *vice versa*.

^g Forest inventories implicitly include the effect of disturbance on growing stock, the bookkeeping method by Houghton (1999) does not.

^h calculated from generic modules.

Tab. 1.1: Different methods to estimate terrestrial carbon budgets, as discussed in Section 1.3.1. '✓' denote that these processes are included in the flux estimates, and '×' that this process cannot be considered.

Bottom-up methodologies

Eddy-covariance measurements: Measurements of ecosystem-atmosphere CO₂ exchanges on sub-daily time-scales derived with the eddy-covariance technique can be used to estimate annual net C fluxes for areas of typically less than 1 km² (Wofsy *et al.*, 1993; Goulden *et al.*, 1996; Aubinet *et al.*, 2000; Baldocchi, 2003). These studies have led to an improved understanding of the ecophysiological controls of *NEE* (Valentini *et al.*, 2000a). Point-scale estimates from eddy-covariance techniques can be integrated over larger regions using meteorological variables, land-use maps and indices of vegetation activity derived from remotely sensed data (Martin, 1998; Valentini *et al.*, 2000a; Papale and Valentini, 2003). However, such an upscaling is subject to high uncertainty. It is not self-evident that the measurement sites are representative for the entire European forest ecosystem, in particu-

lar since the network is biased towards high productive, middle-aged forest stands (Bolin *et al.*, 2000; Valentini *et al.*, 2000a). Also, upscaled land-atmosphere flux based on these measurements may be biased, because these measurements cover only a limited number of years (typically less than 10 years) and the measured flux exhibits a high interannual variability (Malhi and Grace, 2000; Valentini *et al.*, 2000a). Eddy-covariance techniques have recently also been used for the study of CO₂ fluxes in arable and grasslands, as well as for the examination of the effect of disturbance in forests both natural and by harvest (Churkina *et al.*, 2003; Law *et al.*, 2003; Kowalski *et al.*, 2004; Kolari *et al.*, 2004). This will allow for a more comprehensive assessment in the future.

Forest inventories and bookkeeping methods: Forest inventories give relatively accurate information on regional-scale forest growing stock volume, as they rely on a large amount of field measurements. These are specifically designed to supply statistically sound measurements of timber stocks and forest growth across large heterogeneous regions (Köhl *et al.*, 1997). However, inventories in Europe are not yet harmonised (Köhl *et al.*, 2000). Carbon stocks in vegetation need to be inferred from biomass expansion factors to scale volume data to total vegetation carbon (Kauppi *et al.*, 1992; UN-ECE/FAO, 2000; Watson *et al.*, 2000). These scaling factors to infer vegetation C stocks from volume data are only imprecisely known, particularly those applicable on a larger scale (Lehtonen *et al.*, 2004; Wirth *et al.*, 2004).

Forest inventories are routinely reported for most countries in the temperate and boreal zone since 1948. Inventories are typically carried out in cycles of about 10 years, and thereby integrate all factors affecting forest growth due to forest management activities and changed environmental conditions such as climate change, CO₂- and N-fertilisation (Goodale *et al.*, 2002). Originally designed for commercial purposes, such statistics have recently been used to infer bottom-up carbon balances (Kauppi *et al.*, 1992; Dixon, 1994; Kurz and Apps, 1999; Caspersen *et al.*, 2000; Goodale *et al.*, 2002; Nabuurs *et al.*, 2003; Smith *et al.*, 2004). Uncertainty is introduced into such calculations, because inventory methods have improved over time, affecting the accuracy with which stocks have been measured particular for the 1950s and 1960s (Nabuurs *et al.*, 2003).

Forest inventories only account for C stocks in live or dead woody vegetation. Estimates of forest soil C stocks and their change over time can only be obtained from aggregation of soil surveys or modelling (Liski *et al.*, 2002). Also, forest inventories give insight only into stock changes in forests, and do not account for other parts of the terrestrial biosphere. Bookkeeping models keep track of changes in plant and soil carbon stocks (Dixon, 1994; Houghton, 1999) due to land-use changes based on historic records or reconstructions. While these methods may account for all major land-use types and conversion between them, they rely on standard growth and decomposition curves to infer changes in vegetation, soil and product pools. As such, they do not consider the effect of environmental changes on terrestrial carbon storage.

Terrestrial biosphere models: Terrestrial biosphere models encode process understanding of carbon, water and nitrogen fluxes (Cramer *et al.*, 1999; Arora, 2002). They differ from other process-based land ecosystem models, *e.g.* forest gap models, in their simplified representation of ecosystems, usually having globally applicable parameterisation and low input data requirements. This generality makes them an ideal tool to extrapolate small-scale carbon and water fluxes measured with eddy-covariance techniques to larger scales (Sitch *et al.*, 2003; Krinner *et al.*, 2005). These models have been used to explore the interactions of the complex processes that drive the terrestrial carbon cycle, in particular the effect of climate variability on the global carbon cycle (Kindermann *et al.*, 1996; Heimann *et al.*, 1998; Prentice *et al.*, 2000; Dargaville *et al.*, 2002). Their capacity to replicate the interannual variability in the global carbon cycle – as inferred from atmospheric inversions – can be used to identify the contribution of ecosystem processes to this variability (Peylin *et al.*, 2005). Terrestrial biosphere models can be used to evaluate the effects of future environmental changes on the terrestrial C balance (*e.g.* Cox *et al.*, 2000; Cramer *et al.*, 2001; Friedlingstein *et al.*, 2003).

These models differ in the detail in which ecosystem processes are represented, but share a common base of plant physiological processes, that is a more or less mechanistic treatment of photosynthesis, plant respiration, canopy water balance, the controls of stomatal and canopy boundary-layer conductance, and allocation of carbon and nitrogen to tissue pools (Cramer *et al.*, 1999). Differences in the detail with which processes are represented in ecosystem models are known to lead to substantial differences in modelled results (Cramer *et al.*, 2001; Joos *et al.*, 2001; Knorr and Heimann, 2001a; Kramer and Mohren, 2001). But even if the model structure would perfectly resemble all relevant ecosystem processes, uncertainty in model simulations would still arise from model parameterisation (Saltelli *et al.*, 2000). Ecosystem models encode processes at various temporal and spatial scales for which not all relevant scaling factors, or parameter values, are known well. In principle, these models are able to assimilate data from [CO₂] measurements, remote sensing, or derived variability of terrestrial C fluxes based on atmospheric inversions (Knorr and Heimann, 2001b; Wang *et al.*, 2001; Reichstein *et al.*, 2003; Knorr and Kattge, *in press*; Rayner *et al.*, 2005). Such data assimilation techniques can be used to estimate parameter values and to quantify some aspects of the parameter-based model uncertainty. However, the effect of parameter-based uncertainty on process-based estimates of terrestrial carbon budgets, and their change on longer time-scales in particular, has remained largely unquantified.

Early biosphere models did not consider the consequences of environmental changes on ecosystem structure, which may lead to significant redistribution of vegetation under changed climatic conditions (Neilson, 1993; Smith and Shugart, 1993; Melillo *et al.*, 1995), as well as their feedback to the terrestrial carbon cycle. A new class of terrestrial biosphere models, dynamic global vegetation models (DGVMs), has therefore been developed to predict the transient effects of environmental changes on vegetation dynamics (Steffen

et al., 1996; Woodward, 1996). DGVMs describe vegetation as composed of plant functional types (PFTs) with different physiological, phenological and physiognomic attributes (Woodward *et al.*, 1995; Foley *et al.*, 1996; Friend *et al.*, 1997; Brovkin *et al.*, 1998; Cox, 2001; Smith *et al.*, 2001; Sitch *et al.*, 2003; Krinner *et al.*, 2005). Representation of vegetation structure is usually fairly simplistic, typically consisting of simple rules to partition *NPP* between various plant tissues that represent vegetation as homogeneously distributed over larger areas (typically $0.5^\circ \times 0.5^\circ$, Friedlingstein *et al.*, 1999; Sitch *et al.*, 2003). Vegetation dynamics in DGVMs describes large-scale approximations of the competition of PFTs in natural vegetation structure, without anthropogenic disturbance. The treatment of competition between different PFTs in these models ranges from implicit descriptions of vegetation dynamic to gap-model type oriented approaches, which are generalisations of models that have originally been developed to simulate the forest composition on a landscape scale (Botkin *et al.*, 1972; Prentice *et al.*, 1993; Bugmann, 2001).

Few studies have addressed the effect of human land use and its change on the terrestrial carbon balance (McGuire *et al.*, 2001; Levy *et al.*, 2004; Cramer *et al.*, 2004). The representation of actual land-use patterns has been fairly simple in these studies. Recently, some DGVMs have started to include more detailed representations of croplands (de Noblet-Ducoudre *et al.*, 2004; Bondeau *et al.*, in prep.). Only few attempts have been made so far to include a representation of the dynamics in even-aged, managed forests (Kohlmaier *et al.*, 1995; Häger, 1998). Land-use history and forest management have radically changed the forest structure in Europe (Mather, 1990; Karjalainen *et al.*, 1999; Nabuurs, 2004). The age-structure of forests is of particular importance for the development of the growing stock, as the growth rate of forest stands declines markedly with stand age (Kira and Shidai, 1967; Gower *et al.*, 1996; Ryan *et al.*, 1997). The present forest age-structure of Europe with a larger share of young forests implies a higher growth rate than under steady state conditions and thereby accumulation of biomass (Nabuurs, 2004).

Evaluation of these methods with reference to the objectives of this thesis

No single method provides a definitive estimate of regional-scale terrestrial carbon budgets for all relevant terrestrial carbon pools and fluxes in adequate temporal and spatial resolution (House *et al.*, 2003). Bias in the up-scaling of point-scale estimates (either from data or model results) may occur for instance from the selection of sites and time-period used. Some methods give only estimates of individual elements of the carbon cycle (*e.g.* inventories estimate only forest vegetation biomass, satellites give only direct information about vegetation greenness). In inversions, which in theory account for all land-atmosphere fluxes, the net flux is not well constrained, particularly on a regional scale. Above all, data-based methods can only extrapolate observed trends. The ecosystem processes that control these trends will likely be altered under the environmental changes that are to be expected over the coming decades. Process-based modelling is the only method capable of

attributing observed trends to changes in ecosystem processes. These models can be evaluated against ecosystem measurements for some (representative) regions, and thereafter be used to extrapolate these measurements to other regions for which little or no data are available. As such, modelling provides a prognostic capacity that allows for the assessment of the terrestrial carbon balance under future changes in environmental conditions.

Terrestrial biosphere models provide comprehensive and highly resolved estimate of vegetation and soil carbon pools. However, the uncertainty in the application of these modelled for the assessment of present-day and future environmental conditions is only insufficiently known. Also, the representation of actual land-cover processes and the associated C fluxes from human appropriation of *NPP* is limited, and uncertainty in model results is only poorly quantified. The following Section reviews the existing modelling approaches that link dynamics of managed forests to process-based simulations of growth with the aim to identify key limitations of current modelling approaches.

1.3.2 Bottom-up modelling approaches to estimate forest carbon balances

Table 1.2 summarises different bottom-up modelling approaches that have been used previously to estimate forest carbon balances in Europe for present-day and future climatic conditions. At the stand-level, a variety of forest growth models exists that combine process-based calculation of carbon and water cycles with natural and human-induced vegetation dynamics (*e.g.* Lindner, 2000; Lindner *et al.*, 2000). These models encode detailed descriptions of the response of forest growth to variations in climate and alternative forest management strategies. While they do explicitly simulate the development of trees with stand age, not all of these models replicate the age-related decline in forest growth adequately (Kramer and Mohren, 2001). Application of these models at a range of sites across the European climate space has highlighted their potential to estimate the effect of alternative forest management strategies on forest growth and forest carbon balance under climate change (Kramer and Mohren, 2001; Kellomäki, in prep.). Extrapolation of point-scale model results to regional scales, however, might be biased as the selection of sites might not be representative for all relevant forest types and the entire climate space. Some attempts have been made to use such models for the calculation of forest C balances for the landscape or country scale (*e.g.* Lexer *et al.*, 2002). However, these models require a large amount of initialisation data and detailed parameterisation, which are not commonly available or applicable at larger scales.

Few studies attempt to overcome the scale-gap by linking the dynamics of even-aged, managed forests based on forest statistics (*e.g.* Nabuurs *et al.*, 2001) to process-based calculations of ecosystem carbon exchanges based on terrestrial biosphere models (Häger, 1998; Meyer *et al.*, in review). These model represent forest age-structure at the regional scale based on fixed age-dependent growth functions, thereby implicitly accounting for natural forest stand dynamics. In contrast to point-scale models and DGVMs, these models can directly estimate the regional-scale effect of shifts in forest age-structure, *e.g.* through

	<i>Point-scale Models^a</i>	<i>Forest Statistical Models^b</i>	<i>Terrestrial Biosphere Models^c</i>	<i>Modified Terrestrial Biosphere Models^d</i>	<i>This study (Chapter 4)</i>
Input data requirement	high	medium	low	medium	low
Spatial coverage	sites ^e	inventoried area	all forest area	inventoried area	all forest area
Spatial resolution	sites ^e	regions	spatially explicit	regions	spatially explicit
<i>Pools and fluxes</i>					
Vegetation	✓	✓	✓	✓	✓
Soil	✓	limited	✓	limited	✓
Wood-products	✓	✓	×	×	✓
C fluxes	<i>NEE</i>	<i>NBE</i>	<i>NBE</i>	<i>NBE</i>	<i>NBE</i>
<i>Representation of stand dynamics</i>					
Natural dynamics	✓	implicit ^f	✓	implicit ^f	✓
Forest management	detailed	regional	×	regional	regional
Age structure	✓ ^g	✓	×	✓	✓
<i>Representation of environmental changes</i>					
Climate variability	✓	×	✓	✓	✓
Climate change	✓	✓ ^h	✓	✓	✓
Forest area change	×	✓	×	✓	✓

^a *e.g.* Kramer and Mohren (2001); Kellomäki (in prep.)

^b *e.g.* Nabuurs *et al.* (2001); Meyer *et al.* (in review)

^c *e.g.* Friend *et al.* (1997); Sykes *et al.* (2001)

^d *e.g.* Häger (1998)

^e limited selection of representative sites in terms of climate and forest types

^f prescribed growth functions, not responding to environmental or management change

^g single stands that may be assembled to reproduce the age-structure of an entire forest land-scape

^h scaling growth functions by predictions of a process-based forest growth model

Tab. 1.2: Bottom-up modelling approaches that can be used to estimate future forest carbon storage at the European scale.

forest area changes, on forest growth. However, the representation of land-use change effects of the overall forest C balance is still limited as soil C pools on afforested lands have to be prescribed from other data sources. The growth functions in these models give limited insight into the ecology of vegetation dynamics. They thus do not account for potential changes in forest growth rates resulting from changes in either management practices or environmental conditions, such as climate change, CO₂- and N-fertilisation or atmospheric pollution that are known to alter forest growth (Mund *et al.*, 2002). Forest growth under changing climate may be derived by scaling the growth functions with simulated growth changes from process-based ecosystem models (Häger, 1998; Meyer *et al.*, in review). However, such scaling implicitly assumes that the response of the growth rate would be similar for all age-classes, whereas some evidence suggests that the response is non-linear (Vetter, *pers. comm.*).

Improving the modelling of large-scale dynamics in managed forests requires a com-

bination of these two modelling approaches. Gap-type forest dynamics similar to point-scale forest models have already been generalised and incorporated into the framework of DGVMs (Friend *et al.*, 1997; Smith *et al.*, 2001). The logical next step is to integrate the large-scale representation of forest management into these models. Within the framework of the LPJ dynamic global vegetation model (LPJ-DGVM, Smith *et al.*, 2001; Sitch *et al.*, 2003) both a gap model approach (LPJ-GUESS, Smith *et al.*, 2001) and a representation of croplands and pasture (Bondeau *et al.*, in prep.) have been developed. Integrating managed forests into this framework will lead to (a) an improved process-based estimate of the regional-scale C balance of forests and (b) further link this estimate of the forest C balance to estimates of C fluxes from other major land-uses to provide an improved assessment of the regional-scale terrestrial carbon balance.

1.4 Research questions

This study aims at assessing potential future changes in terrestrial carbon stocks at a European scale, relevant for long-term climate mitigation policies, because of tight interactions between the terrestrial carbon cycle and the climate system. Terrestrial biosphere models are a necessary tool for such an assessment under changed environmental conditions. The above review highlights the unknown uncertainty of model results and lack of representation of actual land-use dynamics, particular in forests, as key limitations of the application of terrestrial biosphere models in regional-scale assessments of present-day and future estimates of terrestrial carbon balances. This study therefore addresses the following questions:

- What is the effect of parameter uncertainty on modelling terrestrial biosphere dynamics, and which model parameters contribute most to model uncertainty?
- What level of physiological detail is necessary to model the age-related decline of forest growth?
- Can biomass development in managed even-aged forests be accurately simulated with a generalised vegetation model on a regional-scale ?
- What is the effect of afforestation and wood-demand changes derived from forest statistics on estimates of the age-structure and carbon balance of European forests simulated by generalised vegetation models?
- What are the joint effects of land-use and climate changes on the terrestrial carbon balance of Europe presently and in the future?

Chapter 2 presents an assessment of the sensitivity of the LPJ-DGVM (Smith *et al.*, 2001; Sitch *et al.*, 2003) to its parameterisation and the associated uncertainty in simulated properties of the terrestrial biosphere. The validity of the most likely hypothesis for the

age-related decline in forest growth is discussed in Chapter 3. In the first part of Chapter 4, differing hypotheses as to the causes of the age-related decline are evaluated within the framework of LPJ. Chapter 4 further combines the improved representation of stand-scale biomass development from ecological theory with a generic description of vegetation dynamics in managed forests to estimate the present-day forest C balance of Europe. In a parallel study, the effect of consistent land-use, climate and atmospheric [CO₂] change scenarios on the terrestrial C budget of the European Union in the 21st century is analysed, considering all major land-use types (Chapter 5). These results are summarised in Section 1.5.

1.5 Results

1.5.1 Parameter-based model uncertainty

Chapter 2 provides an analysis of the uncertainty in model results of the LPJ-DGVM based of uncertainty in the ‘correct’ parameter set to scale mathematical formulations of ecosystem processes. This uncertainty results from uncertainty in (a) the measurement process itself, (b) the scaling of measurements to derive parameters applicable at larger scales, or (c) parameters in semi-empirical process descriptions, which are not readily measurable. The possible parameter spaces for 36 model parameters of LPJ-DGVM are derived from a literature review. Employing a mathematical method (latin-hypercube sampling), these ranges are used to identify parameter importance and assess model uncertainty in a range of experiments, including field measurements of *NPP*, eddy-covariance flux sites, and atmospheric [CO₂] at different monitoring stations across the globe, which have become a standard benchmark for terrestrial biosphere models.

Parameters controlling *NPP* generally have the largest influence on modelled land-atmosphere fluxes, ecosystem C stocks, and also impact substantially on modelled vegetation structure and composition. Some parameters are identified to contribute most to the model error in net C fluxes at a particular site/station, and may thus be constrained from observations. However, the results demonstrate the considerable differences in parameter importance for the model-data agreement across different eddy-covariance sites. A similar result is obtained for the [CO₂] monitoring stations, suggesting that a careful evaluation of the spatial representativeness of the parameter-estimates obtained from data assimilation is needed.

Similar to studies with other terrestrial biosphere models, this study assumes an equilibrium pre-industrial state, implying terrestrial carbon pool sizes and fluxes in balance at the beginning of a transient simulation. Higher annual *NPP* under a particular parameterisation is thus necessarily balanced by higher annual *R_h* in equilibrium. In other words, while modelled present-day *NPP* is relatively uncertain, present-day annual *NBE* estimates of LPJ-DGVM are better constrained. In turn, observations of net C fluxes on local and global scales do not provide a sufficient constraint for modelled annual *GPP*

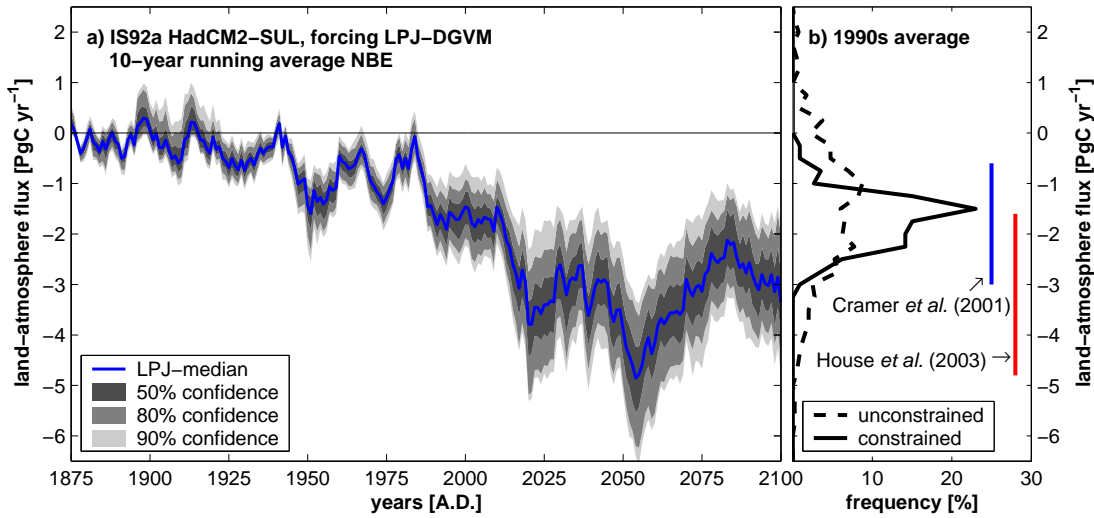


Fig. 1.3: **a)** 10-year running average of the global land-atmosphere flux under the IS92a HadCM2-SUL climate change scenario simulated with LPJ-DGVM [PgC yr^{-1}]. The confidence ranges are based on systematically varying the 14 most important model parameters within their literature range. These results have been constrained from estimates of global A (GPP -leaf respiration), NPP and vegetation C . **b)** Probability distribution function of the mean annual land-atmosphere flux in the 1990s with and without the constraints applied. The range in land-atmosphere flux as simulated by six different DGVMs (blue, Cramer *et al.*, 2001) and the ‘residual’ terrestrial sink (red, House *et al.*, 2003), as inferred from the global carbon budget (see Section 1.3). The latter estimate implicitly includes the effects of N-deposition and land-management that are not considered in the modelling studies.

or NPP in ecosystem models like LPJ-DGVM. As a result, modelled seasonal cycle and interannual variability of NEE at six eddy-covariance sites compare favourably to measurements also under alternative parameterisation. Similarly, seasonal cycle of atmospheric $[\text{CO}_2]$ at a range of different monitoring stations corresponds well to model results despite the parameter-based uncertainty. Persistent model failures that cannot be attributed to parameter-based uncertainty must be the result of a poorly represented or lacking process description in the model. For instance, the time-lag between modelled and observed seasonal cycle at northern $[\text{CO}_2]$ monitoring stations is likely due to snow cover effects on soil thermodynamics, which affect soil respiration and the onset of vegetation growth in spring, that are not represented in the present version of the model (McGuire *et al.*, 2000).

The (parameter-based) uncertainty range in global NPP from one model encompasses the entire uncertainty range obtained from several terrestrial biosphere models (taken as a surrogate for uncertainty in process descriptions; Cramer *et al.*, 1999). Through propagation of uncertainty in NPP , terrestrial C stocks – in particular in soils because of their long turnover time – are the most uncertain model results. Estimates of the ranges of global A (GPP -leaf respiration), NPP and C stored in vegetation are used to constrain the uncertainty in modelled land-atmosphere flux with present-day understanding of the terrestrial biosphere. Application of these benchmarks substantially reduces the spread

of simulated global *NBE* (Fig. 1.3b), hardly affecting the median estimate of the land-atmosphere flux. The reduced range in global *NBE* for the present-day is of a similar magnitude as the uncertainty range resulting from alternative process-formulations in DGVMs (Cramer *et al.*, 2001), and estimates of the ‘residual’ uptake of the terrestrial biosphere (Section 1.3, House *et al.*, 2003, see Fig. 1.3b).

The constrained model is used to assess the effect of parameter-based uncertainty on model projections under climate change. Despite an uncertainty range of about 50% around the median value (90% confidence), interannual, decadal and long-term response of global land-atmosphere fluxes to climate change are fairly robust (Fig. 1.3a). Spatial patterns of change in *NPP* and water-use efficiency are robustly modelled, whereas patterns of change in *NBE* show consistent regional features that are less robust. Present-day uncertainty in mean annual *NBE* derives mainly from uncertainty in global *NPP* because of the proportional response of *NPP* to CO₂-fertilisation. Uncertainty in future land-atmosphere flux is to a much larger extent controlled by the parameterisation of vegetation dynamics and the global average soil C turnover time, and thus soil C stocks.

1.5.2 Age-related decline in forest growth

Various hypotheses have been put forward to explain the observed decline in forest growth with stand age, ranging from increasing autotrophic respiration or nutrient limitation in older stands to hydraulic limitation of photosynthesis in taller trees (Gower *et al.*, 1996; Ryan *et al.*, 1997). The most plausible of these hypothesis, increasing hydraulic resistance with tree height (Ryan and Yoder, 1997), is based on the observation that above-ground plant hydraulic resistance increases with tree height. This theory has been challenged by a theoretical paper of West *et al.* (1999), in which they claim that tapering, the broadening of vessels basipetally, would compensate the effect of increasing path length on plant hydraulic resistance. In Chapter 3, these conflicting hypotheses are reviewed from both theoretical and experimental standpoints. West *et al.*’s conclusions are found to be not convincing. Although tapering may affect hydraulic resistance through increased sapwood conductance, experimental evidence does not suffice to falsify the hydraulic limitation theory. Conversely, evidence supports the idea of increasing leaf-specific aboveground conductance with path-length. Adjustment of plant hydraulic architecture with increasing path length is frequently observed, minimising the direct effect of increased aboveground hydraulic resistance on photosynthesis. However, such an acclimation is an investment of diminishing returns, as carbon resources are allocated away from photosynthetic tissue to supporting tissues, thereby ultimately slowing tree growth.

Alternative hypotheses to predict the age-related decline in forest growth are investigated within LPJ in the first Section of Chapter 4. In particular, a conventional pipe-model type of plant allocation scheme with fixed proportions of leaf area, sapwood cross-sectional area and fine root density (‘size-independent’) is contrasted to a model that allows for changes in these proportions based on changes in the plant hydraulic architecture with

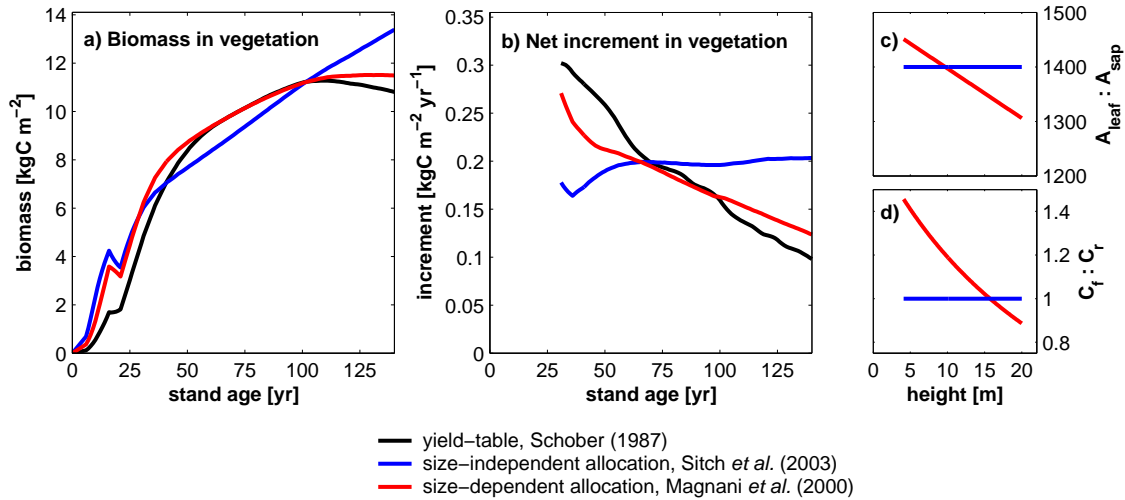


Fig. 1.4: Development of total vegetation carbon [kgC m^{-2}] and net biomass increment [$\text{kgC m}^{-2} \text{yr}^{-1}$] with stand age as predicted from a growth and yield-table (Schober, 1987), and modelled with LPJ using two contrasting hypotheses about the allocation of carbon to plant tissues. **a)** C in vegetation, **b)** net increment, **c)** change in leaf area to sapwood cross-sectional area, as well as **d)** change in leaf to fine root density with tree height. Vegetation biomass is the integral of the net increments minus the biomass removed from thinning (prescribed from the yield-table).

tree height (Magnani *et al.*, 2000, ‘size-dependent’, see Fig. 1.4). Stand-scale predictions of biomass are substantially improved when considering such shifts in plant allocation to compensate for the increased hydraulic resistance with tree height. Nutrient limitation or increased hydraulic limitation of photosynthesis, or alternatively age-dependent tuning factors (as in Waring and McDowell, 2002), are not required to model the age-related decline in forest growth. The subsequent analyses in Section 1.5.3 show that application of this theory provides reasonable estimates of forest growth for different plant functional types, and along larger ecological gradients. However, the applicability of this hypothesis to species other than Scots pine still awaits experimental confirmation.

1.5.3 Evaluation of regional forest growth and carbon balances

In Chapter 4, the improved representation of forest growth rate changes with stand age (Section 1.5.2) is combined with an explicit representation of age-classed, managed forests within the LPJ-framework. The idea behind this is to establish a model that emulates the growth of managed forest stands as observed from yield-tables into a process-based model, but without prescribing the growth rate itself as in Kohlmaier *et al.* (1995) and Häger (1998, see Table 1.2). Instead, gap-model type vegetation dynamics (Prentice *et al.*, 1992; Smith *et al.*, 2001, LPJ-GUESS) are modified to account for the dynamics in even-aged and managed forest stands. The benefits of such an approach are twofold: Firstly, explicit treatment of age-classes allows to evaluate the simulated development of stand biomass with age using biomass estimates obtained from yield-tables and forest inventories, and

not only the average size of the carbon storage in vegetation (as, for instance, in Venevsky, 2001, for LPJ-DGVM and Siberian forests). Secondly, representation of age-classes and forest management allows to force process-based models with historical changes in forest use. Simulated trends in forest vegetation C can thus be evaluated against trends in forest vegetation C stocks as documented in forest statistics (Nabuurs *et al.*, 2003).

The implementation of age-structure in LPJ describes the regional-scale forest structure as composed of even-aged forest stands of different ages for each plant functional type, based on a spatially explicit data-base of present-day forest area and PFT-distribution as well as country-specific information derived from forest statistics. The module is generic, *i.e.* without prescribed management events, and relies only on few, generally available parameters, *e.g.* felling to removal ratio, or total felling intensity. In particular, rotation periods of particular plant functional types are not prescribed but depend dynamically on the landscape level ratio of biomass increment and removals. Feedbacks are considered between management intensity and natural mortality in the stand. Also, landscape-scale disturbance from natural and human-induced fires are taken into account. At present, only even-aged highly productive forests with a long rotation-period (80-150 years) are modelled, but the module is flexible enough to be extended to more complex representation of forest management strategies including ‘coppice with standards’, which are practised in southern Europe, or ‘short-rotation coppice’, which is relevant for estimating bio-fuel production.

Model-based biomass densities for broadleaved and coniferous stands of different age compare favourably with forest inventory based estimates for the dominant tree species in 77 European provinces (average R^2 by province >0.75). Average biomass densities correspond well to forest statistics, with Europe-wide average errors of 2.1 and 3.7 kgC m⁻² for broadleaved and coniferous stands, respectively (expressed as root mean square error, RMSE). Stand biomass is overestimated in older stands for some provinces. Attribution of this model-data disagreement to the failure of the model to correctly simulate either the age-related decline in forest growth, or thinning intensity on a regional scale is hampered by the lack of suitable data to sufficiently constrain either of the two effects. Access to the original forest inventory data, as opposed to the regional-scale statistics based on inventories which are used in this study, for several countries within the EU-funded CarboEurope-IP framework can probably improve this situation. Despite the general agreement, vegetation C is overestimated in boreal regions, probably associated with an overestimation of *NPP* in cold environments. Nevertheless, modelled decline in growth rate with decreasing annual mean temperature agrees well with estimates based on forest inventories of broadleaved and coniferous species. Marked differences between inventoried biomass stocks in different provinces within a particular bioclimatic zone are not modelled adequately by this modified version of LPJ. Most likely, regional differences in soil fertility which are not accounted for in the model, are a major cause of such regional variations in forest growth.

<i>Terrestrial carbon uptake</i>					
	<i>Vegetation</i>	<i>Litter & Soil</i>	<i>Products</i>	<i>Total</i>	<i>Reference area</i>
	[TgC yr ⁻¹]				[10 ⁶ km ²]
LPJ ^a	100.3	7.6	3.2	111.1	1.51
Nabuurs <i>et al.</i> (2003) ^b	98	42	2	142	1.4
Liski and Kauppi (2000) ^b	110				1.76
	<i>Net Ecosystem Exchange</i> [TgC yr ⁻¹]				
LPJ ^a		-190			1.51
Papale and Valentini (2003) ^c		-278			1.51

^a driven with historic climate, atm. [CO₂], forest area and wood demand

^b based on forest statistics

^c derived by scaling annual *NEE* per unit area to the European forest area, as in Janssens *et al.* (2003).

Tab. 1.3: Changes in forest ecosystem C pools and *NEE* ($NEE = R_h - NPP$) of Europe [TgC yr⁻¹] in the 1990s as modelled with the improved version of LPJ, and estimates based on forest inventories and eddy-covariance measurements, respectively.

Based on changes in wood-demand, forest area, climate and atmospheric [CO₂] between 1948 and 2000, the model is able to replicate European scale forest age-structure, absolute level of timber removals, as well as proportion of increment that is removed by harvest in the 1990s. Simulated increases in vegetation C stocks in the 1990s compare favourably with estimates derived from forest statistics (see Table 1.3). This is a marked improvement to the version of LPJ-DGVM presented in Section 1.5.4, which projects much smaller net carbon increases resulting from land-use change (see Section 1.5.5). Average annual *NEE* over the forest area of Europe of -190 TgC yr⁻¹, simulated by the model for the 1990s, compares to an estimate of -278 TgC yr⁻¹ based on the upscaling of eddy-covariance data (see Table 1.3). The data-based estimate is likely to show a larger flux, because the selection of sites is biased towards middle-aged, productive stands, which typically strongly sequester C, whereas the model-based estimate accounts for the entire life-cycle of managed forest stands, with relative contributions of the different age-classes in broad agreement with the actual present-day age-structure of European forests. These comparisons involve a range of uncertainties that are discussed further in Chapter 4. Nevertheless, they do suggest that the C uptake modelled by LPJ is in broad agreement with observations.

More than 50% of the 100 TgC yr⁻¹ uptake of C in forest vegetation in the 1990s is projected to result from historical changes in climate and atmospheric [CO₂]. The remainder is mainly attributed to a shift in the age-structure towards younger stands resulting from a net increase in forest area. Karjalainen *et al.* (1999) suggest that other factors such as tree species selection and N-deposition have contributed substantially to the observed increases in growth. These factors are presently not considered in LPJ. Future work will clarify the relative contribution of the direct effects of N-deposition and improved forest management to the observed increase in forest growth by including these effects into the model.

1.5.4 Analysis of Europe's present-day and future terrestrial carbon balances

In a parallel study to Chapter 4, the joint effects of plausible future land-use and climate change scenarios on the land-atmosphere fluxes over EU* (EU15 plus Norway and Switzerland) are analysed in Chapter 5. Scenarios are based on a detailed interpretation of four illustrative storylines derived from the IPCC Special Report on Emission Scenarios for Europe ('A1F', 'A2', 'B1', 'B2'). Outputs from four different climate models (CGCM2, CSRIO2, HadCM3, PCM2) are used to represent uncertainty in the rate and spatial patterns of climate change. An advanced version of LPJ-DGVM is employed that simulates land-atmosphere C exchanges for different land-use types, including a representation of crop- and grasslands (Bondeau *et al.*, in prep.), as well as the effect of land-use changes on terrestrial C stocks. Changes in land-atmosphere fluxes are evaluated for the historic (1901-2000) and scenario period (2001-2100) in a factorial design to assess the marginal effects of land-use change and climate change. These simulations do not account for the improvements made in Chapters 3 and 4 of this study. The implications of the simpler representation of vegetation dynamics on the terrestrial C balance as opposed to the explicit treatment of forest age-classes are discussed in Section 1.5.5.

Simulated present-day terrestrial vegetation and soil C estimates are in moderate agreement with independent, data-based estimates. Modelled human appropriation accounts for approximately a third of the total *NPP*. Biomass burning contributes only very little to the European scale land-atmosphere C fluxes, despite its importance in the Mediterranean region. Model-based C uptake rates of forests, primarily resulting from forest area increases and growth enhancement from CO₂-fertilisation, are smaller than data-based estimates, and nearly balanced by the C losses from cropland soils. Mean annual net biome exchange in the 1990s is estimated at -5 TgC yr⁻¹, with a range of -105 to +88 TgC yr⁻¹ associated with interannual climate variability. This model-based estimate is considerably smaller than the biospheric uptake of -95 TgC yr⁻¹ obtained from a compilation of different observational data, but still within the uncertainty range of ±154 TgC yr⁻¹ (Janssens *et al.*, 2003).

Impact of climate change and atmospheric [CO₂]: Rising atmospheric [CO₂] under all scenarios leads to enhanced *NPP*, the main cause for the increased biospheric C uptake from 2000 until the 2050s (Fig. 1.5b). Climate change further enhances growth in boreal regions, where the vegetation period becomes longer, however, increasing drought in the Mediterranean limits growth increases in scenarios of the driest climate model (HadCM3). In the second half of the 21st century, increasing soil C losses resulting from rising temperatures counteract these terrestrial carbon gains, leading to widespread net annual C losses, and a decline in cumulative *NBE*, in the boreal region, where all climate models predict the strongest warming. These changes in soil C stocks are in general agreement with predictions from a more sophisticated model of soil C turnover (Smith *et al.*, 2005a,b). Uncertainty in the response of the climate system to a particular emission scenario accu-

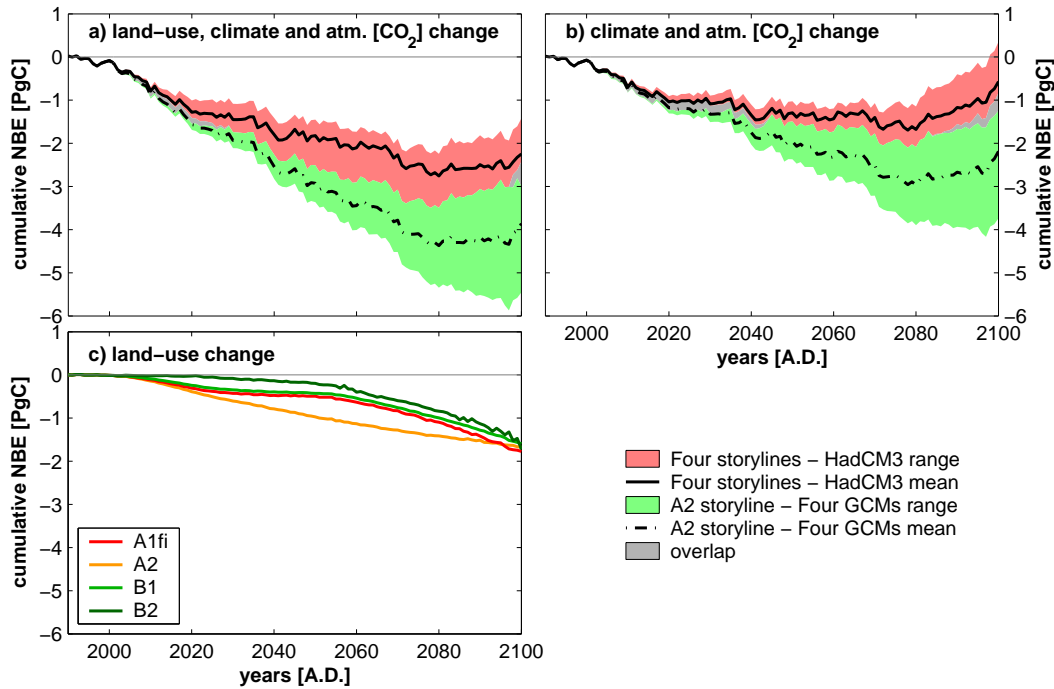


Fig. 1.5: **a)** Cumulative land-atmosphere fluxes [PgC] between 1990 and 2100 for EU* under seven different SRES scenarios of climate and land-use change; split into the components attributable to **b)** climate and atmospheric [CO₂] change, and **c)** land-use change. Displayed are the mean and range of simulation groups based on four different SRES-storylines (‘A1F’, ‘A2’, ‘B1’, ‘B2’) and the HadCM3 GCM, or those based on the ‘A2’ storyline and four different GCMs (HadCM3, CSRIO2, GCGM2, PCM2).

ulates to a ~ 3 PgC difference in cumulative *NBE* by 2100 (Fig. 1.5b). This uncertainty is mainly attributable to different projections of the magnitude in high-latitude warming, and the prevalence of summer drought in the Mediterranean. The climate model related uncertainty is twice as large as the difference in land-atmosphere flux projections under alternative scenario storylines derived from one climate model.

Impact of land-use change: All four land-use change scenarios for Europe foresee a decline in agricultural area, and associated increases in forest and grassland extent. Nonetheless, substantial regional variation exists between these scenarios. Average land-atmosphere fluxes associated with land-use changes across Europe and over the entire scenario period are fairly similar in all scenarios, despite different trajectories (Fig. 1.5c), and of a similar magnitude as the climate change related fluxes. Because of the spatial differences between these scenarios, regional changes in the terrestrial C budget show marked differences under different scenarios. Predicted changes in soil C stock due to land-use change are mainly due to differences in litter fall under different land uses, and in qualitative agreement with the experimental literature (Guo and Gifford, 2002). Uptake in vegetation carbon from land-use changes in these simulations is of a similar magnitude to soil C changes under the ‘A’ scenarios, but twice as large under the ‘B2’ scenario, which envisages the

strongest afforestation. These estimates are qualitatively similar to projections with the forest inventory projection model EFISCEN (Meyer *et al.*, in review, driven with forest growth changes derived from LPJ). However, the magnitude of the C uptake in vegetation is considerably smaller. Section 1.5.5 discusses the potential reasons, and implication on the results obtained in this study.

Combined effects: Average annual C fluxes related to land-use change over the scenario period are equivalent to one fifth of the current EU* Kyoto emission reduction target, a magnitude relevant for mitigation policies. The combined effect of climate, atmospheric [CO₂] and land-use changes on the terrestrial biosphere leads to an average terrestrial carbon uptake rate that compares to 18-68% of the EU* emission reduction target. However, this average terrestrial carbon flux corresponds to only 1-5% of the average EU* CO₂ emission rates over the entire scenario period. Uncertainty in climate change projected from different climate models is the main cause for differences in the simulation results. Nevertheless, the simulations suggest that the terrestrial biosphere will act as a net carbon ‘sink’ during the coming decades under a range of plausible scenarios of climate and land-use change (Fig. 1.5a), although the uptake rate declines and finally turns into a net loss of C under most scenarios in the second half of the 21st century.

1.5.5 Contrasting two alternative formulations of vegetation dynamics and implications for estimates of the terrestrial C balance

Two different formulations of forest vegetation dynamics have been used in Sections 1.5.3 and 1.5.4. One approach describes vegetation as simplified, ageless average over the entire forest area (‘ageless’, Section 1.5.4); the other represents forest area as composed of differently aged stands of even-aged forests (‘age-class’, Section 1.5.3). These approaches differ in the mechanism by which the landscape scale growth rate responds to forest area changes. With the ‘ageless’ approach, increases in forest area decrease stand density and therefore mortality due to self-thinning. Accumulation of biomass is the consequence until self-thinning reaches the level prior to the disturbance. When explicitly accounting for age-classes, *i.e.* with the ‘age-class’ approach, increases in forest area lead to an increased share of younger stands that exhibit a notably larger growth rate than older stands (compare Section 1.5.2).

Figure 1.6 compares the effect of these two alternative approaches on estimates of vegetation C stock changes for the example of the four land-use change scenarios used in Section 1.5.4. These simulations assume constant wood demand and a detrended climatology, *i.e.* excluding any long-term trend in climate or changes in atmospheric [CO₂], to assess the marginal effects of land-use change. Increases in European forest area since the 1950s lead to C uptake in forest vegetation in the 1990s of 6 gC m⁻² yr⁻¹ with the ‘ageless’ approach, but 32 gC m⁻² yr⁻¹ when considering age-classes. Using the ‘age-class’ approach, projected forest age-structure in 2100 differs substantially under the different

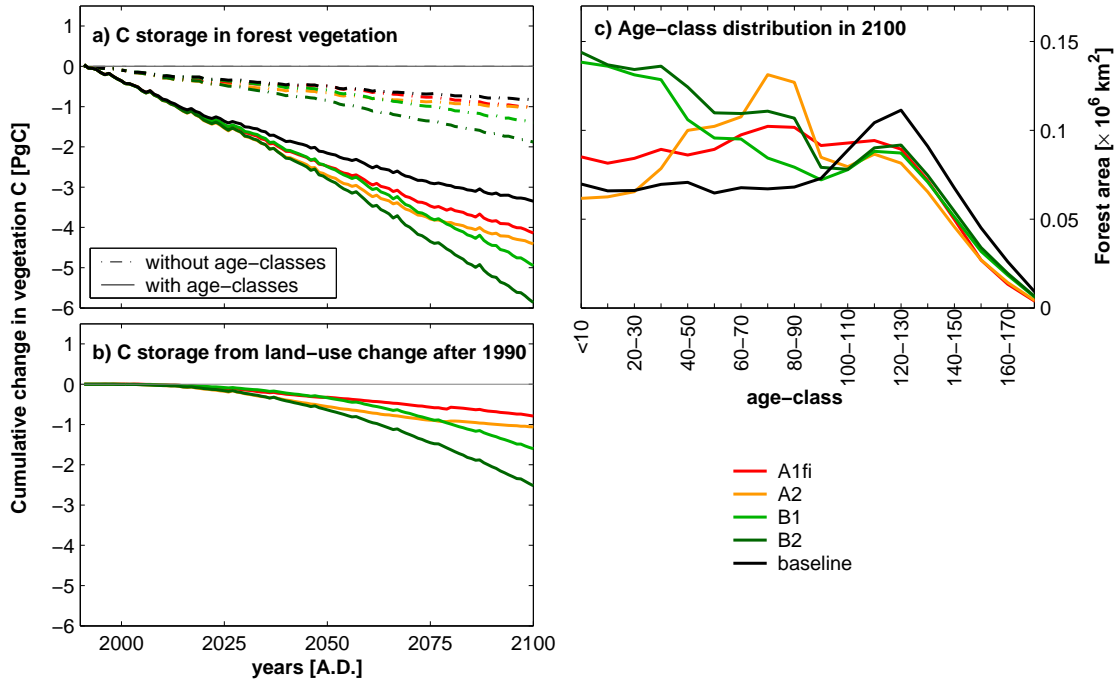


Fig. 1.6: **a)** Cumulative carbon uptake in forest vegetation after 1990 [PgC] with the ‘ageless’ approach as in Chapter 5 (dash-dot) and the ‘age-class’ approach as in Chapter 4 (solid) under the four different land-use change scenarios (but without climate or [CO₂] change). The ‘baseline’ run considers land-use changes until 1990, and constant land-use patterns thereafter. **b)** Net carbon exchange in forest vegetation that is attributed to land-use change after 1990 simulated with the ‘age-class’ approach. **c)** Age-class distribution in 2100 under the four scenarios and the baseline run.

land-use change scenarios (2001–2100, Fig. 1.6c). Consequently, net biomass increments per area average between 20 gC m⁻² yr⁻¹ for the ‘A2’ scenario with the highest average forest age, and 50 gC m⁻² yr⁻¹ for the ‘B2’ scenario with the lowest average age. Changes in average growth rates are much less pronounced using the ‘ageless’ approach. Nevertheless, the proportional differences are more or less maintained (‘A2’: 4 gC m⁻² yr⁻¹, ‘B2’: 16 gC m⁻² yr⁻¹). These results do not affect the qualitative conclusions in Section 1.5.4, but suggest that C sequestration in forest vegetation resulting from land-use change may be underestimated by about 30 TgC yr⁻¹ (Fig. 1.6a). The increased detail in the representation of managed forests (in the ‘age-class’ version) reduces the conceptual difference between the LPJ results of Chapter 5 and projections based on the propagation of present-day forest inventories (Meyer *et al.*, in review) and will allow further evaluation of the difference between model projections. Future work will include an assessment of the effects of climate change and wood demand change on the projected C storage in forest vegetation.

Propagation of present-day age-structure until 2100 without considering future changes in land-use, *i.e.* increases in forest area only until 1990 (thereafter held constant) and wood-demand held constant at 1901 levels, leads to substantial increases in vegetation

C over the 21st century as the result of the past disturbance ('baseline' in Fig. 1.6a,b). These results demonstrate quite clearly that past changes in forest area have substantial impact on the future forest C exchanges (as suggested by Nabuurs, 2004). This has two implications. Firstly, this corroborates results from Kohlmaier *et al.* (1995), who find that land-use history has a strong effect on future C accumulation in forests. Secondly, the long-term effect of the past disturbance contributes substantially to the cumulative carbon uptake between 1991 and 2100 under various land-use scenarios. Only a small fraction of the modelled C sequestration in forest vegetation resulting from land-use change would thus be accountable for emission reductions under Art. 3.4 of the Kyoto protocol for the first commitment period (2008-2012, Fig. 1.6b). Nevertheless, afforestation in the early decades of the 21st century does have a substantial long-term effect on terrestrial C storage (Fig. 1.6b). Changes in wood-demand, species selection or other forest management actions after 1990 that could contribute to the terrestrial C sequestration eligible under the Kyoto protocol, have not been considered in these simulations.

1.6 Discussion

Of the methods available to estimate present-day terrestrial carbon balances, only process-based modelling allows to evaluate the effect of potential future environmental changes. The Chapters of this thesis evaluate the parameter-based uncertainty in model projections, discuss ecological theory relevant for an improved representation of forest growth, and provide a regionalisation of a globally applicable land vegetation model for regional-scale impact assessments in Europe as a highly managed region. These studies aim at assessing the confidence that can be placed into process-based estimates of terrestrial carbon budgets, both for present-day conditions and under a range of potential future scenarios.

Despite the uncertainties that are involved in comparing model results and forest statistics, the comparison suggests that incorporating a stand-scale hypothesis about structural changes in plant allometry leads to improved modelling of forest growth on the regional scale. The evaluation provides some confidence into the modelled growth patterns as well as their response to environmental changes, and thereby demonstrates the usefulness of forest statistics as an additional benchmark for global vegetation models. This benchmark will be useful to evaluate future model developments, including the effect of N-deposition or forest management on forest growth, which likely contribute to changes in European growth rates (Karjalainen *et al.*, 1999; Kellomäki, in prep.). The results of this study are an improvement to earlier studies that have either incorporated forest age dynamics into a global terrestrial biogeochemical model (Häger, 1998), or coupled terrestrial biosphere and forest statistical models offline (Meyer *et al.*, in review). Feedbacks between forest growth and changes in vegetation dynamics due to changed management practices or environmental conditions are explicitly taken into account. Substantial differences in the future C uptake rates projected by 'conventional' terrestrial biosphere models and propa-

gation of forest statistics, as noted in Chapter 5, have been highlighted also from earlier model comparisons (Kramer and Mohren, 2001). The incorporation of forest age-structure into the framework of LPJ has led to simulated uptakes that are better compatible with independent results of a forest statistical model (Meyer *et al.*, in review). The accuracy of the simulations may be further improved by accounting for more regional detail in forest management strategies.

Observations of seasonal and interannual variability of the terrestrial net C fluxes also provide a useful model test, and allow to evaluate the model's response to climate variability (Prentice *et al.*, 2000). Data assimilation of C flux measurements offers some potential in reducing the parameter-based uncertainty in the simulation of this seasonal and interannual variability (as assessed in Chapter 2) by constraining parameters governing short-term ecosystem processes (Knorr and Kattge, in press; Rayner *et al.*, 2005). However, short-term observations of ecosystems provide only insufficient information to reduce uncertainty in the long-term response of the terrestrial biosphere (see Chapter 2). Integration of forest statistics into process-based models, as shown in Chapter 4, aims at an improved representation of the longer-term dynamics in managed forests. The advanced model is also applicable to managed temperate and boreal forests in other continents, because it does not involve specific regional parameterisations of either management of forest growth. It thus provides a framework to integrate process-based understanding of the terrestrial carbon cycle with changes in forest use in the temperate and boreal zone. Such wider analysis may be useful for (a) assimilating historic trends in forest growth into a carbon cycle data assimilation system (Rayner *et al.*, 2005), and (b) analysing the effect of future forest use under different scenarios of land-use and climate change for the entire temperate and boreal zone.

Both European case-studies in this thesis integrate process-based representations of forest and cropland vegetation with a spatially explicit data-base on climate, land use and soils. As such, the study provides an improved assessment of the terrestrial carbon balance on a continental scale in comparison to earlier studies (*e.g.* Kramer and Mohren, 2001; Sykes *et al.*, 2001). Nevertheless, terrestrial C balances in highly managed regions such as Europe are not only the product of present-day land-use distribution, but more importantly their land-use history (Valentini *et al.*, 2000a). The effect of land-use history has been accounted for in terms of land-cover conversions based on country statistics, improving the spatial detail with which these changes are represented in comparison to other studies (McGuire *et al.*, 2001; Cramer *et al.*, 2004). However, these statistics document only net changes, not accounting for the absolute amount of conversions between different land uses within a region. For instance, the deforestation rate of the Netherlands over the last decade is of a similar magnitude as present tropical deforestation, even though the Dutch forest area has slightly increased over the same period of time (Nabuurs, *pers. comm.*). In addition, the extent of past land-use conversions is only poorly known for the period prior to the 1950s, such that considerable uncertainty is inherent in the analysis of

their effect on the terrestrial C balance on a continental scale (House *et al.*, 2003). Nevertheless, the data available are sufficient to adequately model present-day regional-scale forest age-structure, and the associated shifts in forest growth, from past land-use changes.

The effect of past and present land-management practices on terrestrial soil C stocks, resulting from soil degradation for instance due to litter raking and nutrient export, are not assessed in the current study, because knowledge about these processes is only incomplete on the regional scale. In the case of forests, these past land-management practices are the most likely cause for the contemporary increase in soil C stocks (Glatzel, 1999; Schulze *et al.*, 2000). It is thus not surprising that the simulated present-day uptake rates are much lower than these data-based estimates. Recent analyses of the temperature response of soil organic matter decomposition rates indicate that soil organic matter fractions of different lability have similar response rates to increasing temperature (Knorr *et al.*, 2005; Fang *et al.*, 2005). Despite the uncertainty about the current rate of change in soil C stocks, this suggests that the qualitative results on the effect of climate change on soil C stocks – a weakening of the terrestrial carbon uptake – are robust.

Considerable uncertainties in future land-atmosphere flux projections result from differences between climate change scenarios derived from different general circulation models. Similar findings are reported from a global and a tropical study (see Schaphoff *et al.*, in review; Cramer *et al.*, 2004, respectively). Notably, the climate-model related uncertainty is larger than the difference in land-atmosphere flux projections under alternative scenario storylines derived from one particular climate model. Regional details of climate change projections are thus important for the assessment of future changes of the terrestrial C balance, and likely also for assessment of the vulnerability of other terrestrial ecosystem services (Schröter *et al.*, 2004). Despite this uncertainty, qualitative trends, such as the decline in the terrestrial C uptake in the second half of the 21st century due to increasing soil C losses, are similar among different scenarios. These results agree broadly with findings from other models within the EU-funded ATEAM-project, which focused on particular aspects of the terrestrial C cycle, for both vegetation and soil (see Schröter *et al.*, 2004). The general trends are also consistent with findings from earlier global studies (Cox *et al.*, 2000; Cramer *et al.*, 2001; Friedlingstein *et al.*, 2003) performed by a range of different terrestrial biosphere models. Notably, qualitatively similar results on the global scale have been obtained under a range of alternative parameterisations of plant uptake and ecosystem C turnover times in the uncertainty analysis of Chapter 2.

The direct human impact through land-use changes on the terrestrial C balance of Europe, resulting from the projected decline in European agricultural area, may account for one fifth of the EU* Kyoto-emission reduction target (Chapter 5). When the effect of forest age-structure is taken into account, the terrestrial uptake may be even more pronounced (Section 1.5.5), because of the non-linear response of landscape-scale forest growth to changes in the age-structure. The effects of changing forest use on vegetation C stock development have not been addressed in the present study, but are important for the

development of forest resources, as demonstrated in the study of Meyer *et al.* (in review). In addition, increasing average longevity of forest products has not been addressed, but could be analysed with the methods provided in this study. Nevertheless, while the terrestrial C fluxes projected in this study are of a magnitude relevant to climate mitigation strategies under the Kyoto-protocol and beyond, their contribution to the overall C budget of Europe (considering anthropogenic emissions as well as terrestrial fluxes) will likely remain small.

1.7 Conclusions

This study provides an extensive evaluation of model-based estimates of the terrestrial C balance and their uncertainty. Potential future changes in this balance have been investigated using a comprehensive set of climate and land-use change scenarios. The major findings of this study are:

- Parameters controlling plant assimilation rate, plant respiration and plant water balance are the most important sources of uncertainty in simulated *NPP*. Terrestrial C stocks, particularly in soils, are the most uncertain model results through propagation of the uncertainty in *NPP*. Nevertheless, seasonal and interannual variations in land-atmosphere fluxes are relative robust model results of LPJ-DGVM. Within quantifiable uncertainty bounds, robust estimates of future changes in the *NBE* can be obtained from a suitably constrained model. Model robustness, however, must not be understood as certainty. Uncertainty associated with the representation of the relevant processes may be equally important, as demonstrated in the comparison of the effect of two alternative representation of vegetation dynamics.
- Evidence supports the hypothesis that hydraulic path length does affect plant growth. Representation of plant hydraulic architecture and its change with plant size by implementing a hypothesis of hydraulic acclimation with path length allows for a plausible simulation of forest growth changes with age. Results obtained from the application of this theory along environmental gradients, and across different plant functional types are promising. However, these results remain provisional as long as adequate field studies have not been conducted to evaluate the predictions of the hypothesis applied for different plant functional types.
- Simulated terrestrial productivity and vegetation biomass have been assessed by evaluating model-based estimates for different forest age-classes with inventory-based estimates of 77 provinces in Europe. Regional biomass estimates from the improved model correspond well with the data for different plant functional types. Discrepancies remain, most likely related to regional differences in soil fertility that are currently not modelled by LPJ.

- Representation of forest age-classes and management as drivers of forest vegetation C storage reduces the theoretical gap between terrestrial ecosystem models and forest statistics. The advanced model produces realistic estimates of forest age-structure, harvest to removal ratio and net carbon uptake in vegetation on the European scale. Carbon uptake estimates based on forest inventories provide an additional benchmark for simulated growth changes under historic changes in environmental conditions, and will allow to evaluate the effects of future model developments, such as nutrient interactions of the C-cycle and more detailed representation of forest management, on modelled forest growth.
- Land-use and climate changes during the coming decades will substantially impact the terrestrial carbon balance of Europe. Projected terrestrial carbon uptake rates – averaged over the 21st century – correspond to 18-68% of Europe’s present Kyoto emission reduction target. Average carbon sequestration rates over the 21st century, resulting from the projected decline in European agricultural area, may account for at least one fifth of this emission reduction target. When the effect of forest age-structure is taken into account, the terrestrial uptake may be even more pronounced. Increasing soil C losses in a warmer climate will weaken carbon sequestration from land-use activities and increased terrestrial net primary productivity due to increased atmospheric [CO₂] and climate change. Nevertheless, all but one scenario (‘A1fi-HadCM3’) suggest a net terrestrial uptake over the 21st century. Qualitatively, these results are obtained under all scenarios, notwithstanding substantial differences in the magnitude of future land-atmosphere fluxes. The climate model related uncertainty is larger than the difference in land-atmosphere flux projections under alternative scenario storylines derived from one particular climate model. In particular, high-latitude warming and Mediterranean drying differ between the projections of the climate models and are the main cause for these different magnitudes of C fluxes. These results demonstrate that for a comprehensive assessment of the effects of climate change on the terrestrial biosphere, the uncertainty in climate change needs to be taken into account.

In summary, the results show that seasonal, interannual and longer-term variability of the terrestrial carbon balance are consistently modelled under a range of alternative parameter combinations, and provide estimates of the parameter-based uncertainty in simulated fluxes. The study successfully combines process-based modelling with forest statistics to improve process-based estimates of vegetation carbon stocks and their change over time. It is demonstrated that the magnitude of terrestrial carbon fluxes resulting from future land-use and climate changes will likely be of a magnitude relevant to climate mitigation policies. Three different aspects of uncertainty in projections of future terrestrial carbon balances have been addressed separately (uncertainty in model parameters, in the representation of processes, and in the forcing, *i.e.* climate change scenarios). Non-linear interactions between model and climate change uncertainty are still incompletely understood, and an

integrative approach is required to assess the relative importance of these three factors in determining the uncertainty in process-based projections of land-atmosphere fluxes.

Further Research

- Present-day carbon exchanges in Europe are strongly affected by land-use history, which is merely known qualitatively on a continental scale. Better quantification of land-use history, and particular land-management practices, appear most urgent to reduce the apparent disagreement between observations and model simulations, which assume equilibrium at the start of the transient simulation.
- Forest statistics have been integrated into the framework of LPJ-DGVM in this study by better representation of plant physiology and vegetation dynamics. The next steps would be to (a) apply and evaluate the model for other regions in the temperate and boreal zone, and (b) subject the advanced model to a formal constraint process. The carbon cycle data assimilation system (CCDAS, Rayner *et al.*, 2005) already includes different short-term measures of the terrestrial carbon cycle, *e.g.* eddy-covariance and atmospheric [CO₂] data. An additional long-term constraint of the land-atmosphere flux may further improve the confidence in the carbon fluxes modelled with a CCDAS.
- The discrepancy of modelled versus inventoried growth suggests that nutrient limitation needs to be accounted for to accurately model forest growth. Existing physiological knowledge on C-N interactions should be incorporated into the modelling of terrestrial biosphere dynamics.
- Plant hydraulic architecture has been useful in improving the model's performance in terms of biomass development, but also improved representation of plant hydraulics themselves (Hickler *et al.*, 2004). However, open questions remain in the variation of hydraulic properties across different plant functional types, and in particular the variation of the maximum transpiration rate per unit leaf area.
- The advanced representation of forest vegetation dynamics provides a framework for the assessment of socio-economic changes on the forest carbon balance under future environmental conditions. Future work could focus on increasing the detail with which regional differences or tree species are considered to enhance the regional applicability of the model.

1.8 The author's contribution to the individual papers of this thesis

- Paper 1 (Chapter 2): I prepared the literature search for parameters, developed the modelling protocols, and did the relevant coding. I performed the simulations, did the statistical post-processing and interpreted the results. I drafted the several versions of the manuscript. Stephen Sitch and Ben Smith introduced me to the details of process-based modelling of the terrestrial biosphere, and Fred Hattermann to the concept of latin hypercube sampling.
- Paper 2 (Chapter 3): This paper is based on a discussion I had with Colin Prentice in May 2003. I prepared the review, did the mathematical analysis, and formulated the manuscript, to which Colin Prentice and Stephen Sitch contributed in discussions.
- Paper 3 (Chapter 4): I prepared the relevant review of the literature, did the relevant coding, analysed and processed the inventory data, designed and ran the experiments, and interpreted the results. I also drafted the several versions of this manuscript. Colin Prentice and Thomas Hickler contributed to the discussions about plant hydraulic architecture. Jari Liski and Markus Erhard were involved in the development of the yield-table and the inventory data comparison. Stephen Sitch guided the whole process.
- Paper 4 (Chapter 5): I developed the land-use interface, as well as the land-use change and forest management part of the code. Markus Erhard and I pre-processed the relevant input data. I constructed the historical land-use data set, performed the simulations, interpreted the results and drafted the manuscript. The overall task for this manuscript was defined by the ATEAM project (Advanced Terrestrial Ecosystem Assessment and Modelling). The modelling protocol was set up by myself after discussions with Martin Sykes and Colin Prentice. Alberte Bondeau and Pascale Smith prepared the cropland code of LPJ.

2. EFFECTS OF PARAMETER UNCERTAINTIES ON THE MODELLING OF TERRESTRIAL BIOSPHERE DYNAMICS

Sönke Zaehle* Stephen Sitch*[†] Benjamin Smith [‡] Fred Hattermann*

As if someone were to buy several copies of the morning newspaper to ensure himself that what was said was true.

(L. Wittgenstein)

An edited version of this manuscript is published (American Geophysical Union, 2005) as Zaehle, S., Sitch, S., Smith, B., Hattermann, F. Effects of parameter uncertainties on the modelling of terrestrial biosphere dynamics, *Global Biogeochemical Cycles*, in press
Reproduced with permission of the American Geophysical Union, not subject to US copyright.

Abstract

Dynamic global vegetation models (DGVMs) have been shown to broadly reproduce seasonal and interannual patterns of carbon exchange, as well as realistic vegetation dynamics. To assess the uncertainties in these results associated with model parameterisation the Lund-Potsdam-Jena-DGVM (LPJ-DGVM) is analysed in terms of model robustness and key sensitive parameters. Present-day global land-atmosphere carbon fluxes are relatively well constrained, despite considerable uncertainty in global net primary production mainly propagating from uncertainty in parameters controlling assimilation rate, plant respiration and plant water balance. In response to climate change, water-use efficiency driven increases in net carbon assimilation by plants, transient changes in vegetation composition and global warming effects on soil organic matter dynamics are robust model results. As a consequence, long-term trends in land-atmosphere fluxes are consistently modelled despite an uncertainty range of $-3.35 \pm 1.45 \text{ PgC yr}^{-1}$ at the end of the 21st century for the specific scenario used.

Keywords: LPJ-DGVM, sensitivity analysis, parameter-based uncertainty, terrestrial carbon cycle, vegetation structure.

*Potsdam Institute for Climate Impact Research (PIK), e.V., Telegrafenberg, PO Box 601203, D-14412 Potsdam, Germany

[†]present address: Met Office (JCHMR), Crowmarsh-Gifford, Wallingford, OX10 8BB, U.K.

[‡]Geobiosphere Science Centre, Physical Geography and Ecosystems Analysis, Lund University, Sölvegatan 12, S-22362 Lund, Sweden

2.1 Introduction

The terrestrial biosphere plays an important role in regulating the increase of atmospheric CO₂ (Prentice *et al.*, 2000). Process-based models of terrestrial biogeochemical cycles (TBMs) have been successfully used to explain a large proportion of the interannual variation in the CO₂ growth rate (Kindermann *et al.*, 1996; Dargaville *et al.*, 2002). TBMs, and dynamic global vegetation models (DGVMs), which further couple terrestrial biogeochemistry to vegetation dynamics, are important tools to investigate the net effect of the complex feedback loops in the global carbon cycle in response to changing environmental forcing such as climate change (Houghton *et al.*, 2001). Inter-model comparison studies (Melillo *et al.*, 1995; Heimann *et al.*, 1998; Kicklighter *et al.*, 1999; Cramer *et al.*, 1999, 2001) and recent applications of TBMs in coupled earth-system models (Friedlingstein *et al.*, 2003; Jones *et al.*, 2003) have shown that large uncertainty in the response of the global carbon cycle to future climate warming arises as a result of the typical behaviour of the particular model used to simulate vegetation changes. Since future projections of atmospheric CO₂ content depend on plausible estimation of the processes governing global carbon exchange, an assessment of the uncertainty associated with these terrestrial ecosystem models is essential to identify key model strengths and deficiencies.

Uncertainty in model simulations can arise from both uncertainty as to the correct (mathematical) description of mechanisms driving ecosystem processes, and from uncertainty in the parameter set to scale mathematical formulations of these processes. Process-based uncertainty can, to some extent, be addressed by inter-model comparison or studies testing different process formulations in one modelling framework (*e.g.* Joos *et al.*, 2001; Knorr and Heimann, 2001a; Smith *et al.*, 2001). Parameter-based uncertainty can result from (a) uncertainty in the measurements used to parameterize a model, (b) the method used to scale, for example, point measurements to the larger scale on which a model operates, as well as (c) the parameterisation of semi-empirical process descriptions, for which parameter values are not readily measurable. Only few studies have so far analysed the effects of propagating parameter uncertainty in global vegetation models. Most of these studies have used a local design, *i.e.* changed one parameter at a time within a given range around the standard value (*e.g.* Knorr, 2000; Knorr and Heimann, 2001a; Maayar *et al.*, 2002), or used minimum and maximum values from the literature (Hallgren and Pitman, 2000). Although these approaches are able to identify main effects of parameters (Kleijnen, 1998), they neglect possible interactions between different parameters, which are important in complex ecosystem models (Saltelli *et al.*, 2000). Factorial designs (*e.g.* White *et al.*, 2000a) that allow the assessment of such interactive effects require many model runs and are therefore prohibitive for complex models with a large number of parameters and a high computational demand (Campolongo *et al.*, 2000). Recently, adjoint methods have been used to infer optimal parameter combinations in terrestrial biosphere models from observations, as well as to gain insight into parameter sensitivities and the uncertainty in output variables (Wang *et al.*, 2001; Barrett, 2002; Randerson *et al.*, 2002;

Rayner *et al.*, 2005).

We adopt a Monte Carlo-type stratified sampling approach (latin hypercube sampling, LHS, McKay *et al.*, 1979) as an efficient method to identify functionally important parameters and simultaneously estimate the uncertainty range of the modelled results. Like other probability-based methods, LHS allows interactions between different parameter combinations to be studied, and can identify the contributions of parameters alone and in combination to the uncertainty of the modelled results. LHS has previously been used to construct a reduced form of a land surface model for sensitivity tests (Beringer *et al.*, 2002), and has been shown to provide reliable estimates of the distribution function of model output variables (Helton and Davis, 2000).

Dynamic global vegetation models are fairly general, globally parameterised models, describing vegetation in terms of plant functional types (PFTs), and its response to variation in climate, atmospheric CO₂ and soil properties (Steffen *et al.*, 1996; Cramer *et al.*, 2001). They incorporate more or less mechanistic formulations of physiological, biophysical and biogeochemical ecosystem processes (*e.g.* canopy biophysics, vegetation physiology, phenology, and ecosystem carbon (C) and water (H₂O) cycling) coupled to a description of the major processes governing changes of vegetation structure and composition (Cramer *et al.*, 2001). Although DGVMs differ in the detail with which particular processes or scales are represented, they tend to follow a similar structure and share a largely common base of process descriptions and parameters, *e.g.* with respect to canopy energy balance, photosynthesis, water balance, respiratory processes, carbon allocation and turnover within the plant, litter and soil organic matter (SOM) decomposition, and plant mortality and establishment (Woodward *et al.*, 1995; Foley *et al.*, 1996; Friend *et al.*, 1997; Daly *et al.*, 2000; Sitch *et al.*, 2003).

In this study, we use the Lund-Potsdam-Jena model (LPJ-DGVM, Smith *et al.*, 2001; Sitch *et al.*, 2003), which is typical of DGVMs as a family of models, both with respect to its representation of structural ecosystem components (plants and soil) and ecosystem processes. LPJ-DGVM has been used recently to study the sensitivity of equilibrium C storage to climate and atmospheric CO₂ (Gerber *et al.*, 2004) and to assess the uncertainty in simulations of the future terrestrial C balance with respect to both different formulations of ecosystem processes in a DGVM inter-comparison study (Cramer *et al.*, 2001) and different climate change projections from several global circulation models driven with the same radiative forcing (Schaphoff *et al.*, in review).

The aim of this paper is to systematically analyse the sensitivity of LPJ-DGVM, as a representative DGVM, to its parameterisation, and to evaluate the resulting uncertainty in model outcomes both for current and potential future climatic conditions. We examine the relative importance of different parameters for determining specific model results, and analyse the effects of parameter-based uncertainty on modelling terrestrial biosphere dynamics. We also explore possibilities to constrain model uncertainty using independent observations. To facilitate comparison to previously published studies using LPJ-DGVM

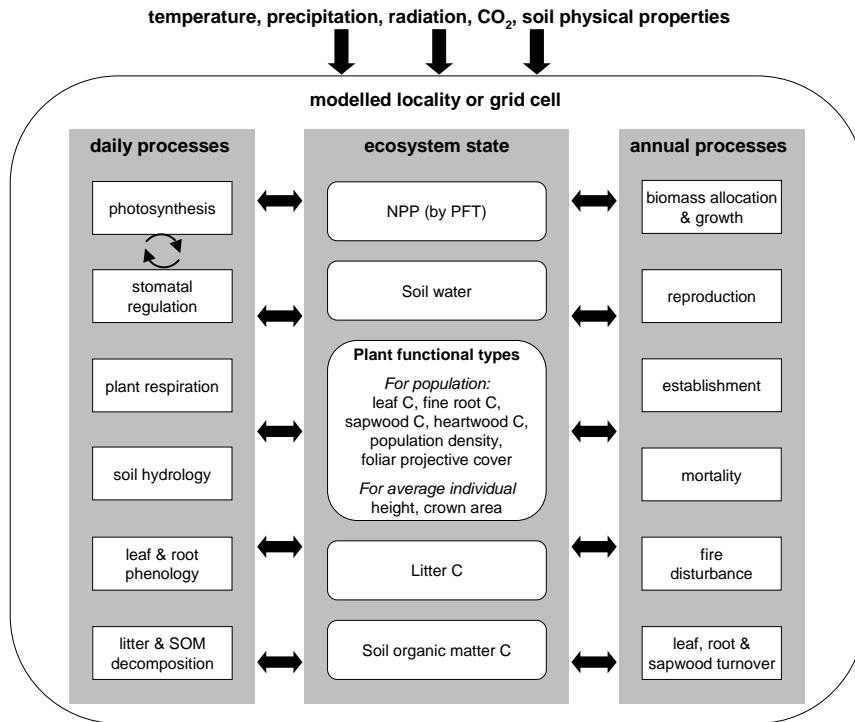


Fig. 2.1: The main processes, state variables and driving data for the model LPJ-DGVM (Sitch *et al.*, 2003). Other dynamic global vegetation models (DGVMs) generally have a similar structure.

we repeat the simulation experiment of the IGBP DGVM inter-comparison study (Cramer *et al.*, 2001) using climate data from HadCM2-SUL (Mitchell *et al.*, 1995; Johns *et al.*, 1997) forced by the IS92a emission scenario (Houghton *et al.*, 1992). We assume that many of our conclusions in terms of the importance of certain groups of parameters, or their functional equivalents in alternative process formulations, would be similar for DGVMs and similar ecosystem models other than LPJ-DGVM.

2.2 Methods

2.2.1 LPJ-DGVM

LPJ-DGVM (Smith *et al.*, 2001; Sitch *et al.*, 2003) is one of a family of models derived from BIOME (Prentice *et al.*, 1992). The model simulates distribution and dynamics of 10 plant functional types (PFTs) with different photosynthetic (C3, C4), phenological (deciduous, evergreen), and physiognomic (tree, grass) attributes, based on bioclimatic limits for plant growth and regeneration, and PFT-specific parameters that govern plant competition for light and water.

Photosynthesis is calculated as a function of absorbed photosynthetically active ra-

diation (PAR), temperature, atmospheric CO₂ concentration, day length, and canopy conductance using a form of the Farquhar scheme (Farquhar *et al.*, 1980; Collatz *et al.*, 1992) with canopy-level optimised nitrogen allocation (Haxeltine and Prentice, 1996a) and an empirical convective boundary layer (Monteith, 1995) to couple the C and H₂O cycles. Soil hydrology is simulated using two soil layers (Haxeltine and Prentice, 1996b).

Annual net primary production (*NPP*) is allocated to the four C pools (leaves, sapwood, heartwood, and fine-roots) of each PFT population on the basis of allometric relationships linking height, diameter and the leaf-area to sapwood-area ratio to the size of these pools (Shinozaki *et al.*, 1964a; Huang *et al.*, 1992). Litter fall from vegetation enters separate above- and below-ground litter pools, which in turn provide input to a fast and a slow decomposing soil C pool. Decomposition rates of soil and below-ground litter organic C depend on soil temperature (Lloyd and Taylor, 1994) and soil moisture (Foley, 1995). Fire fluxes are calculated based on litter moisture content, a fuel-load threshold, and PFT-specific fire resistances (Thonicke *et al.*, 2001). Vegetation dynamics are modelled based on light competition, resource stress mortality, fire disturbance, re-establishment rates, and a set of temperature-related limits to survival or establishment (Sitch *et al.*, 2003). Monthly net ecosystem C exchange (*NEE*), which represents the C balance at a point scale, is the difference between predicted heterotrophic respiration (R_h) and *NPP* for each grid cell, *i.e.*

$$NEE = R_h - NPP \quad (2.1)$$

where negative fluxes denote a net C flux from the atmosphere to the terrestrial biosphere. Annual land-atmosphere flux (the so called net biome exchange, *NBE*), which represents the landscape-scale C balance, is calculated as the sum of the monthly *NEEs* over the year plus annual C lost from biomass burning for each grid cell, *i.e.*

$$NBE = NEE + BiomassBurning \quad (2.2)$$

This study uses the LPJ-DGVM version as described in Sitch *et al.* (2003), with modifications by Gerten *et al.* (2004), and the dark respiration formulation as in Haxeltine and Prentice (1996b). In order to ensure comparability with previous studies using LPJ-DGVM, including Cramer *et al.* (2001), stochastic disaggregation of monthly precipitation to daily values, as implemented by Gerten *et al.* (2004), was not applied in the present study. Instead, precipitation data were – like the other climate variables – interpolated linearly to daily values.

2.2.2 Parameter values and sampling procedure

Estimates of the ranges of 36 model parameters were, where possible, obtained from an extensive search of the ecological literature to provide a comprehensive overview of the parameter uncertainty (Table 2.1). For all parameters except leaf longevity the probability density function (PDF) was assumed to be uniform. For leaf longevity a triangular

distribution was chosen based on data presented by Reich *et al.* (1992). Following Sitch *et al.* (2003), root turnover time was assumed to be inversely related to leaf longevity. The choice of the parameter-PDF does not influence the ranking of individual parameters in terms of their importance, but could affect the PDF of the modelled output variables. In the case of parameters for which values differ between the different PFTs (*i.e.* for a_{leaf} , g_{min} , int_{loss} , r_{maint} , r_{fire} , and m_e , see Table 2.1), proportional differences between the PFT-specific values were conserved when the overall level was adjusted.

Latin hypercube sampling (McKay *et al.*, 1979, see Appendix 2.6) was employed to generate a stratified sample of random sets of parameter values. Unless otherwise stated, parameters were assumed not to be correlated. The stability of the results obtained with LHS needs to be tested for each application (Helton and Davis, 2000). LHS samples with differing sample sizes ($n=30-10000$) were generated to assess, for a representative set of cells and for each model output variable, the degree of convergence to a stable PDF. Three independently-generated LHS samples with $n=1000$ were also produced to assess the stability of the PDFs obtained using different random number sequences. These analyses indicated that for 36 (14) parameters under consideration, a sample size of 1000 (400) sets was sufficient to generate, for each model output variable, a reliable estimate of the mean, standard deviation, 90% confidence interval, and ranking of the parameter importance (*results not shown*). The choice of the random number seed required to create LHS samples had only a very minor influence on the results.

2.2.3 Data-sets

Fields of mean temperature, precipitation and cloudiness (1901-2000) were taken from the CRU2000 monthly climate dataset on a $0.5^\circ \times 0.5^\circ$ global grid, provided by the Climate Research Unit (CRU, Mitchell *et al.*, 2004). Data on the annual CO_2 content of the atmosphere were obtained from Keeling and Whorf (2003). Time-series of monthly temperature, precipitation and PAR were obtained for six sites of the EUROFLUX network, *i.e.* those for which more than 3 years' measurements were available (Valentini *et al.*, 2000a). Soil texture data were based on the FAO soil data set (FAO, 1991; Zobler, 1986; Haxeltine and Prentice, 1996b). The response of the terrestrial biosphere to climate change was simulated using monthly climate data (1861-2100) on a $3.75^\circ \times 2.5^\circ$ grid, derived from HadCM2-SUL (Mitchell *et al.*, 1995; Johns *et al.*, 1997) forced by CO_2 concentrations corresponding to the IPCC IS92a scenario (Houghton *et al.*, 1992), as used in Cramer *et al.* (2001).

An assessment of the uncertainty in model results requires some understanding of the typical variation of the considered variables in reality. Spatially referenced data useable for the evaluation of global vegetation models are still very sparse (Cramer *et al.*, 1999; Scurlock *et al.*, 1999). We evaluated model performance against *NPP* data from the Ecosystem Model Data Inter-comparison project (EMDI) for 81 sites from the class A data set (Olson *et al.*, 2001) that include measurements for all major biomes. Seasonality

Tab. 2.1: Key LPJ-DGVM parameters: Standard value, literature range, parameter description and literature sources. Equation numbers refer to the equations in Sitch *et al.* (2003). For parameters, for which no literature source is given, value ranges were estimated. Nomenclature of the plant functional types (PFTs): TrBE: tropical broadleaved evergreen, TrBR: tropical broadleaved rain green, TeNE: temperate needle-leaved evergreen, TeBE: temperate broadleaved evergreen, TeBS: temperate broadleaved summer green, BNE: boreal needle-leaved evergreen, BNS: boreal needle-leaved summer green, BBS: boreal broadleaved summer green, TeH: temperate herbaceous, TrH: tropical herbaceous. Parameters marked with * belong to the reduced set of 14 parameters (see Section 2.2.4).

<i>Parameter</i>	<i>Standard value</i>	<i>Minimum value</i>	<i>Maximum value</i>	<i>Description</i>	<i>Reference</i>	
<i>Photosynthesis</i>	θ^*	0.7	0.2	0.996	Co-limitation shape parameter; eq. 14	Leverenz (1988); Collatz <i>et al.</i> (1990)
	k_{beer}^*	0.5	0.4	0.7	Extinction coefficient; eq. 7	Larcher (1995)
	α_a^*	0.4	0.3	0.7	Scaling parameter (leaf to canopy)	Haxeltine and Prentice (1996a)
	$\lambda_{\text{max,C3}}$	0.8	0.6	0.8	Optimal c_i/c_a for C3 plants (all PFTs except TrH)	Haxeltine and Prentice (1996a)
	α_{C3}^*	0.08	0.02	0.125	Intrinsic quantum efficiency of CO ₂ uptake in C3 plants	c.f. Hallgren and Pitman (2000)
	a_{C3}^*	0.015	0.01	0.021	Leaf respiration as a fraction of Rubisco capacity in C3 plants	estimated from Farquhar <i>et al.</i> (1980)
	$\lambda_{\text{max,C4}}$	0.4	0.31	0.4	Optimal c_i/c_a for TrH	Collatz <i>et al.</i> (1992)
	α_{C4}	0.053	0.3	0.054	Intrinsic quantum efficiency of CO ₂ uptake in C4 plants	Ehleringer and Bjorkman (1977); Collatz <i>et al.</i> (1992)
	a_{C4}	0.035	0.0205	0.0495	Leaf respiration as a fraction of Rubisco capacity in C4 plants	Collatz <i>et al.</i> (1992)
	<i>Respiration</i>	r_{maint}	0.0495 (0.008)	0.066 (0.011)	0.0825 (0.013)	Tissue respiration rate at 10°C (gC gN ⁻¹ d ⁻¹) (value for TrBE TrBR); eq. 22
r_{growth}^*		0.25	0.15	0.4	Growth respiration per unit <i>NPP</i> ; eq. 25	Sprugel <i>et al.</i> (1996)
e_a		308.56	275	325	Activation energy for respiration; eq. 23	estimated from Lloyd and Taylor (1994)
<i>Hydrology</i>	z_1	0.667	0.5	0.9	fraction of fine roots in upper soil layer (trees)	Jackson <i>et al.</i> (1996)
	E_{max}	5.0	2.4	6.2	Maximum daily transpiration rate (mm d ⁻¹)	Steward and Gay (1989); Whitehead <i>et al.</i> (1993)
	g_m^*	5.0	2.5	18.5	Maximum canopy conductance analogue (mm d ⁻¹)	Magnani <i>et al.</i> (1998)

Tab. 2.1: Continued.

<i>Parameter</i>	<i>Standard value</i>	<i>Minimum value</i>	<i>Maximum value</i>	<i>Description</i>	<i>Reference</i>	
<i>Hydrology</i>	g_{\min}	0.3/0.5	0.22/0.42	0.38/0.58	Minimum canopy conductance (mm d^{-1})	Körner (1994)
	α_m	1.4	1.1	1.5	Empirical evapotranspiration parameter	Monteith (1995)
	$loss_{\text{int}}$	0.2/0.6	0.15/0.45	0.25/0.75	Interception loss parameter (herbaceous/tree PFTs)	Kergoat (1998)
<i>Allometry</i>	k_{allom1}	100	75	125	$\text{crownarea} = k_{\text{allom1}} * \text{height}^{**} k_{\text{rp}}$; eq.4	Huang <i>et al.</i> (1992) Huang <i>et al.</i> (1992) Waring <i>et al.</i> (1982) Zeide (1993); Enquist and Niklas (2002)
	k_{allom2}	40	30	50	$\text{height} = k_{\text{allom2}} * \text{diameter}^{**} k_{\text{allom3}}$; eq.3	
	k_{allom3}	0.5	0.5	0.8	$\text{height} = k_{\text{allom2}} * \text{diameter}^{**} k_{\text{allom3}}$; eq.3	
	$k_{\text{la:sa}}^*$	8000	2000	8000	leaf-to-sapwood area ratio; eq. 1	
	k_{rp}	1.6	1.33	1.6	$\text{crownarea} = k_{\text{allom1}} * \text{height}^{**} k_{\text{rp}}$; eq.4	
	CA_{max}	15.0	7.5	30	Maximum woody PFT crown area	
<i>Vegetation dynamics</i>	k_{mort1}^*	0.01	0.005	0.1	Asymptotic maximum mortality rate (yr^{-1}); eq. 32	
	k_{mort2}	35	20	50	growth efficiency mortality scalar; eq. 32	
	est_{max}^*	0.24	0.05	0.48	Maximum sapling establishment rate ($\text{m}^{-2} \text{yr}^{-1}$); eq. 41	
<i>Fire dynamics</i>	r_{fire}	0.12/0.5/1.0	-10%	+10%	Fire resistance Tree PFTs / TrBR,TeBE / herbaceous	
	m_e	0.3 (0.2)	0.0225 (0.15)	0.375 (0.25)	Litter moisture of extinction (herbaceous PFTs)	
	$fuel_{\min}$	0.2	0.01	0.4	Minimum fuel load for fire spread	
<i>PFT characteristics</i>	f_{sapwood}^*	0.05	0.01	0.2	sapwood turnover rate (yr^{-1})	Bartelink (1998)
	a_{leaf}	0.5/1.0/2.0	0.11	8.0	leaf longevity (yr) (herbaceous and deciduous/broadleaved evergreen/needleleaved PFTs)	Reich <i>et al.</i> (1992)
	$dens_{\text{wood}}$	200	180	220	specific wood density (kgC m^{-3})	
<i>Soil organic matter pools</i>	τ_{litter}^*	2.85	1.23	5.26	litter turnover time at 10°C	Meentemeyer (1978)
	f_{air}^*	0.7	0.5	0.9	fraction of the decomposed litter emitted as CO_2 to the atmosphere	Jenkinson (1990)
	f_{inter}^*	0.985	0.85	0.99	fraction of soil-bound decomposed litter entering the intermediate soil pool	Foley (1995)

<i>Section</i>	<i>Number of Parameters</i>	<i>Number of LHS-samples</i>	<i>Spatial coverage and resolution</i>	<i>Output Variable</i>
2.3.1	36	1000	81 EMDI class A sites	(R)PCC for several model output variables
2.3.2	14	400 ^{a,b,c}	global 3.25° × 2.5° HadCM2-SUL	<i>A</i> , <i>NPP</i> , vegetation <i>C</i>
2.3.3	14	400 ^c	81 EMDI class A sites	<i>NPP</i>
2.3.3	14	400 ^c	6 EUROFLUX sites	<i>NEE</i> ^d
2.3.3	14	400 ^c	global 3.0° × 3.0° CRU2000	seasonal cycle of CO ₂ ^e
2.3.3	14	400 ^c	global 3.25° × 2.5°	<i>NBE</i> , ecosystem <i>C</i> pools,
2.3.4			HadCM2-SUL	vegetation structure

^a 400 LHS samples for 14 completely uncorrelated parameters.

^b 400 LHS samples as above, but with correlation between α_{C3} and α_a (R^2 : 0.8), as well as α_{C3} and k_{beer} (R^2 : 0.7).

^c 400 LHS samples as in ^b, used for the calculation of RPCCs, however, for all figures, and output variable ranges, only those of the 400 runs were used that conformed to the benchmarks in Section 2.3.2.

^d simulations without fire.

^e using TM2 for atmospheric transport.

Tab. 2.2: Overview over the experimental setup used in this study, as described in Section 2.2.4.

of net C fluxes was compared to (a) point-scale measurements of *NEE* obtained with eddy-covariance techniques at six sites of the EUROFLUX network (Valentini *et al.*, 2000a) and (b) the seasonal cycle of CO₂ observed at 27 monitoring stations from a program of the National Oceanographic and Atmospheric Administration (GLOBALVIEW-CO₂, 1999).

2.2.4 Modelling protocol

For each LHS set the model was run for a “spin-up” period of 900 years to achieve equilibrium in terms of pre-industrial stable vegetation structure and C pools. During the spin-up phase 30 years of varying climate from the beginning of the respective climate dataset were repeated continuously with pre-industrial atmospheric CO₂ content. The model was thereafter driven with the transient climatology and observed atmospheric CO₂ content. Table 2.2 summarises the experimental setup of this study.

Running LPJ-DGVM several hundred times for the entire globe at 0.5° resolution is computationally not feasible. In order to assess the parameter-based uncertainty on the global scale, we attempted to identify the most important parameters contributing to overall model uncertainty, and performed a global-scale uncertainty analysis with this reduced set. Parameter importance for all 36 parameters was determined at a set of locations spanning all major biomes and corresponding to EMDI class A sites. 30-year average values (1961-1990) of each model output variable were used to analyse the parameter importance (Section 2.3.1). Fourteen parameters could be identified as having the greatest influence on the ecosystem carbon cycling (Section 2.3.2 absolute ranked partial correlation coefficient, $|\text{RPCC}| > 0.25$, see Appendix) as well as being of substantial importance in modelling vegetation dynamics and terrestrial water balance. We chose $|\text{RPCC}| = 0.25$

as a lower threshold for parameter importance because visual inspection of correlation plots between parameter and model output did not show any notable trend for RPCCs below this value. By using this reduced set of 14 parameters, we could reduce the numbers of required runs to a practically attainable level of 400, while still accounting for most of the model uncertainty.

CRU2000 monthly climate data were used to estimate 30-year average *NPP* (1961-1990) for 81 EMDI sites (Section 2.3.3). Site-specific regressions between measured meteorology and the nearest grid cell from the CRU climatology for each of the six EUROFLUX sites were used for the spin-up and in the transient run up to the period for which site-specific meteorological data were available; site-specific data were used where possible (Section 2.3.3). For consistency in the comparison to eddy-covariance measurements, fire disturbance was not included in the simulations performed for this comparison. Site history may influence the magnitude and sign of the annual C exchange (Thornton *et al.*, 2002), but we did not find any notable effect on the modelled seasonal cycle (Stephen Sitch, *unpublished results*), consistent with recent findings from flux measurements (Kolari *et al.*, 2004). Global fields of averaged and detrended monthly *NEE* for the period 1983-1992 were obtained using CRU2000 monthly climatology aggregated to $3.0^\circ \times 3.0^\circ$ resolution (Section 2.3.3). This is the highest resolution possible given the computational constraints associated with performing 400 global simulations. These data were passed into a reduced-form version of the atmospheric transport model TM2 (Heimann *et al.*, 1998; Kaminski *et al.*, 1999a,b). Modelled seasonal cycles were compared to the global network of atmospheric CO₂ monitoring sites, following the approach of Heimann *et al.* (1998). Global C cycle simulations for 1861-2100 were performed with the HadCM2-SUL climate data at $3.75^\circ \times 2.5^\circ$ resolution (Cramer *et al.*, 2001, Sections 2.3.3 and 2.3.4). No notable differences in terms of global *A* (gross primary production, *GPP*, minus leaf respiration, *R_l*), *NPP* and ecosystem C pools were observed between simulations using climatologies at 0.5° and 3.0° or climate model resolution under the standard parameterisation. Also the seasonal cycle of CO₂ at all 27 stations was very similar between simulations using climatologies at 0.5° and 3.0° resolution.

2.2.5 Parameter constraints and global benchmarking

The parameters scaling various ecosystem processes are likely to be interdependent to a greater or lesser extent, for example because of the existence of syndromes of structural and functional characteristics, such as plant life history strategies. In our analyses, we varied parameters within their literature range without assuming any interdependence. This might cause overestimation of uncertainty, and thereby unjustifiably reduce confidence in model results (Helton and Davis, 2000). Inverse methods have been recommended as an approach to constrain model uncertainty and to infer parameter correlations (Kaminski *et al.*, 2002; Rayner *et al.*, 2005). However, such methods are beyond the scope of this paper.

To limit the overestimation of uncertainty due to parameter interdependence, a simpler approach – taking advantage of existing knowledge of the terrestrial biosphere – is to evaluate model performance against generally agreed benchmarks of the contemporary carbon cycle. If the model in its standard parameterisation produces output that conforms to the benchmarks, the failure to meet the benchmarks in a particular run may be the consequence of unrealistic or implausible *combinations* of particular parameters, even if each individual parameter range may be justified based on literature values. Correlations between these parameters can then be prescribed to avoid these combinations, while still sampling parameter values uniformly across the each parameter range (Iman and Conover, 1982).

In our study, we identified one such set of parameters (Section 2.3.2). Expert judgment would have allowed further exclusion of parameter combinations that produce unrealistic results for particular geographical regions or biomes. In the interest of objectivity, however, we employed the same parameter space globally. We choose to consider only those runs, which satisfy generally agreed global benchmarks of both global production and vegetation C for the assessment of uncertainty in *other* model outcomes, and in particular the uncertainty under climate change scenarios (Sections 2.3.3 and 2.3.4). Net assimilation rate A in the range of 90-160 PgC yr⁻¹, NPP in the range of 45-85 PgC yr⁻¹ and vegetation C in the range of 500-1200 PgC were taken as parameter constraints. The benchmarks were based on top-down studies of the global C cycle (Knorr and Heimann, 1995; Ciais *et al.*, 1997a) and estimates of various process-based models of potential natural vegetation (Houghton and Skole, 1990; Post *et al.*, 1997; Cramer *et al.*, 1999; Gerber *et al.*, 2004). A similar approach has been applied in a comparable study on climate model uncertainty (Knutti *et al.*, 2002).

2.3 Results

2.3.1 Parameter importance

The most important parameters controlling NPP are the intrinsic quantum efficiency for C3 plants α_{C3} (RPCC= 0.85), which influences the amount of energy available for GPP , and the parameter α_a (RPCC= 0.70), which primarily accounts for PAR absorbed by non-photosynthetic structures (*e.g.* branches) and thus lost to canopy photosynthesis (Table 2.3). Of secondary importance are the shape parameter θ (RPCC= 0.47), controlling the degree of co-limitation by light and Rubisco activity in the Farquhar photosynthesis scheme (Haxeltine and Prentice, 1996a), and the canopy light extinction coefficient, k_{beer} (RPCC= -0.27), which determines the shape of the relationship between canopy leaf area index (LAI) and the fraction of incoming PAR absorbed by the canopy. Parameters governing autotrophic respiration (R_a) have also notable, though less pronounced, effects on annual NPP , with higher respiration rates reducing NPP (RPCC = -0.29, -0.27, -0.13, for r_{growth} , a_{C3} , r_{maint} , respectively).

<i>Rank</i>	<i>A</i>		<i>NPP</i>		<i>R_h</i>		<i>Biomass burning</i>	
1	α_{C3}	0.864	α_{C3}	0.846	α_{C3}	0.801	α_{C3}	0.722
2	α_a	0.733	α_a	0.704	α_a	0.662	α_a	0.484
3	θ	0.513	θ	0.474	g_m	0.467	f_{sapwood}	0.411
4	g_m	0.463	g_m	0.463	θ	0.429	k_{mort1}	-0.377
5	a_{C3}	-0.309	r_{growth}	-0.297	k_{beer}	-0.303	θ	0.311
6	k_{beer}	-0.249	k_{beer}	-0.270	r_{growth}	-0.255	$k_{\text{la:sa}}$	-0.250
7	$\lambda_{\text{max,C3}}$	0.149	a_{C3}	-0.268	a_{C3}	-0.242	E_{max}	0.234
8	E_{max}	0.143	f_{sapwood}	0.230	a_{leaf}	0.201	k_{est}	-0.232
9	α_m	-0.127	a_{leaf}	-0.217	f_{sapwood}	-0.192	m_e	0.203
10	a_{leaf}	-0.089	r_{maint}	-0.134	α_m	0.112	a_{C3}	-0.185
11	z_1	-0.077	$\lambda_{\text{max,C3}}$	0.132	r_{maint}	-0.110	g_m	0.171
12	$k_{\text{la:sa}}$	0.050	E_{max}	-0.128	$\lambda_{\text{max,C3}}$	-0.109	r_{growth}	-0.157

Tab. 2.3: The twelve most important parameters in controlling net assimilation rate A , net primary production NPP , heterotrophic respiration R_h and C loss by ecosystems through biomass burning. The ranking was performed according to the average RPCC across all 81 grid cells. Regionally, the importance ranking may vary, as discussed in the text. Parameters specific to C4 plants have similar importance than the respective parameters for C3 plants locally, however, they are of minor importance globally because of the limited geographical distribution of C4 plants.

Although these parameters have a similar effect on A and NPP worldwide, differences in parameter importance can be observed in water-limited regions as characterised by a low ratio of actual to potential evapotranspiration. In such regions, parameters controlling plant water balance, *i.e.* g_m (RPCC= 0.46), E_{max} (RPCC= 0.13) and α_m (RPCC= -0.11) are relatively important (Fig. 2.2). E_{max} controls the water extraction supply, whereas g_m and α_m describe the coupling of the atmospheric water demand to the leaves. Assuming constant non-water stressed stomatal conductance, higher α_m increases the demand, whereas higher values of the canopy conductance analogue g_m reduces it. Together these parameters scale stomatal regulation and C uptake. Since stomata couple the C and H₂O cycles, the same parameters also control actual evapotranspiration and freshwater recharge (Table 2.3). Other parameters influential in regulating the water balance are those determining photosynthetic activity, LAI and the stomatal conductance associated with a certain assimilation rate, which in turn depends on the choice of the optimal ratio of intercellular to ambient CO₂ partial pressure, $\lambda_{\text{max,C3}}$.

NPP determines the amount of C available for tissue production and thereby controls C storage in vegetation (Table 2.4). The rate of conversion of sapwood to heartwood, f_{sapwood} (RPCC= 0.54), and the leaf to sapwood-area ratio, $k_{\text{la:sa}}$ (RPCC= -0.40), control C residence times in trees, and therefore the size of the vegetation C pool. Larger f_{sapwood} values result in trees with proportionally less sapwood, smaller associated losses to R_a , and proportionally more heartwood, and thus generally larger C stocks and a higher C accumulation rate after disturbance. Larger values for $k_{\text{la:sa}}$ decrease the amount of

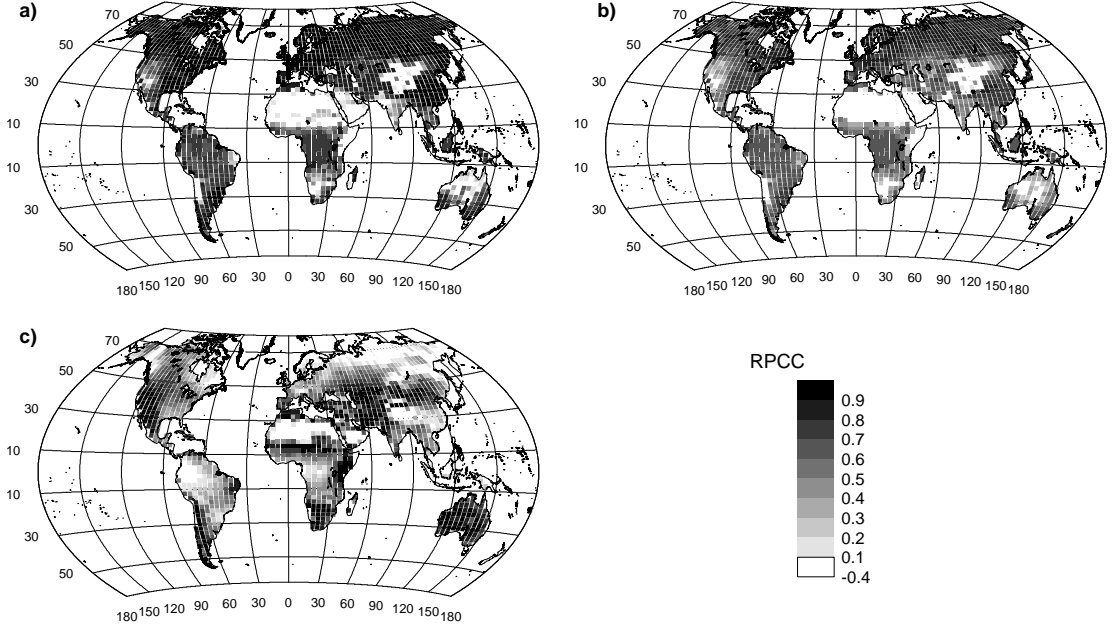


Fig. 2.2: Parameter importance of **a)** α_{C3} , **b)** α_a , **c)** g_m for *NPP* from a global simulation using 14 parameters and 400 LHS (uncorrelated) samples, measured as RPCC. α_{C3} and α_a show very similar spatial patterns of importance, whereas g_m is most important in regions with seasonal water limitation.

C required for leaves and their associated transport tissue (“pipe-model”), and thereby enhance LAI (RPCC=0.60), light interception and *NPP*. At the same time, increased C storage in leaves in connection with larger $k_{la:sa}$ values lead to reduced C accumulation as wood. Vegetation dynamics processes are the third major control on vegetation C. Higher disturbance rates (higher maximum mortality, k_{mort1} , RPCC= -0.46) and higher establishment rates est_{max} (RPCC= -0.32) lead to younger average vegetation, with less C stored.

Soil C stocks are controlled by f_{inter} and f_{slow} (RPCC= -0.81, -0.80), which together determine the mean residual time of C as SOM. Parameters governing litter fall are almost as important (α_{C3} RPCC= 0.75, α_a RPCC= 0.58). Notably, uncertainty in τ_{litter} has very little influence on overall SOM stock, as litter C very quickly comes to equilibrium with annual litter fall, and the size of the litter pool, though controlled by τ_{litter} , is small compared to overall soil C stocks. Fire frequency is influenced by parameters regulating fuel load (vegetation and litter C), and fire susceptibility, *e.g.* the moisture threshold for fire extinction (m_e : RPCC= 0.48). Dryness of the litter layer – a third important factor – depends on parameters governing the root water uptake (z_1 : RPCC= 0.43; E_{max} : RPCC= 0.35), and plant water use (g_m : RPCC= -0.34), as in the model soil moisture in the top layer is taken as a surrogate for litter moisture. The C flux from biomass burning depends very strongly on the vegetation C pool ($f_{sapwood}$: RPCC= 0.41;

<i>Rank</i>	<i>Vegetation C</i>		<i>Litter C</i>		<i>Intermediate Soil C</i>		<i>Slow Soil C</i>	
1	α_{C3}	0.607	α_{C3}	0.791	f_{air}	-0.837	f_{inter}	-0.873
2	f_{sapwood}	0.536	τ_{litter}	0.742	α_{C3}	0.783	f_{air}	-0.720
3	k_{mort1}	-0.459	α_a	0.593	α_a	0.691	α_{C3}	0.657
4	$k_{\text{la:sa}}$	-0.398	θ	0.405	θ	0.392	α_a	0.473
5	g_m	0.379	g_m	0.397	g_m	0.298	θ	0.289
6	α_a	0.370	f_{sapwood}	0.321	k_{beer}	-0.244	g_m	0.270
7	est_{max}	-0.318	r_{growth}	-0.252	r_{growth}	-0.205	k_{beer}	-0.188
8	θ	0.257	a_{C3}	-0.224	a_{C3}	-0.200	a_{C3}	-0.153
9	k_{mort2}	0.186	a_{leaf}	-0.193	a_{leaf}	-0.177	r_{growth}	-0.149
10	k_{allom2}	0.171	E_{max}	0.149	f_{inter}	0.160	$\lambda_{\text{max,C3}}$	0.133
11	z_1	-0.149	k_{beer}	-0.146	$\lambda_{\text{max,C3}}$	0.159	E_{max}	0.123
12	a_{C3}	-0.143	r_{maint}	-0.121	E_{max}	0.140	a_{leaf}	-0.106

Tab. 2.4: The twelve most important parameters in controlling vegetation, litter and soil C pools (soil C partitioned into pools with intermediate and slow turnover times). The ranking was performed according to the average RPCC across all 81 grid cells.

k_{mort1} : PRCC= -0.38; Table 2.3a).

Since LPJ-DGVM is spun up to equilibrium in terms of its pre-industrial C pools, the annual C release from R_h and biomass burning must balance annual C inputs from NPP , averaged over the final few years of the spin-up. The size of the different C pools, their average turnover time and their C inputs are then in balance. Despite large uncertainty in vegetation and soil C pools, R_h is thus strongly controlled by parameters regulating NPP (Table 2.3). With increased productivity, an ecosystem exhibits a larger seasonal amplitude of NEE as a consequence of greater C uptake in summer and greater C release in winter associated with larger ecosystem C stocks, in effect amplifying the differential responses of NPP and R_h to seasonal variations in climate. Most of the remaining uncertainty in the seasonal cycle of NEE is associated with the sensitivity of photosynthesis to water stress (Fig. 2.5 inset). A set of model parameters that describes high non-water-stressed stomatal conductance (a result of high potential daily GPP), with a well-coupled canopy-atmosphere system (high α_m and low g_m , and low water uptake rates E_{max}), increases the sensitivity of actual stomatal conductance, and thus actual GPP , to plant water stress. Particularly in water-limited environments and/or dry conditions, this higher sensitivity increases the effect of summer drought on stomatal conductance, and thus reduces NPP . R_h is less sensitive to seasonal variations in soil moisture, due to its direct dependence on the size of the litter and soil C pools, which varies comparatively little between seasons. Thereby NPP is the main source of uncertainty in magnitude and interannual variations of modelled NEE .

Most of the variation in vegetation composition, expressed as foliar projective cover (FPC) of individual PFTs, can be explained by (a) factors that control the competitive balance between dominant and subdominant PFTs for a given climate and pedographic

<i>Parameter</i>	<i>Dominant PFT</i>	<i>Subdominant PFT</i>	<i>Herbaceous PFT</i>	
<i>Vegetation</i>				
<i>Dynamics</i>	k_{mort1}	-0.398	0.185	0.201
	k_{mort2}	0.107	-0.011	-0.104
	est_{max}	0.278	-0.183	-0.073
<i>Allometry</i>				
	k_{allom1}	0.138	-0.083	-0.091
	k_{allom3}	0.154	0.008	-0.121
	$k_{\text{la:sa}}$	0.073	0.017	-0.083
	k_{rp}	-0.207	0.016	0.156
	CA_{max}	0.081	-0.035	-0.006
<i>Photosynthesis</i>				
	θ	0.073	0.075	-0.131
	k_{beer}	0.013	0.143	-0.806
	α_{a}	0.102	0.139	-0.281
	α_{C3}	0.256	0.278	-0.455
<i>Autotrophic</i>				
<i>Respiration</i>	r_{maint}	-0.164	0.135	0.054
	r_{growth}	0.042	-0.124	0.081

Tab. 2.5: Parameter importance (RPCC) for the foliage projective cover (FPC) of PFTs in grid cells that are tree-dominated biomes under the standard model configuration.

setting; and (b) factors influencing the competitive strength of a specific plant functional trait (Table 2.5). Generally, parameters determining ecosystem level productivity and key vegetation dynamics parameters appear to have the greatest influence on the vegetation structure. Water balance and stand structure related parameters are of lesser importance, except under arid conditions in which Savanna type ecosystems prevail. This is a result of changes in the delicate balance between water demand and supply. In general, forest ecosystems are favoured by higher maximum soil water extraction rates, E_{max} , and higher g_{m} , since a less coupled canopy-atmosphere system mitigates the effect of high atmospheric water demand on plant transpiration. Parameter combinations describing stable vegetation dynamics (lower maximum mortality, stronger effect of growth efficiency on mortality, and higher re-establishment rate) tend to increase the FPC of the dominating PFT. A faster rate of canopy closure, resulting from higher k_{allom1} , k_{allom3} , and a lower self-thinning coefficient k_{rp} also favour the dominant PFT, with the strongest effect on the herbaceous understorey. The predominant influence on the FPC of herbaceous PFTs is exerted by the canopy light extinction coefficient, k_{beer} , with reduced PAR within the canopy increasing the available radiation at the forest floor and tipping the competitive balance towards the herbaceous PFTs. The response of FPC to k_{beer} is highly non-linear (PRCC= -0.81; PCC= -0.41), as the canopy light extinction, and thus PAR-utilisation, follow the Lambert-Beer law.

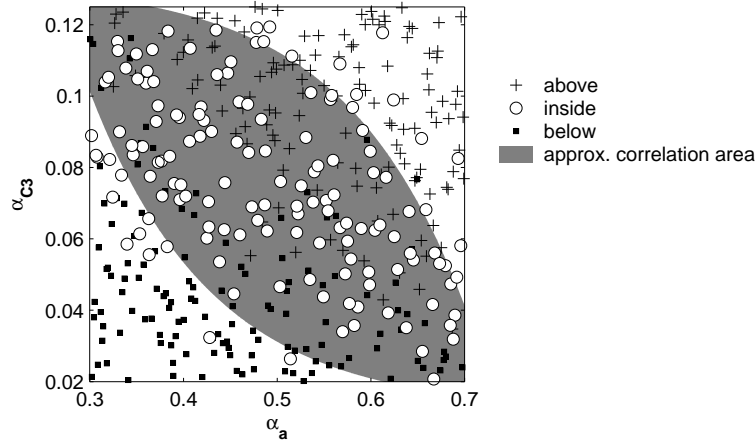


Fig. 2.3: Parameter combinations of α_{C3} and α_a that result in simulated global A and NPP either above (+), inside (o), or below (■) the global benchmarks of 90-160 and 45-85 PgC yr⁻¹ for (A) and (NPP), respectively, as discussed in Section 2.2.5. The grey area shows approximately the parameter space included in the correlation introduced in Section 2.3.2. Note that some variation in A and NPP also results from other co-varying parameters.

2.3.2 Constraints to the parameter space

Of the 36 parameters in Table 2.1, 14 parameters are identified as having a dominant influence on the terrestrial carbon cycling ($|R_{PCC}| > 0.25$, see Section 2.2.4; marked in Table 2.1 with *). Global simulations using the reduced set of parameters result in an uncertainty range in global NPP – for one model – of 29.8 to 133.3 PgC yr⁻¹, spanning the complete range of NPP estimates reported from an earlier model inter-comparison (44.4 - 66.3 PgC yr⁻¹, Cramer *et al.*, 1999), and exceeding the variable constraints set in Section 2.2.5. Uncertainty in global A and NPP mainly results from uncertainty in α_{C3} , α_a , and k_{beer} , and in particular from the consequences of extreme combinations of these parameters for light-use efficiency (Fig. 2.3). By prescribing correlations between these parameters, while still sampling parameter values uniformly across the total parameter range, as described in Section 2.5, implausible combinations are avoided, and uncertainty in modelled NPP substantially reduced (43.1 to 103.3 PgC yr⁻¹). Similar reductions were achieved for A (without parameter correlation: 51.5 to 224.1, with parameter correlation: 71.9 to 172.6 PgC yr⁻¹).

The set of parameter combinations is further reduced by excluding runs in subsequent analyses that do not conform to global benchmarks on the contemporary carbon cycle (see Section 2.2.5). 73% of the 400 simulations satisfied the global constraints for A or NPP , whereas only 41% satisfy the constraint on vegetation C . Only 28% out of the 400 runs satisfy the benchmarks for both global production and vegetation C . Most of the runs excluded have extreme parameter combinations of either α_{C3} versus g_m or $f_{sapwood}$ and k_{mort1} versus $k_{la:sa}$. The first case is associated with low quantum efficiency combined with high water stress, leading to low C uptake. The second is tied to unrealistic vegetation

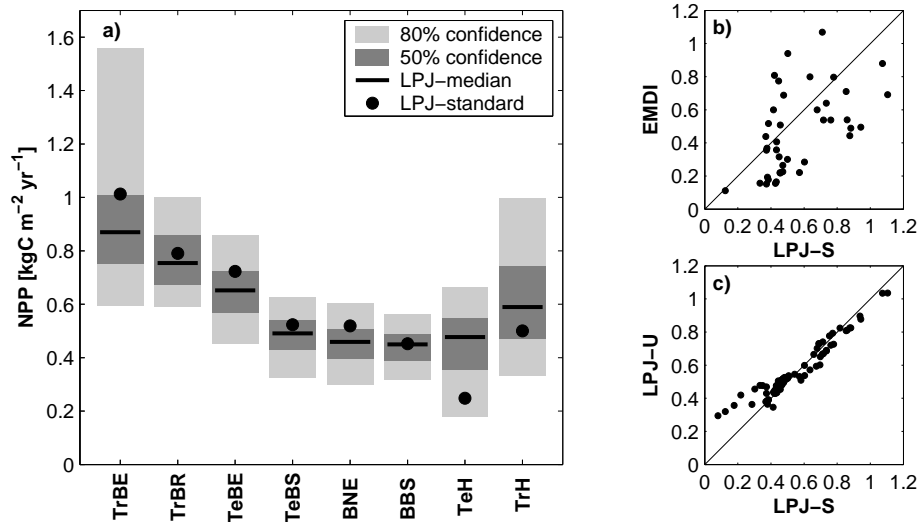


Fig. 2.4: a) Average annual NPP [$\text{kgC m}^{-2} \text{yr}^{-1}$] for various biomes for 1961-1990, and its parameter-based uncertainty range (see Table 2.1 for biome definitions). Correlation of annual NPP [$\text{kgC m}^{-2} \text{yr}^{-1}$] between b) LPJ-DGVM (standard parameterisation, LPJ-S) and EMDI NPP -data (EMDI), for sites at which modelled and observed vegetation type are in agreement ($R^2=0.28$); and c) LPJ-DGVM under standard parameterisation (LPJ-S) and the median of the uncertainty experiment (LPJ-U, $R^2=0.92$).

dynamics in regions with stable growing conditions for forests (*e.g.* Amazonia and tropical Africa) for very low $k_{\text{la:sa}}$ in combination with low k_{mort1} and high f_{sapwood} .

2.3.3 Parameter-based uncertainty in modelling the present-day carbon cycle

Local scale annual net primary production

NPP estimates of LPJ-DGVM are in rather modest agreement with the NPP data from the EMDI dataset. However, the fit is comparable to the fit observed with other terrestrial ecosystem models (EMDI, 2003, *unpublished data*, Fig. 2.4a). In principle, parameter-based uncertainty suffices to explain the difference observed between modelled and measured NPP for most sites (Fig. 2.4b). The results of running LPJ-DGVM with its standard parameterisation agree very well with the median of the uncertainty experiment (Fig. 2.4c). Sources of disagreement between model and data, apart from parameter-based model uncertainty, include the intrinsic difference between site measurements and values applicable at larger (*e.g.* regional, biome, global) scales, taking account of variation in climate, pedography, topography, land management etc. at intermediate scales. In addition, uncertainty arises from the measurements themselves, in particular from the assumptions made to estimate below-ground C allocation (Clark *et al.*, 2001). Previously, the utility of field measurements to evaluate the performance of TBMs has been questioned based on the observation that – as in this study – the NPP data-set did not show any particular

<i>Site</i>	<i>Location</i>	<i>RMSE</i>	<i>R</i> ²
Loobos	(52.1°N, 5.4°E)	35 (32-41)	0.68 (0.66-0.70)
Sarrebourg	(48.4°N, 7.5°E)	54 (45-65)	0.77 (0.65-0.81)
Sorø	(55.3°N, 11.4°E)	31 (24-41)	0.87 (0.78-0.89)
Bayreuth	(50.1°N, 11.5°E)	25 (20-40)	0.65 (0.57-0.70)
Tharandt	(50.6°N, 13.3°E)	56 (53-62)	0.72 (0.68-0.73)
Hyytiälä	(61.5°N, 24.2°E)	27 (25-32)	0.75 (0.70-0.80)

Tab. 2.6: Root mean square error [RMSE, $\text{gC m}^{-2} \text{ month}^{-1}$] and coefficient of determination (R^2) between measured and modelled monthly *NEE* for the period 1996-2000 for six eddy-covariance sites. Measured monthly fluxes are obtained from Valentini *et al.* (2000b).

sensitivity to annual precipitation (Knorr and Heimann, 2001a). The explanation for this may lie in differences in the period of *NPP* sampling and climate measurements.

Seasonal cycle of net ecosystem exchange

Simulated *NEE* of the median of the sensitivity experiment and the standard parameterisation agree reasonably well with the seasonal phasing and amplitude observed at the six eddy covariance sites considered (Fig. 2.5, Table 2.6). Generally, the seasonal cycle is well captured by all simulations of the uncertainty experiment, compared to the standard run. The uncertainty range of *NEE* is considerably smaller than the uncertainty range of modelled *NPP*. For Sorø and Sarrebourg the simulations agree well on the seasonality; however, peak C uptake in summer is consistently underestimated by the simulations. Simulated net C uptake is consistently too low in Tharandt, whereas the seasonality matches the measurements reasonably well.

The root mean square error (RMSE, see Appendix 2.6; Table 2.6) between the flux measurements and simulations is most influenced by α_{C3} , α_{a} and r_{growth} for Loobos, Sarrebourg, Sorø and Bayreuth, since these govern the amplitude of the seasonal cycle. However, the effect is the opposite for Sarrebourg/Sorø, where LPJ-DGVM underestimates the seasonal cycle, compared with Bayreuth/Loobos, where peak C uptake is well matched. Variation of g_{m} can, as noted earlier, lead to considerable uncertainty in monthly *NEE*, most pronounced in an exceptionally dry summer for Hyytiälä (Fig. 2.5 inset). The effect of parameters on the modelled error varies between the measurements sites, both in terms of their average importance and ranking, as well as the seasonal cycle of parameter importance.

LPJ-DGVM is capable of simulating the dominant features of the seasonal cycle of CO_2 as measured at the global network of atmospheric CO_2 monitoring stations (Fig. 2.6). The normalised mean square deviation (NMSD, see Appendix 2.6) between model and measurements considering all 27 stations is only slightly larger than the deviation observed with six TBMs, including a previous model, BIOME-2, related to LPJ-DGVM (Heimann

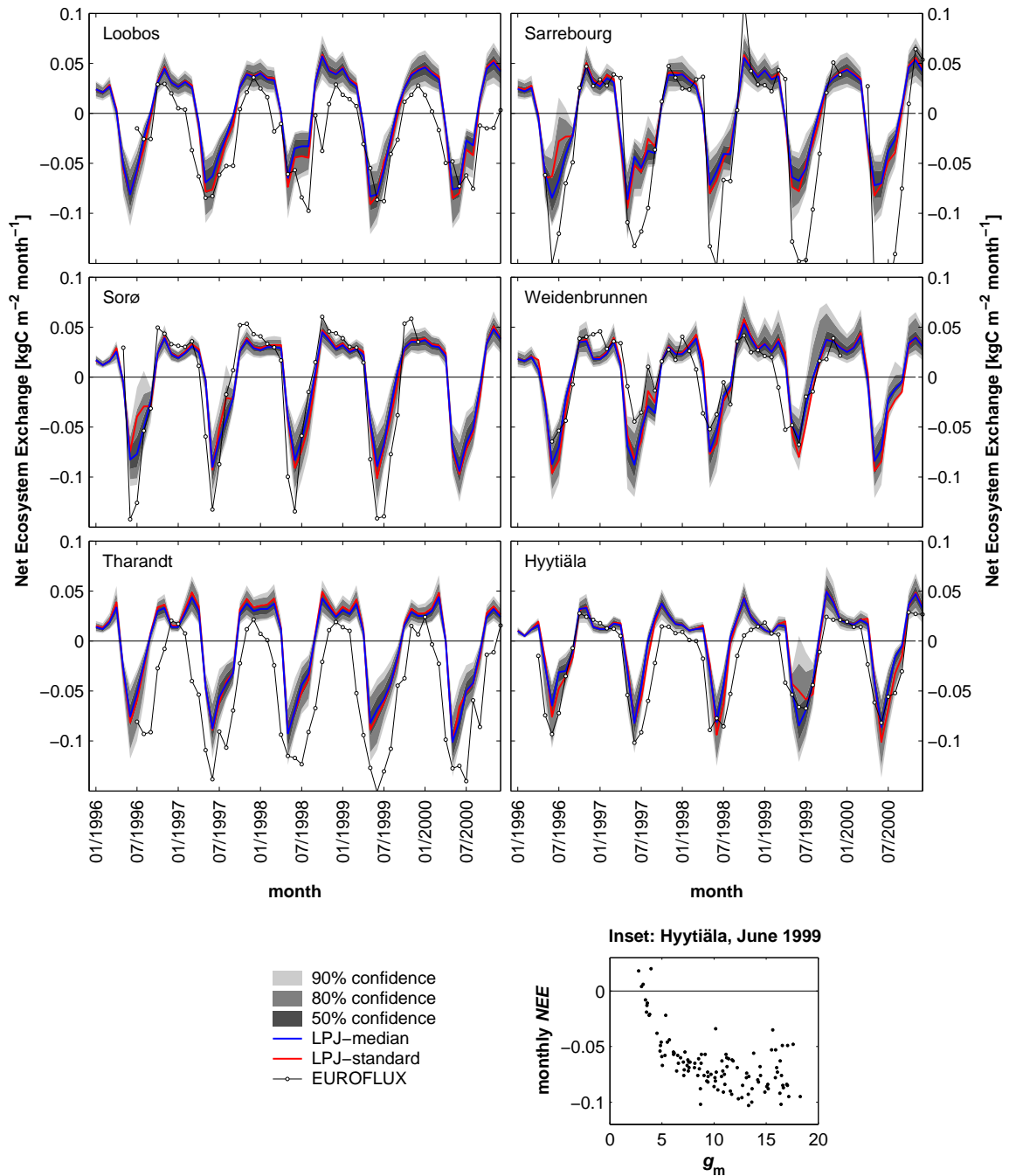


Fig. 2.5: Simulated and observed net ecosystem exchange [NEE , $\text{kgC m}^{-2} \text{ month}^{-1}$] for 1996-2000 at six eddy-covariance sites of the EUROFLUX network. Observed monthly fluxes are obtained from Valentini *et al.* (2000b). **Inset:** Effect of g_m on modelled monthly NEE at Hyytiälä, June 1999.

et al., 1998). The range of NMSD obtained from the uncertainty experiment is of similar magnitude when pooled into three latitudinal categories (Table 2.7). The strong influence of the terrestrial biosphere on the seasonal cycle at northern high-latitude stations is reflected in a relatively high uncertainty in the modelled seasonal cycle of CO_2 . The

	<i>All stations</i>	<i>Northern Stations</i> ($>25^\circ N$)	<i>Tropical Stations</i> ($25^\circ N - 30^\circ S$)	<i>Southern Stations</i> ($>30^\circ S$)
<i>NMSD</i>				
median	13.1	17.6	10.0	7.6
min	1.5	5.0	1.2	1.1
max	38.8	35.9	40.6	39.7
<i>RPCC</i>				
g_m	0.78	-0.02	0.78	0.89
α_{C3}	-0.50	-0.63	-0.63	0.53
τ_{litter}	-0.44	-0.34	-0.42	-0.34
α_a	-0.36	-0.48	-0.55	0.35
θ	-0.30	-0.50	-0.36	0.45
r_{growth}	0.23	0.44	0.31	-0.37

Tab. 2.7: Normalised mean standard deviation (NMSD) between measured and modelled mean seasonal cycle of CO₂ at 27 stations from the GLOBALVIEW network, pooled into northern stations (12), tropical stations (9) and southern stations (6); and parameter importance determining NMSD, measured as average RPCC over all the stations within a specific group.

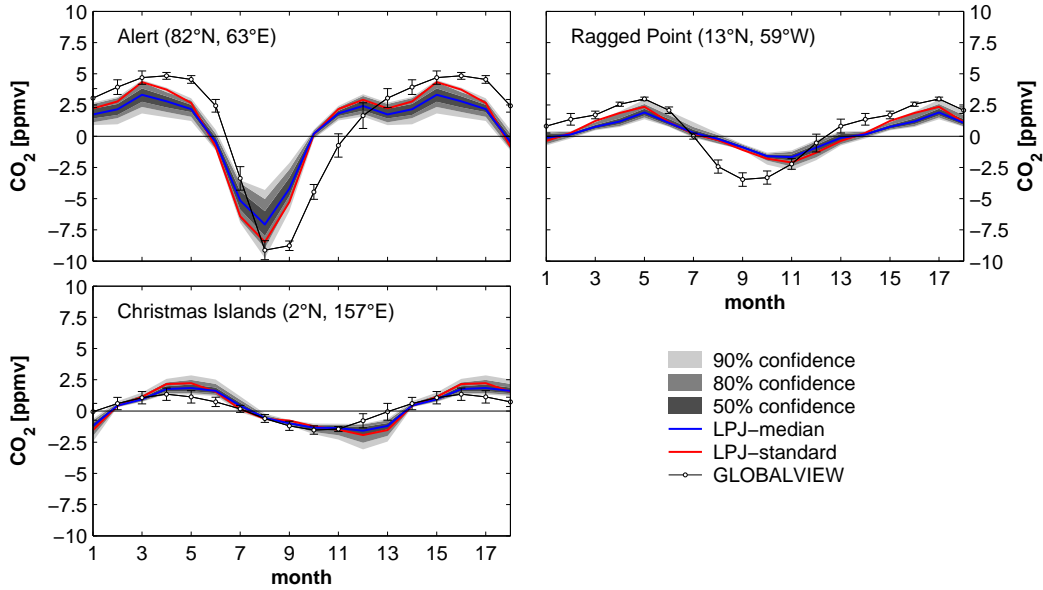


Fig. 2.6: Average seasonal cycle of CO₂ at the Alert, Ragged Point and Christmas Island stations for 1983-1992. Data points are observed concentrations from Conway *et al.* (1994). Months 1-6 are repeated for clearer visualisation.

consistent too early draw down and recovery of CO₂ for these stations, which was already apparent in a predecessor model to LPJ-DGVM, BIOME-2 (Heimann *et al.*, 1998), cannot be related to uncertainty in the parameters examined, and thus appears to be a robust model feature. Likely causes are the effect of snow cover on soil thermodynamics and hence rates of R_h (McGuire *et al.*, 2000) and the delayed onset of the growing season associated with snow cover and frozen soils.

	1980s		1990s	
	<i>standard</i>	<i>median (90% conf.)</i>	<i>standard</i>	<i>median (90% conf.)</i>
<i>A</i>	111.6	109.0 (89.9 - 143.7)	114.8	112.5 (92.8 - 148.8)
<i>NPP</i>	61.9	60.8 (48.9 - 78.1)	63.3	62.7 (50.5 - 80.1)
<i>Rh</i>	55.1	54.3 (42.8 - 70.6)	56.7	56.0 (44.9 - 72.5)
<i>Biomass burning</i>	5.5	5.1 (3.0 - 7.5)	5.4	5.1 (3.0 - 7.4)
<i>NBE</i>	-1.5	-1.5 (-0.4 - -2.4)	-1.7	-1.7 (-0.4 - -3.3)
<i>Vegetation C</i>	995	902 (556 - 1151)	1004	912 (566 - 1157)
<i>SOM</i>	1441	2323 (877 - 5181)	1450	2329 (884 - 5191)
<i>Annual AET</i>	37.9	34.1 (26.2 - 45.0)	37.4	33.8 (26.0 - 44.7)
<i>Annual runoff</i>	36.0	45.0 (34.7 - 55.1)	35.6	44.6 (34.2 - 54.5)

Tab. 2.8: Standard results, median and 90% confidence interval of present-day global C fluxes [PgC yr⁻¹], terrestrial C storage [PgC] and H₂O fluxes [10¹² m³ yr⁻¹].

Parameters governing plant C uptake generally play an important role (α_{C3} : RPCC=-0.50; α_a : RPCC= -0.36) in determining NMSD. In particular, higher values for α_{C3} and α_a increase the agreement between model and observations at the northernmost stations, mainly because of increased summer draw down of CO₂ concentrations by ecosystems. Of the parameters controlling vegetation and SOM dynamics only τ_{litter} appears to be important globally (PRCC= -0.43), with increasing litter residence time amplifying the seasonal cycle at all stations. A marked reduction in global average NMSD is apparent for low values of g_m (RPCC= 0.77). However, this reduction is mainly associated with tropical and southern stations, which have a low amplitude and little modelled uncertainty in the seasonal cycle of CO₂, so that the reduced absolute model error is rather small. Notably we did not find a significant relationship between the overall model performance with respect to the CO₂ network and predicted biosphere properties such as global *A* and *NPP*.

Contemporary terrestrial biosphere dynamics

Parameter-based uncertainty in present-day vegetation composition is typically within $\pm 12.5\%$ of the median FPC (90% confidence) for tropical and temperate tree PFTs, with a larger range for boreal ($\pm 15\%$) and particularly herbaceous PFTs ($\pm 21.5\%$). Global vegetation maps of the distribution of evergreen, deciduous, and mixed forests, grasslands and deserts show good agreement (average $\kappa=0.74$, Prentice *et al.*, 1992) with the median vegetation composition. Global *A* and *NPP* under the standard parameterisation and the respective median estimates from the uncertainty experiment are within 10% of the most plausible estimates of global *A* and *NPP* from observations (Table 2.8). Estimates of C lost from biomass burning are of a similar magnitude to the 4.3 PgC yr⁻¹ ($\pm 50\%$) estimated from observations by Andreae and Merlet (2001). Mean annual global land-atmosphere fluxes for the 1980s and 1990s are estimated at -1.48 (-0.37 to -2.43) and -1.71 (-0.37 to

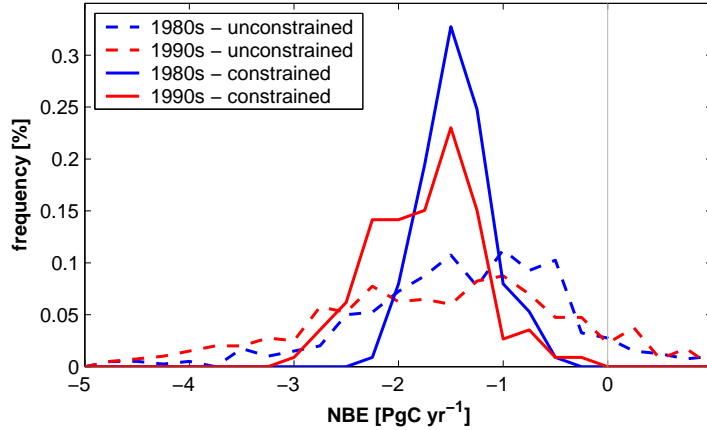


Fig. 2.7: Average annual global land-atmosphere flux [PgC yr^{-1}] in the 1980s (blue lines) and 1990s (red lines), resulting from historic climate and atmospheric CO_2 changes. Dashed lines show the full uncertainty range, solid lines the uncertainty range for those model realisations that conform to contemporary observations of A , NPP and vegetation C .

-3.25) PgC yr^{-1} , respectively.

Fig. 2.7 shows the spread of NBE estimates with and without the constraints discussed in Section 2.2.5. Median estimates of annual NBE are within $\pm 0.1 \text{ PgC yr}^{-1}$ for the period in 1981-2000; the unconstrained median is in the direction of a stronger C uptake. The larger spread without the constraints results mainly from parameter combinations affecting present-day A and NPP , whereas vegetation C contributes only little to the uncertainty in present-day NBE , except for some outliers. The response of A and NPP to observed climate and CO_2 changes relative to present-day A and NPP is comparable between all runs. This means that, in absolute terms, the response is amplified by larger values of A and NPP . As a consequence, 68% and 54% of the variance in the increase in magnitude of NBE are explained by present-day A and NPP , respectively, using linear regression without the constraints. Uncertainty in global A accounts for only 22% of the uncertainty in the contemporary C uptake for the constrained case.

The range of NBE estimated in this study may be compared to -0.6 to -3.0 PgC yr^{-1} (1990s) among six DGVMs (including LPJ-DGVM) obtained by Cramer *et al.* (2001) using the same driving data. Model based NBE estimates of the 1980s range between -1.1 and -2.3 PgC yr^{-1} among four TBMs (likewise including LPJ-DGVM, McGuire *et al.*, 2001). The “residual terrestrial sink”, as inferred from the global C budget, which also accounts for effects on vegetation that are not modelled by LPJ-DGVM such as nitrogen deposition and tropospheric ozone, has been estimated -0.3 to -4.0 PgC yr^{-1} (1980s) or -1.6 to -4.8 PgC yr^{-1} (1990s, House *et al.*, 2003). In the absence of any land-use change that could alter the terrestrial C balance due to deforestation or forest regrowth, the modelled present-day land C uptake is located in roughly equal strength in the tropics (between 20°S and 5°N) and the northern extra tropics, with a particularly strong uptake above 40°N (Fig. 2.8), which is consistent with earlier findings (Kicklighter *et al.*, 1999).

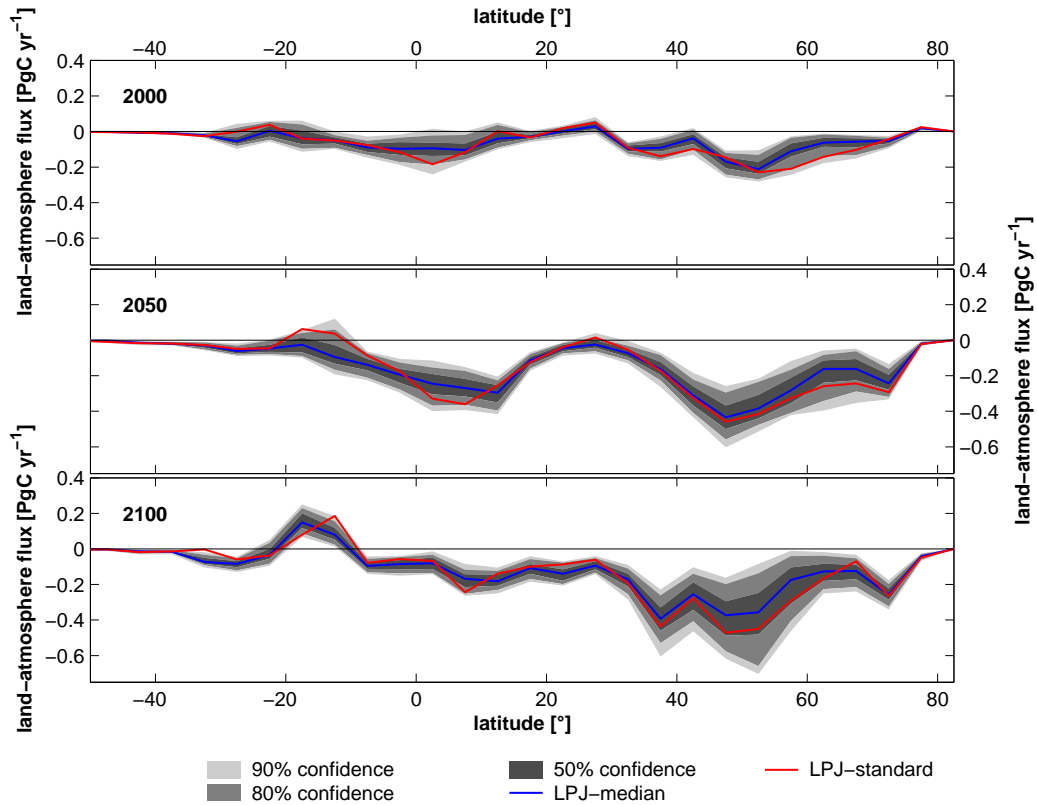


Fig. 2.8: Average annual *NBE* for 5° latitudinal bands [PgC yr^{-1}] in 1991-2000, 2041-2050 and 2091-2100 under the IS92a HadCM2-SUL climate change scenario.

2.3.4 Model projections to 2100

The increases in A and NPP under the climate change scenario from HadCM2-SUL, forced with the IS92a emissions scenario, are a robust model feature, and are driven by the continuous increase in atmospheric CO_2 as well as CO_2 induced increases in water-use efficiency (Fig. 2.9). Despite the uncertainty in A , NPP , vegetation distribution and modelled water stress (allowed for by varying the parameter g_m over a wide range), projected changes in water-use efficiency are robust model results in the sense that alternative parameter values do not change the direction of this important process response. As a result of the rise in A , global *NBE* increases in magnitude by the 2050s to -4.85 (-3.34 to -6.58) PgC yr^{-1} , but then decreases to -3.36 (-1.84 to -4.80) PgC yr^{-1} by the end of the 21st century (Fig. 2.10a). This decline is a consequence of the levelling off of C uptake in vegetation and the decline in soil C uptake with land-atmosphere fluxes of around -2.51 (-1.63 to -3.38) PgC yr^{-1} (Fig. 2.10b) and -0.75 (-0.01 to -1.88) PgC yr^{-1} (Fig. 2.10c), respectively, towards the end of the 21st century. These trends are relatively robust on a long time-scale (50-years; average R^2 with linear regression: 0.98), and in reasonable agreement with previously published LPJ-DGVM results (Cramer *et al.*, 2001). Most of the deviation among the suite of runs in this study occurs in the last two decades of the 21st century, where some

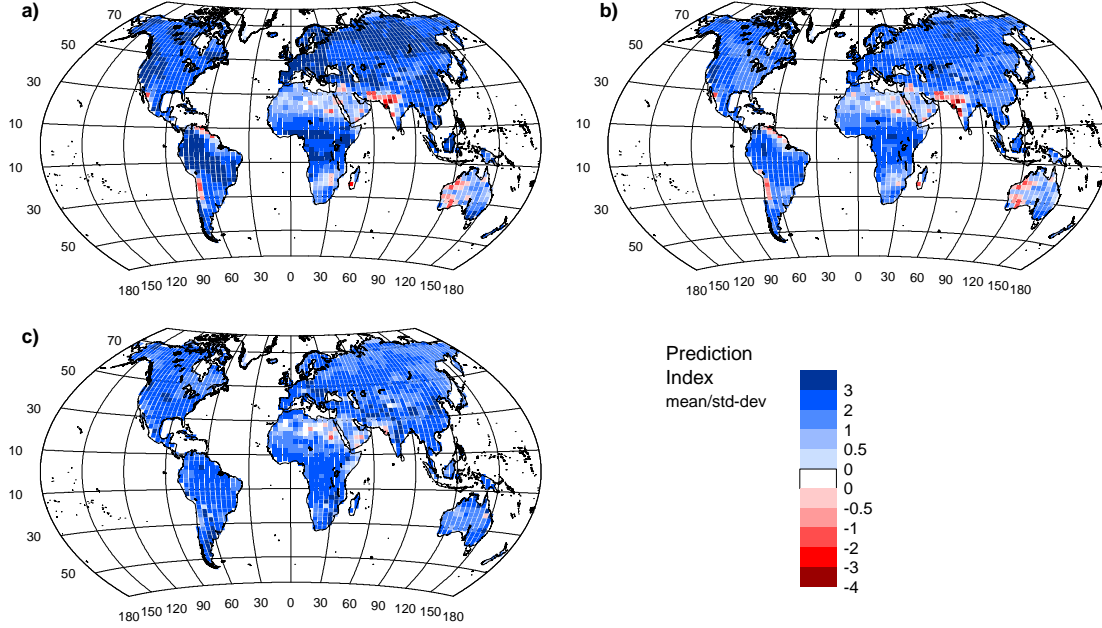


Fig. 2.9: Change in a) A , b) NPP and c) water-use efficiency between the periods 1991-2000 and 2091-2100 under the IS92a HadCM2-SUL climate change scenario, expressed as Prediction Index (PI, see Appendix 2.6), *i.e.* mean change / standard deviation of change from the uncertainty experiment. $|PI| > 2$ indicates a robust model result. Typically, trends have similar directions for much smaller values of $|PI|$.

simulations show a stagnation of the biospheric C uptake, whereas others exhibit a strong decrease, mainly as result of C losses from soil. Decadal and inter-annual variations are less well constrained (average $R^2 = 0.88 / 0.86$ for decadal and inter-annual variability, respectively), but still reasonably similar to the median of the uncertainty experiment.

Parameters governing present-day plant C uptake (α_{C3} , a_{C3} , θ) exert some influence on the rate of increase in A and NPP , but have only little impact on the rate of vegetation C build-up, which are much more strongly controlled by vegetation dynamics (0.67% explained variance with ANalysis of VAriance, ANOVA, for the parameters k_{mort1} and k_{est}). Global SOM C uptake at the end of the 21st century, by contrast, is influenced to a similar extent by parameters controlling present-day NPP (0.45% explained variance by α_{C3} , α_a , θ and r_{growth}) and parameters governing vegetation and SOM dynamics (0.40% explained variance by f_{inter} , τ_{litter} and k_{est}).

Projected NBE at the end of the 21st century shows distinct regional patterns, however, the changes compared to present-day NBE are not as robust as modelled changes in A and NPP . The latitudinal breakdown of the development of NBE over the 21st century shows that the rise in atmospheric CO_2 increases C storage in both the tropics and the northern extra tropics up to 2050 (Fig. 2.8). Thereafter climate change substantially weakens the capacity of ecosystems to sequester C in the tropics and southern mid-latitudes by the end of the 21st century, in agreement with the results of Cramer *et al.* (2001). This effect can

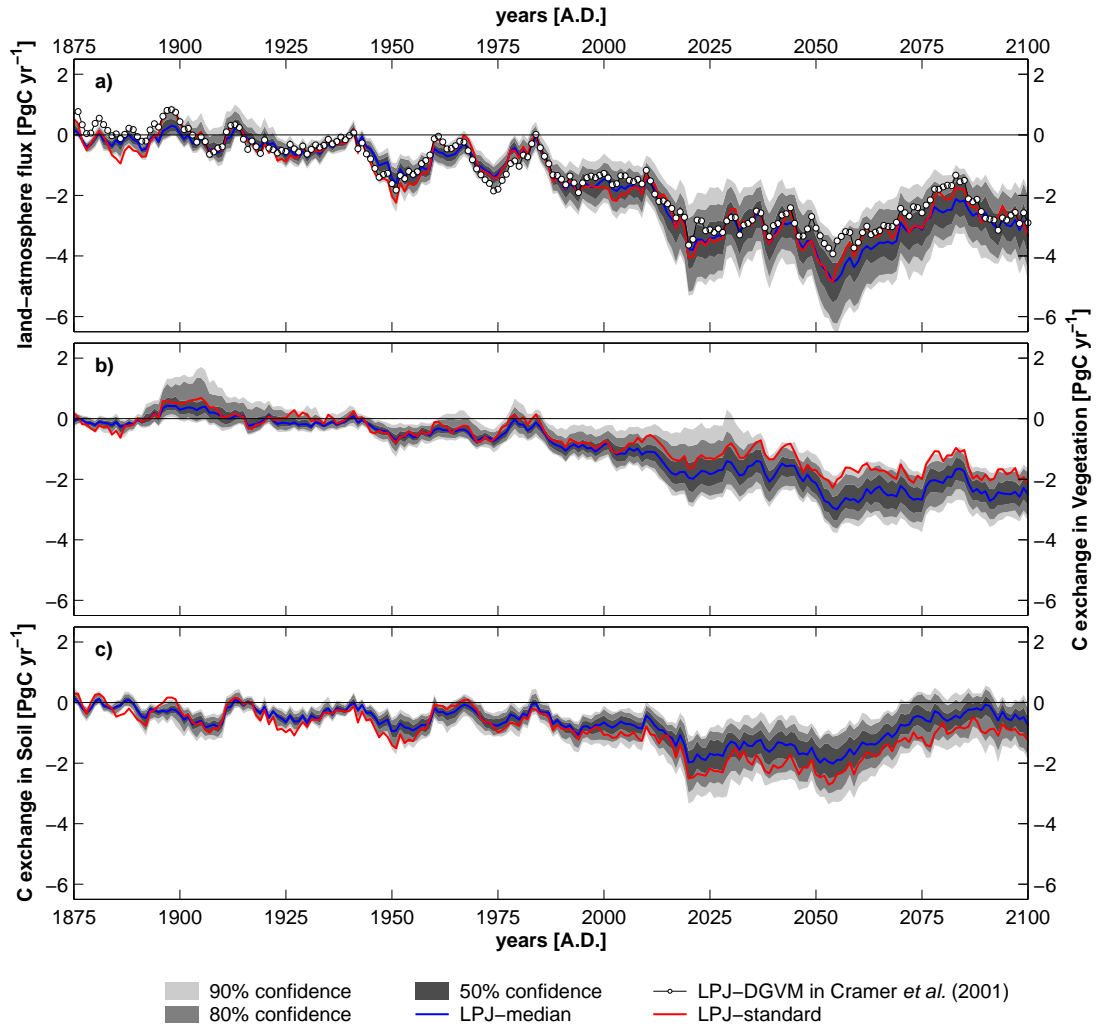


Fig. 2.10: Global land-atmosphere flux [10-year running average, PgC yr^{-1}] under the IS92a HadCM2-SUL climate change scenario: **a)** *NBE* of the terrestrial biosphere, **b)** C exchange of the vegetation, **c)** C exchange of SOM pools. Negative values indicate C storage in the respective pool, whereas positive values denote release to the atmosphere.

be attributed to a strong decline in precipitation over the tropics, a particular feature of the climate scenario used in this study. In the northern extra tropics, where the strongest climate change is simulated under this scenario, C sequestration is still substantial by the end of the 21st century, but there is considerable uncertainty associated equally with soil and vegetation processes.

Despite the large range of uncertainty in modelled water-stress (a result of varying g_m over a wide range) the expansion of savanna into arid grasslands of the tropics is common to all simulations (Fig. 2.11a). All simulations show an expansion of high latitude forests as well as an increased deciduousness of temperate and southern boreal forests (Fig. 2.11b,c). The greater part of the vegetation C sink is located in this area, and its

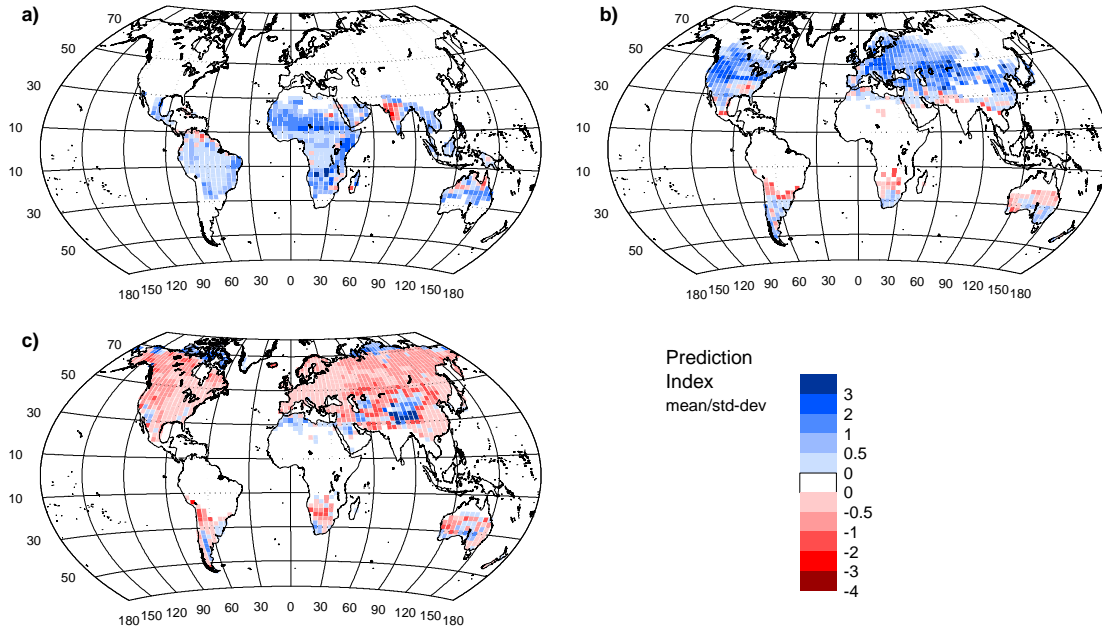


Fig. 2.11: Change in foliage projective coverage between 2000 and 2100 under the IS92a HadCM2-SUL climate change scenario for **a)** tropical rain green (TrBR), **b)** temperate deciduous (TeBS), and **c)** temperate herbaceous (TeH) PFTs; expressed as Prediction Index (PI, see Appendix 2.6), *i.e.* mean change / standard deviation of change from the uncertainty experiment. $|PI| > 2$ indicates a robust model result. Typically, trends have similar directions for much lower values of PI.

uncertainty controlled by the parameter f_{sapwood} , which governs the rate of vegetation C accumulation in newly establishing PFTs. A concurrent decline in precipitation and increase in deciduousness in parts of Southern Africa and America leads to a reduction in *NBE*.

2.4 Discussion

Of the 36 parameters included in the survey only few have an overriding influence on the modelled terrestrial biosphere dynamics. In particular, LPJ-DGVM shows little sensitivity to many of those parameters whose ‘correct’ values, in the absence of suitable measurements, are particularly uncertain, *e.g.* several parameters describing allometry (k_{allom1} , k_{allom2} , k_{allom3}), stand structure (CA_{max}), and fire dynamics (r_{fire} , fuel_{min}). Parameters that contribute most to overall model uncertainty are those controlling net assimilation rate and water exchange. This is in general agreement with the results obtained by Knorr (2000) and Knorr and Heimann (2001a) for the BETHY model, and White *et al.* (2000b) for BIOME-BGC. In particular, only a few parameters are associated with the uncertainty in A at equilibrium, reflecting the big-leaf approach employed in these models (Friend, 2001).

The uncertainty range of *NPP* is of a similar magnitude to the range among models reported from model inter-comparison studies (Heimann *et al.*, 1998; Cramer *et al.*, 2001). This suggests that these differences might to a large extent be associated with parameter-based uncertainty. Since *NPP* is the major driving force for plant performance and vegetation dynamics, parameters that influence *NPP* have a strong influence on the overall ecosystem dynamics simulated by the model. *NPP* plays the dominant role in determining the sizes of the various C pools in equilibrium, as also noted by Gerber *et al.* (2004).

Despite considerable uncertainty in modelled present-day and future net assimilation and primary production, as well as C storage, some robust features are apparent from the scenario analyses. Substantial increases in *A* because of increased water-use efficiency occurred consistently in all simulations (as noted by Kicklighter *et al.*, 1999), suggesting that alternative parameter values do not change the direction of the process response. All major regional responses of vegetation to changes in climate are simulated consistently for the majority of simulations. Resulting regional patterns of C uptake or loss from vegetation and soil are also consistently modelled, even though the magnitude of the effect is relatively uncertain.

We evaluated the effect of parameter uncertainty on future responses of the terrestrial biosphere as simulated by one particular DGVM, whereas Cramer *et al.* (2001) assessed uncertainties associated with the different process representations encapsulated by different models (*i.e.* six DGVMs, one climate scenario), while Schaphoff *et al.* (in review) investigated uncertainties associated with different climate change projections produced by different climate models (*i.e.* one DGVM, five different climate models, all driven with the IS92a emission scenario). Results from the three studies agree well in terms of modern *NPP*, R_h and *NBE*, as well as in inter-annual variability, and the overall decadal trend for the scenario period when forced with the same climate data. Uncertainty in present-day *NBE* is equally large among different DGVMs and results obtained using different parameterisations of one particular model. Under climate change, all three studies point to an initial increase in terrestrial carbon stocks, followed by a decline in net C uptake in the second half of the 21st century. The decline of biospheric C uptake and a potential net C loss towards the end of the 21st century are in agreement with other model studies (Cox *et al.*, 2000; White *et al.*, 2000a; Joos *et al.*, 2001; Dufresne *et al.*, 2002; Jones *et al.*, 2003; Friedlingstein *et al.*, 2003).

The uncertainty range in modelled C uptake integrated over the entire 21st century in the present study is 201 (117 to 264) PgC (vegetation) and 107 (32 to 212) PgC (soil). These ranges compare to 151 to 340, and 28 to 220 PgC for vegetation and soil pools, respectively, from the DGVM inter-comparison (Cramer *et al.*, 2001), and to 0 to 150 PgC (vegetation) and -70 to 41 PgC (soils) for four different climate scenarios (excluding the ‘older’ HadCM2 scenario, Schaphoff *et al.*, in review). In all three studies, models predict a trend towards increased *NPP* and vegetation growth as response to increased

atmospheric CO₂ and temperature, particularly at high northern latitudes, concurrent with an expansion of boreal forests. This trend is consistently modelled among different DGVMs, future climate scenarios and model parameterisations. Strong regional differences in changes of vegetation composition were, however, observed for tropical regions among different climate scenarios, mainly as a result of different regional changes in precipitation (Schaphoff *et al.*, in review). The present study shows that simulated shifts in dominant vegetation types, regional patterns of *NBE* and their change over time are relatively robust to the choice of model parameterisation.

We applied a relatively simple method to constrain the parameter-based model uncertainty in an attempt to approach a realistic uncertainty range for modelled present-day and potential future *NEE*, as well as to demonstrate the effect of parameter-based uncertainty on modelling terrestrial biosphere dynamics. A more sophisticated method of constraining distribution functions for model output variables, assigning a probability to results from each model run based on the distance between the run and the ‘best-guess’ region of a particular benchmark, was tested for the present-day analysis. However, results were similar to those obtained using the simpler approach, and would not greatly affect the conclusions of our study.

The obvious starting point to reduce parameter-based uncertainty would be to constrain *NPP* directly from observations, because of the importance of *A* and *NPP* in global vegetation models. As detailed in Section 2.3.3, currently available *NPP* measurements are probably insufficient for this purpose. C flux estimates from eddy-covariance measurements that integrate C and H₂O fluxes at the ecosystem scale offer some potential to constrain the parameter space using inverse methods (Wang *et al.*, 2001; Reichstein *et al.*, 2003; Knorr and Kattge, in press). α_{C3} and α_a contribute most to the uncertainty in the modelled seasonal cycle by amplifying its magnitude. However, the importance of these parameters in determining monthly *NEE* were in most cases strongly anti-correlated with r_{growth} , r_{maint} and r_{ea} . This implies that a particular modelled seasonal cycle of *NEE* might be obtained from a multitude of combinations of these parameters, such that these parameters might be difficult to constrain based on net C fluxes. Partitioning the net flux into uptake and respiratory components could potentially help to identify parameter contributions, especially for respiratory processes (Wang *et al.*, 2001). However, large uncertainty still exists with respect to the correct flux separation (Janssens *et al.*, 2001; Ogee *et al.*, 2004). Parameter correlations could, however, be derived by constraining model results with flux data and thus reducing the parameter space (Reichert and Omlin, 1997; Knorr and Kattge, in press). The findings of the present study demonstrate clearly that parameter importance varies between different sites. A representative collection of high quality seasonal *NEE* data sets for all major biomes would thus allow uncertainty in global terrestrial modelling to be reduced.

Measurements of the seasonal variations of atmospheric CO₂ concentrations integrate carbon fluxes over larger regions; hence they have the potential to avoid spatial bias.

The largest reduction in absolute error may be obtained in the northern latitudes, where the seasonal cycle appears to be most strongly controlled by light-use efficiency effects on vegetation productivity. Atmospheric inversion studies likewise point to light-use efficiency as a major controlling factor for seasonal variation in CO₂ exchange (Kaminski *et al.*, 2002; Still *et al.*, 2004). However, uncertainty in the concurrent fluxes of anthropogenic and oceanic origin, atmospheric transport fields used to map emissions of the terrestrial biosphere to the CO₂ monitoring stations, as well as data availability and quality (Rayner *et al.*, 2005) limit the degree to which uncertainty in parameter values can be effectively reduced.

Both eddy-covariance and CO₂ measurements could potentially be used to constrain parameters that govern short-term ecosystem processes (*e.g.* α_{C3} , α_a , θ , r_{growth}). These parameters contribute most to the parameter-based uncertainty in present-day *NEE*, and amplify the rate of *A* and *NPP* increase as a response to future climate scenarios. However, in our global change case study these parameters contribute to only 4% and 45% of the uncertainty in C uptake by vegetation and soil, respectively. Transient projections of climate change effects on vegetation C storage are influenced to a much greater extent by uncertainty in vegetation dynamics, primarily the rate at which forests can accumulate C after disturbance, or in response to changing environmental conditions. Similarly, uncertainty in modelled SOM change – although showing a strong influence of uncertainty in litter fall – is strongly linked to parameters governing the average turnover time of the SOM pools, particularly in regions in which soils become a source of CO₂ in the future in these scenario analyses. These results highlight the need for improved understanding of the response of SOM to changing environmental conditions (*e.g.* Fang *et al.*, 2005; Knorr *et al.*, 2005), as well as for improved understanding of potential changes in the competitive balance between PFTs under climate change.

We evaluated parameter importance for average present-day conditions, and constrained the parameter space further using present-day observations of the global C cycle. Parameters that appear of little importance in this approach may still have substantial impact on model simulations under other than present-day conditions. For instance, Fang *et al.* (2005) showed that uncertainty in the apparent Q₁₀ of soil respiration could lead to an up to 70% difference in projected soil C losses under future climate change in temperate regions. Joos *et al.* (2001, using LPJ-DGVM) demonstrated that cumulative land-atmosphere fluxes (2000-2100) differ by 188 PgC depending on whether a Lloyd-Taylor temperature dependence of soil respiration or no temperature dependence at all is assumed. Uncertainty in soil C changes through the 21st century, as simulated in this study, is of a comparable magnitude (see Fig. 2.10), but associated with different parameters: The rate parameter of the Lloyd-Taylor equation was found not to be important in determining present-day C cycling, and was thus not included in estimating the uncertainty in the future C balance. Data assimilation, as discussed above, may improve the identification of parameters that are of importance also under changing environmental

conditions. These methods rely on present-day observations to test model performance (*e.g.* Rayner *et al.*, 2005), which still might be insufficient to reduce uncertainty of the long-term response of some terrestrial processes, *e.g.* the long-term responses of photosynthesis to enhanced CO₂ concentrations, or soil respiration to global warming. Uncertainty due to gaps in process understanding and uncertainties associated with alternative process formulations at scales relevant to global terrestrial biosphere modelling (*e.g.* Knorr and Heimann, 2001a) are important, but beyond the scope of the present study.

The uncertainty range of a particular model output variable depends on the choice of distribution function for the parameters in question. We chose to apply the principle of parsimony in assuming a uniform distribution function for all but one parameter. An alternative choice would be for instance a bell-shaped function, simulating parameter values distal from the mean of ‘best guess’ values with reduced probability. This would tend to reduce the spread in model results, giving a more conservative estimate of the potential model uncertainty. Some parameters are likely to co-vary but were assumed – with one exception – to vary independently in our study; again, our approach is likely to overestimate rather than to underestimate the true uncertainty range.

The exact ranking of the uncertainty contribution of individual parameters, or their functional equivalents in other models, will be influenced by the structure of the particular model under investigation. Nevertheless, LPJ-DGVM may be considered exemplary for the DGVM family of models, and we anticipate that many of our results in terms of the importance of certain groups of parameters may be representative for the sensitivity of DGVMs and other similar ecosystem models to their parameterisation. These models generally follow similar approaches to simulate plant C and H₂O exchanges with the atmosphere. Certain parameter groups, for instance those controlling the light-use efficiency of photosynthesis at the ecosystem scale, will very likely play a pivotal role in model uncertainty for any DGVM, due to of the central role of *NPP* in determining vegetation structure and dynamics. The methodology presented here could be readily applied to other models to further corroborate our findings.

This study focuses on the uncertainty in process-based terrestrial biosphere models due to imperfect knowledge (or implicit uncertainty) of the ‘correct’ parameter values used in scaled representations of ecosystem processes, and aims at providing quantitative information about the confidence that can be placed in model results. However, other aspects of model uncertainty were not addressed; for example, uncertainty due to incomplete knowledge of the true mechanisms underlying certain ecosystem phenomena, as well as uncertainty in the driving environmental data, which may be equally important (*e.g.* Knorr and Heimann, 2001a). Future steps towards a quantitative assessment of the uncertainty in modelling terrestrial biosphere dynamics will need to account for uncertainty related to model assumptions, *e.g.* the equilibrium of C cycle at the beginning of the 20th century, and to consider driving factors other than climate and atmospheric CO₂ change, such as land-use change (McGuire *et al.*, 2001) and N deposition (Vitousek *et al.*,

1997). It should be noted that model robustness does not necessarily imply that model predictions are correct. In fact, model failure to correctly predict observations considering model uncertainty can point to areas in which model improvements are required. Better evaluation data and improved process understanding, *e.g.* of the response of ecosystem to disturbances, are indispensable for the reliable modelling of the terrestrial biosphere.

2.5 Conclusions

We presented an assessment of parameter-based uncertainty in modelling the present-day and future terrestrial biosphere dynamics using one particular DGVM. Of the 36 parameters in our survey, only a limited subset of parameters is associated with most of the present-day model uncertainty. An improved understanding of the scaling of leaf-level photosynthesis to ecosystems, the hydraulic coupling of vegetation and atmosphere, and plant respiration processes appear to be the most important priorities to reduce parameter-based uncertainty in the modelling of present-day ecosystem C cycling. The rate of C accumulation in vegetation and the turnover time of SOM were identified as major contributors to uncertainty in future C balance estimates, highlighting the need for more appropriate experiments and better validation data sets to improve model performance.

The substantial uncertainty range in *NPP* in this study is of a similar magnitude to the range observed between different DGVMs and other model-based estimates of global *NPP*. Uncertainty propagation leads to considerable uncertainty in sizes of C pools. Soil C pools, due to their long turnover times, represent the most uncertain model outputs. Despite this, contemporary global vegetation distribution and *NBE* are relatively robust model results. The overall response of LPJ-DGVM to a particular climatic forcing is maintained among most of the alternative parameterisations tested in this study. In particular, the response of vegetation to increased levels of CO₂, shifts in vegetation patterns as a result of climate change, and the effect of global warming on SOM pools are reasonably robust model results. In effect, long-term trends in *NBE* are reliably modelled, although the uncertainty range reaches $-3.35 \pm 1.45 \text{ PgC yr}^{-1}$ by the end of the 21st century under the particular climate scenario used in this study.

Based on our analysis we recommend that uncertainty analyses should be an integral part of the development and validation process for all process-oriented ecosystem models.

Acknowledgements

The authors are grateful to Stefano Tarantola (JRC, Italy) for kindly providing the software tool SimLab to generate the latin hypercube samples and to Christoph Müller (PIK) for providing the aggregated 3.0° CRU climatology. We also thank Kathrin Poser, Wolfgang Cramer, Markus Reichstein and two anonymous reviewers for helpful comments on earlier versions of this manuscript. SZ acknowledges funding from the HSP Brandenburg (AZ: 24-04/323;200). BS acknowledges funding through the Swedish Research Council for

Environment, Agriculture Sciences and Spatial Planning. The study was part of the Advanced Terrestrial Ecosystem Analysis and Modelling (ATEAM) initiative (EVK2-2000-00075) of the fifth European Community Framework Programme.

2.6 Appendix

In latin hypercube sampling (LHS, McKay *et al.*, 1979) the value range of each variable x_j is divided into n intervals of equal probability, and one value is selected at random from each of these. The sample obtained for x_1 is paired at random and without replacement with LHS values for x_2 , and so on, to create a set of n x_j -tupels (Helton and Davis, 2000). Iman and Conover (1982) developed a method to induce correlation between individual parameters to account for known or deduced relationships between parameters.

Partial correlation coefficients (PCC) were calculated to identify the relative importance of the uncertainty contribution of a particular parameter to the total model output uncertainty. The PCC is defined as the correlation coefficient between the terms $x_j - \hat{x}_j$ and $y - \hat{y}$ where x_j and y are a particular parameter and output variable, respectively. \hat{x}_j and \hat{y} are the estimated values of the linear regression:

$$\hat{x}_j = a_0 + \sum_{\substack{p=1 \\ p \neq j}}^n a_p x_p \quad (2.3)$$

and

$$\hat{y} = b_0 + \sum_{\substack{p=1 \\ p \neq j}}^n b_p x_p \quad (2.4)$$

The concept of partial correlation allows the identification of the contribution of a parameter x_j to the variation in the output variable y when the variation in y is influenced by a number of co-varying factors, or parameters, x_p . Since PCC relies on linear regression, it provides a measure for the linear relationship between x_j and y with the linear effects of all other parameters x_p removed. To identify potential non-linear monotonic effects, these analyses were repeated using rank-transformed input variables (RPCC, Conover and Iman, 1981). We did not find any non-monotonic effects with respect to the parameters in this study. The PCC is independent of the probability distribution function of parameter and output variable (for more details on properties of this coefficient see Helton and Davis, 2000). Parameters were ranked for each model output variable in terms of their absolute value in PCC or RPCC, respectively. In this study, PCC and RPCC were similar for most of the cases. We therefore report RPCC-values, and refer to PCC in those cases only, where both correlation coefficients differ substantially, indicating a non-linear sensitivity of the model to that specific parameter.

Root mean square error (RMSE) was calculated between modelled and measured C exchanges for six forest sites of the EUROFLUX network as

$$RMSE = \sqrt{\frac{1}{n} \sum_{m=1}^n (C_{sim,m} - C_{obs,m})^2} \quad (2.5)$$

where $C_{sim,m}$ and $C_{obs,m}$ are the modelled and measured C exchanges for a particular

month m , and n is the number of month in the record.

Model performance against the observed seasonal signal of atmospheric CO₂ at a monitoring station was evaluated as the normalised mean square deviation (NMSD), as in Heimann *et al.* (1998),

$$NMSD = \frac{1}{12} \sum_{m=1}^{12} \left(\frac{C_{T,m} + C_{F,m} + C_{O,m} - C_{OBS,m}}{\sigma_m} \right)^2 \quad (2.6)$$

where $C_{T,m}$, $C_{F,m}$, and $C_{O,m}$ are the monthly CO₂ concentrations resulting from the corresponding biospheric, fossil fuel and ocean flux, respectively. $C_{OBS,m}$ is the 10-year mean observed monthly atmospheric CO₂ concentration (1983-1992) and σ_m the corresponding standard deviation of the observed value for each month between modelled and measured monthly concentrations.

The robustness of modelled responses to climate change was evaluated as prediction index (PI)

$$PI = \frac{x_{sim,2100} - x_{sim2000}}{\sigma_{sim}} \quad (2.7)$$

either as difference between 10-year mean values for model output x in 2000 and 2100, or in the case of *NBE* as difference from zero. Model responses were considered robust when the absolute value of PI exceeded 2.0; usually trends agreed in sign far below this value.

3. EFFECT OF HEIGHT ON TREE HYDRAULIC CONDUCTANCE INCOMPLETELY COMPENSATED BY XYLEM TAPERING

Sönke Zaehle*

The great tragedy of science – the slaying of a beautiful hypothesis by an ugly little fact.

(T.H. Huxley)

An edited version of this manuscript is published as

Zaehle, S. (2005). Effect of height on tree hydraulic conductance incompletely compensated by xylem tapering, *Functional Ecology* **19**: 359-364.

Abstract

The hydraulic limitation theory proposes that the decline of forest productivity with age is a consequence of the loss of whole-plant and leaf-specific hydraulic conductance with tree height caused by increased friction. Recent theoretical analyses have suggested that tapering (the broadening of xylem vessel diameter from terminal branches to the base of the stem) could completely compensate for the effect of tree height on hydraulic conductance, and thus on tree growth. The data available for testing this hypothesis are limited, but they do not support the implication that whole-tree and leaf-specific hydraulic conductance are generally independent of tree height. Tapering cannot exclude hydraulic limitation as the principle mechanism for the observed decline in growth. Reduction of the leaf-to-sapwood area ratio, decreased leaf water potential, loss of leaf-cell turgor or osmotic adjustments in taller trees could reduce the effect of increased plant hydraulic resistance on stomatal conductance with height. However, these mechanisms operate with diminishing returns, as they infer increased costs to the tree that will ultimately limit tree growth. To understand the decline in forest growth, the effect of these acclimation mechanisms on carbon uptake and allocation should be considered.

Keywords: plant hydraulic architecture, hydraulic limitation theory, leaf-specific conductance, pipe-model, WBE

*Potsdam Institute for Climate Impact Research (PIK), e.V., Telegrafenberg, PO Box 601203, D-14412 Potsdam, Germany

3.1 Introduction

The growth rate of trees declines with age. The leading hypothesis to explain this is decreased hydraulic conductance as a consequence of increased tree height (Ryan and Yoder, 1997). Assuming a simple pipe-model of the plant's hydraulic system, *i.e.* a leaf attached to a unit stem and a unit root pipe (Shinozaki *et al.*, 1964a,b; Jarvis, 1975), the hydraulic path length – and along with it the resistance of the plant's hydraulic system due to friction – increases with tree height (Whitehead and Hinckley, 1991). Increased stomatal closure to prevent a breakdown of the hydraulic transport system due to cavitation (Ryan and Yoder, 1997), or lower leaf water potentials triggering leaf-cell turgor loss or osmotic adjustment would reduce daily net photosynthesis. Less growth would be the ultimate result, as the other carbon costs (respiration, foliage production and root growth) vary little, or increase slightly with stand age (Ryan and Waring, 1992; Mencuccini and Grace, 1996b). Increased respiration by itself, as a consequence of the increasing amount of living woody biomass with tree size (Yoda *et al.*, 1965), cannot explain the decline in forest productivity. Maintenance respiration of the sapwood accounts for only 5-12% of the annual carbon fixation (Ryan *et al.*, 1995), and the larger fraction of respiration is associated with growth processes that generally decline as growth declines (Ryan and Waring, 1992).

The hydraulic limitation theory has been controversial (Becker *et al.*, 2000b; Bond and Ryan, 2000; Mencuccini and Magnani, 2000). From the formal hydraulic model of Whitehead *et al.* (1984), one might expect acclimation of the ratio between supporting sapwood area and transpiring leaf area. Such an acclimation could result in homeostatic balance between the plant's transport capacity and transpirational demand of the leaves, to either minimise, or compensate for the potential hydraulic limitation of stomatal conductance due to height. Tree height would still affect tree growth, because hydraulic adjustment would increase the relative share of carbon production that is allocated to sapwood construction and maintenance, thereby diminishing the returns per unit carbon investment.

Recent theoretical analyses (West *et al.*, 1999; Enquist, 2002) have suggested that the observed tapering of xylem conduits, *i.e.* the broadening of xylem vessels basipetally (Zimmermann, 1978; Pothier *et al.*, 1989), could produce hydraulic homeostasis of the plant. This conclusion is derived from a model of plant branching networks based on the assumption of minimised internal transport resistance while maximising the plant's surface area. This model describes the plant's architecture and hydraulic system as a self-similar fractal, and in a more detailed way than the pipe model as it allows for branching and for changes in the xylem anatomy between different branch segments. A basipetal increase in conduit diameter would permit the total resistance of a tube running from trunk to petiole to remain constant, independent of tube length (West *et al.*, 1999).

Here, the published evidence relevant to the scaling of hydraulic resistance as predicted by West *et al.*'s model is reviewed. I discuss whether the data support the assumptions of the model and the conclusions drawn from it. The aim is to evaluate whether tapering

would suffice to discard the hydraulic limitation theory as the most likely explanation for the observed age-related decline in forest productivity.

3.2 Review of theory and experimental evidence

Can vessel tapering compensate for height growth?

The architecture of the branching network in the general plant model (hereafter WBE) by West *et al.* (1999) is described by the scaling of branch diameter, branch length, and conduit diameter of adjacent branch segments of the tree according to simple power laws (Appendix 3.4, eq. 3.5). Three parameters define the relationships between branch diameter, branch length, and conduit diameter of adjacent branch levels. Conduits are assumed to operate as if they were tightly bundled, not interconnected, and to have a uniform diameter within a branch segment. They form a continuous tube, represented by a linear series of vessels, conserving the total numbers of tubes in each segment. Thus, total plant hydraulic resistance depends linearly on the total resistance of a single tube. Total plant resistance can be approximated by the Hagen-Poiseuille formula, which describes capillary flow (Nobel, 1983; Becker *et al.*, 2000a). Tapering is included into the model by scaling conduit diameter such that it increases basipetally, thus allowing the ratio of conductive to non-conductive tissue to vary between branch segments.

An intuitive way to see why tapering can compensate for the longer path length of the tree with increasing tree height in the WBE model is to look at total path length L and resistance Z with increasing number of segments. Since, in the WBE model, length and conduit diameter, and thus resistance, of the petiole are assumed to be invariant, the total path length and resistance of a single tube can be described as simple sums of petiole length l_N and resistance Z_N , respectively, with N the number of branching levels in the network:

$$L = \sum_{k=0}^N l_k = l_N \sum_{k=0}^N m^{N-k} \quad (3.1)$$

and

$$Z = \sum_{k=0}^N Z_k = Z_N \sum_{k=0}^N i^{N-k} \quad (3.2)$$

The scaling factors m and i linking the two adjacent levels k and $k-1$ can be derived from the basic equations of WBE (see Appendix 3.4 for derivations):

$$m = \frac{l_{k-1}}{l_k} = n^{\beta/3} \quad (3.3)$$

$$i = \frac{Z_{k-1}}{Z_k} = n^{\beta/3-2\bar{\alpha}} \quad (3.4)$$

where n is the number of daughter branches per branch, $\bar{\alpha}$ and β are the scaling factors for segment conduit diameter and length, respectively. For simplicity, n , $\bar{\alpha}$ and β

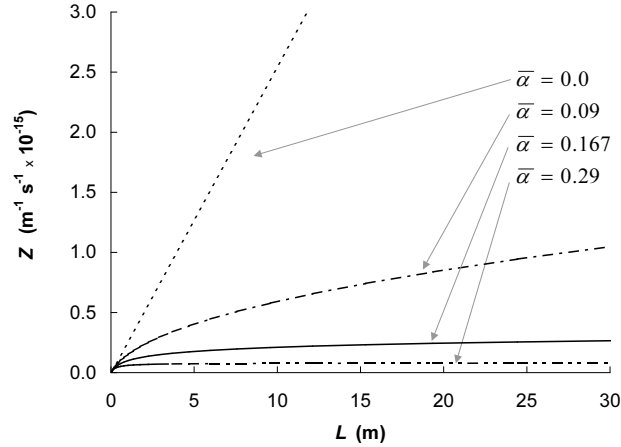


Fig. 3.1: Total plant hydraulic resistance (Z , in $m^{-1}s^{-1} \times 10^{-15}$) as a function of total path length (L , in m), assuming that $l_N = 0.05m$, $a_N = 10\mu m$, and $\beta = 1.0$ for different tapering coefficients $\bar{\alpha}$. 0.0 is the pipe-model theory; 0.167 WBE; 0.09 and 0.29 are estimates of the 95% confidence interval of the tapering parameter estimated by Becker and Gribben (2001), assuming $\beta = 1.0$

are assumed to be level-independent, that is constant for all branch segments (although, as shown below, this is not a requirement). Three conclusions can be drawn from the limiting behaviour of length and resistance for a large number of branching levels:

1. For a network without tapering ($\bar{\alpha} = 0$, pipe-model), hydraulic resistance grows in proportion to path length ($m=i$), consistent with the hydraulic limitation theory in its original form (Yoder *et al.*, 1994; Ryan *et al.*, 1997).
2. Any (level-independent) tapering ($\bar{\alpha} > 0$) will cause hydraulic resistance to grow slower than path length, since then m always exceeds i . The extent to which this effect influences the capacity of trees to compensate for height growth is sensitive to assumptions about the scaling of tapering and branch length (Fig. 3.1, Becker *et al.*, 2000b).
3. Total plant hydraulic resistance (eq. 3.2) approaches an asymptotic value with increasing number of segments when $i < 1$. Unlike hydraulic resistance, path length (eq. 3.1) always increases in the WBE model, because $m \geq 1$ for any plausible value of β . Thus, total plant hydraulic resistance becomes independent of total path length, when the tapering exponent $\bar{\alpha}$ fulfils the inequality $\bar{\alpha} > \beta/6$ (eq. 3.4). Two assumptions are introduced in the WBE model, namely that biomechanical constraints and tapering are uniform, and the branching network is volume-filling, leading to the special case of a self-similar fractal model with $\beta = 1$ (West *et al.*, 1999). Eq. 4 thus implies for the WBE model that $\bar{\alpha}$ would have to be greater than or – in the limiting case of very large trees – equal to $1/6$.

The original version of WBE (West *et al.*, 1997) minimised the energy required to

distribute resources without any variation in xylem diameter. Tapering was introduced in a subsequent version of the model, ostensibly because hydraulic constrictions would otherwise preclude the existence of tall trees and cause leaves high in the canopy to receive less water than leaves deeper in the canopy (West *et al.*, 1999). However, WBE describes a fractal-like structure, so that all leaves have equal supply irrespective of their position within the canopy and even with zero tapering, since all tubes have equal path length.

Evidence even for quite small trees (Zimmermann, 1978; Mencuccini, 2002, citing Magnani, *unpublished results*) indicates that the degree of tapering diminishes basipetally. Also, James *et al.* (2003) found that conduits tapered within the crown of several tropical tree species, but lumen diameters were virtually constant below the base of the crown. These results raise concerns that the assumption of a uniform tapering might be too strong (Mencuccini, 2002; Becker and Gribben, 2001). A declining rate of tapering does not necessarily invalidate tapering as a mechanism to avoid the adverse effects of tree height, contrary to the assumption of Becker and Gribben (2001). In the derivation of equation 3.4, no assumptions were made that require the coefficients to be level-independent (see Appendix 3.4). In fact, any combination of n , β and $\bar{\alpha}$ that results in $i < 1$ for a particular segment k will achieve this. It is not necessary to assume fractality to minimise the hydraulic resistance and to decouple total plant hydraulic resistance from plant height, agreeing with the more mathematically exact account of Dodds *et al.* (2001).

Recent results from McCulloh *et al.* (2003) for vines and ring-porous trees suggest that the total number of conduits per segment varies between adjacent segments, conflicting with the assumption made in WBE. This would be expected from the application of Murray's law to the hydraulic architecture of plants. If conduits serve transport purposes only (as in ring porous trees), the construction cost of conduits can be assumed to be proportional to conduit volume (McCulloh *et al.*, 2003). Murray's law applied to plant vascular systems implies for such a case that the original pipe-model (*i.e.* $\bar{\alpha} = 0$ or no taper) would be optimal for a constant number of conduits. Any degree of taper without variation in total tube number would be less efficient and therefore violate the energy minimisation principle. If the number of conduits were allowed to vary between segments in the WBE model, as suggested by the data in McCulloh *et al.* (2003), the required taper to decouple hydraulic resistance from path length cannot be calculated by eqns. 3.1-3.4. Whole-plant hydraulic conductance then becomes difficult to predict, limiting the capacity of the WBE to actually predict the whole-plant effect of tapering on hydraulic conductance.

Are the predictions of WBE confirmed by observations?

To judge whether WBE adequately describes the hydraulic architecture of trees, the distribution of hydraulic resistance within the tree needs to be modelled correctly, and the model predictions of the scaling between size parameters (*e.g.* diameter) and hydraulic resistance should agree with relevant measurements. Unfortunately, although plant hy-

draulic architecture has long been identified as an important subject (Zimmermann, 1978), surprisingly few relevant data are available. Only a few studies have been designed to exclude the effect of differences in environmental factors (*e.g.* understorey versus canopy trees, unequal access to groundwater resources, Bond and Ryan, 2000), and few analyses allow the assessment of whole-plant hydraulic resistance (Mencuccini, 2002).

West *et al.* (1999) claimed that the degree of tapering predicted by their model agrees with the observed distribution of hydraulic resistance in the two *Acer* species analysed by Yang and Tyree (1993). However, no data on the scaling of conduit tapering and branch length are available from Yang and Tyree (1993) to confirm that the observed agreement is a consequence of a correct assumption of the WBE model. In a re-analysis of data by Zimmermann (1978), Becker and Gribben (2001) found that the parameter estimate for the tapering parameter $\bar{\alpha}$ is sensitive to the assumptions made on the – unknown – scaling of segment length. As only a slight deviation will yield strongly different results in terms of the overall hydraulic resistance (Figure 3.1), these data cannot indicate if the predicted degree of tapering is sufficient to compensate for height growth.

Becker and Gribben (2001) showed that WBE is potentially useful in interpreting conduit tapering by producing a good fit of the model to the data of Zimmermann (1978), although the estimated value of the tapering parameter $\bar{\alpha}$ was uncertain. A meta-analysis of existing studies on tree hydraulic architecture by Mencuccini (2002) corroborates the capacity of the WBE model to predict the scaling of hydraulic conductivity of segments to the segment's diameter, illustrating the fact that larger stems are more permeable (Mencuccini and Grace, 1996a; Becker *et al.*, 2000b). However, the data do not support the scaling of whole-tree hydraulic resistance to diameter (and total plant biomass): the observed scaling coefficients are smaller than predicted (Table 3.1), and whole-plant hydraulic conductance declines with increasing size, contradicting the WBE model.

Smaller scaling coefficients than predicted by WBE do not necessarily imply that the water supply to leaves (leaf-specific hydraulic conductance) is reduced with height, as data also support the hypothesis that leaf-to-sapwood area ratio declines with tree height (Whitehead *et al.*, 1984; Mencuccini and Magnani, 2000; McDowell *et al.*, 2002b). Yet, there is a significant reduction of leaf-specific hydraulic conductance with height in three out of the four studies summarised in Table 3.1; in the fourth, the sample size was too limited to draw any significant conclusion (Mencuccini and Magnani, 2000). Similar results were obtained for *Pinus ponderosa* (Ryan *et al.*, 2000) and *Fagus sylvatica* (Schäfer *et al.*, 2000). Saliendra *et al.* (1995) found no evidence for acclimation of either specific sapwood conductance or leaf area with increasing path length in *Betula occidentalis*, however a more than two-fold decline in whole-plant leaf specific conductance between juvenile and adult individuals. Apparently, the acclimation of leaf area with height is not sufficient to prevent leaf-specific hydraulic conductance from declining with height; it merely minimises the reduction in leaf-specific hydraulic conductance (McDowell *et al.*, 2002a).

<i>Species</i>	<i>Segment diameter</i>			<i>Stem diameter</i>			<i>Biomass</i>		
	<i>b</i>	<i>SE</i>	<i>P</i>	<i>b</i>	<i>SE</i>	<i>P</i>	<i>b</i>	<i>SE</i>	<i>P</i>
<i>Acer rubrum</i> ^a	2.66	0.05	ns	1.72	0.08	***	0.65	0.03	**
<i>Acer saccharum</i> ^b				1.68	0.12	*	0.65	0.05	ns
<i>Pinus sylvestris</i> ^c	2.63	0.08	ns	1.23	0.14	***	0.50	0.05	***
<i>Pinus banksiana</i> ^d				1.34	0.22	*	0.52	0.09	*
All four species				1.32	0.06	***	0.54	0.02	***

^a Yang and Tyree (1994)

^b Tyree and Sperry (1988); Yang and Tyree (1994)

^c Mencuccini and Grace (1996a)

^d Pothier *et al.* (1989)

Tab. 3.1: Allometric scaling of hydraulic conductivity of stem-segment hydraulic conductance to stem-segment diameter, and aboveground hydraulic conductance to diameter at breast height and aboveground biomass based on reduced-major-axis regression (*c.f.* Mencuccini, 2002). Analyses using ordinary least square regression obtained similar results. Abbreviations: *b* = regression coefficient, *SE* = standard error, and *P* = significance of the t-test for the difference between the regression coefficient and theoretical slopes predicted by the WBE (2.67 for segment diameter, 2.0 for stem diameter, and 0.75 for biomass). ns = not significantly different $P > 0.05$; * $P < 0.05$; ** $P < 0.01$; *** $P < 0.001$.

Does acclimation to increased hydraulic resistance affect forest growth?

A recent study on a moist-tropical *Eucalyptus saligna* plantation suggested that a decline in growth occurred, even though an acclimation of leaf area with height compensated for the hydraulic effect of height (Barnard and Ryan, 2003). Direct and indirect evidence suggest that maintenance and growth respiration costs of the stem are not greater in taller trees (Ryan and Waring, 1992; Mencuccini and Grace, 1996b), so one cannot invoke increasing respiration as an explanation. Instead, the hydraulic limitation theory might need to be extended. Even in the absence of any hydraulic limitation related to path length, tree height might affect leaf water potential through gravity (Woodruff *et al.*, 2004). Osmotic adjustments as a response to loss of turgor (Woodruff *et al.*, 2004), or increased leaf construction costs to maintain lower minimum leaf water potentials (Barnard and Ryan, 2003; Koch *et al.*, 2004) in taller trees, could only partly offset reductions in growth, since these adaptations would divert resource allocation from photosynthesis. Similarly, increased belowground carbon allocation and decreased leaf-to-sapwood area ratios to minimise the increase of total plant hydraulic resistance with height (Magnani *et al.*, 2000) could mitigate the effect of tree height on stomatal conductance, but only at increased costs per unit foliage, thereby ultimately limiting tree growth.

3.3 Concluding remarks

The WBE model shows that theoretically tapering could compensate for the effect of tree height on hydraulic resistance, and therefore limit the hydraulic effect of tree height on tree growth. The predicted scaling of hydraulic conductance matches observed scaling

on a segment scale, but not at more aggregated levels. Thus, either the WBE model lacks an important process, or one or more of its assumptions (*e.g.* conservation of total tube number, uniformity of tapering, or the volume-filling and area-preserving branching network) are invalid. However, the data available are insufficient to evaluate all of the assumptions underlying the WBE model, even though they indicate that the assumption of constant tube numbers is too strong. The data nevertheless do not support the prediction of the WBE model that whole-tree hydraulic conductance is generally independent of height. Tapering cannot exclude the hydraulic limitation hypothesis as being the principal mechanism for the observed decline in stand productivity with age. Instead, the hydraulic limitation theory should be extended to account for hydraulic acclimation and the associated consequences for gross primary production and carbon allocation. For the mechanistic modelling of forest development with age it is essential to understand tree hydraulic architecture and its implications for tree growth.

Acknowledgements

This review was supported by the HSB-programme of the Federal State of Brandenburg, Germany (AZ: 24-04/323;200). The author is grateful to Stephen Sitch, I. Colin Prentice and two anonymous reviewers for helpful comments on previous versions of this manuscript.

3.4 Appendix

The initial equations from the West *et al.* (1999) model (WBE) describe a fractal network for the adjacent levels of branches k and $k+1$:

$$\frac{r_{k+1}}{r_k} = n_k^{-\alpha_k/2} \quad \frac{a_{k+1}}{a_k} = n_k^{-\bar{\alpha}/2} \quad \frac{l_{k+1}}{l_k} = n_k^{-\beta_k/3} \quad (3.5)$$

where n is the number of daughter branches, α , $\bar{\alpha}$ and β are the scaling coefficients for branch diameter r , tube radius a , and segment length l , respectively. Since in the WBE assumes invariant petiole conduit diameter and length, it is more convenient to invert the equations in A1. The hydraulic resistance Z of a single tube j within a branch segment k can be approximated by the Hagen-Poiseuille formula, which describes capillary flow. This formula neglects the substantial contribution of the pit membrane resistance to total resistance, but this does not affect relative comparisons of resistance Nobel (1983); Becker *et al.* (2000b).

$$Z_k^j = \frac{8 \times \eta \times l_k}{\pi \times a_k^4} \quad (3.6)$$

where η is viscosity. Assuming the number of total tubes are preserved, the ratio of resistances i between adjacent levels is given by

$$i = \frac{Z_{k-1}}{Z_k} \propto \frac{l_{k-1}}{a_{k-1}^4} \cdot \frac{a_k^4}{l_k} \longrightarrow \frac{n_{k-1}^{-4\bar{\alpha}_{k-1}}}{n_{k-1}^{-\beta_{k-1}/3}} = n_{k-1}^{\beta_{k-1}/3 - 2\bar{\alpha}_{k-1}} \quad (3.7)$$

4. THE HYDRAULIC ACCLIMATION THEORY AND IMPLICATIONS FOR MODELLING REGIONAL CARBON BALANCES

Sönke Zaehle* Stephen Sitch† I. Colin Prentice‡ Jari Liski§¶
Wolfgang Cramer* Markus Erhard|| Thomas Hickler** Benjamin Smith**

All models are wrong, but some are useful.

(G. Box)

An edited version of this manuscript is in review for *Ecological Applications*.

Abstract

Changing carbon allocation in trees to counteract increasing hydraulic resistance with tree height has been hypothesised to lead to the commonly observed age-related decline in aboveground productivity of forests. We show the implications of this decline in forest growth, and hence forest age structure, on the carbon dynamics of European forests in response to historical changes in environmental conditions. Incorporating hydraulic acclimation into a global terrestrial biosphere model (LPJ) improves the simulated increase in biomass with stand age. Application of the advanced model, including a generic representation of forest management in even-aged stands, for 77 European provinces shows that model-based estimates of biomass development with age compare favourably with inventory-based estimates for different tree species. Model estimates of biomass densities on province and country-levels, and trends in growth increment along an annual mean temperature gradient are in broad agreement with inventory data. However, the level of agreement between modelled and inventory-based estimates varies markedly between countries and provinces. The model is able

*Potsdam Institute for Climate Impact Research (PIK), e.V., Telegrafenberg, PO Box 601203, D-14412 Potsdam, Germany

†Met Office (JCHMR), Crowmarsh-Gifford, Wallingford, OX10 8BB, U.K.

‡Department of Earth Sciences, University of Bristol, Queen's Road, Bristol BS8 1RJ, UK

§European Forest Institute, Torikatu 34, FI-80100 Joensuu, Finland

¶Finnish Environment Institute, Research Programme for Global Change, PO Box 140, FI-00251 Helsinki, Finland

||Institut für Meteorologie und Klimaforschung (IMK-IFU), Forschungszentrum Karlsruhe GmbH, Kreuzeckbahnstr. 19, D-82467 Garmisch-Partenkirchen, Germany

** Geobiosphere Science Centre, Physical Geography and Ecosystems Analysis, Lund University, Sölvegatan 12, S-22362 Lund, Sweden

to reproduce the present-day age structure of forests and the ratio of biomass removals to increment on a European-scale based on observed changes in climate, atmospheric CO₂ concentration, forest area and wood demand between 1948 and 2000. Vegetation in European forests is modelled to sequester carbon at a rate of 100 TgC yr⁻¹, which corresponds well to forest inventory-based estimates.

Keywords: age-related decline, plant hydraulic architecture, Magnani-hypothesis, LPJ, DGVM, forest management

4.1 Introduction

The growth rate of forests declines markedly with stand age after canopy closure (Kira and Shidai, 1967; Gower *et al.*, 1996). A profound understanding of this phenomenon is important, as changes in the age structure of forests influence large-scale accumulation of biomass. The current net C uptake in forest ecosystems is partly attributed to both changes in age structure from afforestation and forest management (Goodale *et al.*, 2002; Nabuurs *et al.*, 2003). Propagating present forest age structure into the future, Kohlmaier *et al.* (1995) have demonstrated that age-related changes of forest growth can have significant effects on land-atmosphere flux estimates under changing environmental conditions. Two approaches are frequently used to estimate regional carbon balance in forests. The first, book-keeping methods, are based on forest inventories and consider stand dynamics, and thus evidence for the age-related decline in forest growth, implicitly through changes in measured stocks through time. The second approach uses ecosystem models which mechanistically describe processes of growth and turnover in forests and simulate forest growth also under changing environmental conditions.

Consecutive forest inventories are routinely carried out at least since the 1960s for most of the countries in the Northern hemispheric temperate and boreal zone. These inventories integrate all factors affecting forest growth on stand and regional scale from forest management activities and changed environmental conditions such as climate change, CO₂- and N-fertilisation (Goodale *et al.*, 2002). Originally designed for commercial forestry purposes, such inventories have recently been used to infer bottom-up carbon balances (Kauppi *et al.*, 1992; Dixon, 1994; Kurz and Apps, 1999; Caspersen *et al.*, 2000; Goodale *et al.*, 2002; Nabuurs *et al.*, 2003; Smith *et al.*, 2004). Nabuurs *et al.* (2003), for instance, used inventory data to estimate a net C uptake of 0.14 PgC yr⁻¹ over 1.4×10^6 km² of European forests in the 1990s based on a book-keeping approach and including the wood-products cycle. Inventories give only limited insight into the ecology of vegetation dynamics, and therefore cannot be used directly for predictive analysis of potential future environmental changes in forest ecosystems. However, they provide a data-base to study regional variations in forest stock as well as forest growth changes over stand age, and thereby a useful constraint for aboveground vegetation carbon estimates from process-based ecosystem models (Venevsky, 2001; Waring and McDowell, 2002).

Terrestrial biosphere models provide a mechanism to scale detailed process knowledge obtained from field and laboratory experiments to larger regions, and are thus important tools to investigate the response of the terrestrial biosphere to changing environmental conditions (Prentice *et al.*, 2000). These models are frequently used to assess the impact of climate change on the terrestrial carbon cycle (Cox *et al.*, 2000; Cramer *et al.*, 2001; Dufresne *et al.*, 2002). There have been first attempts to include land-use history into terrestrial biosphere models (McGuire *et al.*, 2001; Levy *et al.*, 2004), however, inclusion of realistic stand development has been limited to the application of static rules derived from forest statistics (Kohlmaier *et al.*, 1995; Häger, 1998). Most of these models consider only elementary representations of ageless grid scale vegetation with simple allocation rules to partition net primary production into different carbon pools representing plant tissues. However, even complex stand-scale forest growth models are not generally able to adequately reproduce the age-related decline, thus requiring age-dependent factors to fit observed growth curves (Kramer and Mohren, 2001; Waring and McDowell, 2002).

Hypotheses to explain the age-related decline in forest growth have been the subject of intensive debate (Ryan *et al.*, 1997; Becker *et al.*, 2000a; Mencuccini and Magnani, 2000; Ryan *et al.*, 2004; Zaehle, 2005). Hydraulic limitation, resulting from increased hydraulic resistance of the plant's vascular system with increasing path length has been suggested to be the dominant cause (Yoda *et al.*, 1965; Ryan *et al.*, 1997). The original hypothesis proposed that increased friction of the plant vascular system of taller trees would result in earlier stomatal closure, and subsequently in reduced photosynthetic carbon uptake (Ryan and Yoder, 1997). A decline in leaf-specific hydraulic conductance of the sapwood has been reported for a number of tree species (Yang and Tyree, 1993; Mencuccini and Grace, 1996a; Hubbard *et al.*, 1999; Schäfer *et al.*, 2000; Delzon *et al.*, 2004). An accompanying decrease in the ratio of transpiring leaf area to supporting sapwood area, as expected from the application of Darcy's law to plant hydraulics (Waring *et al.*, 1982), has been frequently, though not always, observed (McDowell *et al.*, 2002a). While such an acclimation apparently minimises the effect of path length on leaf-specific hydraulic conductance (McDowell *et al.*, 2002a), it still bears a cost, because carbon is allocated away from photosynthetically active tissue (Zaehle, 2005).

Summarising various aspects of the 'hydraulic limitation' hypothesis, Magnani *et al.* (2000) suggested that homeostasis in plant hydraulic architecture is responsible for this decline, based on data on growth, allocation and hydraulic conductance in Scots pine (*Pinus sylvestris* L.). They proposed that allocation of carbon to conductive sapwood and absorbing roots should be optimal with respect to achieving minimal whole-plant leaf-specific hydraulic resistance whilst supporting a maximum of transpiring leaf-tissue, thereby maximising *NPP*. Increased allocation to fine roots with tree height decreases below-ground plant hydraulic resistance. This decrease in below-ground resistance is assumed to compensate for the increase in leaf-specific resistance of the stem as path length increases with tree height, thereby maintaining a near-constant whole-plant leaf-specific hydraulic con-

ductance. Increasing investment costs to maintain similar levels of whole-plant leaf-specific hydraulic conductance with increasing tree height reduces growth efficiency, resulting in a decline in forest growth. Magnani *et al.* (2002) have investigated the functional relationship predicted from this hypothesis to variations in annual mean temperature and climatic water deficit and showed that this theory is adequate for larger-scale predictions of carbon allocation to plant tissues, and therefore suitable for the inclusion in large-scale ecosystem models.

An advanced representation of the age-dependent forest growth rate in terrestrial modelling may improve estimates of regional-scale biomass development, and thereby increase confidence in the predictive capacities of such models under changed environmental conditions (Venevsky, 2001). Using this comprehensive theory of changing carbon allocation with plant size (Magnani *et al.*, 2000), we test the capacity of a particular terrestrial biosphere model, the Lund-Potsdam-Jena dynamic global vegetation model (LPJ, Smith *et al.*, 2001; Sitch *et al.*, 2003), to correctly predict age-dependent changes in forest growth at scales that are relevant to regional scale carbon budgets. Vegetation dynamics in LPJ are modified to represent growth dynamics in managed, even-aged forests. We evaluate the stand-scale growth function in the model (with both the advanced and original allocation formulations) and its ability to simulate the age-related decline in forest growth with biomass estimates obtained from forest growth and yield-tables (Schober, 1987). Biomass estimates at a regional scale, at which the model is commonly applied, are compared with estimates derived from a collection of forest inventory data for different European provinces, covering a large ecological gradient (Schelhaas *et al.*, 1999). Europe is particularly suitable for such a model test, as its forests are predominately managed and even-aged. The present-day forest C balance is influenced by the response of forest growth to past changes in land-use, intensity of wood-harvesting, and other environmental factors such as climate and atmospheric carbon dioxide concentrations ($[\text{CO}_2]$). The effect of these factors on vegetation C stock dynamics are modelled with the advanced LPJ model. Results are compared with estimates derived from consecutive forest inventories.

4.2 Methods

Model performance is assessed in three steps (see Section 4.2.3). First, stand-scale predictions of biomass are evaluated. Secondly, the applicability of the theory to other stands representative of European forest ecosystems is assessed. Finally, the present-day forest ecosystem C-balance in European forests is inferred from a regional application of the model. The steps are detailed below:

1. In Section 4.3.1, the age-related shifts in growth rate are evaluated within the LPJ-framework of coupled C and H_2O cycles at the stand scale. Growth trends generated by the advanced (*i.e.* based on Magnani's theory on C allocation) and original LPJ model formulations are compared against a yield-table for Scots pine stands in

Germany (see Section 4.2.2). Yield-tables provide detailed descriptions of increment and removals in the typical development of forest stands that allow to assess the changes in growth rate with forest age. Mortality in the stand, which influences the development of biomass with stand age, is prescribed in the simulations from the yield-table to achieve consistency between model and data. Forest growth has substantially increased since the time of the construction of these tables, resulting from improved site management and environmental changes (*e.g.* Mund *et al.*, 2002). These changes need thus to be accounted for in the model-data comparison.

2. Terrestrial biosphere models are typically applied on larger scales, where less information is available to constrain the stand scale dynamics of forests. A generic representation of vegetation dynamics in managed forests is implemented into LPJ to model stand establishment and mortality on a regional scale (see Section 4.2.1). In Section 4.3.2, model performance is evaluated against a comprehensive data-set of forest biomass estimates in terms of ecological gradients and a broad range of species based on forest inventories for different tree species and 77 provinces in Europe obtained from the EEFR-database (see Section 4.2.2). At this stage we assume Magnanis theory holds for all tree species. We evaluate whether the modelled biomass densities are consistent with the data, and thereby infer the broad applicability of the theory within and across plant functional types.
3. Regional forest carbon balances largely depend on the transient effects of land-use and other environmental changes on forest growth, while Section 4.3.2 only gives an evaluation of the model representation of forest growth with age. In Section 4.3.3, the effects of land-use, wood-demand and environmental changes (climate and atmospheric [CO₂]) on the present-day C balance are analysed by explicitly considering forest age-structure in a terrestrial biosphere model. These factors are hypothesised to be to a large extent responsible for the European forest growth trends as inferred from forest inventory for the period 1948-2000.

4.2.1 LPJ

The Lund-Potsdam-Jena model (LPJ, Smith *et al.*, 2001; Sitch *et al.*, 2003) is one of a family of models derived from the BIOME equilibrium biogeography model (Prentice *et al.*, 1992). This study uses the LPJ version as described in Sitch *et al.* (2003), with improved representation of hydrological processes as described in Gerten *et al.* (2004), the leaf dark respiration formulation as in Haxeltine and Prentice (1996a), and adapted for the use of stand scale forest simulations (LPJ-GUESS) as in Smith *et al.* (2001). Sitch *et al.* (2003) give an extensive overview on the model. Here, only the model detail relevant to this study is described.

Vegetation is described in terms of plant functional types (PFTs), with different photosynthetic (C3, C4), phenological (deciduous, evergreen), and physiognomic (tree, grass)

attributes. Of these, boreal and temperate needleleaved evergreen and broadleaved sum-mergreen PFTs are considered in this study, as well as an herbaceous understorey. Gross primary production (*GPP*) is calculated as a function of absorbed photosynthetically ac-tive radiation, temperature, atmospheric $[\text{CO}_2]$, day length, and canopy conductance using a modified form of the Farquhar scheme (Farquhar *et al.*, 1980; Collatz *et al.*, 1992), with implicit leaf-level optimised nitrogen allocation (Haxeltine and Prentice, 1996a). F.-W. Badeck (*unpublished data*) adapted the model to avoid unrealistically high leaf nitrogen concentrations at low temperatures. Carbon and water cycling is coupled through an empirical convective boundary layer parameterisation (Monteith, 1995). Soil hydrology is simulated using two soil layers (Haxeltine and Prentice, 1996b). Plant water uptake is mod-elled taking into account the plant hydraulic architecture (this study, see Appendix 4.6.2). Annual net primary production (*NPP*) is calculated by subtracting autotrophic respiration (R_a) from *GPP*. *NPP* is allocated to three carbon pools representing leaves, sapwood, and fine-roots on the basis of allometric relationships. Turnover of plant tissue, plant mortality and/or management redistribute C from living biomass to above and below-ground litter pools, which in turn provide input to a fast and a slow decomposing soil carbon pool. Decomposition depends on a modified Arrhenius formulation (Lloyd and Taylor, 1994), which implies a decline in apparent Q_{10} values with temperature, and an empirical soil moisture relationship (Foley, 1995).

Changes to the original model formulation

C allocation in plants: The original LPJ allocation scheme assumes a constant ratio of leaf area to sapwood cross-sectional area, a plant size independent, but drought controlled ratio of leaf to root mass and a fixed height to diameter relationship (‘size-independent al-location’, Sitch *et al.*, 2003, Fig. 4.1). In the hydraulic acclimation theory (‘size-dependent allocation’, as in Magnani *et al.*, 2000, see Appendix 4.6.1 for derivation of the allocation scheme), the leaf to sapwood cross-sectional area ratio decreases with increasing height, in response to increasing friction with path length. Simultaneously, plants allocate relatively more C to fine roots, thereby reducing plant below-ground hydraulic resistance, to main-tain a constant leaf-specific water supply with increasing tree height (Fig. 4.1). Table 4.1 summarises the key model parameters introduced into the model that differ from Sitch *et al.* (2003).

Vegetation dynamics in managed forests: Each $10' \times 10'$ grid cell in LPJ is subdivided into fractions of forests, crops and grasslands, as described in (Zaehle *et al.*, in prep.). These fractions, as well as the fractional coverage of each PFT in the forest part of the grid cell, are prescribed from land-use data (Section 4.2.2). To model an entire forest landscape comprising forest stands of different ages, the fraction of the grid cell covered by each PFT is further subdivided into stands consisting of even-aged 10-year age-classes (or cohorts) with a herbaceous understorey. Appendix 4.6.3 gives the details of this module;

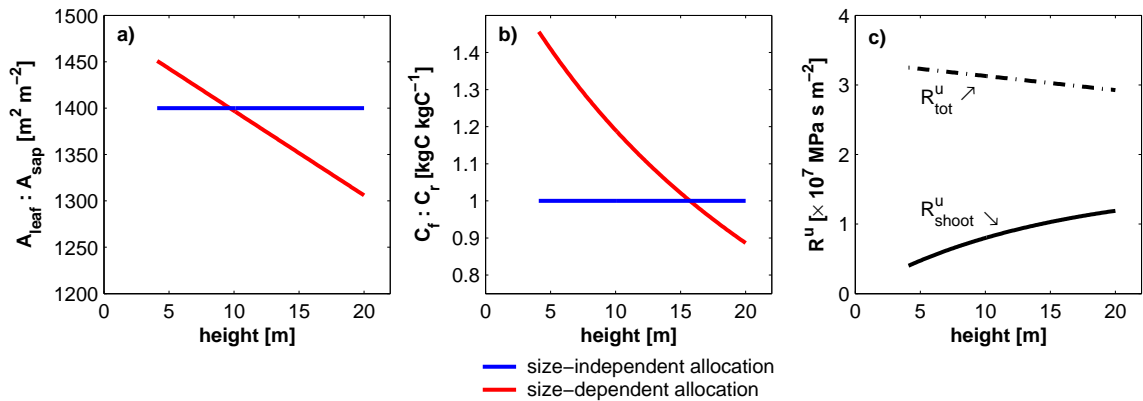


Fig. 4.1: Height dependence of **a)** the ratio of leaf to sapwood cross-sectional area, **b)** the ratio of leaf to root mass, for the original LPJ formulation (‘size-independent’, Sitch *et al.*, 2003), and the acclimation hypothesis by Magnani *et al.* (2000, ‘size-dependent’), under constant environmental conditions. **c)** Changes in leaf-specific hydraulic resistance of the whole-plant (R_{tot}^u) and the shoot (R_{shoot}^u) with tree height as predicted with the size-dependent allocation scheme under constant environmental conditions. Note that R_{tot}^u must decline with height to ensure comparable water supply to leaves, as the gravitational potential increases with height (see Appendix 4.6.1, eq. 4.7).

	k_r^a	k_s^b	τ_r^c	τ_s^d	E_{un}^e	SLA^f	$\Psi_{leafmin}^g$	T_{rot}^h
TeNE	2.3	1.3	1.5	0.025	4.2	9.8	-2.0	120
TeBS	2.3	3.0	1.5	0.02	4.2	41.2	-2.0	150
BNE	2.3	1.3	1.5	0.025	4.2	9.8	-2.0	100
BBS	2.3	3.0	1.5	0.02	4.2	41.2	-2.0	80
TeH	2.3	n.a.	1.5	n.a.	4.2	41.2	-1.5	n.a.

^a specific root hydraulic conductance [$10^{-7} \text{ m}^3 \text{ kg}^{-1} \text{ s}^{-1} \text{ MPa}^{-1}$]; Roberts (1977); Magnani *et al.* (2000), similar to Rüdinger *et al.* (1994); Steudle and Meshcheryakov (1996); Nardini *et al.* (1998).

^b specific sapwood conductance [$10^{-3} \text{ m}^2 \text{ s}^{-1} \text{ MPa}^{-1}$]; Magnani *et al.* (2000); Larcher (2001).

^c turnover time of fine roots [yr^{-1}]; Vogt *et al.* (1996); Eissenstat and Yanadi (1997); Eissenstat *et al.* (2000); Magnani *et al.* (2000).

^d turnover time of sapwood [yr^{-1}]; Bartelink (1998); Magnani *et al.* (2000).

^e maximum transpiration rate per unit leaf area [10^{-8} m s^{-1}]; Magnani *et al.* (2000).

^f specific leaf area; Reich *et al.* (1992); Magnani *et al.* (2000).

^g minimum leaf water potential [MPa]; Larcher (2001); Hickler *et al.* (2004).

^h PFT-specific rotation period length in equilibrium [yr]; Nabuurs and Mohren (1995).

Tab. 4.1: Parameter values for the ‘size-dependent’ allocation scheme (see Appendix 4.6.1), as well as rotation period length in equilibrium for woody PFTs (see Appendix 4.6.3).

TeNE: temperate needle-leaved evergreen, TeBS: temperate broadleaved summergreen, BNE: boreal needle-leaved evergreen, BBS: boreal broadleaved summergreen, TeH: temperate grass (C3). All other parameters as in Sitch *et al.* (2003)

the important features are summarised as follows:

Balances and fluxes of C and H₂O are calculated for each stand separately. The average current annual increment at equilibrium (see Section 4.2.3) is used to determine the grid cell specific productivity, and thereby the initial amount of total fellings from forest management for each PFT. This locally adapted level of harvesting allows to scale country-wide trends in wood demand derived from forest statistics (Section 4.2.2) to a fine-resolution grid in the transient phase of a simulation. However, this assumes steady-state at the beginning of the transient simulation (1901). Estimates of the natural self-thinning in each stand (adapted from Smith *et al.*, 2001), as well as the amount of clear-cut felling required to maintain a PFT specific rotation-period (T_{rot}) are used to partition the total fellings into thinnings and clear-cut fellings. The fraction of forest lost due to stand-replacing fires in each age-class are estimated with the regional fire module of LPJ (Reg-FIRM, Venevsky *et al.*, 2002), taking account of aboveground litter stocks and moisture and PFT-specific fire resistances. Cleared fractions of the grid cell, either by management or fire, are transferred into an ‘area pool’ from which new cohorts are established every ten years. The level of total fellings can have an effect on the average rotation time of the forests, and on the area available for replanting, thereby affecting forest age-structure in addition to changes in forest area.

Representation of autotrophic respiration (R_a): Two alternative hypotheses exist to calculate R_a . The approach implemented in LPJ deduces R_a from tissue size, a tissue-specific, temperature-dependent maintenance respiration rate and a substrate-dependent growth respiration rate (‘LPJ-g&m’, Sitch *et al.*, 2003). An alternative approach is to assume R_a to be entirely substrate dependent (‘LPJ-sub’). This implies that R_a is a constant fraction of GPP , as often observed over longer time-scales (Waring *et al.*, 1998), or as emergent property of a model (Dewar *et al.*, 1999). With increasing temperature, the fraction of GPP lost to R_a is greater in ‘LPJ-g&m’ than in ‘LPJ-sub’. In this study, the ‘LPJ-g&m’ formulation is used unless explicitly stated otherwise.

4.2.2 Data

Forest yield-tables and inventory data

Estimates of the typical age-dependent development of growing stock, gross annual increment, biomass losses due to harvesting and natural mortality in German Scots pine stands are obtained for high, medium and low productivity site-classes from yield tables by Schober (1987). Biomass expansion equations from Marklund (1988) and the CO2FIX model (Version 2.0, Maser *et al.*, 2003) are used to estimate total stand C and increments, as described in Kaipainen *et al.* (2004).

Timber stocks and increments across large heterogeneous regions can be obtained from forest inventories. These rely on a large number of field measurements – typically taken from managed forests – specifically designed to supply statistically sound measurements on

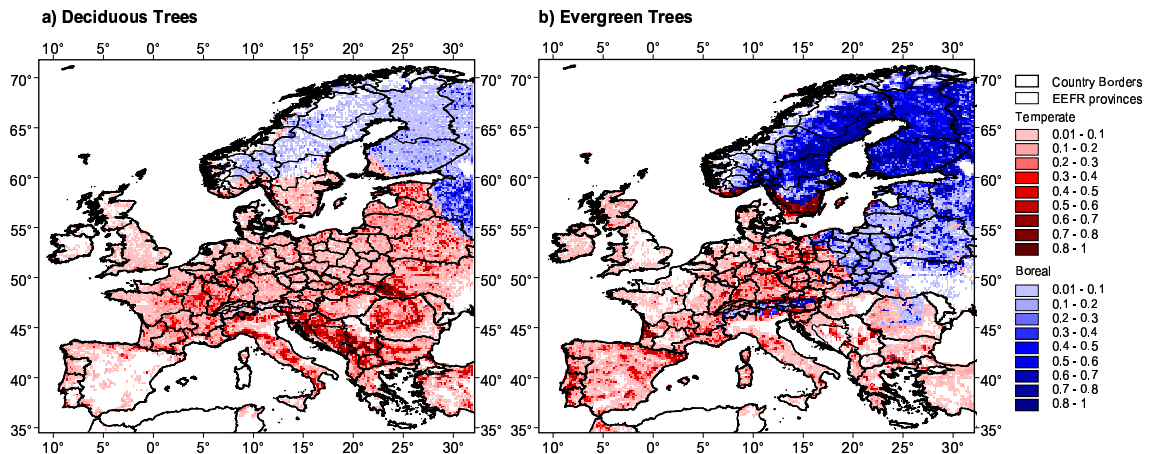


Fig. 4.2: Provinces of the EEFR-data base and fractional coverage of **a)** broadleaved and **b)** evergreen forests, separated into boreal (blue) and temperate (red) PFTs by bioclimatic limits.

larger scales (Köhl *et al.*, 1997). Forest inventories give relatively accurate information on the aboveground growing stock volume in forests. However, total C stocks in vegetation need to be inferred using biomass expansion factors (BEFs, Kauppi *et al.*, 1992; UN-ECE/FAO, 2000; Watson *et al.*, 2000). Estimates of soil C stocks can only be derived from modelling (*e.g.* Liski *et al.*, 2002).

Forest inventories of European countries are yet to be harmonised, and differ in their method of estimating growing stock, sometimes even between provinces within countries (Köhl *et al.*, 2000). Estimates of standing volume and gross annual increment are taken from the EEFR-database (Schelhaas *et al.*, 1999), which is a collection of national inventories of 32 European countries on a provincial level. These data have been collected mainly between 1985 and 1999. For the evaluation of regional growth patterns, data are standardised in 20-year age-classes by tree species and province to achieve comparability between countries. Sufficient data are available for 74 (broadleaved trees) and 77 (coniferous trees) provinces. Estimating total vegetation C from growing stock is still a subject of intensive research (Laitat *et al.*, 2000; Lehtonen *et al.*, 2004). Since the database contains no information to enable conversion of volume data into total vegetation C, such as diameter at breast height and tree height (Wirth *et al.*, 2004), country-specific BEFs for coniferous and broadleaved trees were used, based on UN-ECE/FAO (2000, see Table 4.2).

Data to drive the model

Monthly fields of mean temperature, precipitation and cloudiness are taken from the CRU2000 monthly climate data on a $10' \times 10'$ European wide grid, for the years 1901-2000, provided by the Climate Research Unit (CRU, Mitchell *et al.*, 2004). Data on the annual CO₂ content of the atmosphere are obtained from Keeling and Whorf (2003). Available water holding capacity, percolation coefficients and soil water characteristics are derived

<i>Country</i>	<i>Below-ground Biomass (Broadleaved & Conifers)</i>	<i>Above-ground biomass (Conifers)</i>	<i>Above-ground biomass (Broadleaved)</i>
Belgium (BE)	0.09	0.39	0.52
Denmark (DK)	0.18	0.40	0.55
Finland (FI)	0.10	0.53	0.64
France (FR)	0.07	0.40	0.53
Germany (DE)	0.14	0.50	0.50
Italy (IT)	0.12	0.42	0.56
Luxembourg (LU)	0.12	0.52	0.66
Netherlands (NL)	0.27	0.61	0.74
Norway (NO)	0.10	0.51	0.69
Poland (PL)	0.07	0.41	0.58
Sweden (SE)	0.11	0.58	0.67
Switzerland (CH)	0.18	0.41	0.68
United Kingdom (UK)	0.14	0.43	0.83

Tab. 4.2: Country-scale conversion factors to scale inventoried volume data to total vegetation biomass [Mt oven-dry m⁻³ o.b.], taken from Annex 3B.1 (UN-ECE/FAO, 2000). Data are transformed to carbon density assuming a carbon density in biomass of 0.5 kgC kg⁻¹.

from soil texture (IGBP-DIS, 2000, aggregated to the 10' × 10' grid), based on Saxton *et al.* (1986). Soil thermal properties are also based on the IGBP-DIS soil data set (2000), as in Melillo *et al.* (1995).

Actual distribution of tree species is derived from a compilation of an area corrected forest cover map (Schuck *et al.*, 2002), an analysis of ICP level 1 and 2 data (Köble and Seufert, 2001), and bioclimatic limits as in Sitch *et al.* (2003, Fig. 4.2). Land-use history for Europe on the 10' × 10' grid are constructed from FAO land-use statistics (1961-2000, FAOSTAT, 2004) and forest resource assessments (1948-1960, FAO, 1948, 1955, 1960), see Appendix 4.6.4. Changes in felling intensity and country-specific parameters describing stem volume to total tree biomass ratios, harvest efficiency, partitioning of removals to fuel and industrial wood are also based on FAO forest resource assessments (FAO, 1948, 1955, 1960, 1976; UN-ECE/FAO, 1985, 1992, 2000). Sufficient data are available for all European countries with the exception of Belarus, Moldova, Russia and Ukraine.

4.2.3 Modelling protocol

Stand-level model evaluation

LPJ is run at a typical location (52°N, 10°E) with constant, thirty-years monthly average climatology and atmospheric CO₂ concentration (averaged over the years 1941-1970) to reduce a potential bias due to confounding effects of past changes in environmental conditions on stand development (Mund *et al.*, 2002). Diameter and height from the yield-tables are used to estimate the parameters k_{allom2} and k_{allom3} in LPJ's diameter to height relationship (Eq. 4.12, see Appendix 4.6.1), using a Nelder-Mead simplex method. Vegetation

dynamics are controlled in this experiment by prescribing mortality in the stand from the volume loss of the yield table. We vary one parameter at a time by $\pm 10\%$ around the standard value to estimate parameter sensitivity, and then vary all parameters at the same time, equally by $\pm 10\%$, to examine the extreme cases.

Regional evaluation of modelled growth patterns

The model, including the generic representation of vegetation dynamics in managed forests (see Section 4.2.2), is spun up to pre-industrial equilibrium in terms of stable vegetation and soil C pools, as well as vegetation dynamics, including age-class distribution and total fellings. For this spin-up, LPJ is run for 900 simulation years recycling monthly climatology for the years 1901 to 1930 with pre-industrial atmospheric $[\text{CO}_2]$, as well as assigned present-day forest area and tree species distributions. In the transient phase, climate and atmospheric $[\text{CO}_2]$ vary as observed between 1901 and 2000. For comparison with regional inventory data, averages of growing stock in 1986-1995 are calculated and aggregated to twenty-year age-classes for each district of the EEFR-database. Model-data agreement for each of these regions and tree species is assessed as root mean square error (RMSE),

$$RMSE = \sqrt{\frac{1}{n} \sum_{i=1}^n (m_i - d_i)^2} \quad (4.1)$$

where m_i and d_i are the simulated and inventory-derived estimates of biomass in kgC m^{-2} for an age-class i , respectively.

Regional application of the model to infer forest C balance

LPJ is spun up to equilibrium as in Section 4.2.3 above, but reconstructed land-use patterns from the beginning of the century are incorporated. This section follows a factorial design with three separate runs in order to attribute changes in age-structure, vegetation biomass and land-atmosphere fluxes to observed changes in climate and atmospheric $[\text{CO}_2]$ ('C'), changes in land-use ('L'), and changes in wood demand ('D') between 1948 and 2000. In 'C', only climate and atmospheric $[\text{CO}_2]$ are varied, with forest area and wood demand held constant at 1901 levels. In 'L', land-use patterns are changed in addition (see Section 4.2.2, and Appendix 4.6.4), with wood demand on a per grid cell basis held constant at 1901 levels, implying a change in removals per area inversely proportional to the change in forest area. In 'D', in addition to climate, atmospheric $[\text{CO}_2]$, and land-use, wood demand is adjusted for the period 1948-2000 as derived from the FAO forest resource assessments (Section 4.2.2). Afforestation after 1948 is the only factor (apart from environmental changes) influencing forest soil C stocks, in 'L' and 'D'. Soil C pools of afforested land are initialised with results of LPJ's cropland module (Bondeau *et al.*, in prep.), taking account of the actual crop and grassland distribution. Cropland soil C

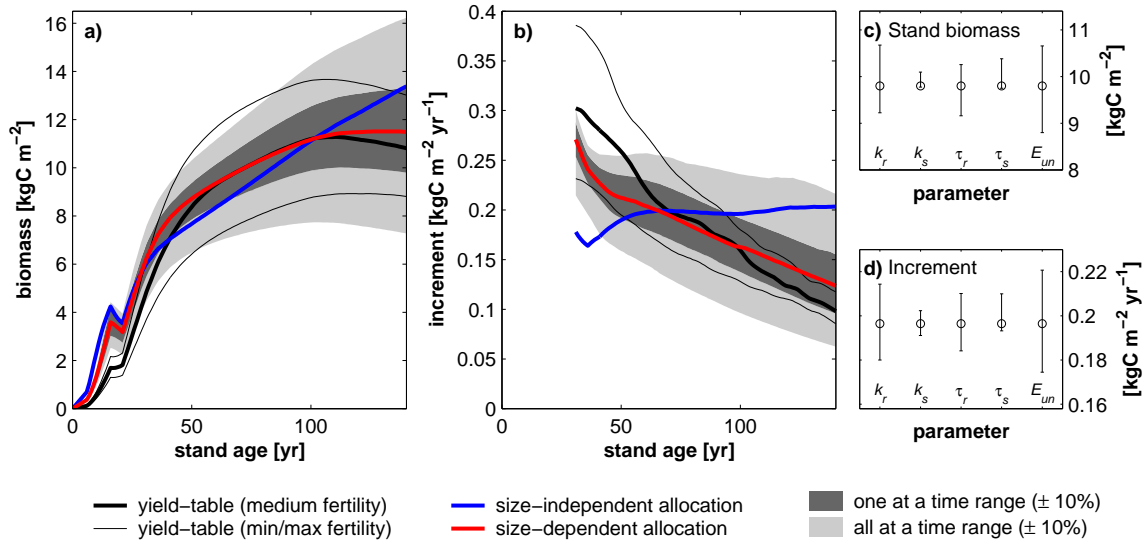


Fig. 4.3: Five-year running mean of **a)** biomass in vegetation [kgC m^{-2}], and **b)** net increment [$\text{kgC m}^{-2} \text{yr}^{-1}$] of *Pinus sylvestris* in Germany (Schober, 1987) for low, medium and high fertility site classes, compared to a model run of LPJ with size-independent allocation scheme (Sitch *et al.*, 2003), and size-dependent allocation (Magnani *et al.*, 2000). Vegetation biomass is the integral of net increments and removals from thinnings. **c)** and **d)** show the parameter sensitivity for the five parameters of the size-dependent allocation scheme (see Table 4.5 for parameter-key) as difference in vegetation biomass and increment in a 60-years old stand.

stocks are typically lower than soil C stocks in forests (Guo and Gifford, 2002). Effects of previous land degradation (*e.g.* Glatzel, 1999) are not taken into account.

4.3 Results

4.3.1 Stand-level model evaluation

Figure 4.3 shows that, in the yield-table, the growth rate declines markedly after canopy closure for all three site classes considered, attaining peak biomass at around 100 years. In the original LPJ formulation, carbon is allocated to plant tissues with fixed proportions of leaf, root and sapwood area (Fig. 4.1). After canopy-closure, this scheme predicts an increasing proportion of *GPP* lost through maintenance respiration to support the increasing living biomass with stand age (Yoda *et al.*, 1965; Kira and Shidai, 1967). On the stand level, this increase contributes little to the age-related decline in the net increment of trees, seen in Figure 4.3 as constant growth rate in stands older than 45 years. These results agree with experimental evidence presented in Ryan and Waring (1992) and Ryan *et al.* (1995). A slight increase in growth with age is modelled, resulting from larger per-unit leaf area photosynthesis at lower LAI as stands become less dense with age.

Following Magnani *et al.* (2000), the proportional allocation of C to fine roots and shoot increases with increasing tree height to maintain comparable levels of canopy conductance

compensating for an increase in above-ground hydraulic resistance with path length (see Fig. 4.1). The resulting additional allocation of biomass away from photosynthetic tissue is costly, and results in reduced growth efficiency with age. However, while the relative decline in growth is correctly modelled in LPJ with the size-dependent allocation scheme by Magnani *et al.* (2000), the actual size of growing stock and increment is less than predicted from the yield table with the original parameterisation of physiology in LPJ (results not shown). In the size-dependent scheme below-ground costs are higher, because of the considerably higher turnover of fine roots compared to the original value in LPJ (fine root longevity of 0.65 years as opposed to 3.0 years). Setting the growth predicted from the yield-table and the biomass-allocation patterns derived from Magnani as a constraint to modelled gross primary production from LPJ, values for LPJ parameters affecting the rate of assimilation per unit leaf area can be inferred. After adjusting the radiation use efficiency in LPJ (by changing α_a from 0.5 to 0.75) both simulated biomass and net increment compare well with the yield-table based estimates, as demonstrated in Figure 4.3.

The size-dependent allocation scheme has five parameters that functionally link root, shoot and leaf C pools (k_r , k_s , τ_r , τ_s , E_{un} , see Table 4.1). The decline of forest growth is robustly modelled, when varying one parameter at a time by $\pm 10\%$ around its standard value (dark grey area in Fig. 4.3). Decreasing growth efficiency still leads to a decline of forest growth with age when varying all parameters at the same time by $\pm 10\%$. However, the decline is considerably less, if the costs of sustaining a unit leaf area are low (*e.g.* high k_r in combination with low E_{un}), seen as the upper uncertainty bound in Figure 4.3b. While changes in the allometric ratios of leaf mass to sapwood area or leaf to root mass with height are similar between alternative parameterisations, modelled biomass density in 140-years old stands differs by up to $\pm 50\%$ from the result obtained under standard parameterisation. The investment costs of roots, *i.e.* root hydraulic conductance and root longevity, are more important than the corresponding parameters for sapwood. The maximum transpiration rate per unit leaf area (E_{un}) exerts the strongest influence on model results. Lower values of E_{un} decrease the investment costs per unit leaf area, thereby enhancing growth, however, at the increased risk of water limiting photosynthesis in dry conditions.

4.3.2 Regional evaluation of modelled growth patterns

Modelled biomass densities for different age-classes compare favourably with estimates derived from the EEFR-database for most regions and for both coniferous and broadleaved PFTs (Table 4.3), as shown exemplary for a boreal (Northern Finland), temperate (Germany, Hessen), and Mediterranean (Italy) province/country in Figure 4.4. The coefficient of determination between biomass estimates of different age-classes from EEFR-data and LPJ for individual provinces is typically higher than 0.75, with few exceptions in provinces where inventoried biomass is very low (*e.g.* northern Norway), or shows unrealistic changes

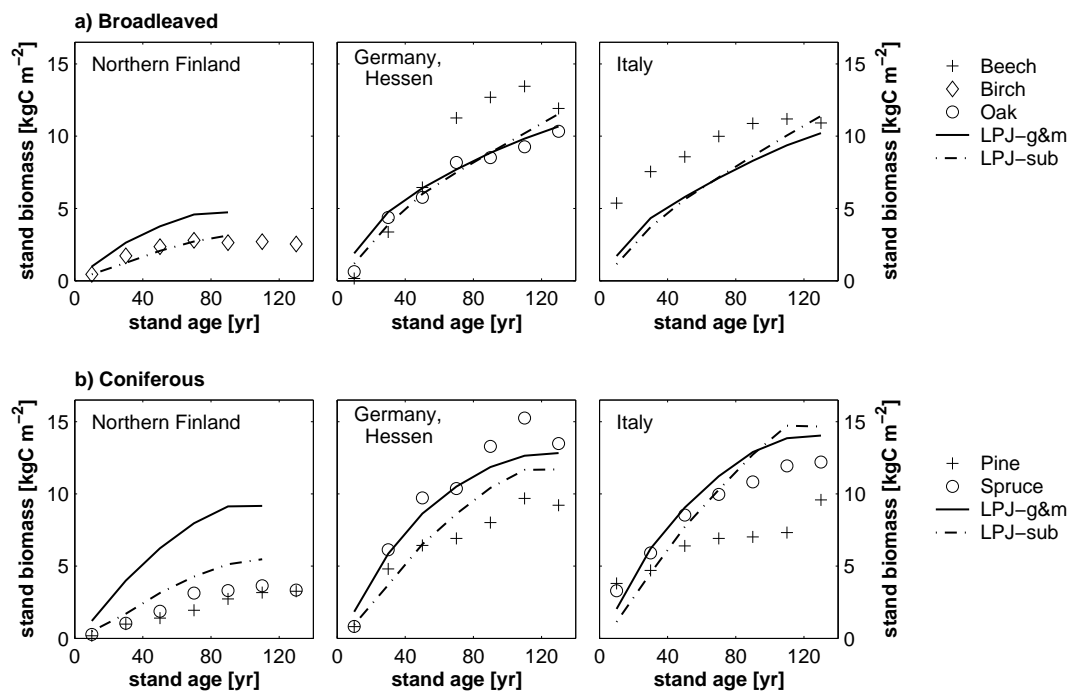


Fig. 4.4: Comparison of vegetation C estimates (including the below-ground component) derived from the EEFR-data base (Beech, Birch, Oak, Pine and Spruce) to estimates by LPJ for a boreal (Northern Finland), temperate (Hessen, Germany), and mediterranean (Italy) province. **a)** Boreal or temperate broadleaved summer green PFT, **b)** boreal and temperate needle-leaved evergreen PFT.

from age-class to age-class (*e.g.* Scots pine in Wales). For a given province, the largest contribution to the model error is typically due to overestimation of biomass in old stands. This could be attributed to either under prediction in the age-related decline or underestimated harvest intensity/mortality in older stands. It is not possible to confirm either hypothesis from the data available.

Figure 4.5 shows that the average biomass densities of data and model compare relatively well for most countries, for which suitable data are available. Average model errors (expressed as RMSE, see Section 2.3.2) by region are 3.70 (0.49-8.89) kgC m^{-2} for coniferous and 2.07 (0.56-7.02) kgC m^{-2} for broadleaved PFTs (Table 4.3). The disagreement is larger for conifers because of systematic overestimation of biomass by the model in parts of France, Poland and Scandinavia (see below). The fact that inventoried biomass differ substantially between coniferous species (*i.e.* spruce and pine), but are quite similar for broadleaved species (*i.e.* oak, beech and birch) also contributes to the larger difference in conifers. For instance, the coniferous PFT modelled by LPJ agrees well with Scots pine in the southern German provinces of Bavaria and Baden-Württemberg, where vegetation C stocks are generally high, but better with Norway spruce in the eastern province of Brandenburg, where inventoried biomass densities are low. Average conifer RMSE for all three regions are, however, fairly similar, resulting from the substantial difference in

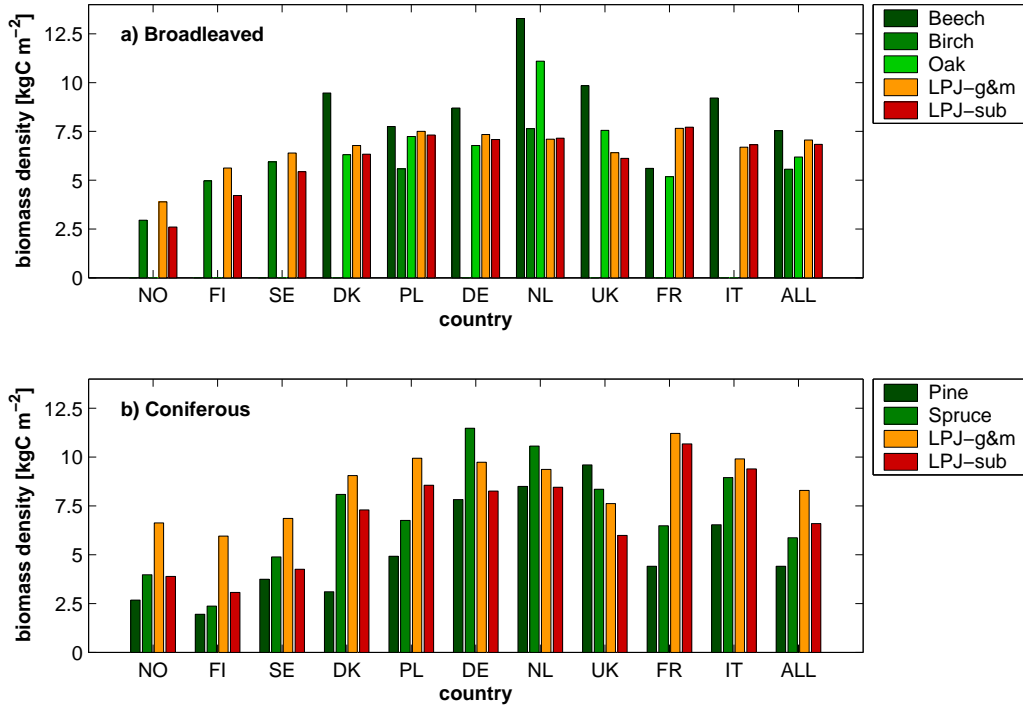


Fig. 4.5: Biomass densities [kgC m^{-2}] in European forests by country as estimated from the EEFR-database (Beech, Birch, Oak, Pine and Spruce) and simulated with LPJ, giving equal weight to each age-class to facilitate comparison between data and model (see Table 4.2 for country-key). **a)** Boreal or temperate broadleaved summer green PFT, **b)** boreal and temperate needle-leaved evergreen PFT.

Country	LPJ-g&m			LPJ-sub			LPJ-g&m		LPJ-sub	
	Beech	Birch ^a	Oak	Beech	Birch ^a	Oak	Pine	Spruce	Pine	Spruce
Norway	n.a.	1.96	n.a.	n.a.	1.79	n.a.	4.60	3.18	1.99	1.35
Finland	n.a.	0.76	n.a.	n.a.	0.90	n.a.	4.59	4.09	1.86	1.44
Sweden	n.a.	2.04	n.a.	n.a.	2.10	n.a.	3.63	2.44	1.59	1.46
Denmark	3.93	n.a.	0.95	4.02	n.a.	0.47	6.27	1.45	4.58	1.09
Poland	2.14	2.11	1.38	2.00	2.23	1.25	4.28	1.46	4.36	1.88
Germany	2.30	n.a.	1.19	2.23	n.a.	1.18	2.47	2.80	2.02	3.95
Netherlands	7.02	1.93	4.78	6.82	2.01	4.44	1.38	2.52	1.67	3.12
United Kingdom	5.04	n.a.	1.96	5.00	n.a.	2.03	4.89	3.00	3.53	3.70
France	2.19	n.a.	2.57	2.39	n.a.	2.82	7.40	5.25	7.31	5.30
Italy	2.68	n.a.	n.a.	2.82	n.a.	n.a.	3.31	2.68	4.36	3.62
Average	2.44	1.83	1.95	2.51	1.90	2.03	4.25	3.15	2.77	2.34

^a Data for Norway and Sweden are for all broadleaved species, assembled in group.

Tab. 4.3: Country average root mean square error [RMSE, kgC m^{-2}] of biomass estimates of LPJ as compared to the EEFR-database according to tree species (see Section 4.2.3). Averages for all European countries are obtained as forest area-weighted mean. ‘LPJ-g&m’ refers to the standard LPJ formulation of R_a , whereas ‘LPJ-sub’ refers to the substrate limited mode (see Section 4.2.3).

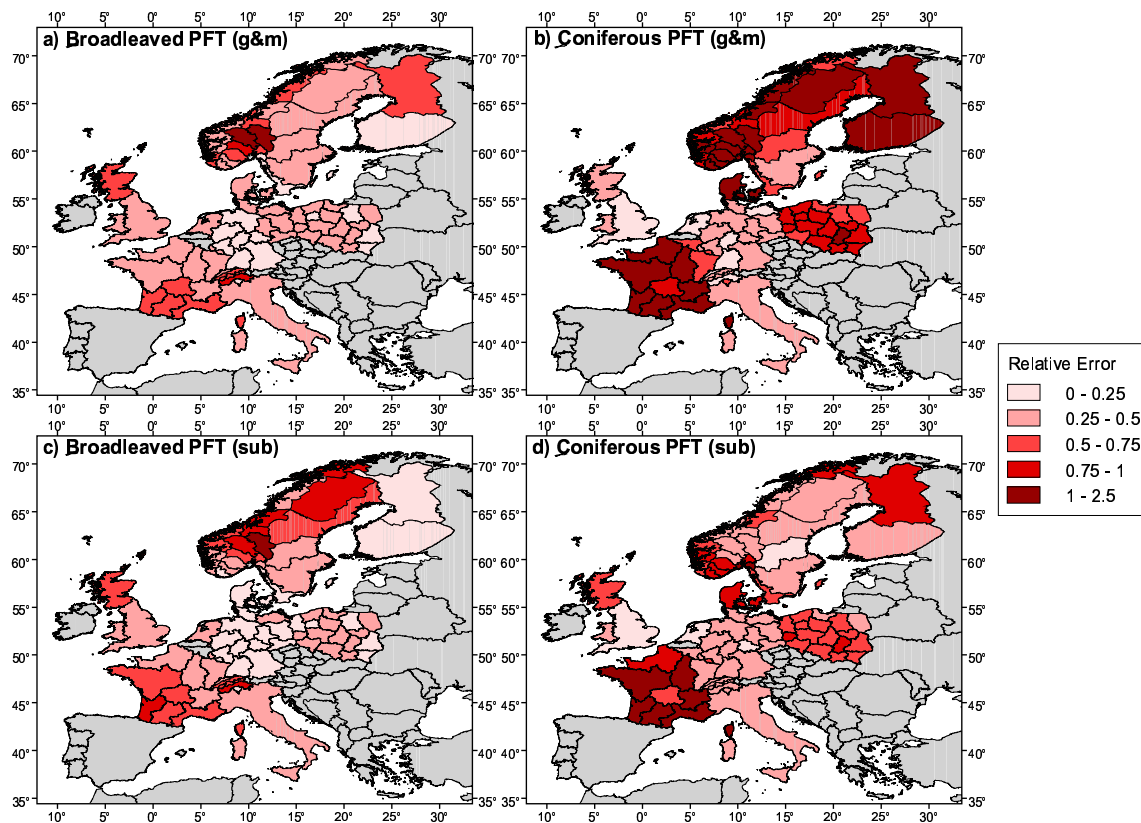


Fig. 4.6: Average relative error of biomass estimates by LPJ, expressed as the ratio of root mean square error and inventory-based biomass density for **a,c**) broadleaved and **b,d**) coniferous PFTs (or tree species), using either ‘LPJ-g&m’ or ‘LPJ-sub’.

biomass density between Norway spruce and Scots pine in these provinces.

Spatial maps of the relative model-data difference (Fig 4.6 a,c) suggest that for broadleaved species relative differences between model and data are largest in southern Norway and southern France, but relatively low for most other regions. The error in these regions results from over prediction in simulated biomass. However, in Norway the largest error occurs in regions where inventoried stocks range between 1.5 and 2.4 kgC m⁻², such that the absolute over prediction is quite low, whereas in southern France inventoried biomass ranges between 5.0 and 6.5 kgC m⁻². The error mostly results from overpredicted simulated biomass stocks in older stands. However, it is not clear, whether past disturbance or a too slow decline in the simulated growth rate is the cause for this.

Similar maps for conifers (Fig. 4.6b,d) show the largest model-data differences in France, Poland and Scandinavia. In Poland and France, larger model-data differences may be partly attributed to the low coefficients to scale volume data to biomass (Table 4.2). The systematic overestimation is reduced when the European average BEFs are used instead of the country-specific coefficients for the volume-biomass conversion (Table 4.2, *results not shown*). However, modelled biomass densities in southern France would still be too high. A comparison of *NPP* modelled by LPJ with results from the *NPP*-intercomparison

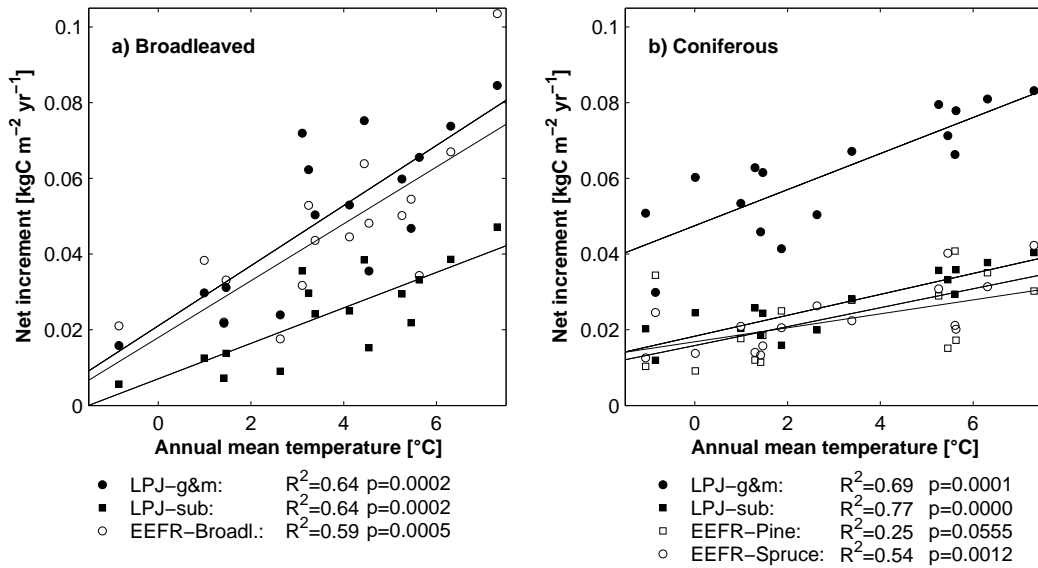


Fig. 4.7: Average growth rate in the first 20 years after stand establishment along a gradient in annual mean temperature for EEFR-provinces in Norway, Sweden and Finland for a) broadleaved and b) coniferous PFTs (or tree species).

(Cramer *et al.*, 1999; Kicklighter *et al.*, 1999), and data from the Ecosystem Model-Data Intercomparison project (EMDI, Olson *et al.*, 2001) suggests that *NPP* in boreal ecosystems is overestimated with the standard LPJ formulation of R_a ('LPJ-g&m'; *results not shown*). Using the alternative formulation ('LPJ-sub'), this overestimation is reduced. Biomass estimates for Scandinavian conifers simulated with 'LPJ-sub' are in better agreement with the data (see Fig. 4.6d). However, improvement with this alternative formulation is not unequivocal, with slight deterioration in the model-inventory data agreement for temperate conifers, and broadleaved species. This increased difference results partly from a smaller age-related decline in growth rate predicted with 'LPJ-sub', as increasing sapwood respiration costs no longer contribute to R_a . Overall model error is, however, substantially reduced (Table 4.3), primarily because of the improved estimation of biomass in boreal Europe.

Figure 4.7 shows that net increments estimated for the first 20 years of stand development from the EEFR-database decline significantly with decreasing annual mean temperature on a South to North gradient in Scandinavia, for Scots pine and Norway spruce, and broadleaved species (pooled into one group to obtain a greater spatial coverage). Such a trend is also apparent in estimates of increment from LPJ, irrespective of the hypothesis used to model R_a . In the EEFR-data, no trend is notable with respect to climatic water deficit within a country. It is not possible to assess the gradient across countries along a East-West transect, because different country-specific biomass expansion factors lead to significant, but artificial, gradients when pooling the data of two or more countries.

4.3.3 Regional application of the model to infer the forest carbon balance

Simulated C stocks in vegetation (11.3 PgC, corresponding to 7.4 kgC m^{-2}) as well as litter and soil (17.9 PgC, corresponding to 11.8 kgC m^{-2}) are larger than estimates based on forest inventories for vegetation (7.7 PgC excluding woodlands, plus 1.0 PgC dead wood, the total corresponding to 6.0 kgC m^{-2}) and soil (13.0 PgC, plus 0.7 PgC forest floor, the total corresponding to 9.2 kgC m^{-2}) (Goodale *et al.*, 2002). Some overestimation of vegetation C would be expected based on the results in Section 4.3.2, particularly in boreal ecosystems (see Figure 4.6b). In addition, all forests were assumed to be managed as ‘high forest’ with rotation period lengths between 80 and 150 years, whereas management strategies may differ regionally. Management strategies such as ‘coppice with standards’, as practiced in the Mediterranean region, or forests with shorter rotation times would imply lower average vegetation C stocks. The biomass estimate of LPJ also accounts for understorey vegetation, whereas inventory-based estimates typically only account for biomass in trees above a diameter threshold. Considering model and data uncertainty, however, the simulated C stock estimates appear acceptably close to the inventory-based estimates.

Figure 4.8a shows that observed climatic changes and CO_2 fertilisation in the 20th century (‘C’) lead to a continuous rise in simulated forest vegetation C stocks between 1950 and 2000, reaching an average rate of increase of about $40 \text{ gC m}^{-2} \text{ yr}^{-1}$ over Europe in the 1990s. Forest area increase (depicted in Fig. 4.8d) more than compensates the growth enhancement per unit area until the 1960s (‘L’) because of the large proportion of very young stands (but see also Appendix 4.6.3). Thereafter forest vegetation C increases per unit area are quicker than with environmental changes alone (1990s average: $58 \text{ gC m}^{-2} \text{ yr}^{-1}$) as the afforested stands reach their maximum growth rate. Increasing harvest rates since the 1950s lead to somewhat smaller increases in the growth rate after 1975, when changes in wood demand are also considered (‘D’). Growth rates reach similar levels in the late 1990s, when wood demand shows a marked decline (Fig. 4.8c).

Observed climatic changes and CO_2 fertilisation in the 20th century (‘C’) result in a net increase in the vegetation carbon stock of about 57 TgC yr^{-1} in the 1990s, distributed almost equally across Europe (Table 4.4). Afforestation since 1948 in addition to changing environmental conditions (‘L’) leads to a net uptake of 107 TgC yr^{-1} in vegetation. The simulated forest age-class distribution is in good agreement with present-day inventory-based estimates from (UN-ECE/FAO, 2000, see Fig. 4.8b). This shift towards younger forests increases overall forest increment, as demonstrated in Figure 4.3. The amount of wood removed from forests has not been constrained by inventory-based estimates of removals (see Appendix 4.6.3). Instead, it is based on the average forest increment in equilibrium, modified by the observed changes in removals since 1948 (‘D’). The modelled removals of about 95 TgC yr^{-1} in the 1990s are surprisingly close to the 96 TgC yr^{-1} estimated for 1990 from inventory data (Nabuurs *et al.*, 2003, Fig. 4.8c). In ‘D’, the modelled removal to increment ratio in the 1990s of 0.53 is very close to the 0.55 obtained

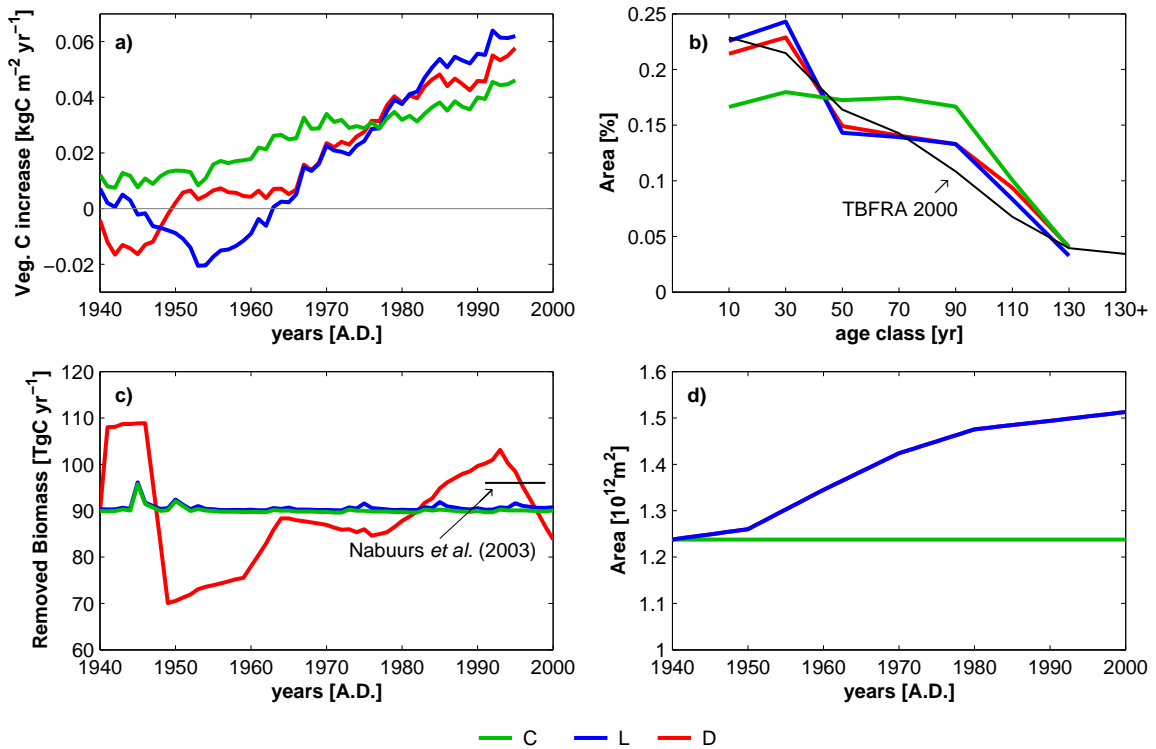


Fig. 4.8: **a)** 10-year running average of the net increase in vegetation C stocks resulting from the effect of observed changes in climate and atmospheric $[\text{CO}_2]$ ('C'), the former plus increasing forest area ('L') and all of the aforementioned factors and including changes in wood demand ('D') for Europe, excluding Belarus, Moldova, Russia and Ukraine. **b)** Age-structure of forests in the 1990s, as simulated by LPJ and documented in forest statistics (black line, UN-ECE/FAO, 1992, 2000). **c)** Removals of timber from forests, including an estimate based on forest statistics from Nabuurs *et al.* (2003). **d)** Change in forest area, as derived from forest statistics (similar in 'L' and 'D').

from (UN-ECE/FAO, 1992, 2000). Taking all forcing factors into consideration, modelled net C uptake in forest vegetation is about 100 TgC yr^{-1} in the 1990s.

Estimates of present-day net C uptake are within the range of estimates obtained by inventory-based studies (see Table 4.4). Nabuurs *et al.* (2003) estimate an average increase in vegetation C of 48 TgC yr^{-1} between 1950 and 1999, tracking net increments and removals in European forest based on inventory data between 1948 and 2000. They note that net increments in the inventory data prior to 1976 may have been underestimated, resulting in an underestimation of C uptake of up to 15 TgC yr^{-1} . Average net C uptake in vegetation would still be 10 TgC yr^{-1} smaller than the average uptake between 1950 and 1999 of about 73 TgC yr^{-1} estimated in this study.

A full forest sector carbon balance comprises includes changes in litter and soil C stocks, as well as in wood products. For a given grid cell, the development of net ecosystem production (NEP ; the difference of NPP and carbon losses from heterotrophic respiration, R_h , where positive values denote terrestrial C uptake) with stand age is in

<i>Terrestrial carbon uptake</i>					
	<i>Vegetation</i>	<i>Litter & Soil</i>	<i>Products</i>	<i>Total</i>	<i>Reference area</i>
	[TgC yr ⁻¹]				[10 ⁶ km ²]
LPJ					
Climate and [CO ₂] change	57.1	-1.9	0.1	55.4	1.23
+ Land-use change	106.7	9.7	-0.1	116.3	1.51
+ Wood-demand change	100.3	7.6	3.2	111.1	1.51
Literature					
Nabuurs <i>et al.</i> (2003)	98	42	2	142	1.4
Liski and Kauppi (2000)	110				1.76
Päivinen <i>et al.</i> (1999)	69				1.4
Kauppi and Tomppo (1993)				130-194 ^a	1.44
<i>Net Ecosystem Production</i>					<i>Reference area</i>
	[TgC yr ⁻¹]				[10 ⁶ km ²]
LPJ					
Climate and [CO ₂] change		146.0 ^b			1.23
+ Land-use change		194.2 ^b			1.51
+ Wood-demand change		189.8 ^b			1.51
Literature					
Papale and Valentini (2003)		278 ^{cd}			1.51

^a but excluding wood products. Also this estimates refers to the 1980s.

^b flux estimates do not account for C losses from wood products or biomass burning

^c flux estimates do not account for C losses from any disturbance

^d derived from scaling the average annual uptake per unit area to the European forest area, as in Janssens *et al.* (2003).

Tab. 4.4: Changes in terrestrial C pools [TgC yr⁻¹] in the 1990s as modelled with LPJ, and from inventory-based studies, as well as net ecosystem production [$NEP=NPP-R_a$, TgC yr⁻¹] estimated with LPJ and from eddy-covariance measurements. Positive NEP denotes an increase in terrestrial C stocks.

general agreement with several chronosequence studies of NEP in different forest ecosystems based on eddy-covariance data (Churkina *et al.*, 2003; Law *et al.*, 2003; Campbell *et al.*, 2004; Kolari *et al.*, 2004; Kowalski *et al.*, 2004, *results not shown*). Clear-cut felling turn forest stands from a moderate C sink to a moderate net C source. Stands begin to sequester C some years after the disturbance, however, the exact timing of this varies between regions depending on the growth rate of forests and the amount and decay rate of slash. Net C uptake generally peaks around the time of canopy closure, however, as long as thinning, *i.e.* C removal from the site, continues, stands exhibit a positive NEP . LPJ estimates of annual C exchange are generally lower than eddy-covariance based estimates (*e.g.* Kolari *et al.*, 2004). However, a detailed analysis of the causes for this is beyond the scope of the present analysis, and site specific management actions may have contributed to the apparent underestimation.

European scale forest NEP obtained from upscaling eddy-covariance measurements of several forest stands (Papale and Valentini, 2003) amounts to 278 TgC yr⁻¹. This

is substantially higher than the 189 TgC yr⁻¹ obtained in this study, taking account of forest age structure – and the associated shifts in *NEP* – which is in agreement with European-scale forest age structure from forest statistics. However, the present study probably underestimates soil C uptake, as it does not account for the effect of earlier soil degradation (Glatzel, 1999). The effect of the cessation of litter raking alone is estimated to cause a net uptake of 42 TgC yr⁻¹ in soils (Table 4.4, Nabuurs *et al.*, 2003). On the other hand, the flux-data based estimate might overestimate whole European forest *NEP*, because most of the sites considered are middle-aged forests, which typically show a strong C uptake, and the sparse network may not be representative for the European forest structure (Valentini *et al.*, 2000a).

Wood products do not contribute to a large proportion of the overall C uptake in forests in this study (Table 4.4). This is in agreement with findings from (Nabuurs *et al.*, 2003), although they used estimates of wood products stored in Germany to initialise the products pools. In contrast, the pools are assumed to be in equilibrium at the start of the simulation in this study. Given that the products-pool sizes and the resulting flux are small compared to the fluxes of *NPP* and R_h , uncertainty in the estimation of these pools will not change the overall results of this study.

4.4 Discussion

In this study, we evaluated biomass predictions of a generalised ecosystem model with forest inventory data. We demonstrated that the original pipe-model formulation of LPJ does not suffice to model stand development adequately and proposed an improved model formulation (Section 4.4.1). The advanced model, coupled to a generic representation of forest management, captures the important features of regional forest inventories, however, substantial differences remain (Section 4.4.2). Nonetheless, the model is able to reproduce present-day age-structure and harvest ratio, and predicts a net carbon uptake in vegetation that is compatible with observations (Section 4.4.3).

4.4.1 Tree growth in LPJ

This study has shown that Magnani’s hypothesis on changing C allocation to plant tissues with tree height can be successfully used within the framework of a general ecosystem model to predict stand-scale evolution of biomass densities with stand age (Section 4.3.1). Furthermore, it has been demonstrated that a suitably parameterised model using this algorithm can be used to estimate plausible biomass stocks at a regional scale despite the fact that the model was only calibrated for one tree species (Section 4.3.2, Fig. 4.6). Clearly, the results presented here show how simulations can be improved by using the Magnani-hypothesis but do not constitute a proof of the hypothesis in itself. Such a test would comprise intensive field work along a chronosequence for several different plant functional types and across different ecotones. However, this study demonstrates the

potential applicability of such a theory. Further field work is highly desirable, particularly because the hypothesis is of an adequate complexity to be incorporated into generalised ecosystem models. Such data would either confirm the results in this study, or point to further improvements on the algorithms used.

Two aspects that specifically require more ecological understanding are the maximum transpiration rate per unit leaf area (E_{un}), and how this rate changes along environmental gradients, as well as the increase in below-ground allocation with stand age for which evidence is still conflicting (see discussion in Ryan *et al.*, 2004). Fine root investment in the size dependent allocation scheme depends primarily on the assumed specific root hydraulic conductance, and fine root turnover times. Although data available for specific root hydraulic conductivity (Roberts, 1977; Rüdinger *et al.*, 1994; Steudle and Meshcheryakov, 1996; Nardini and Tyree, 1999; Magnani *et al.*, 2000) are sparse and do not allow generalisation, the estimates are of the same magnitude. Field data suggest that fine root longevity is similar to the time-scale suggested by Magnani *et al.* (2000), and conservative across different plant functional types (Vogt *et al.*, 1996; Eissenstat *et al.*, 2000).

Evidence supports the hypothesis that despite considerable differences in sapwood leaf-specific conductivity across species, leaf-specific whole plant conductance of well-watered mature plants is rather conservative even across different angiosperm and coniferous species (Becker *et al.*, 1999). A constant maximum transpiration rate is also supported by long-term ecosystem manipulation experiments (Cinnirella *et al.*, 2002). The precise value of the parameter E_{un} is likely the result of a compromise between high carbon gains due to low water limitation and low investment costs into supporting tissue (Givinish, 1986; Cannell and Dewar, 1999; Sperry *et al.*, 2002), and probably a function of environmental conditions (Magnani *et al.*, 2002). However, little is known about the variation of this parameter in response to the climatic water deficit (*i.e.* long-term average humidity).

4.4.2 Evaluation of simulated growth patterns using inventory data

The comparison of simulated and inventory-based biomass estimates has shown that, in general, a simple, globally parameterised model is capable of reproducing large-scale trends in growth, both with respect to time (age structure, Fig. 4.4) and location (*e.g.* temperature gradient, Fig. 4.7). The data of the EEFR-database provide a plausibility check of simulated biomass densities with age, but they are of limited use in attributing causes to the model-data differences. Nevertheless, the large-scale differences between model and data do suggest that *NPP* in boreal ecosystems modelled with the standard LPJ R_a formulation is overestimated (Fig. 4.6).

Inventory-based biomass estimates differ substantially between provinces of the same country, and far more pronounced than simulated estimates, leading to substantial differences in the coincidence between simulations and data. The inventory-based estimates have been obtained using country specific BEFs that may not adequately represent regional differences in carbon allocation within a country. More likely, however, these differ-

ences are due to regional variations in soil fertility, and thus nutrient limitation on plant photosynthesis, which are not taken into account in the current version of LPJ. Further refinement of LPJ to increase the accuracy with which regional variations in biomass are modelled therefore requires an advanced representation of nutrient limitation, and in first order C-N interactions, on plant growth. Differences in inventoried biomass stocks between tree species of the same plant functional type suggest that more physiological detail to model the differential growth rates of different tree species would further enhance the models capacity to provide accurate biomass estimates in regional scale applications.

The overestimation of biomass in old stands in LPJ-simulations may be a consequence an underestimation of either the age-related growth decline or thinning intensity. The removals of biomass from each age-class cannot be inferred from the EEFR data-base itself. Yield-tables, which are representative of typical management regimes in a particular region, may provide volume loss and tree density data for different age-classes. The LPJ forest management module shows a broad agreement in biomass loss with stand age with a limited number of these yield-tables. Further evaluation systematically using yield-tables from different countries, and for different forest types, may further increase the confidence placed in the thinning intensity predicted by LPJ. Nevertheless, a gap will remain between these idealised, and sometimes outdated, data and forest inventories that take account of actual, present-day forest management and the effect of past natural disturbances on growing stocks. Access to higher resolution inventory data, comprising stand-level information and also tracking stand volume removals, would greatly help to reduce this type of uncertainty.

The average European-wide harvest ratio modelled with LPJ agrees surprisingly well with the average harvest ratio from the 1992 and 2000 forest resource assessments. Despite the overall agreement the modelled and observed ratios differ considerably for individual regions, but in a non-systematic way. Modelled harvest ratios for some Central European countries are higher than in reality, suggesting that modelled growth stimulation has not been as strong as observed in these countries. Countries with a high proportional share of young forests due to reforestation, for instance Ireland, show a much lower simulated harvest index than documented in the forest statistics. Probably some of the forests in Ireland are in reality quite intensively managed with short rotation times, *e.g.* to prevent losses to infectious diseases, whereas in the simulations final felling of afforested forests is only allowed after these have reached the prescribed PFT-specific rotation period time. Theoretically, the framework of LPJ is flexible enough to account for these regional differences in management, which will probably be most important in southern Europe, where ‘coppices with standards’ occupy significant fractions of the area that is classified as forest. Data to improve simulation results would not only encompass a consistent description of management practices, *e.g.* timing and extent of thinning, across Europe, but also geolocation of the different management types.

4.4.3 European forest C balance

Carbon uptake in vegetation estimated from the advanced model is well within the uncertainty bound of the estimates based on forest inventories (Liski *et al.*, 2003). The simulations in this study suggest that observed climate change, and even more so, CO₂-fertilisation account for more than 50% of this uptake. Nitrogen availability is unlikely to have limited the fertilising effect of CO₂ because of the very high levels of N-deposition over large parts of Europe in the recent decades. On the other hand, forest growth is directly affected by increased N-deposition, and other air pollutants such as SO₂ and O₃, even though the magnitude of these effects is still uncertain (Spieker *et al.*, 1996; Townsend *et al.*, 1996; Lloyd and Farquhar, 1999; Nadelhoffer *et al.*, 1999). Similarly, past changes in forest management in Europe focused on enhancing forest growth by improving site quality through selection of better provenances, cessation of litter raking and soil amelioration and peatland drainage programmes (Kauppi *et al.*, 1992; Spieker *et al.*, 1996). The inventory-based estimate of the present-day net increase in vegetation C with its ‘known’ uncertainty of -20% to +25% (for all 55 countries of the TBFRA data set, Liski *et al.*, 2003) gives an appropriate constraint to the growth changes as predicted by terrestrial biosphere models. Future work will have to clarify the relative contribution of the direct effects of N-deposition and improved forest management to the observed increase in forest growth by including these effects into the model.

Simulated changes in forest litter and soil C pools are very small compared to other studies (Schulze *et al.*, 2000; Nabuurs *et al.*, 2003), as in this study these pools were assumed to be in equilibrium at the beginning of the 20th century. Deforestation as early as the medieval period had left many parts of Europe with forest area of less than 10% (Mather, 1990). Forest soil carbon stocks today are probably far below their equilibrium size, resulting from reforestation of former agricultural land since the late 19th century and traditional forest management practices. These management practices, for example fuelwood collection and litter raking that were practiced until the mid 20th century (Karjalainen *et al.*, 1999), caused soil degradation mainly from nutrient export, thereby reducing site fertility and, because of reduced productivity, litter inputs to the soils (Glatzel, 1999). However, only the effect of increasing forest area from 1948 levels onwards is considered in the simulations. Litter and soil C stock uptake rates in this study average around 20 gC m⁻² yr⁻¹ for the 1990s, with considerable interannual variability. Inventory-based soil C uptake is approximately 50 gC m⁻² yr⁻¹ (Nabuurs *et al.*, 2003), using an initialisation that was not necessarily in equilibrium with litter fall in 1948, and including the effect of litter raking and its cessation in the latter part of the 20th century. By comparison of litter fall and rates of heterotrophic respiration, Schulze *et al.* (2000) derived a soil C uptake rate of 110 gC m⁻² yr⁻¹, after correction for soil C losses after disturbances by harvest (Janssens *et al.*, 2003). It appears unlikely that the uncertainty in estimated soil C stock change can be substantially reduced by a simple extension of the historic land-use data set. A reduction in uncertainty would furthermore require a quantification of the

effects of past soil degradation on current soil C stocks.

4.5 Conclusions

A generalised ecosystem model considering plant hydraulic architecture and its influence on C allocation with tree height captures the age-related decline in forest growth. The advanced model is able to simulate the development of biomass with age at the stand and regional scale. Despite the general agreement in growth trends between model and inventory-based estimates along a large-scale temperature gradient, notable differences occur regionally. These may be related to regionally varying soil fertility, which is currently not considered in LPJ.

The model-data agreement in forest biomass increment, as well as the agreement of the predicted absolute level of removals, harvest ratio, and forest age-structure after accounting for changes in forest area and wood demand since 1948 suggest that the proposed forest management scheme in LPJ captures the main effects of forest management on forest growth on a regional scale. The remaining inaccuracies may be addressed by including for example more detailed information on the tree-species level, and on regional forest management practices, such as country-specific rotation times, felling to thinning ratios, or management types such as coppices with standards, which are important in the Mediterranean region.

The present study links process-based simulation of growth processes with statistical information on land-use change and forest use, and thereby reduces the theoretical gap in C accounting between inventory and process-based approaches. Modelled increases in vegetation C storage are in good agreement with previous inventory-based estimates, and allow the attribution of fluxes to different causes. The results confirm earlier findings (*e.g.*, Kohlmaier *et al.*, 1995) that forest management and forest area changes that impact on forest age-structure are important to understand the present-day, and hence also future patterns of net C exchange. From the wide range of different estimates of soil C exchanges obtained by different approaches, resulting partly from the uncertainty in historical soil C stocks of forest soils, it is clear that soil C uptake rates are critical in determining the net forest C exchange.

This study uses forest statistics to evaluate both simulated tree growth and C dynamics. It provides an essential step forward in providing a comprehensive estimate of net carbon exchanges of the terrestrial biosphere, and a framework in which to study the impacts of future environmental changes on European forests.

Acknowledgements

The authors are grateful for fruitful discussions with Thies Eggers and Gert-Jan Nabuurs. The corresponding author was supported by a PhD-scholarship of the federal state of Brandenburg (AZ: 24-04/323; 200), and a European Forest Institute member-scholarship.

The work presented is a contribution to the ATEAM project (EVK2-2000-00075) of the fifth European Community Framework Programme, and CarboEurope-IP in the sixth European Community Framework (GOCE-CT2001-00125).

4.6 Appendix

4.6.1 Hydraulic acclimation theory

Table 4.5 (page 111) gives an overview of all abbreviations and parameter used, Table 4.1 details the parameter values and their units.

The flow of water from the soil through the plant may be described by the Ohm's law analogy (Slayter, 1967), where the instantaneous transpiration rate E_s is function of the pressure gradient between soil and atmosphere that is bridged by the plant, ΔP , and the hydraulic resistance of the plant, R_{tot} :

$$E_s = \frac{\Delta P}{R_{tot}} \quad (4.2)$$

The pressure gradient ΔP is constrained by the difference between soil and leaf water potentials (Ψ_{soil} and Ψ_{leaf} , respectively) reduced by a gravitational component (Ψ_{grav}), imposed by the vertical transport of water. Plants have been observed to operate close to the minimum level of leaf water potential $\Psi_{leafmin}$ that can be safely maintained without inducing catastrophic xylem embolism (Tyree and Sperry, 1988; Sperry *et al.*, 1994). The maximal transpiration rate will thus depend on:

$$\Delta P = \Psi_{soil} - \Psi_{grav} - \Psi_{leafmin} = \Psi_{soil} - H \times g \times \rho_w - \Psi_{leafmin} \quad (4.3)$$

where H is tree height, g the gravitational acceleration, and ρ_w density of water. Neglecting any differences in transpiration and hydraulic resistance among leaves in the canopy, total plant resistance can be considered as the sum of the resistances of a root and a shoot component, arranged in series. Root hydraulic resistance (R_{root}) is mainly determined by the radial resistance of the root (Weatherly, 1982; Magnani *et al.*, 1996; Steudle, 2000), and therefore inversely related to root surface, and in first order to fine root mass (C_r):

$$R_{root} = \frac{\rho_c}{k_r \times C_r} \quad (4.4)$$

where k_r is the specific root hydraulic conductance and ρ_c the carbon density of root biomass. Hydraulic resistance of the shoot can be expressed as a function of plant height H and sapwood cross-sectional area A_s (Whitehead *et al.*, 1984). Following the pipe-model, cumulative cross-sectional area of the sapwood in stem and branches is constant along the whole pathway. Assuming furthermore that specific sapwood conductance k_s is independent of tree size, shoot resistance can then be expressed as

$$R_{shoot} = \frac{H}{k_s \times A_s} = \frac{H^2 \times \rho_s}{k_s \times C_s} \quad (4.5)$$

where C_s is the sapwood mass. Stand transpiration can be assumed to be proportional to leaf-area in open and aerodynamically well coupled canopies with small environmental

gradients (Jarvis *et al.*, 1976; Schulze *et al.*, 1994). This has been found for Scots pine, where stomatal conductance, transpiration and photosynthesis per unit leaf mass showed only small vertical gradients. More generally, stand transpiration is a function of absorbed radiation, which results in a strongly non-linear relationship for higher leaf area indices:

$$E_s = SLA \times C_l \times E_{un} \quad (4.6)$$

where the maximum transpiration rate per unit leaf area, E_{un} , is a constant for given environmental conditions, but assumed to decrease linearly in response to drought stress (modelled in LPJ as the ratio of supply over demand), corresponding to Magnani *et al.* (2002).

Functional homeostasis implies that the hydraulic resistance of a plant does not exceed the limit given by

$$\frac{\rho_c}{k_r \times C_r} + \frac{H^2 \times \rho_s}{k_s \times C_s} = \frac{\Psi_{soil} - H \times g \times \rho_w - \Psi_{leafmin}}{E_s} \quad (4.7)$$

The optimality constraint, proposed by Magnani *et al.* (2000), requires that R_{tot} exactly matches the limit imposed. Biomass would be allocated to root and shoot tissues so as to minimise whole-plant leaf-specific hydraulic resistance, while maximising leaf surface area, and thereby NPP . Thus, considering the different hydraulic conductivities as well as the lifetime of the different tissues, optimal growth requires that the ratio of the marginal total plant hydraulic return to marginal carbon costs in either root or shoot tissue to be equal:

$$\frac{\partial R_{tot}}{\partial C_r} \frac{1}{\tau_r} = \frac{\partial R_{tot}}{\partial C_s} \frac{1}{\tau_s} \rightarrow \frac{\rho_c}{k_r \times C_r^2} \frac{k_s \times C_s^2}{H^2 \times \rho_s} = \frac{\tau_r}{\tau_s} \quad (4.8)$$

Defining

$$c = \sqrt{\frac{k_r \tau_r \rho_s}{k_s \tau_s \rho_c}} \quad \text{and} \quad c0 = \frac{\tau_r}{\tau_s \times c} \quad (4.9)$$

the following allometric constraints can be derived:

$$A_s = C_l \times SLA \frac{E_{un}}{\Delta P \times k_s} (H + c0) \quad (4.10)$$

$$C_r = C_l \times SLA \frac{E_{un}}{\Delta P \times k_r} (H + c0) / c0 \quad (4.11)$$

Together with the diameter-height relationship

$$D = k_{allom2} \times H^{k_{allom3}} \quad (4.12)$$

these relationships form the size-dependent allocation scheme that is used to replace the original, size-independent allocation scheme of LPJ. See Figure 4.1 for a description

of the allometric changes with tree height.

4.6.2 Plant water uptake considering hydraulic architecture

From equation 4.2 it follows that the instantaneous maximum daily water supply rate for an individual tree, *i.e.* with canopy conductance regulated such that leaf water potential reaches $\Psi_{leafmin}$, is a simple linear function of the actual soil water potential, and inversely related to whole plant hydraulic resistance. Accounting for plant hydraulic architecture allows for a more plausible treatment of soil water status on canopy conductance than in the original version of LPJ (see Hickler *et al.*, 2004, for an evaluation of simulated AET using a similar approach at point and larger scales). Daily supply rates, and thereby canopy conductance, are obtained by integrating demand and supply over the course of the day following Prentice *et al.* (1993).

Canopy conductance is regulated to prevent xylem pressure values that would lead to catastrophic embolism. However, cavitation, and thus the loss of conductivity of xylem vessels, still commonly occurs in water-limited environments (Tyree and Ewers, 1991). The loss of conductivity can be described as a function of the xylem water potential, which is in first order equal to the sum of soil water and gravitational potential ($\Psi_{xylem} = \Psi_{soil} + \Psi_{grav}$) (Sperry *et al.*, 1998; Hickler *et al.*, 2004).

$$R_{root/shoot} \propto 1 - \exp\left(-(\Psi_{xylem}/w1)^{w2}\right) \quad (4.13)$$

where $w1$ corresponds to the xylem water potential at which 50% of the conductance is lost and $w2$ is a shape parameter (Hickler *et al.*, 2004).

Stomatal conductance has been shown to be sensitive to temperature even under a constant water potential gradient (Smit-Spinks *et al.*, 1984; Cochard *et al.*, 2000; Matzner and Comstock, 2001). Changes in the conductance are well explained by changes in water viscosity over a wide range of temperatures, and therefore including the temperature effect on conductance gives:

$$R_{root/shoot} \propto \frac{1}{a1 + a2 \times T_c} \quad (4.14)$$

where $a1 = 0.555$ (relative viscosity at 0°C), $a2 = 0.022$ and T_c temperature in °C (Cochard *et al.*, 2000; Lide, 2002).

4.6.3 Forest management in LPJ

Forest management of even-aged cohorts in LPJ is described in three different components to model forest C balances at a landscape-scale:

1. The changes of the age-class distribution over time
2. The total level of fellings, and the partitioning of these fellings into thinning and final felling.

3. The distribution of thinnings and final fellings over all age-classes.

Table 4.6 (page 112) gives an overview of all abbreviations and parameter used. The module is described as follows:

Age-structure and area propagation

Each $10' \times 10'$ grid cell consists of a forest fraction, F_{forest} , that is sub-divided into separate stands S for each PFT (p) of 10-years age-classes ($i = 1, \dots, n$). These stands occupy a fractional area, $a_{i,p}$, of F_{forest} that can be decreased by losses from fire or final (clear-cut) fellings. The fractional changes in area for each $S_{i,p}$ are updated annually. Ten years have been chosen as the resolution of the age-class cohorts as a compromise between a realistic representation of the forest dynamics and computational demand.

At the end of each simulation year t , before the start of the forest management module, the fraction of area lost due to fire is subtracted from each age-class

$$a_{i,p} = (1 - fab) \times a_{i,p}^{t-1} \quad (4.15)$$

where fab is the fraction of area burnt, as estimated from LPJ's regional fire module (Venevsky *et al.*, 2002), depending on aboveground litter stocks, moisture, and a PFT-specific fire-resistance. Areas $a_{i,p}$ are then updated to account for the fractional loss from clear-cut fellings in this year (Eq. 4.24):

$$a_{i,p}^{t+1} = \left(1 - frac_{i,p}^{fell}\right) \times a_{i,p} \quad (4.16)$$

Areas from fire or clear-cut (for all PFTs) enter a 'non-forest' stand S_0 (with only herbaceous vegetation) with the fractional coverage a_0 . Changes in the (grid cell scale) fractional forest area F_{forest} are also allocated to S_0 . New cohorts (for all PFTs) are established from S_0 every 10 years. In equilibrium, the mean residence time of area in S_0 is 5 years.

The propagation of age-classes over time is best illustrated on a time-step ts of 10 years, because new cohorts are established only every 10 years. The proportion of $a_{i,p}$ that are either burnt or felled in a time-step ts , $l_{i,p}$, can be obtained by integrating the fractional changes from eqns. 4.15 and 4.16 over 10 years. The age-class propagation can then be described as a modified Leslie-Matrix (Leslie, 1945), as in Kohlmaier *et al.* (1995) and Häger (1998):

$$A_{ts+1} = P.A_{ts} \quad (4.17)$$

where

$$A_{ts} = (a_{1,p}, \dots, a_{n,p})^T \quad (4.17a)$$

and

$$P = \begin{pmatrix} l_{1,p} & l_{2,p} & l_{3,p} & \cdots & l_{n-1,p} & 1 \\ 1 - l_{1,p} & 0 & 0 & & 0 & 0 \\ 0 & 1 - l_{2,p} & 0 & & 0 & 0 \\ 0 & 0 & 1 - l_{3,p} & & 0 & 0 \\ \vdots & & & \ddots & & \\ 0 & 0 & 0 & & 1 - l_{n-1,p} & 0 \end{pmatrix} \quad (4.17b)$$

Total fellings and partitioning amongst thinning and felling

The grid cell scale (G) current annual biomass increment of a PFT p , $CAI_{G,p}$, is the area-weighted sum of the annual gross increment $\Delta C_{i,p}^{veg}$ in roundwood over all age-classes i :

$$CAI_{G,p} = \sum_{i=1}^n CAI_{i,p} = \sum_{i=1}^n a_{i,p} \times \Delta C_{i,p}^{veg} \quad (4.18)$$

where ΔC^{veg} is the gross increment in a stand over one year (not discounting for removals). Total woody vegetation carbon estimates (sapwood and heartwood) by LPJ are converted into roundwood estimates using a conversion factor of 0.6, and in addition accounting for an average of 10% fellings that are not recovered, and thus remain in the forest (UN-ECE/FAO, 2000, based on country-specific data).

The thirty-year average $CAI_{G,p}$ at equilibrium (corresponding to the 30-years spin-up cycle used; see Section 4.2.3) is used to adapt the level of total fellings, $F_{G,p,eq}^{total}$, to the local growing conditions. In the transient phase, total fellings $F_{G,p,t}^{total}$ vary according to

$$F_{G,p,t}^{total} = \delta(t) \times F_{G,p,eq}^{total} \quad (4.19)$$

where t is time in years, and $\delta(t)$ the relative change in wood demand derived from forest statistics (FAO, 1948, 1955, 1960, 1976; UN-ECE/FAO, 1985, 1992, 2000). This approach allows to scale local harvesting rates with country-scale changes in wood demand, without prescribing $F_{G,p,eq}^{total}$ and $F_{G,p,t}^{total}$ directly from forest statistics. The benefits are twofold: Firstly, forest statistics are typically on a country-basis, whereas modelled and observed growth differ substantially between regions, a simple scaling is therefore inappropriate. Secondly, modelled increment may not accurately represent observed increment, such that a drift may be introduced into the calculations because of an inaccurate increment to harvest ratio at the beginning of the simulation. Assuming steady-state at the beginning of the simulation is also an unrealistic assumption (because the beginning of the simulation refers to the year 1901). However, this does not result in model drift, and therefore allows to assess the consequence of land-use, wood demand and other causes for forest growth changes.

The partitioning of $F_{G,p,t}^{total}$ into final fellings ($F_{G,p,t}^{fell}$) and thinning ($F_{G,p,t}^{thin}$) follows the ob-

jectives of maintaining a PFT-specific rotation period and minimising loss of wood to self-thinning. To achieve this, $F_{G,p,t}^{total}$ is first allocated to the requirements for thinning $\tilde{F}_{G,p}^{thin}$ (Eq. 4.20) and final felling $\tilde{F}_{G,p}^{fell}$ (Eq. 4.21). The remainder of $F_{G,p,t}^{total}$ is distributed to $F_{G,p,t}^{thin}$ and $F_{G,p,t}^{fell}$ with the aim to partition $F_{G,p,t}^{total}$ with a constant ratio $c = 2/3$. A similar approach is used within the EFISCEN forest statistical model (Nabuurs *et al.*, 2001).

Mortality in each stand $S_{i,p}$ from natural self-thinning $m_{i,p}$ is estimated from growth efficiency and stand density (Smith *et al.*, 2001). Forest management is assumed to act to prevent losses of timber in the forest, thus $m_{i,p}$ is increased if stand density becomes large (if foliage projective cover approaches 95%, Sitch *et al.*, 2003) to avoid any loss from self-thinning. The landscape scale requirement for thinning to prevent natural mortality is thus computed as

$$\tilde{F}_{G,p}^{thin} = \sum_{i=1}^n \tilde{F}_{i,p}^{thin} = \sum_{i=1}^n m_{i,p} \times a_{i,p} \times C_{i,p}^{veg} \quad (4.20)$$

In this way, trees dying from self-thinning are assumed to be removed as salvage logging, and also, stand density is held at a level slightly below that level at which substantial self-thinning would occur.

Forest management aims at a (PFT-specific) rotation period length ($T_{rot,p}$), because of the age-related decline in growth and also to avoid increasing mortality in older stands because of their increased susceptibility to infections. This is implemented into LPJ as a requirement for clear-cut felling, $\tilde{F}_{G,p}^{fell}$, once a particular $S_{i,p}$ reaches a stand age, *age* larger than $T_{rot,p}$. A lag of ten years is required to match the annual time-step of the management module with the ten year time-step of new stand establishment. Thus,

$$\tilde{F}_{G,p}^{fell} = \sum_{i=1}^n \tilde{F}_{i,p}^{fell} = \sum_{i=1}^n f_{i,p} \times a_{i,p} \times C_{i,p}^{veg} \quad (4.21)$$

where

$$f_i = \begin{cases} age \leq T_{rot,p} - 10 & \rightarrow f_i = 0.0 \\ T_{rot,p} - 10 < age \leq T_{rot,p} & \rightarrow f_i = 1/(T_{rot,p} + 1 - age) \\ age > T_{rot,p} & \rightarrow f_i = 1.0 \end{cases} \quad (4.21a)$$

Harvesting rates per age-class and fate of harvested C

The landscape scale demand for thinning, $F_{G,p,t}^{thin}$, is allocated to stands $S_{i,p}$ by first allocating thinning to those stands in which natural mortality would occur, and which did not

receive a thinning within the last five years:

$$frac_{i,p}^{thin} = \begin{cases} y_{lt} < 5 & \rightarrow frac_{i,p}^{thin} = 0 \\ y_{lt} \geq 5 & \rightarrow frac_{i,p}^{thin} = m_{i,p} \end{cases} \quad (4.22)$$

where y_{lt} is the number of years since the last thinning for this $S_{i,p}$. The remaining demand for thinning ($\hat{F}_{G,p,t}^{thin}$) is allocated to those stands $S_{i,p}$ which had not been thinned for at least 10 years, with a cap of 7% on removal ($frac_{max}^{thin}$):

$$frac_{i,p}^{thin} + = \begin{cases} y_{lt} < 10 & \rightarrow 0 \\ y_{lt} \geq 10 & \rightarrow \min(\hat{F}_{G,p,t}^{thin} / C_{i,p}^{veg} / a_{i,p}, frac_{max}^{thin}) \end{cases} \quad (4.23)$$

Any remaining demand for thinnings is allocated to those stands $S_{i,p}$ that would receive a thinning in this year ($frac_{i,p}^{thin} > 0$) by iteratively adjusting these fractions until all demand is allocated. Partitioning of the thinnings amongst age-classes is - within reason - similar to estimates obtained from several European yield-tables (*data not shown* Koivisto, 1959; Garcia Abejon and Loranca Gomez, 1984; Schober, 1987). Additionally, pre-commercial thinning at the age 15 (typically corresponding to a height of 6-8 meters) is carried out to reduce natural mortality in early stand development.

Final fellings are only carried out in the the oldest age-class, *old*, of a given PFT. The fraction of the age-class felled is determined by

$$frac_{old,p}^{frac} = F_{G,p,t}^{fell} / C_{old,p}^{veg} / a_{old,p} \quad (4.24)$$

without affecting other stands. If the felling demand cannot be met by felling the oldest age-class completely, the second oldest age-class is used to satisfy the remaining demand. The rotation-period length $T_{rot,p}$ is not strictly enforced, *i.e.* if in the transient phase increments exceed demand for felling – forest area changes, changes in relative wood demand, or changes in increment due to changed environmental conditions –, forests may become older than $T_{rot,p}$, and *vice versa*.

Only the harvestable fraction of the vegetation C on the stand is actually removed, *i.e.* about 54% of the sap- and heartwood (see above). The biomass remaining on site together with litter of foliage and fine roots are added to the respective litter pools for decay. Harvested biomass, H_p , is added to a fast ($k_1 = 1 \text{ yr}^{-1}$) and a slow ($k_2 = 1/25 \text{ yr}^{-1}$) wood products pool, as in Nabuurs *et al.* (2003), with country-specific partitioning coefficients, $w_{1,2}$ derived from UN-ECE/FAO (2000):

$$\frac{dWP_i}{dt} = k_i \times WP_i + w_i \times H_p \quad (4.25)$$

where $i=1,2$.

4.6.4 Gridded forest area, 1948-2000

Data of past distribution and extent of different land-use types in Europe are sparse; a consistent spatially explicit data-base is still lacking. Global data-sets by Ramankutty and Foley (1999) and Goldewijk (2001) map past changes in agricultural and pasture areas, however, the remainder cannot be simply assumed to be forests. Also, these data-sets treat Europe as only one or two homogeneous regions with similar land-use change trends, which is unduly coarse for a detailed European study. To account for the need of such a data-base for modelling land-use change effects with spatially explicit ecosystem models, a variety of data sources on area changes for agriculture, pasture, and forests for the period 1900-2000 are used, with an emphasis on the second half of the century owing to a lack of suitable data earlier in the century. An approach similar to Ramankutty and Foley (1999) and Goldewijk (2001) is used to scale country-level trends in land-use types to the spatial $10' \times 10'$ grid. Present-day land-use patterns are derived from a combination of the CORINE data-set (CORINE, 1997) for those countries, for which these data are available, and PELCOM (Mücher *et al.*, 2000), as in Erhard *et al.* (in prep.). Land-use change trends in agriculture, grasslands and forests between 1961 and 2000 are derived from country statistics (FAOSTAT, 2004). Forest area (1948-1961) is taken from FAO forest resource assessments (FAO, 1948, 1955, 1960, 1976; UN-ECE/FAO, 1985, 1992, 2000). Agriculture and grasslands are obtained from Goldewijk (2001) for the period before 1960. Instead of assuming a linear trend within a region, we weighted trends such that increases were stronger in areas of a high percentage of this land-use, and *vice versa*, to account for the effect that marginal sites would be abandoned by that land-use first. Erhard *et al.* (in prep.) give a more detailed overview of the procedure to construct these data.

<i>Parameter</i>	<i>Description</i>	<i>Unit</i>
A_s	sapwood basal area	
C	stand carbon density (subscript: l, leaf; r, root; s, sapwood)	kgC m ⁻²
D	stem diameter	m
ΔP	soil-atmosphere pressure gradient	MPa
E	transpiration rate (subscript: s, stand; un, per unit leaf area)	mm s ⁻¹
g	acceleration due to gravity	m s ⁻²
H	stand height	m
$kallom_{2,3}$	scaling parameters in equation 11	
k_r	specific hydraulic conductance of fine roots	m ³ kg ⁻¹ s ⁻¹ MPa ⁻¹
k_s	specific hydraulic conductance of the sapwood	m ² s ⁻¹ MPa ⁻¹
R	hydraulic resistance (superscript u: per unit leaf area; subscripts: root, shoot, total)	MPa s m ⁻¹
ρ_c	carbon density of biomass	kgC kg ⁻¹
ρ_s	carbon density of sapwood	kgC m ⁻³
ρ_w	density of water	kg m ⁻³
SLA	specific leaf area	m ² kgC ⁻¹
τ	turnover time (subscript: r, root; s, sapwood)	yr ⁻¹
Ψ	hydraulic water potential (subscript leaf; xylem; soil; grav, gravitational; leaf-min, critical leaf-water potential)	MPa

Tab. 4.5: Parameters and variables used of the size-dependent allocation module and plant hydraulics.

<i>Parameter</i>	<i>Description</i>	<i>Unit</i>
subscript i	denoting a particular age-class	
subscript G	denoting the sum over all age-classes of one PFT p in a grid cell	
subscript p	denoting a particular PFT	
a	fractional coverage of the forest fraction F_{forest} of the grid cell	%
A_{ts}	Vector containing fractional areas a_1, \dots, a_n at the time ts	%
C^{veg}	roundwood density of a stand S , <i>i.e.</i> (sapwood+heartwood) $\times 0.6 \times \sim 0.9$	kgC m ⁻²
CAI	current annual increment of roundwood	kgC
ΔC^{veg}	change in roundwood density of a stand S over one year, not accounting for losses due to harvesting or natural mortality <i>i.e.</i> (sapwood+heartwood) $\times 0.6 \times \sim 0.9$	kgC m ⁻² yr ⁻¹
$\delta(t)$	relative change in wood demand over time	
fab	fraction of area burnt	%
F_{forest}	fraction of the grid cell covered by forest	%
$frac^{fell}$	fraction of a stand S felled from clear-cut	%
$frac^{thin}$	thinning intensity of a stand S	%
F	fellings (superscript: fell: final fellings, thin: thinning, total: total fellings)	kgC
\tilde{F}	required fellings to avoid loss due to self-thinning or to maintain T_{rot} , (superscript: fell: final fellings, thin: thinning)	kgC
H_p	C removed from harvesting	kgC
$k_{1,2}$	decay constants of the wood products pool	yr ⁻¹
l	propagation coefficient in the Leslie-Matrix	
m	estimated mortality from self-thinning	
S	stand, subfraction of the forest fraction of a grid cell	
t, ts	t time in years, ts 10year time-steps	
T_{rot}	PFT-specific rotation period, see Table 4.1	yr
$w_{1,2}$	country-specific partitioning coefficient of harvested wood to the wood products pool	
$WP_{1,2}$	C stored in the wood products pool with 1: 1 year, and 2: 25 years turnover times	kgC
y_{it}	years since last thinning of a stand	yr

Tab. 4.6: Parameters and variables of the forest management module.

5. PROJECTED CHANGES IN TERRESTRIAL CARBON STORAGE IN EUROPE UNDER CLIMATE AND LAND-USE CHANGE, 1990-2100

Sönke Zaehle* Alberte Bondeau* Pascale C. Smith*[†] Wolfgang Cramer*
Markus Erhard*[‡] I. Colin Prentice[§] Stephen Sitch*[¶] Benjamin Smith^{||}
Martin Sykes^{||}

The future is the only kind of property that the masters willingly concede to the slaves.

(A. Camus, The Rebel)

manuscript in preparation for *Regional Environmental Change*

Abstract

Changes in climate and land use, caused by socio-economic changes, greenhouse gas emissions, agricultural policies and other factors, are known to affect both natural and managed ecosystems, and will likely impact on the European terrestrial carbon balance during the coming decades. This study presents a comprehensive European Union wide (EU15 plus Norway and Switzerland, EU*) assessment of potential future changes in terrestrial carbon storage considering these effects based on four illustrative IPCC-SRES storylines ('A1fi', 'A2', 'B1', 'B2'). A process-based land vegetation model (LPJ-DGVM), adapted to include a generic representation of land-use types, is forced with changing fields of land-use patterns from 1901-2100 to assess the effect of land-use and cover changes on the terrestrial carbon balance of Europe. Furthermore, the uncertainty in the future carbon balance associated with the choice of a climate change scenario is assessed by forcing LPJ-DGVM with output from four different

*Potsdam Institute for Climate Impact Research (PIK), e.V., Telegrafenberg, PO Box 601203, D-14412 Potsdam, Germany

[†]present address: Laboratoire des Science du Climat et de l'Environnement, Orme des Merisiers, F-91191 Gif-sur-Yvette, France

[‡]present address: Institut für Meteorologie und Klimaforschung (IMK-IFU), Forschungszentrum Karlsruhe GmbH, Kreuzackbahnstr. 19, D-82467 Garmisch-Partenkirchen, Germany

[§]Department of Earth Sciences, University of Bristol, Queen's Road, Bristol BS8 1RJ, UK

[¶]present address: Met Office (JCHMR), Crowmarsh-Gifford, Wallingford, OX10 8BB, U.K.

^{||}Geobiosphere Science Centre, Physical Geography and Ecosystems Analysis, Lund University, Sölvegatan 12, S-22362 Lund, Sweden

climate models (GCMs: CGCM2, CSIRO2, HadCM3, PCM2) for the same SRES storylines.

Decrease in agricultural areas, and afforestation leads to simulated carbon sequestration for all land-use change scenarios with an average net uptake of $\sim 16 \text{ TgC yr}^{-1}$ between 1990 and 2100, corresponding to one fifth of the EU*'s Kyoto emission reduction target. Projections of total European carbon sequestration are similar among the land-use change scenarios despite substantial differences in regional trajectories. Soil C losses resulting from climate warming more than offset growth enhancement from climate change and increasing atmospheric CO_2 concentrations in the second half of the 21st century in most scenarios. Differences in future climate change projections among GCMs are the main cause for uncertainty in the cumulative land-atmosphere fluxes.

Keywords: terrestrial carbon balance, scenario analysis, climate change, land-use change, LPJ-DGVM, Kyoto protocol.

5.1 Introduction

Terrestrial carbon (C) sinks resulting from land-use and management changes play an important role in the Kyoto process under Article 3.3 and 3.4 (UNFCCC, 1998). Indeed, although the terrestrial biosphere in Europe currently acts as a small, but uncertain C sink, it sequesters annually up to 12 % of the European 1995's fossil fuel emissions (Janssens *et al.*, 2003). Reforestation and decreased forest use for wood production, for instance, are believed to contribute substantially to the present-day net C uptake of the terrestrial biosphere in Europe (Nabuurs *et al.*, 2003). Potential future changes in terrestrial carbon stocks resulting from land-use or land-management changes are therefore of critical importance for climate mitigation policies.

Environmental changes may also have profound impacts on the amount of C stored in the terrestrial biosphere (Prentice *et al.*, 2001). Deposition of reactive nitrogen and fertilisation from increasing atmospheric carbon dioxide concentrations, $[\text{CO}_2]$, may stimulate plant production (Amthor, 1995; Vitousek *et al.*, 1997), leading to net C uptake in terrestrial ecosystems. On the other hand, climate change resulting from fossil fuel emissions may significantly alter the capacity of terrestrial ecosystems, in particular soils, to sequester C (Cramer *et al.*, 2001; Fang *et al.*, 2005). There is a risk of net losses from the terrestrial biosphere which in turn act to amplify rather than dampen the climatic change (Cox *et al.*, 2000; Friedlingstein *et al.*, 2003).

Only few studies have so far addressed the interactions between future human transformations of the landscape, and changes in climate and atmospheric $[\text{CO}_2]$ on the terrestrial C cycle (Leemans *et al.*, 2002; Levy *et al.*, 2004; Sitch *et al.*, 2005). These studies have shown that important feedbacks may be expected from both climate and land-use change in regional carbon budgets. Substantial uncertainty in future global land-atmosphere fluxes arises from uncertainty in climate change projections (Cramer *et al.*, 2004; Schaphoff *et al.*,

in review). However, no study has so far systematically evaluated the relative impact of land use and uncertainty in climate change projections on land-atmosphere fluxes using a consistent set of future land-use and climate change scenarios.

The present study aims to assess the magnitude of the terrestrial carbon fluxes that can be expected from these changes over the coming century, as well as to provide a comprehensive analysis of the uncertainty that arises in such projections from uncertainty about climatic changes in response to a particular emission scenario. Trajectories of future land-atmosphere fluxes are analysed using such a consistent set of land-use and climate change scenarios for a domain including the member states of EU15, as well as Norway and Switzerland (hereafter ‘EU*’). The assessment is based on an advanced version of the widely used Lund-Potsdam-Jena dynamic global vegetation model (LPJ-DGVM; Smith *et al.*, 2001; Sitch *et al.*, 2003) that has been adapted to represent actual land-cover as well as land-use changes. Plausible future development of land-use and greenhouse gas emissions are based on four of the six illustrative storylines from the IPCC Special Report on Emission Scenarios (SRES-storylines: ‘A1fi’, ‘A2’, ‘B1’, ‘B2’; Nakicenovic *et al.*, 2000, see Box 5.1). The effect of these scenarios on the terrestrial carbon balance is evaluated under a range of climate change projections derived from four different general circulation models (GCMs: CGCM2, CSIRO2, HadCM3, PCM2, see Table 5.1 on page 120; Mitchell *et al.*, 2004) to gain understanding of the individual and combined effects of climate, atmospheric [CO₂] and land-use changes, as well as the uncertainties associated with climate change projections.

5.2 Material and Methods

5.2.1 Overview

The SRES-storylines give plausible paths of future development in socio-economic driving forces, fossil-fuel emissions, atmospheric greenhouse gas concentrations, as well as estimates of global land-use changes (Nakicenovic *et al.*, 2000). Based on these storylines, future land-use scenarios have been constructed under special consideration of EU policies and societal trends (Kankaanpää and Carter, 2004; Ewert *et al.*, submitted; Reginster and Rounsevell, submitted; Rounsevell *et al.*, submitted, see Section 5.2.1). These scenarios project changes in arable land, grasslands, forests and urban area for 2020, 2050 and 2080 on highly resolved maps (10' × 10' grid) for a domain including the member states of EU15, as well as Norway and Switzerland (‘EU*’).

Emission scenarios based on the four storylines cover 68% of the range in future fossil-fuel emissions from all 40 SRES scenarios. Climate models differ in their climate sensitivity, *i.e.* their response to a doubling of the radiative forcing, and in particular with respect to the spatial pattern of changes in temperature and precipitation. Output from four different climate models, for the same SRES storylines, form the basis of climate change scenarios to represent this uncertainty (see Mitchell *et al.*, 2004, and Section 5.2.2). Outputs from these

Box 5.1: The four storylines of the Special Report on Emission Scenarios (SRES) used in this study; see Nakicenovic *et al.* (2000) for a detailed description.

The SRES-scenario narratives are differentiated along two axes: one describing 'material consumption' (denoted with 'A') and 'sustainability and equity' ('B'), and the second differentiating either 'globalisation' ('1') and 'regionalisation' ('2'). Along these axes, the four of the six illustrative storylines analysed in this study are 'A1fi' ('world markets - fossil fuel intensive'), 'A2' ('provincial enterprise'), 'B1' ('global sustainability') and 'B2' ('local stewardship'). 'A1fi' envisages rapid economic growth, and high technological advance, with strong reliance on fossil fuel based energy. Materialist-consumerist values are predominant, with low population growth. This narrative describes a strong globalisation, and reduced differences in affluence between different regions. 'A2' describes a heterogeneous, market-led world, with emphasis of regional social and economic development, and a continuous increase in population. The 'B1' narrative has a similar low population growth as 'A1', but represents a more convergent world emphasising global solutions towards a more environmentally sustainable pathway, including the introduction of clean technologies. 'B2' represents a world with local emphasis, intermediate economic development, and a population that stabilises at the end of the 21st century. As such, no probabilities can be attributed to scenarios.

four models are projected onto a common grid, preserving interannual and decadal climate variability of the 20th century to allow for a comprehensive and consistent assessment of the effect of climate change uncertainty on land-atmosphere flux calculations. The set of 16 future climatologies (four GCMs times four emission scenarios) covers 93% of the range in global warming reported in (Houghton *et al.*, 2001). In this study, a subset of eight scenarios is selected to illustrate:

- the range of land-atmosphere flux resulting from the four socio-economic scenarios of land-use changes and consistent climatic changes based on one climate model (HadCM3),
- the uncertainty in these calculations from uncertainty in the rate and spatial patterns of projected climate change (using the 'A2' storyline for all four GCMs),
- a scenario combining moderate climatic changes with substantial afforestation ('B2'-PCM2) to complement the 'extreme' climate change scenario 'A1fi'-HadCM3 (see Table 5.1).

The aim of the subset selection is to be encompassing, comprehensive without having to run all scenarios; see Mitchell *et al.* (2004) for detailed discussion. Here, 'interannual climate variability' refers to historic interannual and decadal climate variability with the longer time-scale variation removed.

Figure 5.1 gives an overview of the experimental setup of this study. For each scenario, three sets of simulations are performed (see details in Section 5.2.2):

- a control simulation accounting only for detrended interannual climate variability (S1),

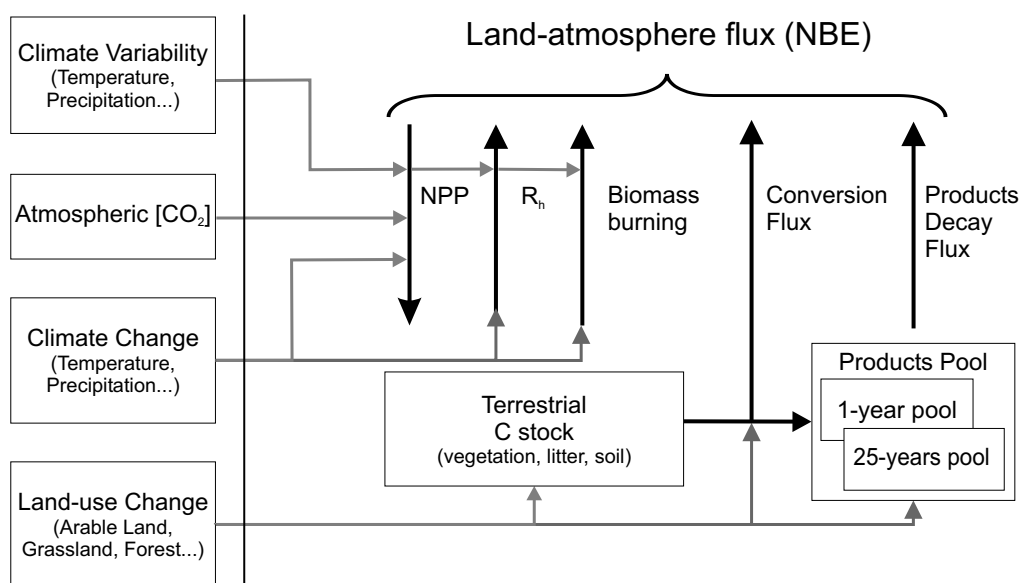


Fig. 5.1: Overview of the experimental setup of this study to simulate the combined effects of climate variability, climate change, increasing atmospheric $[CO_2]$, and land-use changes on the European terrestrial carbon balance between 1901-2100. Data-sets of CO_2 concentration, climate and land-use for the historic period (1901-2000), and future scenarios (2001-2100) are used to force LPJ on a $10' \times 10'$ grid. Simulated land-atmosphere C fluxes (NBE) result from the difference between terrestrial net primary production (NPP), and C releases from heterotrophic respiration (R_h), biomass burning, losses from land-use conversions, and human appropriation of biomass. The latter flux is separated into two products pools with different residence times: a 1-year decay pool (agricultural products and short-lived forest products), and a 25-years decay pool (paper, pulp, wood and other long-lasting products).

- a simulation accounting for historic and predicted changes in climate and atmospheric $[CO_2]$ and interannual climate variability (S2)
- a simulation accounting for all the above, but also land-use changes (S3).

By doing so, the marginal effect of climate and atmospheric $[CO_2]$ change can be inferred by subtracting the effect of interannual climate variability (S1) from S2, and the marginal land-atmosphere flux from land-use change by subtracting the fluxes resulting from interannual climate variability, climate and atmospheric $[CO_2]$ change from the simulations considering all forcing (S3 minus S2).

5.2.2 Data

Soil, and land-use data

For each grid cell, the proportions of land under ‘cropland’, ‘grassland’, ‘managed forests’, urban and ‘other land uses’ are derived from the PELCOM database (Mücher *et al.*, 2000) to construct the baseline land-use data set (assumed to correspond to 2000). Fractions of individual crop functional types (CFTs, see Section 5.2.3) within the agricultural area

are prescribed from the IMAGE2.2 data-set (RIVM, 2001), as described in Erhard *et al.* (in prep.). Partitioning of the forest area into different plant functional types (PFTs, see Section 5.2.3) is based on a combination of the European tree species map (Köble and Seufert, 2001), an area corrected estimate of broadleaved and coniferous forest cover (Schuck *et al.*, 2002), as well as bioclimatic limits (Sitch *et al.*, 2003).

Maps of historic land uses (1901-2000) are a spatial refinement of historic land-use data sets from (Ramankutty and Foley, 1999; Goldewijk, 2001) mainly in terms of more spatial detail in land-use change trends after 1960 (Erhard *et al.*, in prep., see Chapter 4, Appendix 4.6.4). Land-use change scenarios for 2020, 2050 and 2080 are derived by interpreting the SRES storylines (Kankaanpää and Carter, 2004; Ewert *et al.*, submitted; Reginger and Rounsevell, submitted; Rounsevell *et al.*, submitted). These two data-sets are linked by the baseline land-use data (PELCOM, Mùcher *et al.*, 2000, see above) to ensure consistency in the trajectories of land-use change between 1901 and 2100. Gridded time-series for each land-use change scenario, suitable for the use in terrestrial biosphere models, are constructed by linear interpolation between the respective time slices (2000-2020, 2020-2050 and 2050-2080), and extrapolation to 2100 using the trend between 2050 and 2080. The fractions of individual CFTs within 'croplands' and PFTs in 'managed forests' are maintained throughout the simulation. Thus, the scenarios do not account for changes in land management, *e.g.* changes in forest species selection, or crop types. Irrigation is assumed to have increased linearly between 1901 and 2000, and remain constant thereafter, following herein Bondeau *et al.* (in prep.). Note that these simulations do not account for any technological advance to increase plant productivity or retain C in soils. Soil properties are derived from soil texture (IGBP-DIS, 2000), using transfer functions for hydraulic (Saxton *et al.*, 1986) and thermal properties (Melillo *et al.*, 1995).

Land-use changes between 2000 and 2100

Generally, the global oriented scenarios 'A1fi' and 'B1' show strong regional diversification in land use, based on the assumption that land use is optimised for production across the entire domain, whereas in the 'A2' and 'B2' world, trends are more homogeneous because of the tendency for regional subsistence. Gross changes between different land-use types differ strongly amongst the scenarios because of the heterogeneous spatial patterns of land-use change. Key features of the land-use change scenarios are described below (see also Fig. 5.2).

A reduction in the area used for traditional agriculture, *i.e.* mainly for food production, is common to all four land-use scenarios. The decrease results mainly from technological advances and beneficial climate change effects on agricultural productivity; it is thus more pronounced under the technically oriented 'A' scenarios. Biofuel production increases in importance under all scenarios, but particularly so in the environmentally friendly 'B' scenarios. Some of the arable 'surplus' land is used for biofuel production, and therefore remains under agricultural management. Increases in forest area are more widespread

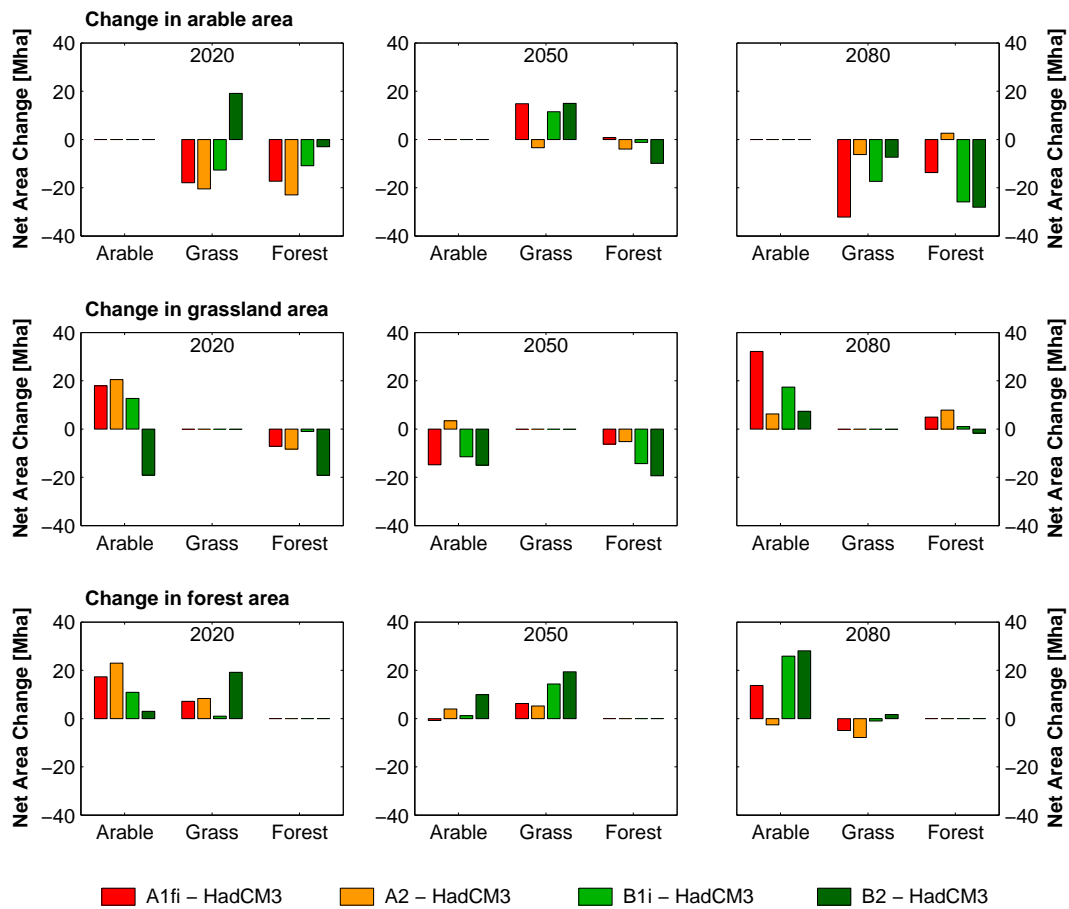


Fig. 5.2: Changing land cover fractions for arable land, grassland, and forests under the four land-use change scenarios ('A1fi', 'A2', 'B1i', 'B2', for the HadCM3-GCM) for 2020, 2050 and 2080 [Mha]. Positive values imply a net gain in cover of given land-use type on the expense of either 'arable', 'grass' or 'forest', and *vice versa*. 'Arable' includes cropland area used for food-production and non-woody biofuels, 'Grass' comprises pastures, and grasslands on agricultural 'surplus' land, 'Forest' include managed forests, and those used for woody-biofuel production.

under the environmentally oriented 'B' scenarios. In all but the 'B2' scenario, increases in forest and biofuel production area do not completely occupy the 'surplus' area from agricultural intensification. The scenario storylines do not give any suggestion as to the fate of these 'surplus' areas. In this study, it is assumed that woody encroachment would be prevented on these areas, since European land legislation would make it difficult to convert the land back to some other land-use, once a forest had been established. Urban areas are projected to expand under all scenarios – mostly on former agricultural land. This trend is most pronounced in 'A2' and least in 'B2', but the changes are small compared to the changes in Arable, Grass and Forest depicted in Figure 5.2. None of the scenarios specifically foresees any policy with the sole intention to enhance terrestrial carbon sequestration.

<i>Scenario</i>		<i>Europe</i>			<i>Finland mon. Temp.</i>		<i>Iberian Peninsula seasonal Precip.</i>			
<i>SRES</i>	<i>GCM</i>	<i>CO₂</i> [ppmv]	<i>Temp.</i> [°C]	<i>Precip.</i> [%(mm)]	<i>DJF</i>	<i>JJA</i>	<i>DJF</i>	<i>MAM</i>	<i>JJA</i>	<i>SON</i>
					[°C]		[%(mm)]			
A2	HadCM3 ^a	870	4.7	-0.5 (-3)	8.0	4.7	-5 (-12)	-31 (-57)	-40 (-36)	-19 (-37)
A2	CSIRO2 ^b	870	4.2	6 (45)	5.8	3.7	3 (7)	-11 (-19)	-27 (-25)	1 (2)
A2	CGCM2 ^c	870	3.7	3 (19)	6.1	3.0	-6 (-14)	-16 (-30)	-29 (-21)	-11 (-22)
A2	PCM2 ^d	870	2.8	3 (23)	7.7	2.4	3 (6)	-10 (-18)	-23 (-20)	-13 (-25)
A1fi	HadCM3 ^a	958	5.8	-1 (-7)	9.5	5.6	-3 (-7)	-35 (-63)	-41 (-37)	-25 (-48)
A2	HadCM3 ^a	870	4.7	-1 (-4)	8.0	4.7	-5 (-12)	-31 (-57)	-40 (-36)	-19 (-37)
B2	HadCM3 ^a	607	3.3	-0 (-1)	6.4	3.3	5 (10)	-19 (-34)	-32 (-29)	-9 (-18)
B1	HadCM3 ^a	516	3.0	-1 (-10)	6.2	3.1	-9 (-20)	-24 (-43)	-28 (-25)	-20 (-40)
B2	PCM2 ^d	607	1.9	(29)	5.1	1.9	2 (5)	-10 (-17)	-22 (-19)	-12 (-23)

^a Mitchell *et al.* (1998)

^b Gordon and O'Farrell (1997)

^c Flato and Boer (2001)

^d Washington *et al.* (2000)

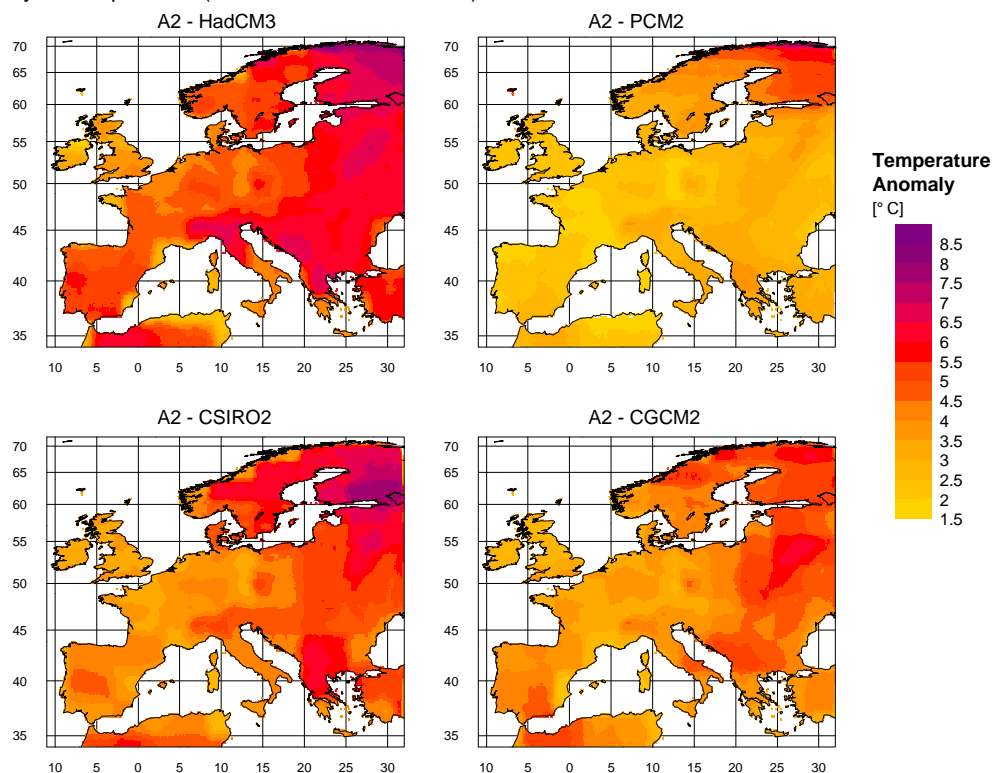
Tab. 5.1: Key characteristics of the climate change scenarios used in this study. Carbon dioxide concentrations are for the year 2100, temperature and precipitation values are anomalies referring to the difference between 1971-2000 and 2071-2100. Seasonal anomalies are given for monthly temperature in Finland (broadly defined as within the ATEAM window north of 60°N and east of 20°E), and seasonal precipitation sum for the Iberian Peninsula; these regions are of special importance to the results in Section 5.3.3. DJF: December, January, February; MAM: March, April, May; JJA: June, July, August; SON: September, October, November.

Climate and atmospheric CO₂ data

Atmospheric [CO₂] are based on Keeling and Whorf (2003) and IMAGE 2.2 (RIVM, 2001), as described in Erhard *et al.* (in prep.). The scenario [CO₂] data include an estimate of the net effect of global land-use change. Monthly fields of temperature, diurnal temperature range, precipitation, number of rain-days and cloudiness for each 10' × 10' grid cell are provided by the Climatic Research Unit (CRU), University of East Anglia (Mitchell *et al.*, 2004). Scenario data for monthly rain-days are not available from this dataset, and held constant at average 1971-2000 levels during the scenario period. Data for the period 1901-2000 are based on meteorological observations. Climate change scenarios for the period 2001-2100 are those constructed by Mitchell *et al.* (2004, see below).

The four GCMs used in this study differ in their spatial resolution, and in the degree with which present-day climate variability is reproduced. Interannual climate variability is an important driver of variability in the terrestrial carbon cycle (Kindermann *et al.*, 1996; Prentice *et al.*, 2000). For a consistent analysis of present and future carbon fluxes, only anomaly fields for each climate variable from the climate models, and climate variability of the 20th century is preserved throughout, including the scenario period. Anomaly fields for each climate variable and each GCM for the period 2070-2099 are superimposed to the

a) Anomaly in Temperature (2071-2100 vs. 1971-2000)



b) Anomaly in Precipitation (2071-2100 vs. 1971-2000)

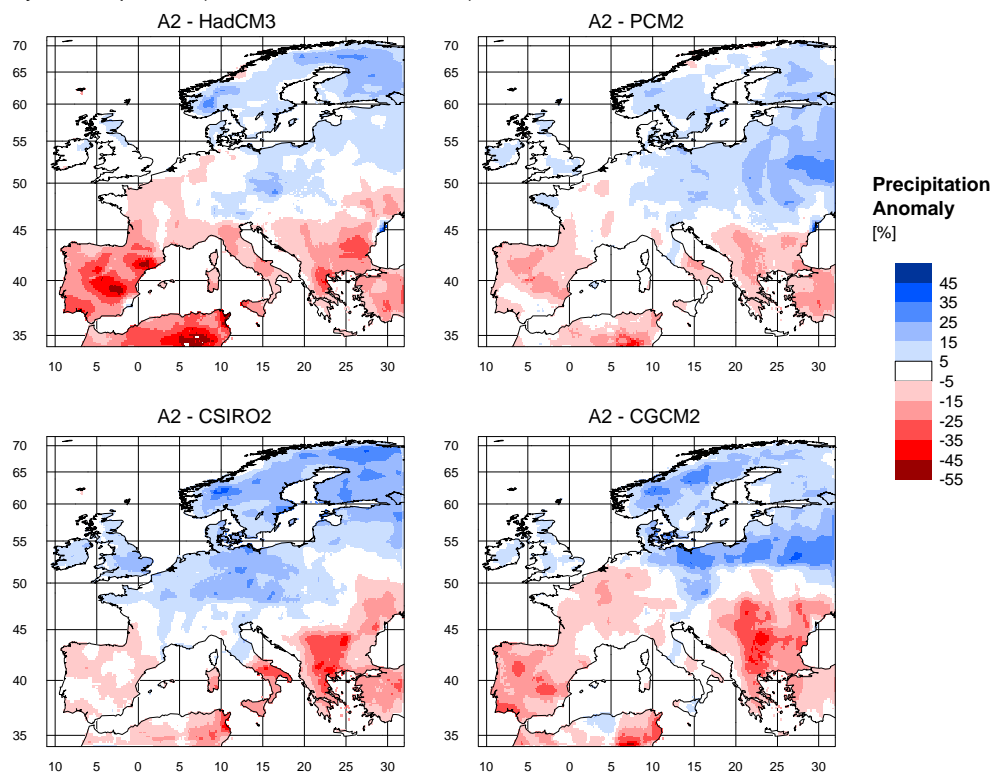


Fig. 5.3: Anomaly (2071-2100 vs. 1971-2000) in a) annual mean temperature (°C) and b) annual precipitation (% change) for the HadCM3, CSIRO2, CGCM2 and PCM2 GCMs, and the 'A2'-SRES emission scenario.

10' × 10' CRU climatology for 1961-1990 to arrive at a high-resolution data-set suitable for regional scale analyses. The transient changes for each climate variable, GCM and scenario in the 21st century are derived from MAGICC (Hulme *et al.*, 2000), thereby also allowing to analyse scenarios for which original GCM data are not available. These transient changes are superimposed to the detrended interannual climate variability of the 20th century. In other words, the interannual and decadal climate variability of the 20th century is repeated in the 21st century, however, with a climate model derived long-term trend of climate change. Thereby, all scenarios share the same, realistic climate variability. To control for the effect of choosing this particular realisation of interannual and decadal variability, and to factor out the influence from short-term variability and long-term trends, a run only forced with the detrended climate variability is performed (S1).

Climate change scenarios 2001-2100

Table 5.1 summarises key characteristics of these scenarios and Figure 5.3 illustrates the spatial patterns of climate change obtained from the different climate models for the 'A2' scenario. Spatial patterns of climate change are relatively similar between different story-lines for each GCM. Generally, the HadCM3 climate model shows the most pronounced rates of warming amongst these GCMs, whereas PCM2 depicts the most modest warming rate. All four climate models project their strongest warming over the high-latitudes of Europe, with a larger rate of change in the winter months. Different emission scenarios for one model (HadCM3) lead to a almost twofold difference in the the change in annual temperature, however, the spatial pattern of change is fairly similar. Overall annual precipitation over Europe changes only slightly under all four climate models, however, notable trends can be seen regionally in Figure 5.3. All four models show a decline in precipitation over the Mediterranean, which is most pronounced in summer. Amongst this suite of models, HadCM3 shows the strongest drying trend both with respect to the seasonal decrease as well as the increase in the length of the dry period, whereas changes with the other three models are more moderate.

5.2.3 Model

LPJ-DGVM

The Lund-Potsdam-Jena dynamic global vegetation model (LPJ, Smith *et al.*, 2001; Sitch *et al.*, 2003) is a model derived from the BIOME family (Prentice *et al.*, 1992; Haxeltine and Prentice, 1996b). The version used in this study has been modified in terms of a representation of human induced fire frequencies (Venevsky *et al.*, 2002), a more detailed treatment of hydrological processes (Gerten *et al.*, 2004), a representation of croplands (Bondeau *et al.*, in prep.), and a module to account for land cover changes (this study, following similar principles as McGuire *et al.*, 2001). A generic representation of forest

management influences the average age and size of the forest population, without explicitly modelling forest age structure and age-dependent effects on tree growth (this study).

Gross primary production (*GPP*) is calculated using a modified form of the Farquhar scheme (Farquhar *et al.*, 1980; Collatz *et al.*, 1992) with canopy-level optimized nitrogen allocation (Haxeltine and Prentice, 1996a, modified by F.-W. Badeck, *unpublished data*) and an empirical convective boundary layer (Monteith, 1995) to couple the C and H₂O cycles. Soil hydrology is simulated using two soil layers (Haxeltine and Prentice, 1996b). Net primary production (*NPP*), *i.e.* *GPP* reduced by C losses to autotrophic respiration, is allocated to plant tissues daily for crop functional types (CFTs, Bondeau *et al.*, in prep.) and annually for woody plant functional types (PFTs, Sitch *et al.*, 2003) satisfying a set of allometric and functional relationships. Turnover of plant tissues, plant mortality and/or management redistribute C from living biomass to above- and belowground litter pools, which in turn provide input to a fast and a slow decomposing soil C pool. Decomposition rates depend on a modified Arrhenius formulation (Lloyd and Taylor, 1994), which implies a decline in apparent Q_{10} values with temperature, and an empirical soil moisture relationship (Foley, 1995).

LPJ has been evaluated against observations of land-atmosphere fluxes at different scales, including field-scale eddy covariance measurements (Sitch *et al.*, 2003; Zaehle *et al.*, 2005; Morales *et al.*, in review), the seasonal cycle of atmospheric [CO₂] at different latitudes (Sitch *et al.*, 2003; Zaehle *et al.*, 2005), the observed trend in the seasonal amplitude of global atmospheric [CO₂] since the 1960s (McGuire *et al.*, 2001), and the interannual variability in its growth rate (Prentice *et al.*, 2000; Peylin *et al.*, 2002). LPJ has been one of four models which first attempted to incorporate the effect of land-use change into terrestrial biosphere models (McGuire *et al.*, 2001). LPJ is used to study aspects of the transient response of the terrestrial biosphere to environmental changes and climate change (Lucht *et al.*, 2002), including an assessment of process-based and parameter-based uncertainty in DGVMs (Cramer *et al.*, 2001; Zaehle *et al.*, 2005), the effect of uncertainty in climate change (this paper; Schaphoff *et al.*, in review), and the equilibrium response to a particular climate forcing (Gerber *et al.*, 2004).

Changes to the original model formulation

Land use and Land-use Change: Each 10' × 10' grid cell is subdivided into fractions of different land uses, *i.e.* 'croplands', 'grasslands/pastures', 'managed forest', 'other land uses' and 'barren' based on the land-use data described in Section 5.2.1. 'Croplands' and 'managed forests' are further subdivided into homogeneous patches for different CFTs or PFTs, respectively. 13 crop functional types are encoded in LPJ with different photosynthetic (C3, C4), phenological and morphological characteristics, representing amongst others temperate cereals, maize and variants, pulses, roots and tubers, oil crops and rice. LPJ distinguishes 10 plant functional types (PFTs) with different photosynthetic (C3, C4), phenological (deciduous, evergreen), and physiognomic (tree, grass) attributes. Of

<i>Ecosystem</i>	<i>Fate upon conversion</i>		<i>Fate as product</i>	
	<i>Below-ground biomass (left dead in soils)</i>	<i>Above-ground biomass (slash left)</i>	<i>1-yr pool (crops, fuel wood)</i>	<i>25-yrs pool (paper, pulp, wood)</i>
Temperate/Boreal forest	100%	30%	67%	33%
Croplands	100%	10% (if any)	90% of aboveground C	n.a.
Grasslands	100%	10%	90% of aboveground C each grass cut	n.a.
Woodlands ('other land use')	100%	33%	67%	33%

Tab. 5.2: The fate of carbon upon conversion, and ecosystem management for different terrestrial ecosystems. Conversion and partitioning coefficients for forest and woodlands are based on (UN-ECE/FAO, 2000; McGuire *et al.*, 2001; Nabuurs *et al.*, 2003), removal of C in croplands and grasslands are based on the agricultural module as described in Bondeau *et al.* (in prep.)

these, the eight PFT that exist in Europe are the temperate and boreal needleleaved evergreen, temperate and boreal broadleaved summergreen, boreal needleleaved summergreen and temperate broadleaved evergreen, as well as C3 and C4 herbaceous PFTs. For each of these subdivisions, fluxes and balances of water and carbon are calculated independently on the basis of the common 'LPJ' physiology. Natural vegetation dynamics are calculated for the 'other land use' grid cell fraction, as in LPJ-DGVM (Sitch *et al.*, 2003).

For each grid cell, fractions for each land-use type are updated annually. The fate of C following land conversion and management is summarised in Table 5.2. Aboveground C of trees on converted land is treated as in McGuire *et al.* (2001), however, partitioning coefficients for the wood products pool are taken from (Nabuurs *et al.*, 2003), which are more appropriate for the use in a European-scale simulation. Slash and belowground litter are added to the respective litter pools of the converted land. Cropping systems are assumed to rotate within any one grid cell, leading to an average soil C pool stocks in the agricultural land-cover corresponding to the difference of average crop plant production and removal by harvest.

Forest Management: Total fellings from forest management are estimated from an approximation of the average felling in a evenly structured forest landscape as a function of maximal stand biomass (Dewar, 1991), as well as characteristic growth curves and rotation-times based on (Nabuurs and Mohren, 1995). Management of forests is described as an additional mortality term in the vegetation dynamics. Vegetation dynamics in 'managed forests' allow for structural changes in response to changing environmental conditions, however, not in terms of changed PFT composition (Sitch *et al.*, 2003). Removals from fellings are based on conversion factors scaling whole-tree biomass to roundwood volume and account for the losses of timber in the forest during harvesting activity (UN-

ECE/FAO, 2000). Timber is partitioned into a 1-year and a 25-years wood-products pool as in Nabuurs *et al.* (2003, Table 5.2). Essentially, although such an approach accounts for the timber removed from forests (and its storage in wood-products), changes in the age structure due to changes in harvest regimes or forest area are not captured, nor are their effects on average forest growth rate. Wood demand changes have not been considered in this study.

Modelling Protocol

LPJ is spun up to equilibrium in terms of pre-industrially stable C pools and vegetation dynamics using the reconstructed land-use patterns of 1901. 30 years of recycled climate (1901-1930) and atmospheric CO₂ concentrations (from 1901) seed this spin-up. In S1, LPJ is forced only with the detrended interannual climate variability, and constant atmospheric [CO₂] and land-use patterns at 1901 levels. In S2, historic (1901-2000) and projected (2001-2100) climatic changes are superimposed on the interannual variability of S1, and [CO₂] levels increase as observed or projected in the scenarios, respectively. In S3, in addition to the above, land -use patterns are varied based on the reconstruction for the period 1901-2000, and scenario projections for 2001-2100.

The land-atmosphere carbon flux, the so called net biome exchange (*NBE*), is calculated separately for each fraction of a grid cell as the net primary production (*NPP*), minus losses via heterotrophic respiration (*R_h*), biomass burning, or by human appropriation. The latter term is the sum of decaying wood products (as described above), and the harvesting flux from croplands, added to the annual fluxes of the grid cell fraction of production.

$$NBE = R_h + BiomassBurning + HumanAppropriation - NPP \quad (5.1)$$

where a negative sign denotes a C flux into the terrestrial biosphere, seen as depletion of [CO₂] in the atmosphere, and *vice versa*. *NBE* of the entire grid cell is then calculated as the area-weighted mean of the fractional land-atmosphere exchanges.

5.3 Results

5.3.1 Present-day European carbon balance

Simulated present-day carbon stocks in soil and vegetation are in modest agreement with independent estimates based on the extrapolation of soil surveys, and forest inventories (Goodale *et al.*, 2002; Smith *et al.*, 2005a,b). About a third of Europe's terrestrial *NPP* is lost to the atmosphere by human appropriation, resulting either from food consumption, or decaying wood products (Fig 5.4, see page 126). The remainder is, to a large extent, lost through *R_h*. Biomass burning, though locally very important, is estimated to play only a minor role in the European scale carbon budget. The modelled land-atmosphere

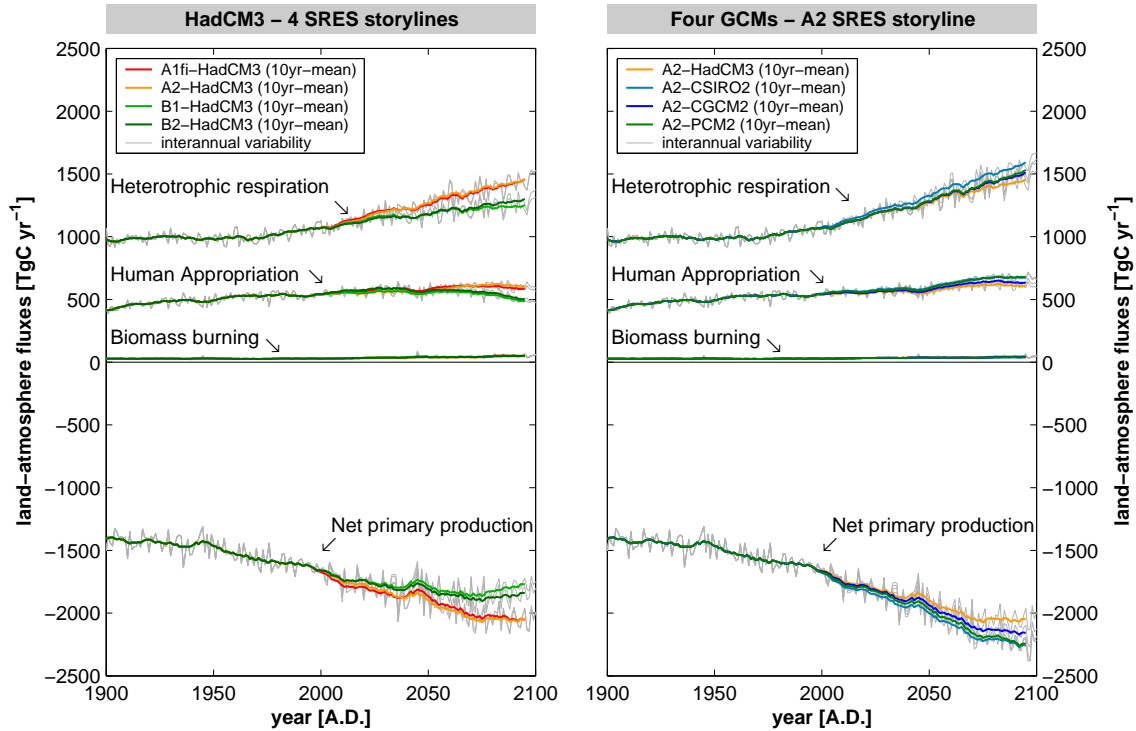


Fig. 5.4: Constituent fluxes of the net land-atmosphere flux [TgC yr^{-1}] considering climate, atmospheric $[\text{CO}_2]$ and land-use change for 1901-2100. **Left:** Results for the four different SRES-storylines ('A1fi', 'A2', 'B1' and 'B2') with climate change projections derived from the Hadley climate model. **Right:** Results for the 'A2'-SRES storyline, with climate change projections based on four different GCMs (HadCM3, CSIRO2, CGCM2, PCM2).

flux of the terrestrial biosphere in the ATEAM-window averages at -5 TgC yr^{-1} for the 1990s (Fig. 5.5a,e, see page 127), with a large interannual variability between -105 TgC yr^{-1} (net uptake) and $+88 \text{ TgC yr}^{-1}$ (net loss). This compares to an estimate of $-95 (\pm 154) \text{ TgC yr}^{-1}$ based on a compilation of bottom-up estimates for different land uses (using numbers and approach from Janssens *et al.*, 2003, but scaling with the area and harvest ratio for the countries within EU*).

5.3.2 Effects of land-use change

Reconstructed historical land-use data suggest that agricultural area increased between 1900 and the 1950s, replacing 'other land-uses' which are assumed to be occupied by natural vegetation. Stagnation and subsequent reversal of this trend around the 1950s, as well as concomitant increases in forest area are the main causes for the decreasing net loss of C from land-use change, reaching a zero balance in about 1990. The net loss of C from land-use change in the 1980s of $+3 \text{ TgC yr}^{-1}$ (Fig. 5.5b,f) compares to the land-atmosphere flux from land-use change based on book-keeping of land-use changes average at about $-20 (\pm 200) \text{ TgC yr}^{-1}$ for geographical Europe, excluding the former Soviet Union

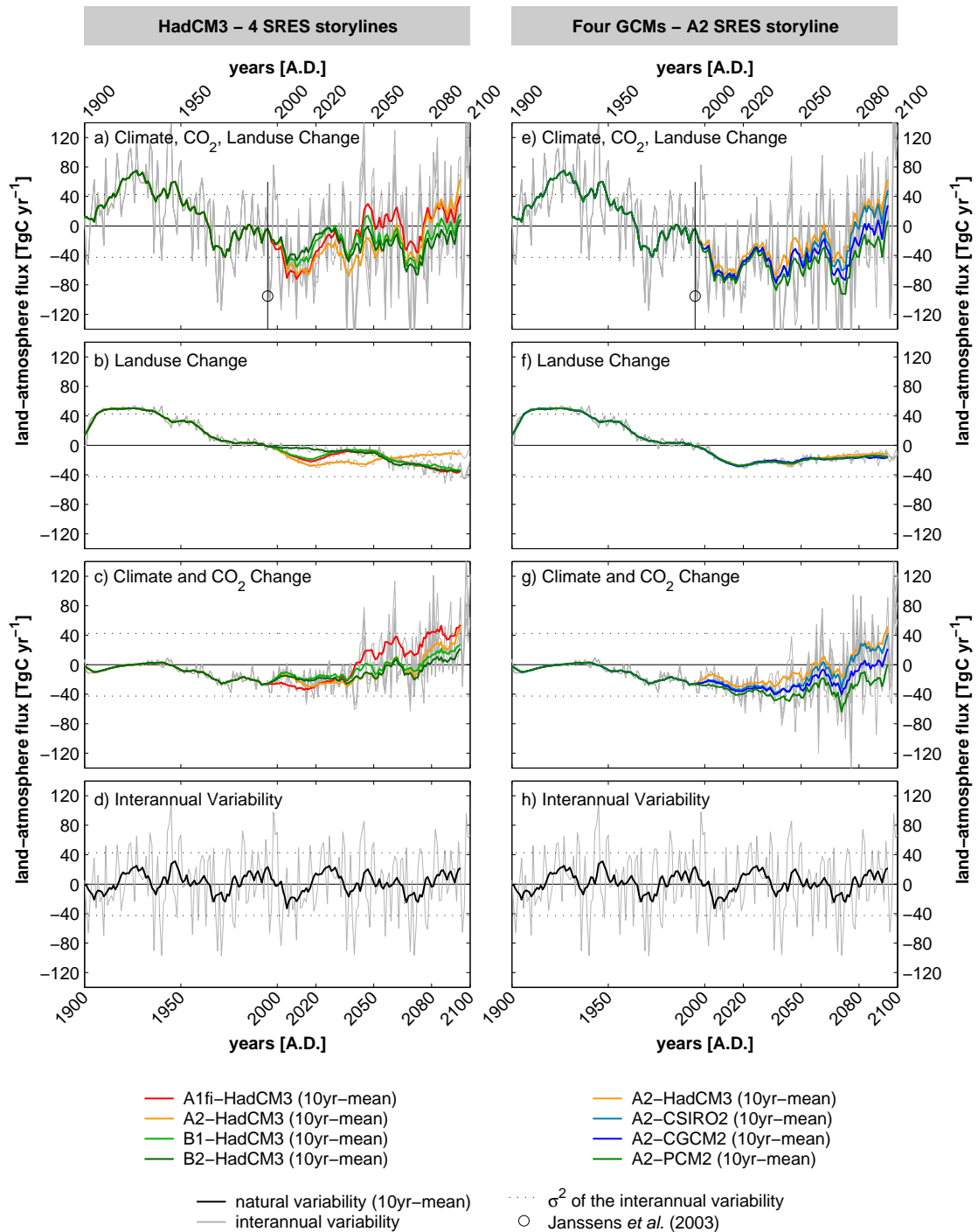


Fig. 5.5: Land-atmosphere flux [TgC yr⁻¹] in the ATEAM-domain 1901-2100. **Left (a-d)**: Results for the four different SRES-storylines ('A1fi', 'A2', 'B1' and 'B2') with climate change projections derived from the Hadley climate model. **Right (e-h)**: Results for the 'A2'-SRES storyline, with climate change projections based on four different GCMs (HadCM3, CSIRO2, CGCM2, PCM2). **a, e**) land-atmosphere flux resulting from climate, atmospheric [CO₂] and land-use change (S3); **b, f**) land-atmosphere flux attributable to land-use change (S3-S2); **c, g**) land-atmosphere flux attributable to climate and atmospheric [CO₂] change (S2-S1); **d, h**) land-atmosphere flux attributable to detrended interannual climate variability (S1). natural variability denotes here the 10-years running average of the land-atmosphere flux resulting from detrended interannual climate variability.

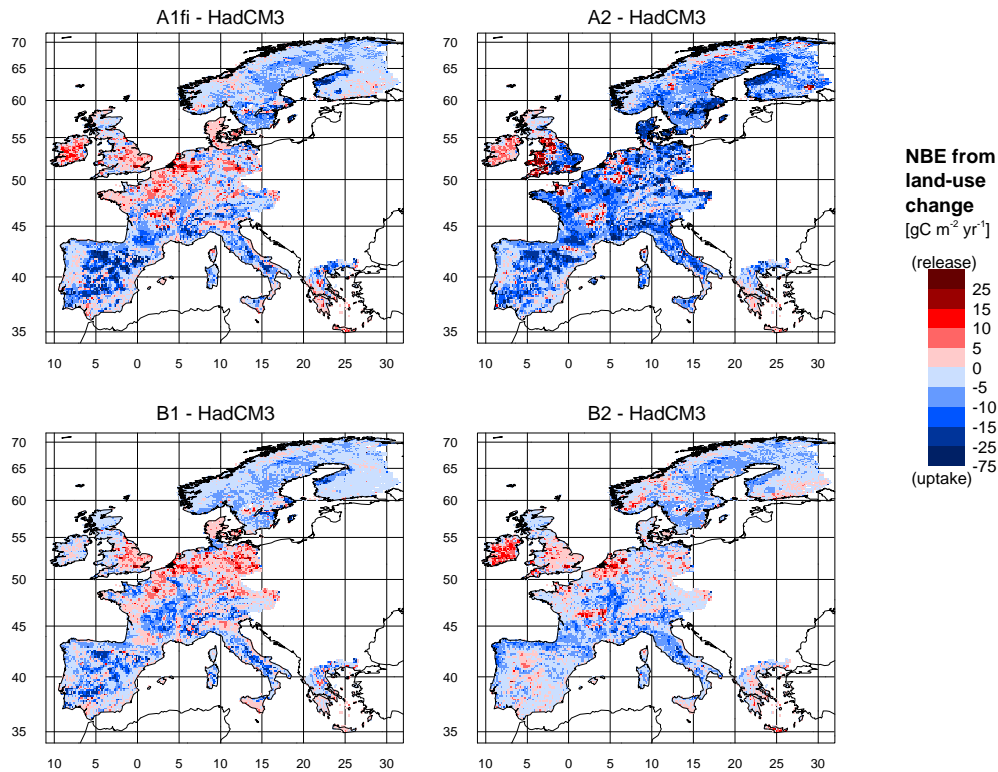


Fig. 5.6: Land-atmosphere fluxes associated with the effects of land-use change, averaged over 2021–2050 for the four SRES storylines ('A1fi', 'A2', 'B1', 'B2') and implemented with HadCM3-GCM.

(Houghton, 1999). Land-use changes in the scenario period are projected to result in net C uptake in all four storylines when averaged over the entire domain (Fig. 5.5b), as an effect of agricultural land abandonment (see Section 5.2.1). The trajectories of land-atmosphere flux from land-use change in the 'A1fi' and 'B1' scenarios are very similar, despite considerable spatial heterogeneity in the land-atmosphere flux between these scenarios (Fig. 5.6, see page 128).

In the 'A1fi' world, agricultural activity is centred in regions of prime productivity, leading to surplus land from agricultural land abandonment in less favoured areas. These areas are – as assumed in this study – converted into grasslands. This results in a net C uptake, as C inputs into the soils are higher in grassland than in croplands, as less C is removed from grazing or cutting, which would otherwise enter the litter and soil pools. Grassland increases as well as afforestation – primarily on previously agriculturally used soils – are the main contributors to the land-atmosphere flux of -20 (2020) and -35 (2080) TgC yr^{-1} under the 'A1fi' scenario. Between 2020 and 2050, C uptake is substantially reduced, as re-expansion of agriculture in intensively used agricultural areas replaces grasslands, which leads to net C losses from soils (Fig. 5.2). This is seen in Figure 5.6 as areas of net C loss *e.g.* in Eastern England and the Benelux-states.

Homogeneous decreases in agricultural area across Europe in the ‘A2’ scenario make land available either for surplus or afforestation, both of which contribute to the fairly evenly distributed land-atmosphere flux of -25 TgC yr^{-1} between 2000 and 2050 (Fig. 5.6). Forest expansion stops in this scenario at around 2050, and clearing of forests occurs between 2050 and 2100 in this scenario in Southern Europe resulting in a net loss of forest area. This decline is the main reason for the reduction in magnitude of the land-atmosphere flux in the second half of the 21st century (Fig. 5.5b). Also, urban expansion, strongest in the ‘A2’ scenario results in net C losses, however, the size of this flux is too small to be seen in regional patterns of land use related land-atmosphere fluxes.

In ‘B1’, agricultural productivity is centred in prime locations as in ‘A1fi’, however, the decline in arable area is less, thus less ‘surplus’ area becomes available. Afforestation is assumed to be more widespread across Europe and most pronounced in Central and Southern Europe, however, before 2020 at half the rate as in ‘A1fi’. These changes result in a land-atmosphere flux of -18 TgC yr^{-1} in 2020. The effect of the strong afforestation on the total net land-atmosphere flux after 2020 is reduced to a net -7 TgC yr^{-1} until 2050 because the area used for cropping, mostly for biofuel production, increases again, primarily at the expense of former grasslands (compare Fig. 5.6). After 2050, even larger increases in forest and grassland area, lead to a land-atmosphere flux of about -35 TgC yr^{-1} in 2080.

The ‘B2’ world is considerably different to the other three scenarios, as no surplus land becomes available from declines in agricultural area. In fact, the decline in area for food production is more than compensated for by increasing biofuel production. A net conversion of grasslands into arable land is required to allocate the land area for biofuel production between 2000 and 2020 (Fig. 5.2). These changes and rapid afforestation on grassland soils, *e.g.* in Ireland (Fig. 5.6), reduces the net effect of the increasing carbon storage in vegetation during until 2050 with land-atmosphere fluxes of around -3 TgC yr^{-1} . Although the increase in forest area in the ‘B2’ scenario is the largest among the four scenarios, more wide-spread afforestation begins to increase biospheric uptake (*NBE*: -35 TgC yr^{-1} in 2080) only after 2050, when afforestation occurs mainly on previously agriculturally used area.

5.3.3 Effects of climate and atmospheric $[\text{CO}_2]$ change

Climate change and increasing atmospheric $[\text{CO}_2]$ lead to a rise in *NPP* under all scenarios (Fig. 5.4). However, in most scenarios this increase levels off around the year 2070. Initially, increases in *NPP* are faster than the rate of increase C release from R_h , thereby sustaining a net C uptake of the terrestrial biosphere between the 1950s and at least 2040 (Fig 5.5c,g). All scenarios show a decline in the C flux towards the biosphere attributed to climate and $[\text{CO}_2]$ change in the second half of the 21st century. The terrestrial biosphere is a C source to the atmosphere towards the end of the scenario period under all HadCM3 scenarios, but also for ‘A2-CSIRO2’ and ‘A2-CGCM2’. Only with very

moderate climate warming, *i.e.* under the two PCM scenarios (*data for 'B2' not shown*), increasing respiration losses only balance increasing *NPP*, reducing the land-atmosphere flux from climate change to zero at around 2100. The simulated trends in *NBE* resulting from climate change and increasing atmospheric $[\text{CO}_2]$ are of a similar magnitude as the variability in land-atmosphere fluxes from 'natural' climate variability alone (Fig. 5.5d,h). There is considerable spread in the magnitude of the land-atmosphere C flux, as well as the timing of the reduction in net terrestrial C uptake, between the different scenarios towards the end of the scenario period (Fig. 5.5c,g).

These differences are less pronounced between the runs using four different SRES storylines and the HadCM3 climate model ('HadCM3 - 4 SRES storylines'). All four 'HadCM3' scenarios show a stabilisation of *NPP* in the last 20 years of the scenario (Fig. 5.4), despite substantial differences between the magnitude of *NPP* between the high ('A1fi' and 'A2') and low ('B1' and 'B2') atmospheric $[\text{CO}_2]$ scenarios. *NBE* trends are fairly similar for all four scenarios. Biospheric C uptake until 2040 turns into a net C release towards the end of the scenario period (Fig. 5.5g). The 'A1fi' scenario is particular since it exhibits the most rapid warming trend, leading already in the 2040s to a net C loss to the atmosphere from climate change alone. In general, initially larger gains from increased *NPP* in high atmospheric $[\text{CO}_2]$ scenarios ('A') are lost due to the larger rates of climate warming in these two scenarios.

Figure 5.7 illustrates the spatial coherence in *NBE* anomalies in 2021-2050 and 2071-2100 resulting from differential climate change projections based on the four GCMs, forced with the same emission scenario ('A2'). In 2021-2050, most of Europe's terrestrial biosphere sequesters C, with only slight differences among the projections based on the four GCMs (Fig. 5.7b). Between 2071 and 2100, the ensemble average *NBE* for large parts of Central Europe is close to zero, resulting in a small positive anomaly since the biosphere acts as a small net sink in 1971-2000. Scenarios agree relatively well over large parts of Central Europe, however disagree in Eastern Scandinavia and the Mediterranean region, especially the Iberian Peninsula (Fig. 5.7d). These are the areas with the most prominent differences in climate change projections between the four GCMs (see Table 5.1).

In Scandinavia, all four climate models show their strongest projected warming in Europe, with anomalies in annual mean temperature between 4.4°C ('A2-CGCM2') and 5.9°C ('A2-HadCM3'; Fig 5.3a). Three out of the four models show the most pronounced warming in winter (Table 5.1), affecting respiratory processes more than photosynthesis. Only subtle differential changes in rates of ecosystem C uptake and release have substantial effect on the net land-atmosphere flux, as boreal forest soil carbon densities are amongst the largest soil C stock densities in Europe. Projected growth enhancement and increasing storage of C in vegetation are outbalanced by increasing losses from soil respiration in all four 'A2' scenarios, however, this effect is more pronounced in those scenarios with higher warming (*i.e.* 'A2-HadCM3' and 'A2-CSIRO').

All four climate models generally predict a decline in summer precipitation over large

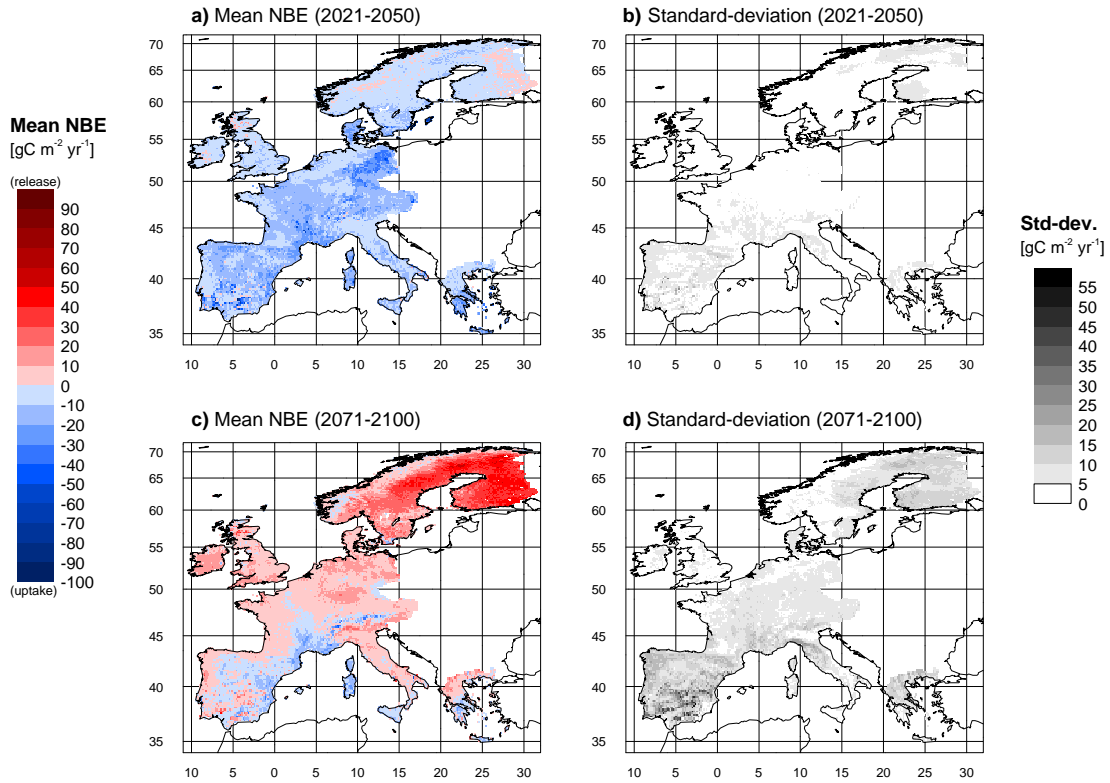


Fig. 5.7: Land-atmosphere fluxes associated with climate change and CO₂-fertilisation under the 'A2'-SRES scenario, as anomalies for 2021-2050 and 2071-2100. The left-hand maps (a,c) show the average over all four S2 simulations ('A2'-storyline, HadCM3, CSIRO2, CGCM2, PCM2), the right-hand maps (b,d) the standard deviation between these four runs.

parts of the Mediterranean (Fig. 5.3b, Table 5.1). A concomitant increase in monthly temperatures is more pronounced in summer in HadCM3 and CGCM2, but spread evenly over the year in two models (PCM2 and CSIRO2). HadCM3 is the most extreme climate model in terms of the increase in seasonal temperatures as well as the decline in annual precipitation and the prolongation of the summer dry-season (see Table 5.1). The differences in *NBE* shown in Figure 5.7 in the Mediterranean result mainly from differences between the 'A2-HadCM3' run and the other three scenarios. On a regional scale, CO₂ induced increases in water-use efficiency more than compensate for the effect of water limitation on photosynthesis in three out of four scenarios ('A2-PCM2', 'A2-CSIRO2', and 'A2-CGCM2'), but not in 'A2-HadCM3'. In 'A2-HadCM3', drought stress leads to a decline in *NPP* in the last 25 scenario years, partly masked by substantial interannual variability. Stabilisation of *NPP* and increasing R_h as a response to increasing temperature reduce the biospheric C uptake most strongly under HadCM3. In addition, the pronounced drying trend projected with the Hadley model leads to a nearly twofold increase in fire danger (increase by 83% between the 30-year averages in 1971-2000 and 2071-2100) relative to the 34-53% increase in fire risk in the other three scenarios. As a

	A1fi	A2				B1	B2	
	<i>HadCM3</i>	<i>HadCM3</i>	<i>CSIRO2</i>	<i>CGCM2</i>	<i>PCM2</i>	<i>HadCM3</i>	<i>HadCM3</i>	<i>PCM2</i>
Climate and [CO ₂] change (S2)								
Vegetation (PgC)	1.69	1.92	2.76	2.41	2.71	1.27	1.79	2.22
Soil (PgC)	-2.00	-1.06	-1.08	0.09	1.03	-0.68	-0.52	0.88
Total (PgC)	-0.31	0.86	1.68	2.50	3.74	0.59	1.27	3.10
Land-use Change (S3 - S2)								
Vegetation (PgC)	0.94	0.84	0.78	0.59	0.78	1.04	1.48	1.53
Soil (PgC)	0.85	0.77	0.97	1.11	0.96	0.57	0.29	0.19
Total (PgC)	1.79	1.61	1.74	1.70	1.74	1.61	1.77	1.72
All forcing (S3)								
Vegetation (PgC)	2.63	2.76	3.53	3.00	3.49	2.31	3.27	3.75
Soil (PgC)	-1.15	-0.29	-0.11	1.21	1.99	-0.11	-0.23	1.07
Total (PgC)	1.48	2.47	3.42	4.21	5.48	2.20	3.04	4.82
Average land-atmosphere flux (1990-2100) as percentage of the EU* Kyoto CO ₂ emission reduction target ^a								
Land-use change	22.4	20.2	21.8	21.2	21.8	20.1	22.2	21.5
All forcing	18.5	30.8	42.8	52.6	68.5	27.5	38.0	60.3
Average land-atmosphere flux (1990-2100) as percentage of the average EU* CO ₂ emissions (1990-2100) ^b								
Land-use change	1.08	1.11	1.20	1.17	1.20	1.66	1.81	1.76
All forcing	0.87	1.68	2.35	2.39	3.77	2.24	3.77	4.93

^a 1990 emissions for EU15: 3.290 Gt CO₂, Switzerland: 0.045 Gt CO₂, Norway: 0.048 Gt CO₂, the total corresponding to 922 TgC yr⁻¹. Accounting for the 'Kyoto' emission targets of 92% (EU15 and Switzerland) and 101% (Norway) gives a EU15* Kyoto emission reduction target corresponding to 72.6 TgC yr⁻¹

^b based on projections of IMAGE 2.0, as in RIVM (2001). 'A1fi': 1,493 TgC yr⁻¹, 'A2': 1,389 TgC yr⁻¹, 'B1': 881 TgC yr⁻¹, 'B2': 887 TgC yr⁻¹.

Tab. 5.3: Cumulative changes in terrestrial vegetation and soil C pools (1990-2100) in PgC under the different scenarios analysed, attributed to climate and atmospheric [CO₂] or land-use change.

result, C releases from biomass burning increase by 87% (29-59%) towards the end of the scenario period.

5.3.4 Cumulative land-atmosphere flux between 1990 and 2100 under climate, atmospheric [CO₂] and land-use change

Notwithstanding the considerable differences in the magnitude and spatial patterns of land-use change related fluxes across the four land-use change scenarios between 1990, the reference year for the Kyoto protocol, and 2100, cumulative land-atmosphere fluxes from land-use change for 1990-2100 are very similar (Fig. 5.8c, Table 5.3). The net uptake 1990-2100 averages at 15.5 TgC yr⁻¹, which corresponds to about 20% of the EU*'s present-day CO₂ emissions. Interactions of the land-use change flux with climate and [CO₂] change lead to only subtle differences in the projected uptake attributed to land-use change.

Uncertainties in cumulative *NBE* attributable to climate change are more pronounced than those in the land-use change related fluxes in this particular set of scenarios. Dif-

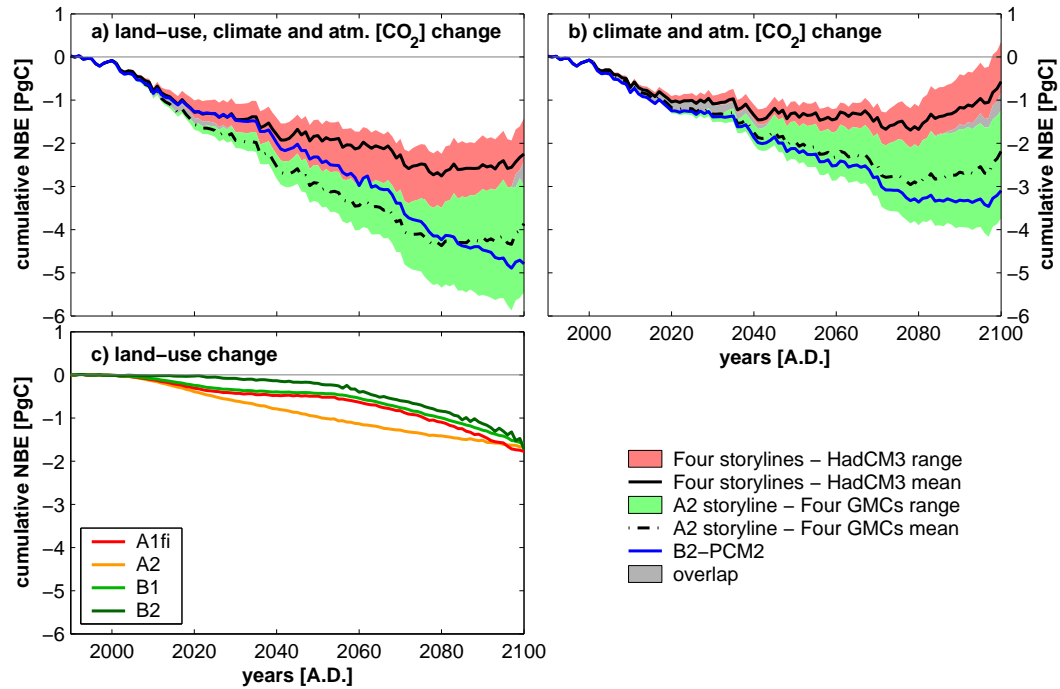


Fig. 5.8: **a)** Cumulative land-atmosphere fluxes [TgC yr^{-1}] between 1990 and 2100; spilt into the components **b)** attributable to climate and $[\text{CO}_2]$ change, and **c)** to land-use change. Displayed are the mean and range of simulation groups based on four different SRES-storylines and HadCM3, based on the ‘A2’ storyline and four different GCMs, as well as the ‘B2’-PCM2 scenario.

ferences in *NBE* resulting from the choice of a particular storyline (*i.e.* the four different storylines and one climate model) are smaller than those resulting from uncertainty in climate change under the same emission scenario (*i.e.* four different climate models and the ‘A2’-storyline) (Fig 5.8b). Notably, the difference in land-atmosphere flux between the ‘A2’ and ‘B2’ scenario modelled with either the PCM2 or HadCM3 climate change scenario is smaller than the difference between C flux projections between the PCM2 and HadCM3 climate change scenario for either of the ‘A2’ and ‘B2’ storyline (see Table 5.3).

Uncertainty in climate change under the same storyline (land-use change and CO_2 scenario) propagates to a 2.1 PgC difference in cumulative land-atmosphere fluxes by the end of the scenario period (Table 5.3). Changes in soil C stock differ widely between these four scenarios (a loss of ~ 1 PgC in ‘A2-HadCM3’ and ‘A2-CSIRO2’ versus and uptake of ~ 0.9 PgC in ‘A2-PCM2’), whereas vegetation stock increases are more similar (see Table 5.3). All four ‘HadCM3’ scenarios predict the strongest decline in soil C stocks, and the smallest increase in vegetation C, related to the pronounced drought in the Mediterranean. These scenarios show the most restricted land uptake of C over the scenario period. The most extreme warming scenario, ‘A1fi-HadCM3’, is the only climate change scenario, which projects Europe as a cumulative net source resulting from substantial net losses of soil C by 2100.

The combined effect of land-use and climate change on the terrestrial biosphere suggests a cumulative net uptake of C between 1990 and 2100 for all scenarios considered in this study (Fig. 5.8a). Climate change, however, weakens the marginal effects of land-use change on terrestrial C sequestration in all but the 'PCM2' scenarios because of increasing soil C losses in the second half of the 21st century. Uncertainty in the spatial pattern of climate change is the largest contributor to the range of projected land-atmosphere fluxes of 1.5-5.5 PgC.

5.4 Discussion

Decrease in agricultural area and increase in managed grassland and forest lead to a net biospheric uptake of about 1.7 PgC under all four plausible future path-ways of land-use change between 1990, the Kyoto baseline year, and 2100. This is equivalent to about 20% of the EU* Kyoto CO₂ emission reduction target and illustrates the relevance of terrestrial C storage for mitigation policies. However, the scenarios show substantial differences in the magnitude of the conversion between the different land uses, and the associated C fluxes. Sequestration in soils plays a stronger role in SRES 'A' scenarios with little afforestation, whereas increasing forest area and thus regrowing vegetation is more important in SRES 'B' scenarios. These effects are discussed in Section 5.4.1.

The C fluxes resulting from climate and [CO₂] change are – on average – of a similar magnitude to the land-use change related fluxes. Yet, they show a much larger difference between different storylines, and even more so between projections of the same scenario based on different climate models. It is interesting to note that the 'low climate change' scenario 'B2'-PCM2, together with rapid reforestation results in less C uptake of the terrestrial biosphere than projected under the 'A2'-PCM2 scenario. The range in cumulative land-atmosphere flux depicted in Figure 5.8 thus likely encompasses the response of the terrestrial biosphere modelled with this particular version of LPJ under all 16 scenarios of the ATEAM-scenario set.

Global warming will likely offset some of the sequestration from land-use and increased productivity, as increasing heterotrophic respiration is not counterbalanced by increasing litter fall. This is a robust finding in this study under all scenarios for larger parts of boreal Europe, however, the magnitude of this effect is subject to considerable uncertainty deriving from uncertainty in Boreal warming. Also, strong drying in the Mediterranean projected in some climate models will likely exacerbate C losses in these ecosystems through decreased productivity and increasing risk of fire. These effects are discussed in Section 5.4.2.

The 1990-2100 average land-atmosphere flux under the combined land-use, climate and [CO₂] change projections (S3) corresponds to 18-69% EU* Kyoto emission reduction target. However, the cumulative land-atmosphere flux in 1990-2100 corresponds only to 1.1-1.8% (from land-use change only) and 0.9-4.9% (all forcing S3) of the total fossil-fuel emissions during that period (Table 5.3). In agreement with earlier studies (House *et al.*,

2002; Sitch *et al.*, 2005), the terrestrial C uptake – and thus its impact on mitigating climate change – is likely to be very small.

5.4.1 Land-use change

Estimates of land-use change related fluxes depend on past land-use changes because of the long response-time of both vegetation and soil C. Consistent data on a continental scale on historical land uses are very sparse, so that substantial uncertainty is inherent in any backward projection of land-use patterns (House *et al.*, 2003). In addition, not only net changes in land use, documented for instance in FAO statistics (FAOSTAT, 2004), but also gross conversions between land-use types and land-management changes (*e.g.* those leading to soil degradation), which are poorly quantified for larger regions, determine the land-use change flux (Glatzel, 1999). This lack of a reliable land-use history contributes to the difference between estimates of the present-day land-atmosphere flux of the European terrestrial biosphere based on process-based modelling that considers past climate, atmospheric [CO₂] and land-use changes and a recent compilation of various data-based bottom-up estimates (Janssens *et al.*, 2003). However, this study focusses on the effect of land-use changes after 1990 on the land-atmosphere flux in the 21st century to give an estimate of the effect of Kyoto-accountable land-use changes on the terrestrial carbon balance. The historical bias is therefore not strongly relevant for the conclusions of this study, however, remains a challenge to reliably model present-day and future carbon budgets.

The change in soil C stock as a consequence of land-use conversion depends on the differential sizes of the soil C pool between the land-use types at equilibrium. Generally, cropland soils have lower C stocks than grasslands, whereas forest soils have similar pool sizes to grasslands (Guo and Gifford, 2002). Such differences are modelled by LPJ, and also conversions between these three land-use types show similar trends to observed studies (see Figure 1 of Guo and Gifford, 2002, and references therein). The accuracy with which the magnitude of the continental scale soil C flux following conversion can be estimated depends on how well the differences between soil stocks of different land-use types are represented in the model. Further validation is required to ascertain the modelled effects. In particular, reliable estimates of forest soil C stocks are required, which are currently poorly quantified at a larger scale. It should be noted that uncertainty in the projections of future soil C arises from potential changes in land management, which could alter the C returns to the soil. Such management effects have not been considered in the present study. However, Smith *et al.* (2005a,b) have demonstrated that these can be expected to significantly affect soil C stock changes, and even more than offset the temperature related soil C losses from this study.

Accompanying studies on the change in forest vegetation C stocks under climate and land-use changes show qualitatively similar changes in forest growth (Meyer *et al.*, in review, Sabate, *unpublished data*). However, propagation of present-day inventoried forest

C stocks and forest age-classes, driven with growth changes predicted from LPJ, lead to larger projected C uptake rates than the increases in vegetation C increases in this study (Meyer *et al.*, in review). Most likely, these differences are related to different treatment of forest dynamics – particularly the age structure – in these models. Kohlmaier *et al.* (1995) have demonstrated the importance of forest age structure in future C balance estimates for the temperate and boreal zone. Currently, a model version of LPJ is being developed that explicitly considers forest age structure. Differences in the projections of a large-scale process-based ecosystem model and propagation of large-scale inventory data can only then be suitably assessed.

5.4.2 Climate change and increasing atmospheric [CO₂]

Climate change and increasing atmospheric [CO₂] affect the terrestrial carbon balance by amplifying terrestrial C uptake (NPP), as well as soil C loss (R_h). CO₂-fertilisation is the main cause for the increase in modelled land-atmosphere flux in before 2050, affecting carbon storage in plants by increasing net primary production as well as water efficiency of plants (Amthor, 1995). This result is typical for the response of terrestrial biosphere models (Cramer *et al.*, 2001; McGuire *et al.*, 2001; Levy *et al.*, 2004; Schaphoff *et al.*, in review). Long-term effects of increased atmospheric [CO₂] on terrestrial carbon storage are still a subject of scientific debate (Prentice *et al.*, 2001), mainly because nutrient availability may limit the long-term growth stimulating effect of enhanced CO₂ responses. Deposition of reactive nitrogen has been identified as one of the dominant causes for the accelerated tree growth in Europe (Spieker *et al.*, 1996). An analysis of growth trends across several European forest plots – including process-based models that link C to N cycles – suggests that N-deposition has been a major contributor to increased forest growth in the past, whereas in the future elevated atmospheric [CO₂] and climate change will likely dominate the environmental effects of forest growth (Karjalainen *et al.*, 1999). Nevertheless, because of the complex interactions between C and N cycles (see *e.g.* Lloyd and Farquhar, 1999), the interaction of N-availability with elevated [CO₂] remain one of the key uncertainties in this study.

The results of this study suggest a decline in soil C stocks from warming particular in boreal regions, which experience the largest warming. This would imply a positive feedback of the terrestrial biosphere to the climate system, as observed also in a range of other modelling studies (*e.g.* Cox *et al.*, 2000; Cramer *et al.*, 2001; Dufresne *et al.*, 2002; Friedlingstein *et al.*, 2003; Schaphoff *et al.*, in review). Some studies have suggested that the resistant pools of soil C might not respond to increasing temperatures (Liski *et al.*, 1999; Giardina and Ryan, 2000; Thornley and Cannell, 2001), contrary to the assumptions made in LPJ. However, recent analyses of experimental evidence (Fang *et al.*, 2005; Knorr *et al.*, 2005) show that soil respiration responses to temperature as modelled by LPJ are compatible with the data. Similar to Jones *et al.* (2005), we find comparable sensitivities of soil C stocks to increasing temperatures as a more sophisticated model of soil C turnover

(RothC) based on the same set of climate change scenarios (Smith *et al.*, 2005a,b). Fang *et al.* (2005) showed that the effect of uncertainty in the temperature sensitivity of soil C lead to some uncertainty in temperate regions, whereas the response in boreal regions, in which we simulate the strongest signal was less affected.

5.4.3 General remarks

The climate model related uncertainty is twice as large as the difference in land-atmosphere flux projections under alternative scenario storylines derived from a particular climate model. Such pronounced differences resulting from uncertainty in climate change projections based on the same emission scenario have been also obtained in a global study of five different GCMs forcing LPJ-DGVM (Schaphoff *et al.*, in review), and in a study using two GCMs to analyse the carbon storage of tropical rainforests under climate and land-use changes (Cramer *et al.*, 2004). These results demonstrate that regional detail of climate projections are an important determinant of terrestrial biosphere responses to climate change. A sound analysis of future scenarios must therefore include not only different plausible storylines to assess the range of potential future climate states, but most also include an assessment of the uncertainty resulting from different climate model projections for a particular radiative forcing.

This study presents a comprehensive assessment of the potential future development of the continental scale terrestrial C balance under different projections of land-use and climate change using one model of the terrestrial biosphere. Zaehle *et al.* (2005) have demonstrated that considerable uncertainty arises in land-atmosphere flux projections from alternative model parameterisations within one modelling framework. However, qualitative trends of land-atmosphere flux, in particular with respect to the source-sink behaviour of the terrestrial biosphere, are reasonably robust model results. Uncertainty in land-atmosphere flux projections arises also from alternative formulations of ecosystem processes in terrestrial biosphere models (Cramer *et al.*, 2001; Joos *et al.*, 2001). Long-term global scale trajectories in land-atmosphere fluxes from six DGVMs show a similar pattern – increasing C uptake in the first half of the 21st century, decline in the second half – under the IS92a HadCM2-SUL climate change scenario despite regional differences primarily because of different assumptions about the effect of changing climate on global *NPP* (Cramer *et al.*, 2001). These results of this study are thus in agreement with earlier studies, but provide a more comprehensive analysis with respect to the uncertainty resulting from different climate model projections, in comparison to the differences in projected land-atmosphere fluxes from alternative scenarios.

5.5 Conclusions

This study provides an analysis of the effect of plausible future land-use changes under a range of different climate change scenarios to estimate the relative contribution of these

two forcing factors on the terrestrial carbon balance of EU* in the 21st century. Under all scenarios, land-use change contributes to a net C uptake equivalent to about one fifth of the EU*'s Kyoto emission reduction target. The influence of climate change and atmospheric [CO₂] increase are of a similar magnitude to the flux inferred by land-use change, leading to an enhanced biospheric uptake rates before 2040, and a weakening of the terrestrial uptake rate thereafter. Considerable uncertainty in the response of the terrestrial biosphere to climate change projections results from uncertainty in climate modelling. Uncertainty in the future European terrestrial carbon balance associated with uncertainty in the rate and spatial pattern of climate change among GCMs for a particular emission scenario is larger than the differences between alternative scenarios of consistent land-use and climate changes interpreted by one particular climate model. This implies that for a sound assessment of climate change impacts, not only different SRES-scenarios, but also a suite of climate models have to be considered.

Acknowledgements

S.Zaehle was supported by the HSB-programme of the Federal State of Brandenburg, Germany (AZ: 24-04/323;200). This work contributes to the EU-funded project ATEAM (Advanced Terrestrial Ecosystem Assessment and Modelling; www.pik-potsdam.de/ateam; EVK2-2000-00075). We are grateful to all members of the ATEAM project for three-and-a-half years of constructive discussions.

6. Bibliography

Lord Polonius: ‘What do you read, my Lord?’

Hamlet: ‘Words, words, words...’

(W. Shakespeare, Hamlet)

- Amthor, J.S. (1995). Terrestrial higher-plant response to increasing atmospheric [CO₂] in relation to the global carbon cycle, *Global Change Biology*, 1: 243–274.
- Andreae, M.O. and Merlet, P. (2001). Emission of trace gases and aerosols from biomass burning, *Global Biogeochemical Cycles*, 15 (4): 955–966.
- Arora, V. (2002). Modelling vegetation as a dynamic component in soil-vegetation-atmosphere transfer schemes and hydrological models, *Reviews of Geophysics*, 40 (2): 1006.
- Arrhenius, S.A. (1896). On the influence of carbonic acid in the air upon the temperature on ground, *Philosophical Magazine and Journal of Science*, 41: 237–276.
- Atjay, G.L., Ketner, P., and Duvigneaud, P. (1979). Terrestrial primary production and phytomass. In: Bolin, B., Degens, E.T., Kempe, S., and Ketner, P., editors, *The Global Carbon Cycle*. John Wiley & Sons, Chichester, USA.
- Aubinet, M., Grelle, A., Ibrom, A., Rannik, U., Moncrieff, J., Foken, T., Kowalski, A., Martin, P.H., Berbigier, P., Bernhofer, C., Clement, R., Elbers, J.A., Granier, A., Grunwald, T., Morgenstern, K., Pilegaard, K., Rebmann, C., Snijders, W., Valentini, R., and Vesala, T. (2000). Estimates of the annual net carbon and water exchange in forests: The EUROFLUX methodology, *Advances in Ecological Research*, 30: 113–175.
- Bakkens, M., Alkemade, J.R.M., Ihle, F., Leemans, R., and Latour, J.B. (2002). Assessing effects of forecasted climate change on the diversity and distribution of European higher plants for 2050, *Global Change Biology*, 8: 390–407.
- Baldocchi, D.D. (2003). Assessing the eddy covariance technique for evaluating carbon dioxide exchange rates of ecosystems: Past, present and future, *Global Change Biology*, 9 (4): 479–492.
- Barnard, H.R. and Ryan, M.G. (2003). A test of the hydraulic limitation hypothesis in fast-growing *Eucalyptus saligna*, *Plant, Cell and Environment*, 26 (8): 1235–1245.
- Barrett, D.J. (2002). Steady state turnover time of carbon in the Australian terrestrial biosphere, *Global Biogeochemical Cycles*, 16 (4): 1108.
- Bartelink, H.H. (1998). A model of dry matter partitioning in trees, *Tree Physiology*, 18 (2): 91–101.
- Becker, P. and Gribben, R.J. (2001). Estimation of conduit taper for the hydraulic resistance model of West *et al.*, *Tree Physiology*, 21: 697–700.

- Becker, P., Gribben, R.J., and Lim, C.M. (2000a). Tapered conduits can buffer hydraulic conductance from path-length effects, *Tree Physiology*, 20 (14): 965–967.
- Becker, P., Meinzer, F.C., and Wullschleger, S.D. (2000b). Hydraulic limitation of tree height: A critique, *Functional Ecology*, 14: 4–11.
- Becker, P., Tyree, M.T., and Tsuda, M. (1999). Hydraulic conductances of angiosperms versus conifers: similar transport sufficiency at the whole-plant level, *Tree Physiology*, 19 (7): 445–452.
- Beringer, J., McIlwaine, S., Lynch, A.H., Chapin, F.S., and Bonan, G.B. (2002). The use of a reduced form model to assess the sensitivity of a land surface model to biotic surface parameters, *Climate Dynamics*, 19: 455–466.
- Bolin, B., Sukumar, R., Ciais, P., Cramer, W., Jarvis, P., Kheshgi, H.S., Nobre, C., Semenov, S., and Steffen, W. L. (2000). Global perspective. In: Watson, R.T., Noble, I., Bolin, B., Ravindranath, N.H., Verardo, D.J., and Dokken, D.J., editors, *IPCC, Land Use, Land-Use Change and Forestry. A Special Report of the IPCC*, pages 23–51. Cambridge University Press, Cambridge, UK.
- Bond, B.J. and Ryan, M.G. (2000). Comment on ‘Hydraulic limitation of tree height: A critique’ by Becker, Meinzer and Wullschleger, *Functional Ecology*, 14: 137–140.
- Bondeau, A., Smith, P.C., and Zaehle, S. *et al.* (in prep.). Modeling the effect of agriculture on the terrestrial carbon cycle during the 20th century, *Global Change Biology*.
- Bopp, L., Le Quéré, C., Heimann, M., Manning, A.C., and Monfray, P. (2002). Climate-induced oceanic oxygen fluxes: Implications for the contemporary carbon budget, *Global Biogeochemical Cycles*, 16: doi: 10.1029/2001GBC001445.
- Botkin, D.B., Janak, J.F., and Wallis, J.R. (1972). Some ecological consequences of a computer model of forest growth, *Journal of Ecology*, 60: 849–872.
- Bousquet, P., Peylin, P., Ciais, P., Friedlingstein, P., Le Quéré, C., and Tans, P.P. (2000). Inter-annual CO₂ sources and sinks as deduced by inversion of atmospheric CO₂ data, *Science*, 290: 870–872.
- Bousquet, P., Peylin, P., Ciais, P., Ramonet, M., and Monfray, P. (1999). Inverse modeling of annual atmospheric CO₂ sources and sinks: 2. Sensitivity study, *Journal of Geophysical Research-Atmospheres*, 104 (D21): 26179–26193.
- Broecker, W.S., Takahashi, T., Simpson, H.J., and Peng, T.H. (1979). Fate of fossil-fuel carbon dioxide and the global carbon cycle, *Science*, 206: 409–418.
- Brovkin, V., Ganoposki, A., Y., Svirezhev., Bloh, W.von, Bondeau, A., Claussen, M., Petoukhov, V., and Rahmstorf, S. (1998). VEgetation COntinuous DEscription Model (VE-CODE). Technical report, Potsdam Institute for Climate Impact Research.
- Bugmann, H. (2001). A review of forest gap models, *Climatic Change*, 51 (3-4): 259–305.
- Campbell, J., Sun, O.J., and Law, B.E. (2004). Disturbance and net ecosystem production across three climatically distinct forest landscapes, *Global Biogeochemical Cycles*, 18: doi:10.1029/2004GB002236.
- Campolongo, F., Kleijnen, J., and Andres, T. (2000). Screening methods. In: Saltelli, A., Chan, K., and Scott, E.M., editors, *Sensitivity Analysis*, Wiley Series in Probability and Statistics, pages 65–80. John Wiley & Sons, Ltd., Chichester, New York, USA.
- Cannell, M.G.R. and Dewar, R.C. (1999). Carbon allocation in trees: A review of concepts in modelling, *Advances in Ecological Research*, 25: 59–104.

- Caspersen, J.P., Pacala, S.W., Jenkins, J.C., Hurtt, G.C., Moorcroft, P.R., and Birdsey, R.A. (2000). Contributions of land-use history to carbon accumulation in US forests, *Science*, 290 (5494): 1148–1151.
- Churkina, C., Tenhunen, J., Thornton, P.E., Falge, E., Elbers, J.A., Erhard, M., Grünwald, T., Kowalski, A., Rannik, U., and Sprinz, D. (2003). Analyzing the ecosystem carbon dynamics of four European coniferous forests using a biogeochemistry model, *Ecosystems*, 6: 168–184.
- Ciais, P., Denning, A. S., Tans, P.P., Berry, J.A., Randall, D.A., Collatz, G.J., Sellers, P.J., White, J.W.C., Trolier, M., Meijer, H.A.J., Francey, R.J., Monfray, P., and Heimann, M. (1997a). A three-dimensional synthesis study of delta O-18 in atmospheric CO₂: 1. Surface fluxes, *Journal of Geophysical Research-Atmospheres*, 102 (D5): 5857–5872.
- Ciais, P., Tans, P.P., Denning, A.S., Francey, R.J., Trolier, M., Meijer, H.A.J., White, J.W.C., Berry, J.A., Randall, D.A., Collatz, G.J., Sellers, P.J., Monfray, P., and Heimann, M. (1997b). A three-dimensional synthesis study of delta O-18 in atmospheric CO₂: 2. Simulations with the TM2 transport model, *Journal of Geophysical Research-Atmospheres*, 102 (D5): 5873–5883.
- Ciais, P., Tans, P.P., Trolier, M., White, J.W.C., and Francey, R.J. (1995). A large northern-hemisphere terrestrial CO₂ sink indicated by the C-13/C-12 ratio of atmospheric CO₂, *Science*, 269 (5227): 1098–1102.
- Cinnirella, S., Magnani, F., Saracino, A., and Borghetti, M. (2002). Response of a mature pinus laricio plantation to a three-year restriction of water supply: structural and functional acclimation to drought, *Tree Physiology*, 22: 21–30.
- Clark, D.A., Brown, S., Kicklighter, D.W., Chambers, J.Q., Thomlinson, J.R., and Ni, J. (2001). Measuring net primary production in forests: Concepts and field methods, *Ecological Applications*, 11 (2): 356–370.
- Cochard, H., Martin, R., Gross, P., and Bogeat-Triboulot, M.B. (2000). Temperature effects on hydraulic conductance and water relations of *Quercus robur* l., *Journal of Experimental Botany*, 51 (348): 1255–1259.
- Collatz, G.J., Berry, J.A., Farquhar, G.D., and Pierce, J. (1990). The relationship between the Rubisco reaction mechanism and models of photosynthesis, *Plant, Cell and Environment*, 13: 219–225.
- Collatz, G.J., M., Ribas-Carbo, and Berry, J.A. (1992). Coupled photosynthesis-stomatal conductance model for leaves of C4 plants, *Australian Journal of Plant Physiology*, 19: 519–538.
- Conover, W.J. and Iman, R.L. (1981). Rank transformation as a bridge between parametric and non-parametric statistics, *American Statistician*, 35 (124-129).
- Conway, T.J., Tans, P. P., and Waterman, L.S. (1994). Atmospheric CO₂ from sites in the NOAA/CMDL air sampling network. In: Boden, T.A. et al., editor, *Trends 93: A Compendium of Data on Global Change*, pages 41–119. CDIAC Oak Ridge National Laboratory, Oak Ridge, Tenn.
- CORINE. (1997). Technical and methodological guide for updating CORINE land cover. Technical report, EEC/JRC.
- Cox, P.M. (2001). Description of the TRIFFID dynamic global vegetation model. Technical report, Met Office. Hadley Centre technical note 24, Reading, UK.
- Cox, P.M., Betts, R.A., Jones, C.D., Spall, S.A., and Totterdell, I.J. (2000). Acceleration of global warming due to carbon-cycle feedbacks in a coupled climate model (vol 408, pg 184, 2000), *Nature*, 408 (6813): 750–750.

- Cramer, W., Bondeau, A., Schaphoff, S., Lucht, W., Smith, B., and Sitch, S. (2004). Tropical forest and the global carbon cycle: Impacts of atmospheric carbon dioxide, climate change and rate of deforestation, *Philosophical Transactions of the Royal Society London B*, 359: 331–343.
- Cramer, W., Bondeau, A., Woodward, F.I., Prentice, I.C., Betts, R.A., Brovkin, V., Cox, P.M., Fisher, V., Foley, J.A., Friend, A.D., Kucharik, C., Lomas, M.R., Ramankutty, N., Sitch, S., Smith, B., White, A., and Young-Molling, C. (2001). Global response of terrestrial ecosystem structure and function to CO₂ and climate change: Results from six dynamic global vegetation models, *Global Change Biology*, 7 (4): 357–373.
- Cramer, W., Kicklighter, D.W., Bondeau, A., Moore, B., Churkina, C., Nemry, B., Ruimy, A., and Schloss, A.L. (1999). Comparing global models of terrestrial net primary productivity (NPP): Overview and key results, *Global Change Biology*, 5: 1–15.
- Daily, G., editor. (1997). *Nature's services: Societal dependence on natural ecosystem*. Island Press, Washington, DC, USA.
- Daly, C., Bachelet, D., Lenihan, J.M., Neilson, R.P., Parton, W., and Ojima, D. (2000). Dynamic simulation of tree-grass interactions for global change studies, *Ecological Applications*, 10 (2): 449–469.
- Dargaville, R.J., Heimann, M., McGuire, A.D., Prentice, I.C., Kicklighter, D.W., Joos, F., Clein, J.S., Esser, G., Foley, J., Kaplan, J., Meier, R.A., Melillo, J.M., Moore, B., Ramankutty, N., Reichenau, T., Schloss, A., Sitch, S., Tian, H., Williams, L.J., and Wittenberg, U. (2002). Evaluation of terrestrial carbon cycle models with atmospheric CO₂ measurements: Results from transient simulations considering increasing CO₂, climate, and land-use effects, *Global Biogeochemical Cycles*, 16 (4).
- Noblet-Ducoudre, N.de, Gervois, S., Ciais, P., Viovy, N., Brisson, N., Seguin, B., and Perrier, A. (2004). Coupling the soil-vegetation-atmosphere-transfer scheme ORCHIDEE to the agronomy model STICS to study the influence of croplands on the European carbon and water budgets, *Agronomie*, 24 (6-7): 397–407.
- Delzon, S., Sartore, M., Burtlett, R., Dewar, R., and Loustau, D. (2004). Hydraulic responses to height growth in maritime pine trees, *Plant, Cell and Environment*, 27: 1077–1087.
- Dewar, R.C. (1991). A model of carbon storage in the trees, soils and wood products of managed forests, *Tree Physiology*, 8: 239–258.
- Dewar, R.C., Medlyn, B.E., and McMurtie, R.E. (1999). Acclimation of the respiration/photosynthesis ratio to temperature: Insights from a model, *Global Change Biology*, 5: 615–622.
- Dixon, R.K. (1994). Carbon pools and flux of global forest ecosystems, *Science*, 265 (5169): 171–171.
- Dodds, P.S., Rothman, D.H., and Weitz, J.S. (2001). Re-examination of the “3/4-law” of metabolism, *Journal of Theoretical Biology*, 209: 9–27.
- Dufresne, J.L., Friedlingstein, P., Berthelot, M., Bopp, L., Ciais, P., Fairhead, L., Le Treut, H., and Monfray, P. (2002). On the magnitude of positive feedback between future climate change and the carbon cycle, *Geophysical Research Letters*, 29 (10).
- Ehleringer, J. and Bjorkman, O. (1977). Quantum yields for CO₂ uptake in C3 and C4 plants, *Plant Physiology*, 59: 86–90.
- Eissenstat, D.M., Wells, C.D., Yanadi, R.D., and Whitbeck, J.L. (2000). Building roots in a changing environment: implications for root longevity, *New Phytologist*, 147: 33–42.

- Eissenstat, D.M. and Yanadi, R.D. (1997). The ecology of root lifespan, *Advances in Ecological Research*, 27: 1–60.
- EMDI. (2003). *Ecosystem Model Data Intercomparison Project*. <http://gaim.unh.edu/Structure/Intercomparison/EMDI/>.
- Enquist, B.J. (2002). Universal scaling in tree and vascular plant allometry: Toward a general quantitative theory linking plant form and function from cell to ecosystems, *Tree physiology*, 22: 1045–1064.
- Enquist, B.J. and Niklas, K.J. (2002). Global allocation rules patterns of biomass partitioning in seed plants, *Science*, 295: 1517–1520.
- Erhard, M., Carter, T.R., Mitchell, T., Reginster, I., Rounsevell, M., and Zaehle, S. (in prep.). Data and scenarios for assessing ecosystem vulnerability across Europe, *Regional Environmental Change*.
- Ewert, F., Rounsevell, M.D.A., Reginster, I., Metzger, M.J., and Leemans, R. (submitted). Future scenarios of European agricultural land use. I: Estimating changes in crop productivity, *Agricultural Ecosystems and Environment*.
- Falkowski, P., Scholes, R.J., Boyle, E., Canadell, J., Canfield, D., Elser, J., Gruber, N., Hibbard, K.A., Hogberg, P., Linder, S., Mackenzie, F.T., Moore, B., Pederson, T., Rosenthal, Y., Seitzinger, S., Smetacek, V., and Steffen, W.L. (2000). The global carbon cycle: A test of our knowledge of Earth as a system, *Science*, 290: 291–296.
- Fang, C., Smith, P., Moncrieff, J., and Smith, J. (2005). Similar response of labile and resistant organic matter pools to changes in temperature, *Nature*, 433: 57–58.
- FAO. (1948). Forest resources of the world, *Unasylva*, 2: 161–182.
- FAO. (1955). *World Forest Resources - Results of the inventory undertaken in 1953 by the forestry division of the FAO*. Food and Agriculture Organisation, Rome, IT.
- FAO. (1960). *World Forest Inventory*. Food and Agriculture Organisation, Rome, IT.
- FAO. (1976). *European Timber Trends and Prospects (1950-2000)*. Food and Agriculture Organisation, Rome, IT.
- FAO. (1991). *The digitized Soil Map of the World (Release 1.0)*, volume 67/1. Food and Agriculture Organization of the United Nations, Rome, IT.
- FAOSTAT. (2004). *FAOSTAT database*. FAO, <http://apps.fao.org>, last update 27.08.2004.
- Farquhar, G.D., Caemmerer, S. von, and Berry, J.A. (1980). A biochemical model of photosynthetic CO₂ assimilation in leaves of C₃ species, *Planta*, 149: 78–90.
- Farquhar, G.D., Lloyd, J., Taylor, J.A., Flanagan, L.B., Syvertsen, J.P., Hubick, K.B., Wong, S.C., and Ehleringer, J.R. (1993). Vegetation effects on the isotope composition of oxygen in atmospheric CO₂, *Nature*, 363: 439–443.
- Fischer, A., Kergoat, L., and Dedieu, G. (1997). Coupling satellite data with vegetation functional models: Review of different approaches and perspectives suggested by the assimilation strategy, *Remote Sensing Review*, 15: 283–303.
- Flato, G.M. and Boer, G.J. (2001). Warming asymmetry in climate change simulations, *Geophysical Research Letters*, 28: 195–198.
- Foley, J.A. (1995). An equilibrium model of the terrestrial carbon budget, *Tellus*, 47B: 310–319.

- Foley, J.A., Prentice, I.C., Ramankutty, N., Levis, S., Pollard, D., Sitch, S., and Haxeltine, A. (1996). An integrated biosphere model of land surface processes, terrestrial carbon balance, and vegetation dynamics, *Global Biogeochemical Cycles*, 10 (4): 603–628.
- Friedlingstein, P., Dufresne, J.L., Cox, P.M., and Rayner, P. (2003). How positive is the feedback between climate change and the carbon cycle?, *Tellus B*, 55 (2): 692–700.
- Friedlingstein, P., Fung, I., Holland, E., John, J., Brasseur, G., Erickson, D., and Schimel, D. (1995). On the contribution of CO₂ fertilization to the missing biospheric sink, *Global Biogeochemical Cycles*, 9 (4): 541–556.
- Friedlingstein, P., Joel, G., Field, C.B., and Fung, I.Y. (1999). Toward an allocation scheme for global terrestrial carbon models, *Global Change Biology*, 5 (7): 755–770.
- Friend, A.D. (2001). Modelling canopy CO₂ fluxes: Are ‘big-leaf’ simplifications justified?, *Global Ecology and Biogeography*, 10 (6): 603–619.
- Friend, A.D., Stevens, A.K., Knox, R.G., and Cannell, M.G.R. (1997). A process-based, terrestrial biosphere model of ecosystem dynamics (Hybrid v3.0), *Ecological Modelling*, 95 (2-3): 249–287.
- Garcia Abejon, J.L. and Loranca Gomez, J.A. (1984). Variable density yield table for *Pinus sylvestris* in central Spain. Comunicaciones inia serie recursos naturales no. 29, Instituto Nacional de Investigaciones Agrarias.
- Gerber, S., Joos, F., and Prentice, I.C. (2004). Sensitivity of a dynamic global vegetation model to climate and atmospheric CO₂, *Global Change Biology*, 10: 1223–1239.
- Gerten, D., Schaphoff, S., Haberlandt, U., Lucht, W., and Sitch, S. (2004). Terrestrial vegetation and water balance - hydraulic evaluation of a dynamic global vegetation model, *Journal of Hydrology*, 286 (1-4): 249–270.
- Giardina, C.P. and Ryan, M.G. (2000). Evidence that decomposition rates of organic carbon in mineral soil do not vary with temperature, *Nature*, 404 (6780): 858–861.
- Gitay, H., Brown, S., Easterling, W., and Jallow, B. (2001). Ecosystems and their goods and services. In: McCarthy, J.J., Canziani, O.F., Leary, N.A., Dokken, D.J., and White, K.S., editors, *Climate Change 2001: Impacts, Adaptation and Vulnerability*, pages 236–341. Cambridge University Press, Cambridge, UK.
- Givinish, T.J. (1986). Optimal stomatal conductance, allocation of energy between leaves and roots, and the marginal costs of transpiration. In: Givinish, T.J., editor, *On the Economy of plant form and function*. Cambridge University Press, Cambridge.
- Glatzel, G. (1999). Historic forest use and its possible implications to recently accelerated tree growth in central Europe. In: Karjalainen, T., Spieker, H., and Laroussinie, O., editors, *Causes and Consequences of Accelerating Tree Growth in Europe*, EFI Proceedings No.27. European Forest Institute, Joensuu, FI.
- GLOBALVIEW-CO₂. (1999). *Cooperative Atmospheric Data Integration Project - Carbon dioxide*. CD-ROM. Boulder, NOAA, CMDL, Colorado.
- Goldewijk, K.K. (2001). Estimating global land use change over the past 300 years: The HYDE database, *Global Biogeochemical Cycles*, 15 (2): 417–433.
- Goodale, C.L., Apps, M.J., Birdsey, R.A., Field, C.B., Heath, L.S., Houghton, R.A., Jenkins, J.C., Kohlmaier, G.H., Kurz, W., Liu, S.R., Nabuurs, G.J., Nilsson, S., and Shvidenko, A.Z. (2002). Forest carbon sinks in the Northern Hemisphere, *Ecological Applications*, 12 (3): 891–899.
- Gordon, H.B. and O’Farrell, S.P. (1997). Transient climate change in the CSIRO coupled model with dynamic sea ice, *Monthly Weather Review*, 125: 875–907.

- Goulden, M.L., Munger, J.W., Fan, S., Daube, B.C., and Wofsy, S. (1996). Exchange of carbon dioxide in a deciduous forest: Response to interannual climate variability, *Science*, 271: 1576–1578.
- Gower, S.T., McMurtrie, R.E., and Murty, D. (1996). Aboveground net primary production decline with stand age: Potential causes, *Trends in Ecology & Evolution*, 11 (9): 378–382.
- Guo, L.B. and Gifford, R.M. (2002). Soil carbon stocks and land use change: A meta analysis, *Global Change Biology*, 8 (4): 345–360.
- Gurney, K.R., Law, R.M., Denning, A.S., Rayner, P.J., Baker, D., Bousquet, P., Bruhwiler, L., Chen, Y. H., Ciais, P., Fan, S., Fung, I. Y., Gloor, M., Heimann, M., Higuchi, K., John, J., Maki, T., Maksyutov, S., Masarie, K., Peylin, P., Prather, M., Pak, B. C., Randerson, J., Sarmiento, J., Taguchi, S., Takahashi, T., and Yuen, C. W. (2002). Towards robust regional estimates of CO₂ sources and sinks using atmospheric transport models, *Nature*, 415 (6872): 626–630.
- Häger, C. (1998). *Die Kohlenstoffbilanz der nördlichen Wälder - Entwicklung eines Simulationmodells unter besonderer Berücksichtigung der Altersklassendynamik und ausgewählter Klimaszenarien*. PhD thesis, Johann Wolfgang Goethe Universität, Frankfurt am Main, DE.
- Hallgren, W.S. and Pitman, A.J. (2000). The uncertainty in simulations by a global biome model (BIOME3) to alternative parameter values, *Global Change Biology*, 6: 483–495.
- Haxeltine, A. and Prentice, I.C. (1996a). A general model for the light use efficiency of primary production, *Functional Ecology*, 10: 551–561.
- Haxeltine, A. and Prentice, I.C. (1996b). BIOME3: An equilibrium terrestrial biosphere model based on ecophysiological constraints, resource availability, and competition amongst plant functional types, *Global Biogeochemical Cycles*, 10 (4): 693–709.
- Heimann, M., Esser, G., Haxeltine, A., Kaduk, J., Kicklighter, D.W., Knorr, W., Kohlmaier, G.H., McGuire, A.D., Melillo, J., Moore III, B., Otto, R.D., Prentice, I.C., Sauf, W., Schloss, A., Sitch, S., Wittenberg, U., and Würth, G. (1998). Evaluation of terrestrial carbon cycle models through simulations of the seasonal cycle of atmospheric CO₂: First results of a model inter-comparison study, *Global Biogeochemical Cycles*, 12 (1): 1–24.
- Helton, J.C. and Davis, F.J. (2000). Sampling-based methods. In: Saltelli, A., Chan, K., and Scott, E.M., editors, *Sensitivity Analysis*, Wiley Series in Probability and Statistics, pages 101–153. John Wiley & Sons, Ltd., Chichester, New York, USA.
- Hese, S., Lucht, W., Schmulius, C., Barnesley, M., Dubayah, R., Knorr, D., Neumann, K., Riedel, T., and Schroter, K. (2005). Global biomass mapping for an improved understanding of the CO₂ balance - the Earth observation mission Carbon-3D, *Remote Sensing of Environment*, 94: 94–104.
- Hickler, T., Prentice, I.C., Smith, B., Sykes, M. T., and Zaehle, S. (2004). Using a global vegetation model to test a comprehensive hypothesis on the effects of plant hydraulic architecture on water uptake in different types of plants. In: Hickler, T., editor, *Towards an integrated ecology through mechanistic modelling of ecosystem structure and functioning*, page 153. Meddelanden fran Lunds Universitets Geografiska Institution; Avhandlingar (ISSN 0346-6787), Lund, SE.
- Houghton, J.T., B.A., Callander, and S.K., Varney. (1992). *Climate Change 1992 - the Supplementary Report to the IPCC Scientific Assessment*. Cambridge University Press, Cambridge.
- Houghton, J.T., Ding, Y., Griggs, D.J., Noguer, M., Linden, P.J.van der, Dai, X., Maskell, K., and Johnson, C.A., editors. (2001). *Climate Change 2001: The Scientific Basis. Contribution of Working Group I to the Third Assessment Report of the Intergovernmental Panel on Climate Change*. Cambridge University Press, Cambridge, United Kingdom and New York, NY, USA.

- Houghton, R.A. (1999). The annual net flux of carbon to the atmosphere from changes in land use 1850-1990, *Tellus*, 51 B: 298–313.
- Houghton, R.A. and Skole, D.L. (1990). Carbon - transformation of the global environment. In: Turner, B.L., editor, *The Earth as Transformed by Human Action - Global and Regional Changes in the Biosphere Over the Past 300 years*, pages 393–408. Cambridge University Press, Cambridge, UK.
- House, J.I., Prentice, I.C., and Le Quéré, C. (2002). Maximum impacts of future reforestation and deforestation on atmospheric CO₂, *Global Change Biology*, 8: 1047–1052.
- House, J.I., Prentice, I.C., Ramankutty, N., Houghton, R.A., and Heimann, M. (2003). Reconciling apparent inconsistencies in estimates of terrestrial CO₂ sources and sinks, *Tellus B*, 55 (2): 345–363.
- Huang, S.M., Titus, S.J., and Wiens, D.P. (1992). Comparison of nonlinear height diameter functions for major Alberta tree species, *Canadian Journal of Forest Research*, 22 (9): 1297–1304.
- Hubbard, R.M., Bond, B.J., and Ryan, M.G. (1999). Evidence that hydraulic conductance limits photosynthesis in old *Pinus ponderosa* trees, *Tree Physiology*, 19 (3): 165–172.
- Hulme, M., Wigley, T.M.L., Barrow, E.M., Raper, S.C.B., Centella, A., Smith, S., and Chipanshi, A.C. (2000). *Using a climate scenario generator for vulnerability and adaptation assessments: MAGICC and SCENGEN Version 2.4 Workbook*. Climatic Research Unit, UEA, Norwich, UK.
- IGBP-DIS. (2000). Global soil data products CD-ROM. Technical report, International Geosphere-Biosphere Programme - Data and Information Services.
- Iman, R.L. and Conover, W.J. (1982). A distribution free approach to inducing rank correlation among input variables, *Communications in Statistics - Simulation and Computation B*, 11: 311–334.
- Jackson, R.B., Canadell, J., Ehleringer, J.R., Mooney, H.A., Sala, O.E., and Schulze, E.D. (1996). A global analysis of root distributions for terrestrial biomes, *Oecologia*, 108: 389–411.
- James, S.A., Meinzer, F.C., Goldstein, G., Woodruff, D., Jones, T., Restom, T., Mejia, M., Clearwater, M., and Campanello, P. (2003). Axial and radial water transport and internal water storage in tropical forest canopy trees, *Oecologia*, 134 (1): 37–45.
- Janssens, I.A., Freibauer, A., Ciais, P., Smith, P., Nabuurs, G.-J., Folberth, G., Schlamadinger, B., Hutjes, R.W.A., Ceulemans, R., Schulze, E.D., Valentini, R., and Dolman, A.J. (2003). Europe's terrestrial biosphere absorbs 7 to 12 % of European anthropogenic CO₂ emissions, *Science*, 300: 1538–1542.
- Janssens, I.A., Lankreijer, H., Matteucci, G., Kowalski, A.S., Buchmann, N., Epron, D., Pilegaard, K., Kutsch, W., Longdoz, B., Grunwald, T., Montagnani, L., Dore, S., Rebmann, C., Moors, E.J., Grelle, A., Rannik, U., Morgenstern, K., Oltchev, S., Clement, R., Gudmundsson, J., Minerbi, S., Berbigier, P., Ibrom, A., Moncrieff, J., Aubinet, M., Bernhofer, C., Jensen, N.O., Vesala, T., Granier, A., Schulze, E.D., Lindroth, A., Dolman, A.J., Jarvis, P.G., Ceulemans, R., and Valentini, R. (2001). Productivity overshadows temperature in determining soil and ecosystem respiration across European forests, *Global Change Biology*, 7 (3): 269–278.
- Jarvis, P., James, G.B., and Landsberg, J.J. (1976). Coniferous forests. In: Monteith, J.L., editor, *Vegetation and the Atmosphere*, volume 2, pages 171–240. Academic Press, London, UK.
- Jarvis, P.G. (1975). Water transfer in plants. In: Vries, D.A.de and Afgan, N.G., editors, *Heat Mass Transfer in the Plant Environment, Part 1*, pages 369–394. Scripta Book Co., Washington D.C., USA.

- Jenkinson, D.S. (1990). The turnover of organic carbon and nitrogen in the soil, *Philosophical Transactions of the Royal Society London B*, 329: 361–368.
- Johns, T.C., Carnell, R.E., and J.F., Crossley. (1997). The second Hadley Centre coupled ocean-atmosphere GCM: Model description, spinup and validation, *Climate Dynamics*, 13: 103–134.
- Jones, C.D., Cox, P.M., Essery, R.L.H., Roberts, D.L., and Woodage, M.J. (2003). Strong carbon cycle feedbacks in a climate model with interactive CO₂ and sulphate aerosols, *Geophysical Research Letters*, 30 (9): 1479.
- Jones, C.D., McConnell, C., Coleman, K., Cox, P.M., Falloon, P., Jenkinson, D.S., and Powlson, D.S. (2005). Global climate change and soil carbon stocks: predictions from two contrasting models for the turnover of organic carbon in soil, *Global Change Biology*, 11: 154–166.
- Joos, F., Prentice, I.C., Sitch, S., Meyer, R., Hooss, G., Plattner, G.K., Gerber, S., and Hasselmann, K. (2001). Global warming feedbacks on terrestrial carbon uptake under the Intergovernmental Panel on Climate Change (IPCC) emission scenarios, *Global Biogeochemical Cycles*, 15 (4): 891–907.
- Kaipainen, T., Liski, J., Pussinen, A., and Karjalainen, T. (2004). Managing carbon sinks by changing rotation length in European forests, *Environmental Science & Policy*, 7: 205–219.
- Kaminski, T., Heimann, M., and Giering, R. (1999a). A coarse grid three-dimensional global inverse model of the atmospheric transport - 1. Adjoint model and jacobian matrix, *Journal of Geophysical Research-Atmospheres*, 104 (D15): 18535–18553.
- Kaminski, T., Heimann, M., and Giering, R. (1999b). A coarse grid three-dimensional global inverse model of the atmospheric transport - 2. Inversion of the transport of CO₂ in the 1980s, *Journal of Geophysical Research-Atmospheres*, 104 (D15): 18555–18581.
- Kaminski, T., Knorr, W., and Rayner, M.P. J. and Heimann. (2002). Assimilating atmospheric data into a terrestrial biosphere model: A case study of the seasonal cycle, *Global Biogeochemical Cycles*, 16 (4).
- Kankaanpää, S. and Carter, T.R. (2004). Construction of European forest land use scenarios for the 21st century. Technical report, Finnish Environment Institute, Helsinki, FI.
- Karjalainen, T., Spieker, H., and Laroussinie, O., editors. (1999). *Causes and consequences of accelerating tree growth in Europe*. EFI proceedings No. 27. European Forest Institute, Joensuu, FI.
- Kauppi, P.E., Mielikäinen, and Kuusela, K. (1992). Biomass and carbon budget of European forests, 1971 to 1990, *Science*, 256: 70–74.
- Kauppi, P.E. and Tomppo, E. (1993). Impact of forests on net national emissions of carbon dioxide in West Europe, *Water, Air and Soil Pollution*, 70: 187–196.
- Keeling, C.D. and Whorf, T.P. (2003). *Atmospheric CO₂ records from sites in the SIO air sampling network*. Carbon Dioxide Information Analysis Center, Oak Ridge National Laboratory, U.S. Department of Energy, <http://cdiac.esd.ornl.gov/trends/co2/sio-mlo.htm>.
- Kellomäki, S., editor. (in prep.). *Management of European Forests under Changing Climatic Conditions - Final report of the FP5 research programme "Silvistrat"*. European Forest Institute, Joensuu, FI.
- Kergoat, L. (1998). A model for hydrological equilibrium of leaf area index on a global scale, *Journal of Hydrology*, 212/213: 268–286.

- Kicklighter, D.W., Bruno, M., Donges, S., Esser, G., Heimann, M., Helfrich, J., Ift, F., Joos, F., Kaduk, J., Kohlmaier, G.H., McGuire, A.D., Melillo, J.M., Meyer, R., Moore, B., Nadler, A., Prentice, I.C., Sauf, W., Schloss, A.L., Sitch, S., Wittenberg, U., and Wurth, G. (1999). A first-order analysis of the potential role of CO₂ fertilization to affect the global carbon budget: A comparison of four terrestrial biosphere models, *Tellus Series B-Chemical and Physical Meteorology*, 51 (2): 343–366.
- Kindermann, J., Würth, G., Kohlmaier, G., and Badeck, F.W. (1996). Interannual variation of carbon exchange fluxes in terrestrial ecosystems, *Global Biogeochemical Cycles*, 10 (4): 737–755.
- Kira, T. and Shidai, T. (1967). Primary production and turnover of organic matter in different forest ecosystems of the western pacific, *Japanes Journal of Ecology*, 13: 70–83.
- Kleijnen, J.P.C. (1998). Experimental design for sensitivity analysis, optimization and validation of simulation models. In: Banks, J, editor, *Handbook of Simulation - Principles, Methodology, Advances, Applications, and Practice*. Wiley, New York, USA.
- Knorr, W. (2000). Annual and interannual CO₂ exchanges of the terrestrial biosphere: Process-based simulations and uncertainties, *Global Ecology and Biogeography*, 9: 225–252.
- Knorr, W. and Heimann, M. (1995). Impact of drought stress and other factors on seasonal land biosphere CO₂ exchange studied through an atmospheric tracer transport model, *Tellus B*, 47 (4): 471–489.
- Knorr, W. and Heimann, M. (2001a). Uncertainties in global terrestrial biosphere modeling: 1. A comprehensive sensitivity analysis with a new photosynthesis and energy balance scheme, *Global Biogeochemical Cycles*, 15 (1): 207–225.
- Knorr, W. and Heimann, M. (2001b). Uncertainties in global terrestrial biosphere modeling, part II: Global constraints for a process-based vegetation model, *Global Biogeochemical Cycles*, 15 (1): 227–246.
- Knorr, W. and Kattge, J. (in press). Inversion of terrestrial ecosystem parameter values against eddy covariance measurements by Monte Carlo sampling, *Global Change Biology*.
- Knorr, W., Prentice, I.C., House, J., and Holland, E. (2005). Long-term sensitivity of soil carbon turnover to warming, *Nature*, 433: 298–301.
- Knorr, W., Smith, B., Wildowski, J.L., Pinty, B., and Gobron, N. (2004). Combining remote sensing techniques with productivity models: A case study for monitoring carbon stocks in northern european forests. In: Stamatiadis, S., Lynch, J.M., and Schepers, J.S., editors, *Remote Sensing for Agriculture and the Environment*, pages 52–64. OECD Publications, Larissa, GR.
- Knutti, R., Stocker, T.F., Joos, F., and Plattner, G.-K. (2002). Constraints on radiative forcing and future climate change from observations and climate model ensembles, *Nature*, 416: 719–723.
- Köble, R. and Seufert, G. (2001). Novel maps for forest tree species in Europe. In: *8th European Symposium on the Physico-Chemical Behaviour of Air Pollutants: "A Changing Atmosphere!"*, Torino, IT.
- Koch, G.W., Sillett, S.C., Jennings, G.M., and Davis, S.D. (2004). The limits to tree height, *Nature*, 428 (6985): 851–854.
- Köhl, M., Päivinen, R., and Traub, B. (2000). Harmonisation and standardisation of multi-national statistics - mission impossible?, *Environmental Monitoring and Assessment*, 63: 361–380.
- Köhl, M., Päivinen, R., Traub, B., and Miina, S. (1997). Study on European forestry and communication systems: Report on forest inventory and survey systems. Technical report, European Commission.

- Kohlmaier, G., Häger, C., Würth, G., Lüdeke, M.K.B., Ramge, P., and Badeck, F.W. (1995). Effects of age class distributions of the temperate and boreal forests on the global CO₂ source-sink function, *Tellus*, 47B: 212–231.
- Koivisto, P. (1959). Growth and yield tables. Communications Instituti Forestalis Fenniae 51 51, Finnish Forest Research Institute.
- Kolari, P., Pumpanen, J., Rannik, U., Ilvesniemi, H., Hari, P., and Berninger, F. (2004). Carbon balance of different aged Scots pine forests in southern Finland, *Global Change Biology*, 10 (7): 1106–1119.
- Körner, C. (1994). Leaf diffusive characteristics in the major vegetation types of the globe. In: Schulze, E.D. and Caldwell, M.M., editors, *Ecophysiology of Photosynthesis*, Ecological Studies 100. Springer Verlag, Berlin, Heidelberg, New York.
- Kowalski, A., Loustau, D., Berbigier, P., Manca, G., Tedeschi, V., Borghetti, M., Valentini, R., Kolari, P., Berninger, F., Rannik, U., Hari, P., Rayment, M., Mencuccini, M., Moncrieff, J., and Grace, J. (2004). Paired comparison of carbon exchange between undisturbed and regenerating stands in four managed forests in Europe, *Global Change Biology*, 10: 1–17.
- Kramer, K. and Mohren, G.M.J. (2001). Long-term effects of climate change on carbon budgets of forests in Europe. Technical Report Green World Research report 194, ALTERRA, Wageningen, NL.
- Krinner, G., Viovy, N., Noblet-Ducoudre, N.de, Ogee, J., Polcher, J., Friedlingstein, P., Ciais, P., Sitch, S., and Prentice, I.C. (2005). A dynamic global vegetation model for studies of the coupled atmosphere-biosphere system, *Global Biogeochemical Cycles*, 19: doi:10.1029/2003/GB002199.
- Kurz, W.A. and Apps, M.J. (1999). A 70-year retrospective analysis of carbon fluxes in the Canadian forest sector, *Ecological Applications*, 9 (2): 526–547.
- Laitat, E., Karjalainen, T., Loustau, D., and Lindner, M. (2000). Towards an integrated scientific approach for carbon accounting in forestry, *Biotechnology, Agronomy, Society and Environment*, 4: 241–251.
- Larcher, W. (1995). *Physiological Plant Ecology*. Springer-Verlag, Berlin, DE, 3rd edition.
- Larcher, W. (2001). *Ökophysiologie der Pflanzen*. Ulmer, Stuttgart, DE, 6th edition.
- Law, B.E., Sun, O.J., Campell, J., Tuyl, S.van, and Thornton, P.E. (2003). Changes in carbon storage and fluxes in a chronosequence of *Ponderosa pine*, *Global Change Biology*, 9: 510–524.
- Le Quéré, C., Aumont, O., Bopp, L., Bousquet, P., Ciais, P., Francey, R.J., Heimann, M., Keeling, C.D., Keeling, R.F., Kheshgi, H.S., Peylin, P., Piper, S.C., Prentice, I.C., and Rayner, P. (2003). Two decades of ocean CO₂ sink and variability, *Tellus B*, 55: 649–656.
- Le Toan, T., Quegan, S., Woodward, I., Lomas, M., Delbart, N., and Picard, G. (2004). Relating radar remote sensing of biomass to modelling of forest carbon budgets, *Climate Change*, 67: 379–402.
- Leemans, R., Eickhout, B., Strengers, B., Bouwman, L., and Schaeffer, M. (2002). The consequences of uncertainties in land use, climate and vegetation response on terrestrial carbon, *Science in China*, 45.
- Lehtonen, A., Makipaa, R., Heikkinen, J., Sievanen, R., and Liski, J. (2004). Biomass expansion factors for Scots pine, Norway spruce and birch according to stand age for boreal forests, *Forest Ecology and Management*, 188: 211–224.
- Leslie, P.H. (1945). On the use of matrices in certain population mathematics, *Biometrika*, 33: 183–212.

- Leverenz, J.W. (1988). The effects of illumination sequence, CO₂ concentration, temperature, and acclimation on the convexity of the photosynthetic light response curve, *Physiologia Plantarum*, 74: 332–341.
- Levy, P.E., Cannell, M.G.R., and Friend, A.D. (2004). Modelling the impact of future changes in climate, CO₂ concentration and land use on natural ecosystems and the terrestrial carbon sink, *Global Environmental Change*, 14: 21–30.
- Lexer, M.J., Honninger, K., Scheifinger, H., Matulla, C., Groll, N., Kromp-Kolb, H., Schadauer, K., Starlinger, F., and Englisch, M. (2002). The sensitivity of Austrian forests to scenarios of climatic change: A large-scale risk assessment based on a modified gap model and forest inventory data, *Forest Ecology and Management*, 162 (1): 53–72.
- Lide, D.E. (2002). *Handbook of Chemistry and Physics*. CRC Press, New York, USA, 3rd edition.
- Lindner, M. (2000). Developing adaptive forest management strategies to cope with climate change, *Tree Physiology*, 20 (5-6): 299–307.
- Lindner, M., Lasch, P., and Erhard, M. (2000). Alternative forest management strategies under climatic change - prospects for gap model applications in risk analyses, *Silva Fennica*, 34 (2): 101–111.
- Lindner, M., Lucht, W., Bouriaud, O., Green, T., Janssens, I.A., Brumme, R., Butterbach-Bahl, K., Grace, J., Lehtonen, A., Lettens, S., Liski, J., Mencuccini, M., Milne, R., Nabuurs, G.J., Olsson, M., Schadauer, K., Troeltzsch, K., Camp, N.van, Vries, W.de, Williams, M., and Zaehle, S. (2004). Specific study on forest greenhouse gas budget. Technical report, Concerted Action CarboEurope-GHG, discussion paper.
- Liski, J., Ilvesniemi, H., Mäkalä, A., and Westman, C.J. (1999). CO₂ emissions from soil in response to climatic warming are overestimated - the decomposition of old soil organic matter is tolerant of temperature, *Ambio*, 28: 171–174.
- Liski, J. and Kauppi, P.E. (2000). Chapter III: Wood supply and carbon sequestration: Situation and changes. (B) Carbon cycle and biomass. In: UN-ECE/FAO, editor, *Temperate and Boreal Forest Resource Assessment 2000*, volume I, pages 102–142. United Nations Economic Commission for Europe, Food and Agriculture Organisation, Geneva, CH, Rome, IT.
- Liski, J., Korotkov, A.V., Prins, C.F.L., Karjalainen, T., Victor, D.G., and Kauppi, P.E. (2003). Increased carbon sink in temperate and boreal forests, *Climatic Change*, 61 (1-2): 89–99.
- Liski, J., Perruchoud, D., and Karjalainen, T. (2002). Increasing carbon stocks in the forest soils of western Europe, *Forest Ecology and Management*, 169 (1-2): 159–175.
- Lloyd, J. and Farquhar, G.D. (1996). The CO₂ dependence of photosynthesis, plant growth responses to elevated atmospheric CO₂ concentrations and their interaction with soil nutrient status. I. General principles and forest ecosystems, *Functional Ecology*, 10: 4–32.
- Lloyd, J. and Farquhar, G.D. (1999). The CO₂ dependence of photosynthesis, plant growth responses to elevated atmospheric CO₂ concentrations and their interaction with soil nutrient status. II: Temperate and boreal forest productivity and the combined effects of increasing CO₂ concentrations and increasing nitrogen deposition at a global scale, *Functional Ecology*, 13: 439–459.
- Lloyd, J. and Taylor, J.A. (1994). On the temperature dependence of soil respiration, *Functional Ecology*, 8: 315–323.
- Lucht, W., Prentice, I. C., Myneni, R. B., Sitch, S., Friedlingstein, P., Cramer, W., Bousquet, P., Buermann, W., and Smith, B. (2002). Climatic control of the high-latitude vegetation greening trend and Pinatubo effect, *Science*, 296 (5573): 1687–1689.

- Maayar, M. el, Price, D.T., Black, T.A., Humphreys, E.R., and Jork, E.-M. (2002). Sensitivity tests of the integrated biosphere simulator to soil and vegetation characteristics in a pacific coastal coniferous forest, *Atmosphere-Ocean*, 40 (3): 313–332.
- Magnani, F., Centritto, M., and Grace, J. (1996). Measurement of apoplasmic and cell to cell components of root hydraulic conductance by a pressure clamp technique, *Planta*, 199: 296–306.
- Magnani, F., Grace, J., and Borghetti, M. (2002). Adjustment of tree structure in response to the environment under hydraulic constraints, *Functional Ecology*, 16: 385–393.
- Magnani, F., Leonardi, S., Tognetti, R., Grace, J., and Borghetti, M. (1998). Modelling the surface conductance of a broad-leaf canopy: Effects of a partial decoupling from the atmosphere, *Plant, Cell and Environment*, 21: 867–879.
- Magnani, F., Mencuccini, M., and Grace, J. (2000). Age-related decline in stand productivity: The role of structural acclimation under hydraulic constraints, *Plant, Cell and Environment*, 23: 251–263.
- Malhi, Y. and Grace, J. (2000). Tropical forests and atmospheric carbon dioxide, *Trends in Ecology & Evolution*, 15: 332–337.
- Mann, M.E. and Bradley, R.S. (1999). Northern hemisphere temperatures during the past millennium: Inferences, uncertainties and limitations, *Geophysical Research Letters*, 26: 759.
- Marklund, L.G. (1988). *Biomassfunktioner för tall, gran och björk I Sverige*. Rapporter-Skog 45. Sveriges lantbruksuniversitetet.
- Marland, G., Boden, T.A., and Andres, R.J. (2000). Global, regional and national CO₂ emissions. In: *Trends: A compendium of data on global change*. Carbon Dioxide Information Analysis Center, Oak Ridge, Tenn. USA.
- Martin, P.H. (1998). New estimate of the carbon sink strength of EU forests integrating flux measurements, field surveys and space observations: 0.17-0.35 GtC, *Ambio*, 27 (7): 582–584.
- Masera, O.R., Garza-Caligaris, J.F., Kanninen, M., Karjalainen, T., Liski, J., Nabuurs, G.J., Pussinen, A., Jong, B.H.J.de, and Mohren, G.M.J. (2003). Modelling carbon sequestration in afforestation, agroforestry and forest management projects: The CO2FIX V.2 approach, *Ecological Modelling*, 164: 177–199.
- Mather, A.S. (1990). Chapter 3: Historical perspectives of forest resource use. In: *Global Forest Resources*, pages 30–57. Timber Press, Portland, OR, USA.
- Matzner, S. and Comstock, J. (2001). The temperature dependence of shoot hydraulic resistance: implications for stomatal behaviour and hydraulic limitation, *Plant, Cell and Environment*, 24: 1299–1307.
- McCulloh, K.A., Sperry, J.S., and Adler, F.R. (2003). Water transport in plants obeys Murray's law, *Nature*, 421 (6926): 939–942.
- McDowell, N., Barnard, H., Bond, B.J., Hinckley, T., Hubbard, R.M., Ishii, H., Kostner, B., Magnani, F., Marshall, J.D., Meinzer, F.C., Phillips, N., Ryan, M.G., and Whitehead, D. (2002a). The relationship between tree height and leaf area: sapwood area ratio, *Oecologia*, 132 (1): 12–20.
- McDowell, N.G., Phillips, N., Lurch, C., Bond, B.J., and Ryan, M.G. (2002b). An investigation of hydraulic limitation and compensation in large, old Douglas-fir trees, *Tree Physiology*, 22 (11): 763–774.

- McGuire, A.D., Melillo, J.M., Randerson, J.T., Parton, W.J., Heimann, M., Meier, R.A., Clein, J.S., Kicklighter, D.W., and Sauf, W. (2000). Modeling the effects of snowpack on heterotrophic respiration across northern temperate and high latitude regions: Comparison with measurements of atmospheric carbon dioxide in high latitudes, *Biogeochemistry*, 48 (1): 91–114.
- McGuire, A.D., Sitch, S., Clein, J.S., Dargaville, R., Esser, G., Foley, J., Heimann, M., Joos, F., Kaplan, J., Kicklighter, D.W., Meier, R.A., Melillo, J.M., Moore, B. III, Prentice, I.C., Ramankutty, N., Reichenau, T., Schloss, A., Tian, H., Williams, L.J., and Wittenberg, U. (2001). Carbon balance of the terrestrial biosphere in the twentieth century: Analyses of CO₂, climate and land use effects with four process-based ecosystem models, *Global Biogeochemical Cycles*, 15 (1): 183–206.
- McKay, M.D., Beckman, R.J., and Conover, W.J. (1979). A comparison of three methods of selecting values of input variables in the analysis of output from a computer code, *Technometrics*, 21: 239–245.
- Meentemeyer, V. (1978). Macroclimate and lignin control of litter decomposition rates, *Ecology*, 59 (3): 465–472.
- Melillo, J.M., Borchers, J., Chaney, J., Fisher, H., Fox, S., Haxeltine, A., Janetos, A., Kicklighter, D.W., Kittel, T.G.F., McGuire, A.D., McKeown, R., Neilson, R., Nemani, R., Ojima, D.S., Painter, T., Pan, Y., Parton, W.J., Pierce, L., Pitelka, L., Prentice, I.C., Rizzo, B., Rosenbloom, N. A., Running, S., Schimel, D. S., Sitch, S., Smith, T., and Woodward, I. (1995). Vegetation ecosystem modeling and analysis project - comparing biogeography and biogeochemistry models in a continental-scale study of terrestrial ecosystem responses to climate-change and CO₂ doubling, *Global Biogeochemical Cycles*, 9 (4): 407–437.
- Mencuccini, M. (2002). Hydraulic constraints in the functional scaling of trees, *Tree Physiology*, 22: 553–565.
- Mencuccini, M. and Grace, J. (1996a). Developmental patterns in aboveground hydraulic conductance in a Scots pine (*Pinus sylvestris* L.) age sequence, *Plant, Cell and Environment*, 19: 939–948.
- Mencuccini, M. and Grace, J. (1996b). Hydraulic conductance, light interception and needle nutrient concentration in Scots pine stands and their relation with net primary productivity, *Tree Physiology*, 16: 459–468.
- Mencuccini, M. and Magnani, F. (2000). Comment on 'Hydraulic limitation of tree height: A critique' by Becker, Meintzer and Wullschleger, *Functional Ecology*, 14: 135–137.
- Meyer, J., Lindner, M., Zudin, S., Liski, J., Zaehle, S., and Pussinen, A. (in review). Forest resource development in Europe under changing climate and land use, *Global Change Biology*.
- Mitchell, J.F.B., Johns, T.C., Gregory, J.M., and Tett, S.F.B. (1995). Climate responses to increasing levels of greenhouse gases and sulphate aerosols, *Nature*, 376: 501–504.
- Mitchell, J.F.B., Johns, T.C., and Senior, C.A. (1998). Transient response to increasing greenhouse gases using models with and without flux adjustment. Technical Report 2, Hadley Centre, UK MetOffice, London Road.
- Mitchell, T.D., Carter, T.R., Jones, P.D., Hulme, M., and New, M. (2004). A comprehensive set of high-resolution grids of monthly climate for Europe and the globe: The observed record (1901–2000) and 16 scenarios (2001–2100). Technical report, no. 5, Tyndall Centre for Climate Change Research, University of East Anglia, Norwich, UK.
- Monteith, J.L. (1995). Accommodation between transpiring vegetation and the convective boundary-layer, *Journal of Hydrology*, 166 (3–4): 251–263.

- Mooney, H., Roy, J., and Saugier, B. (2001). *Terrestrial Global Productivity: Past, Present and Future*. Academic Press, San Diego, USA.
- Morales, P., Sykes, M., Prentice, I.C., Smith, P., Smith, B., Bugmann, H., Zierl, B., Friedlingstein, P., Viovy, N., Sabate, S., Sanchez, A., Pla, E., Gracia, C. A., Sitch, S., and Ogee, J. (in review). Comparing and evaluating process-based ecosystem model predictions of carbon and water fluxes in major European forest biomes, *Global Change Biology*.
- Mücher, C.A., Steinnocher, K., Kressler, F., and Heunks, C. (2000). Land cover characterization and change detection for environmental monitoring of pan-Europe, *International Journal of Remote Sensing*, 21 (6/7): 1159–1181.
- Mund, M., Kummert, E., Hein, M., Bauer, G.A., and Schulze, E.-D. (2002). Growth and carbon stocks of a spruce forest chronosequence in central Europe, *Forest Ecology and Management*, 171: 275–296.
- Myneni, R. B., Nemani, R., and Running, S. (1997). Estimation of global leaf area index and absorbed PAR using radiative transfer models, *IEEE Transactions: Geoscience and Remote Sensing*, 35: 1380–1393.
- Myneni, R.B., Dong, J., Tucker, C.J., Kaufmann, R.K., Kauppi, P.E., Liski, J., Zhou, L., Alexeyev, V., and Hughes, M.K. (2001). A large carbon sink in the woody biomass of Northern forests, *Proceedings of the National Academy of Sciences of the United States of America*, 98: 14784–14789.
- Nabuurs, G.J. (2004). Current consequences from past actions, or how to separate direct from indirect effects. In: Field, C. and Raupach, M.R., editors, *The Global Carbon Cycle*, pages 317–326. Island Press, Washington, USA.
- Nabuurs, G.J. and Mohren, G.M.J. (1995). Modeling analysis of potential carbon sequestration in selected forest types, *Canadian Journal of Forest Research*, 25 (7): 1157–1172.
- Nabuurs, G.J., Päivinen, R., and Schanz, H. (2001). Sustainable management regimes for Europe's forests - a projection with EFISCEN until 2050, *Forest Policy and Economics*, 3: 155–173.
- Nabuurs, G.J., Schelhaas, M.J., Mohren, G.M.J., and Field, C.B. (2003). Temporal evolution of the European forest sector carbon sink from 1950 to 1999, *Global Change Biology*, 9 (2): 152–160.
- Nadelhoffer, K.J., Emmet, B.A., Gunderson, P., Kjonaas, O.J., Koopmans, C.J., Schleppi, P., Tietma, A., and Wright, R. (1999). Nitrogen deposition make a minor contribution to carbon sequestration in temperate forests, *Nature*, 398: 145–148.
- Nakicenovic, N., Alcamo, J., Davis, G., Vries, B.de, and Fenham, J. (2000). *Special Report of Working Group III of the Intergovernmental Panel of Climate Change*. Cambridge University Press, Cambridge, UK.
- Nardini, A., Lo Gullo, M.A., and Salleo, S. (1998). Seasonal changes of root hydraulic conductance (k-rl) in four forest trees: An ecological interpretation, *Plant Ecology*, 139 (1): 81–90.
- Nardini, A. and Tyree, M.T. (1999). Root and shoot hydraulic conductance of seven quercus species, *Annals of Forest Science*, 56 (5): 371–377.
- Neilson, R. (1993). Vegetation redistribution: A possible biospheric source of CO₂ during climate change, *Water, Air and Soil Pollution*, 70 (1-4): 659–673.
- Nemani, R., Keeling, C.D., Hashimoto, H., Jolly, W.M., Piper, S.C., Tucker, C.J., Myneni, R.B., and Running, S. (2003). Climate-driven increases in global terrestrial net primary production from 1982 to 1999, *Science*, 300: 1560–1563.

- Nobel, P.S. (1983). *Biophysical plant physiology and ecology*. W.H. Freeman and Company, San Francisco, USA.
- Ogee, J., Peylin, P., Cuntz, M., Bariac, T., Brunet, Y., Berbigier, P., Richard, P., and Ciais, P. (2004). Partitioning net ecosystem carbon exchange into net assimilation and respiration with canopy-scale isotopic measurements: An error propagation analysis with (CO₂)-C-13 and (COO)-O-18 data, *Global Biogeochemical Cycles*, 18 (2).
- Olson, R.J., Scurlock, J.M.O., Prince, S.D., Zheng, D.L., and R., Johnson K. (2001). *NPP Multi-Biome: NPP and Driver Data for Ecosystem Model-Data Intercomparison. Data set*. Oak Ridge National Laboratory Distributed Active Archive Center, Oak Ridge, Tennessee, U.S.A.; <http://www.daac.ornl.gov>.
- Päivinen, R., Karjalainen, T., and Liski, J. (1999). Carbon removals by European forests. Technical Report Technical Report 35, European Environmental Agency, Copenhagen, DK.
- Papale, D. and Valentini, R. (2003). A new assessment of european forests carbon exchanges by eddy fluxes and artificial neural network spatialization, *Global Change Biology*, 9: 525–535.
- Petit, J.R., Jouzel, J., Raynaud, D., Barkov, N.I., Barnola, J.M., Basile, I., Bender, M., Chappelaz, J., Davis, M., Delaygue, G., Delmotte, M., Kotlyakov, V.M., Legrand, M., Lipengkov, V.Y., Lorius, C., Peplin, L., Ritz, C., Saltzmann, E., and Stievenard, M. (1999). Climate and atmospheric history of the past 420,000 years from the Vostok ice core, Antarctica, *Nature*, 399: 429–436.
- Peylin, P., Baker, D., Sarmiento, J., Ciais, P., and Bousquet, P. (2002). Influence of transport uncertainty on annual mean and seasonal inversions of atmospheric CO₂ data, *Journal of Geophysical Research-Atmospheres*, 107 (D19): Art. 4385.
- Peylin, P., Bousquet, P., Le Quéré, C., Sitch, S., Friedlingstein, P., McKinley, G., Gruber, N., Rayner, P., and Ciais, P. (2005). Multiple constraints on regional CO₂ flux variations over land and oceans, *Global Biogeochemical Cycles*, 19: GB 1011.
- Post, W.M., King, A.W., and Wullschleger, S.D. (1997). Historical variations in terrestrial biospheric carbon storage, *Global Biogeochemical Cycles*, 11 (1): 99–109.
- Pothier, D., Margolis, H.A., and Waring, R.H. (1989). Patterns of change in saturated sapwood permeability and sapwood conductance with stand development, *Canadian Journal of Forest Research*, 19: 432–439.
- Potter, C.S., Klooster, S.A., Myneni, R.B., Genovese, V., Tan, P.N., and Kumar, V. (2003). Continental scale comparison of terrestrial carbon sinks estimated from satellite data and ecosystem modeling 1982-1998, *Global and Planetary Change*, 39: 201–213.
- Prentice, I.C., Cramer, W., Harrison, S.P., Leemans, R., Monserud, R.A., and Solomon, A.M. (1992). A global biome model based on plant physiology and dominance, soil properties and climate, *Journal of Biogeography*, 19 (2): 117–134.
- Prentice, I.C., Farquhar, G.D., Fasham, M.J.R., Goulden, M.L., Heimann, M., Jaramillo, V.J., Khashgi, H.S., Le Quéré, C., Scholes, R.J., and Wallace, D.W.R. (2001). The carbon cycle and atmospheric carbon dioxide. In: Houghton, J.T., Ding, Y., Griggs, D.J., Noguer, M., Linden, P.J.van der, Dai, X., Maskell, K., and Johnson, C.A., editors, *Climate Change 2001: The Scientific Basis. Contribution of Working Group I to the Third Assessment Report of the Intergovernmental Panel on Climate Change*. Cambridge University Press, Cambridge, UK and New York, NY, USA.
- Prentice, I.C., Heimann, M., and Sitch, S. (2000). The carbon balance of the terrestrial biosphere: Ecosystem models and atmospheric observations, *Ecological Applications*, 10 (6): 1553–1573.

- Prentice, I.C., Sykes, M., and Cramer, W. (1993). A simulation model for the transient effects of climate change of forest landscapes, *Ecological Modelling*, 65: 51–73.
- Ramankutty, N. and Foley, J.A. (1999). Estimating historical changes in global land cover: Croplands from 1700 to 1992, *Global Biogeochemical Cycles*, 13 (4): 997–1027.
- Ramaswamy, V., Boucher, O., Haigh, J., Hauglustaine, D., Haywood, J., Myhre, G., Nakajima, T., Shi, G.Y., and Solomon, S. (2001). Radiative forcing of climate change. In: Houghton, J.T., Ding, Y., Griggs, D.J., Noguer, M., Linden, P.J.van der, Dai, X., Maskell, K., and Johnson, C.A., editors, *Climate Change 2001: The Scientific Basis*. Cambridge University Press, Cambridge, UK.
- Randerson, J., Still, C.J., Ballé, J.J., Fung, I., Doney, S.C., Tans, P.P., Conway, T.J., White, J.W.C., Vaughn, B., Suits, N., and Denning, A.S. (2002). Carbon isotope discrimination of arctic and boreal biomes inferred from remote atmospheric measurements and a biosphere-atmosphere model, *Global Biogeochemical Cycles*, 16 (3): 1028, doi:10.1029/2001GB001435.
- Rayner, P.J., Scholze, M., Knorr, W., Kaminski, T., Giering, R., and Widmann, H. (2005). Two decades of terrestrial carbon fluxes from a carbon cycle data assimilation system (CCDAS), *Global Biogeochemical Cycles*, 19: doi:10.1029/2004GB002254.
- Reginster, I. and Rounsevell, M.D.A. (submitted). Future scenarios of urban land use in Europe, *Environment and Planning B*.
- Reich, P.B., Walters, M.B., and Ellsworth, D.S. (1992). Leaf life-span in relation to leaf, plant, and stand characteristics among diverse ecosystems, *Ecological Monographs*, 62 (3): 365–392.
- Reichert, P. and Omlin, M. (1997). On the usefulness of overparameterized ecological models, *Ecological Modelling*, 95: 289–299.
- Reichstein, M., Tenhunen, J.D., Rouspard, O., Ourcival, J-M., Rambal, S., Miglietta, F., Piersantoni, A., Pecchiari, M., Tirone, G., and Valentini, R. (2003). Inverse modelling of season drought effects of canopy CO₂/H₂O exchange in three Mediterranean ecosystems, *Journal of Geophysical Research*, 108 (D23): doi:10.1029/2003JD003430.
- Reichstein, M., Valentini, R., Running, S., Tenhunen, J., Aubinet, M., Bernhofer, C., Buchmann, N., Granier, A., Grünwald, T., Joffre, R., Knohl, A., Kowalski, A., Loustau, D., Ourcival, J.-M., Pereira, J.S., Rambal, S., Seufert, G., Vesala, T., and Zhao, M. (2004). Improving remote-sensing based GPP estimates (MODIS-MOD17) through inverse parameter estimation with CARBOEUROPE eddy covariance flux data, *Geophysical Research Abstracts*, 6: 01388.
- RIVM. (2001). The IMAGE 2.2 implementation of the SRES scenarios. A comprehensive analysis of emissions, climate change, and impacts on the 21st century. Technical Report 481508018, National Institute for Public Health and Environmental Protection.
- Roberts, J. (1977). The use of tree-cutting techniques in the study of the water relations of mature *Pinus sylvestris* L., *Journal of Experimental Botany*, 28 (104): 751–767.
- Rödenbeck, C., Houweling, S., Gloor, M., and Heimann, M. (2003). CO₂ flux history 1982 - 2001 inferred from atmospheric data using a global inversion of atmospheric transport, *Atmospheric Chemistry and Physics*, 3: 1919–1964.
- Rounsevell, M.D.A., Ewert, F., Reginster, I., Leemans, R., and Carter, T.R. (submitted). Future scenarios of European agricultural land use. II: Estimating changes in land use and regional allocation, *Agriculture, Ecosystems and Environment*.
- Rüdinger, M., S.W., Hallgren, Steudle, E., and Schulze, E.D. (1994). Hydraulic and osmotic properties of Spruce roots, *Journal of Experimental Botany*, 45 (279): 1413–1425.

- Ruimy, A., Saugier, B., and Dedieu, G. (1994). Methodology of estimation of terrestrial net primary productivity from remotely sensed data, *Journal of Geophysical Research*, 99: 5263–5283.
- Ryan, M.G., Binkley, D., and Fownes, J.H. (1997). Age-related decline in forest productivity: Pattern and process, *Advances in Ecological Research*, 27: 213–262.
- Ryan, M.G., Binkley, D., Fownes, J.H., Giardina, C.P., and Senock, R.S. (2004). An experimental test of the causes of forest growth decline with stand age, *Ecological Monographs*, 74 (3): 393–414.
- Ryan, M.G., Bond, B.J., Law, B.E., Hubbard, R.M., Woodruff, D., Cienciala, E., and Kucera, J. (2000). Transpiration and whole-tree conductance in Ponderosa pine trees of different heights, *Oecologia*, 124 (4): 553–560.
- Ryan, M.G., Gower, S.T., Hubbard, R.M., Waring, R.H., Gholz, H.L., Cropper, W.P., and Running, S.W. (1995). Woody tissue maintenance respiration of 4 conifers in contrasting climates, *Oecologia*, 101 (2): 133–140.
- Ryan, M.G. and Waring, R.H. (1992). Maintenance respiration and stand development in a sub-alpine Lodgepole pine forest, *Ecology*, 73: 2100–2108.
- Ryan, M.G. and Yoder, B.J. (1997). Hydraulic limits to tree height and tree growth, *BioScience*, 47 (4): 235–242.
- Saliendra, N.Z., Sperry, J.S., and Comstock, J.P. (1995). Influence of leaf water status on stomatal response to humidity, hydraulic conductance, and soil drought in betula-occidentalis, *Planta*, 196 (2): 357–366.
- Saltelli, A., Chan, K., and Scott, E.M., editors. (2000). *Sensitivity Analysis*. Wiley Series in Probability and Statistics. John Wiley & Sons, Ltd., Chichester, New York, USA.
- Sarmiento, J. and Sundquist, E.T. (1992). Revised budget for the oceanic carbon uptake of anthropogenic carbon dioxide, *Nature*, 356: 589–593.
- Saugier, B. and Roy, J. (2001). Estimations of global terrestrial productivity: Converging towards a single number? In: Mooney, H., Roy, J., and Saugier, B., editors, *Global terrestrial productivity: past, present and future*. Academic Press, San Diego.
- Saxton, K.E., Rawls, W.L., Romberger, J.S., and Papendick, R.I. (1986). Estimating generalised soil-water characteristics from texture, *Soil Science Society America Journal*, 50: 1031–1036.
- Schäfer, K.V.R., Oren, R., and Tenhunen, J.D. (2000). The effect of height on crown level stomatal conductance, *Plant, Cell and Environment*, 23: 365–375.
- Schaphoff, S., Lucht, W., Gerten, D., Sitch, S., Cramer, W., and Prentice, I.C. (in review). Terrestrial biosphere carbon storage under alternative climate projections, *Climatic Change*.
- Schelhaas, M.J., Varis, S., Schuck, A., and Nabuurs, G.J. (1999). *EFISCEN's European Forest Resource Database*. European Forest Institute, Joensuu, FI.
- Schimel, D. (1995). Terrestrial ecosystems and the carbon cycle, *Global Change Biology*, 1: 77–91.
- Schimel, D.S., House, J.I., Hibbard, K.A., Bousquet, P., Ciais, P., Peylin, P., Braswell, B.H., Apps, M.J., Baker, D., Bondeau, A., Canadell, J., Churkina, G., Cramer, W., Denning, A.S., Field, C.B., Friedlingstein, P., Goodale, C., Heimann, M., Houghton, R.A., Melillo, J.M., Moore, B., Murdiyarso, D., Noble, I., Pacala, S.W., Prentice, I.C., Raupach, M.R., Rayner, P.J., Scholes, R.J., Steffen, W.L., and Wirth, C. (2001). Recent patterns and mechanisms of carbon exchange by terrestrial ecosystems, *Nature*, 414 (6860): 169–172.
- Schlesinger, W. H. and Melack, J.M. (1981). Transport of organic-carbon in the world rivers, *Tellus*, 33: 172–187.

- Schober, R. (1987). *Ertragstabeln wichtiger Baumarten*. J.D. Sauerländer's Verlag, Frankfurt a.M., DE.
- Schröter, D., Cramer, W., and ATEAM-Members. (2004). *The ATEAM final report 2004 - Detailed report related to overall project duration*. Potsdam Institute for Climate Impact Research, Potsdam, DE, <http://www.pik-potsdam.de/ateam/>.
- Schröter, D., Metzger, M.J., Cramer, W., and Leemans, R. (in press). Vulnerability assessment - Analysing the human-environment system in the face of global environmental change. In: *Environmental Science Section Bulletin, Vol. 2, No. 2*, pages 1–7. Kalmar University, Kalmar, SE.
- Schuck, A., Brusselen, J.van, Päivinen, R., Häme, T., Kennedy, P., and Folving, S. (2002). Compilation of a calibrated European forest map derived from NOAA-AVHRR data. Technical Report EFI Internal Report 13, European Forest Institute, Joensuu, FI.
- Schulze, E.D., Högberg, P., Van Oene, H., Persson, T., Harrison, A.F., Read, D., Kjoller, A., and Matteucci, G. (2000). Interactions between the carbon and nitrogen cycle and the role of biodiversity: a synopsis of a study along a north-south transect through europe. In: Schulze, E.D., editor, *Carbon and nitrogen cycling in European forest ecosystems*, volume 142 of *Ecological Studies*, pages 468–491. Springer, Berlin Heidelberg New York.
- Schulze, E.D., Kelliher, F.M., Körner, C., Lloyd, J., and Leuning, R. (1994). Relationship among maximal stomatal conductance, ecosystem surface conductance, carbon assimilation rate, and plant nitrogen nutrition: a global ecology scaling exercise, *Annual Review of Ecology and Systematics*, 25: 629–660.
- Scurlock, J.M.O., Cramer, W., Olson, R.J., Parton, W.J., and Prince, S.D. (1999). Terrestrial NPP: Toward a consistent data set for global model evaluation., *Ecological Applications*, 9 (3): 913–919.
- Shinozaki, K., Yoda, K., Hozumi, K., and Kira, T. (1964a). A quantitative analysis of the plant form - the pipe model theory, *Japanes Journal of Ecology*, 14 (3): 98–104.
- Shinozaki, K., Yoda, K., Hozumi, K., and Kira, T. (1964b). A quantitative analysis of the plant form - the pipe model theory: II. Further evidence of the theory and its application in forest ecology, *Japanes Journal of Ecology*, 14 (4): 133–139.
- Sitch, S., Brovkin, V., Bloh, W.von, Vuuren, D.van, Eickhout, B., and Ganoposki, A. (2005). Impacts of future land cover changes on atmospheric CO₂ and climate, *Global Biogeochemical Cycles*, 19: [dio:10.1029/2004GB002311](https://doi.org/10.1029/2004GB002311).
- Sitch, S., Smith, B., Prentice, I.C., Arneth, A., Bondeau, A., Cramer, W., Kaplan, J.O., Levis, S., Lucht, W., Sykes, M.T., and Venevsky, S. (2003). Evaluation of ecosystem dynamics, plant geography and terrestrial carbon cycling in the LPJ dynamic global vegetation model, *Global Change Biology*, 9: 161–185.
- Slayback, D.A., Pinzon, J.E., Los, S.O., and Tucker, C.J. (2003). Northern hemispheric photosynthetic trends 1982-99, *Global Change Biology*, 9: 1–15.
- Slyater, R.O. (1967). *Plant water relationships*. Academic Press, New York, USA.
- Smit-Spinks, B., Swanson, B.T., and Markhart, A.H. (1984). Changes in water relations, water flux and root exudate abscisic acid content with cold acclimation of *Pinus sylvestris* l., *Australian Journal of Plant Physiology*, 11: 431–441.
- Smith, B., Prentice, I.C., and Sykes, M.T. (2001). Representation of vegetation dynamics in the modelling of terrestrial ecosystems: Comparing two contrasting approaches within European climate space, *Global Ecology and Biogeography*, 10 (6): 621–637.

- Smith, J., Smith, P., Wattenbach, M., Zaehle, S., Hiederer, R., Jones, R.J.A., Montanarella, L., Rounsevell, M., Reginster, I., and Ewert, F. (2005a). Projected changes in mineral soil carbon of European croplands and grasslands, 1990-2080, *Global Change Biology, in review*.
- Smith, J.E., Heath, L.S., and Woodbury, P.B. (2004). How to estimate forest carbon for large areas from inventory data, *Journal of Forestry*, 102 (5): 25–31.
- Smith, P., Smith, J., Wattenbach, M., Meyer, J., Lindner, M., Zaehle, S., Hiederer, R., Jones, R.J.A., Montanarella, L., Rounsevell, M., and Reginster, I. (2005b). Projected changes in mineral soil carbon of European forests, 1990-2100, *Canadian Journal of Soil Science, in press*.
- Smith, T.M. and Shugart, H.H. (1993). The transient response of terrestrial carbon storage to a perturbed climate, *Nature*, 361: 523–526.
- Sperry, J. S., Nichols, K.L., Sullivan, E.M., and Eastlack, S.E. (1994). Xylem embolism in ring-porous, diffuse porous, and coniferous trees of northern Utah, and interior Alaska, *Ecology*, 75 (6): 1736–1752.
- Sperry, J.S., Adler, F.R., Campbell, G.S., and Comstock, J.P. (1998). Limitation of plant water use by rhizosphere and xylem conductance: Results from a model, *Plant, Cell and Environment*, 21 (4): 347–359.
- Sperry, J.S., Hacke, U.G., Oren, R., and Comstock, J.P. (2002). Water deficits and hydraulic limits to leaf water supply, *Plant, Cell and Environment*, 25: 251–263.
- Spieker, H., Mielikäinen, K., Köhl, M., and Skovsgaard, J.P. (1996). *Growth trends in European Forests*. Springer, Berlin, DE.
- Sprugel, D.G., Ryan, M.G., Brooks, J.R., Vogt, K.A., and Martin, T.A. (1996). Respiration from the organ level to the stand. In: Smith, W.K. and Hinckley, T.M., editors, *Physiological Ecology of Coniferous Forests*.
- Steffen, W.L., Cramer, W., Plöchl, M., and Bugmann, H. (1996). Global vegetation models: Incorporating transient changes to structure and composition, *Journal of Vegetation Science*, 7: 321–328.
- Steddele, E. (2000). Water uptake by plant roots: An integration of views, *Plant and Soil*, 226: 45–56.
- Steddele, E. and Meshcheryakov, A.B. (1996). Hydraulic and osmotic properties of oak roots, *Journal of Experimental Botany*, 47 (296): 387–401.
- Steward, J.B. and Gay, L.W. (1989). Preliminary modelling of transpiration from the FIFE site in Kansas, *Agricultural and Forest Meteorology*, 48: 305–315.
- Still, C.J., Randerson, J.T., and Fung, I.Y. (2004). Large-scale plant light-use efficiency inferred from the seasonal cycle of atmospheric CO₂, *Global Change Biology*, 10 (8): 1240–1252.
- Sykes, M.T., Prentice, I.C., Smith, B., Cramer, W., and Venevsky, S. (2001). An introduction to the European terrestrial ecosystem modelling activity, *Global Ecology and Biogeography*, 10 (6): 581–593.
- Tans, P.P., Fung, I., and Takahashi, T. (1990). Observational constraints on the global atmospheric CO₂ budget, *Science*, 247: 1431–1438.
- Thonicke, K., Venevsky, S., Sitch, S., and Cramer, W. (2001). The role of fire disturbance for global vegetation dynamics: coupling fire into a dynamic global vegetation model, *Global Ecology and Biogeography*, 10 (6): 661–677.
- Thornley, J.H.M. and Cannell, M.G. R. (2001). Soil carbon response to temperature: A hypothesis, *Annals of Botany*, 87: 591–598.

- Thornton, P.E., Law, B.E., Gholz, H.L., Clark, K.L., Falge, E., Ellsworth, D.S., Golstein, A.H., Monson, R.K., Hollinger, D., Falk, M., Chen, J., and Sparks, J.P. (2002). Modeling and measuring the effects of disturbance history and climate on carbon and water budgets in evergreen needleleaf forests, *Agricultural and Forest Meteorology*, 113 (1-4): 185–222.
- Townsend, AR., Braswell, B.H., Holland, E., and Penner, J.E. (1996). Spatial and temporal patterns in potential terrestrial carbon storage due to deposition of fossil fuel derived nitrogen, *Ecological Applications*, 6: 806–814.
- Tyree, M. T. and Sperry, J.S. (1988). Do woody plant operate near the point of catastrophic xylem dysfunction caused by dynamic water stress?, *Plant Physiology*, 88: 574–580.
- Tyree, M.T. and Ewers, F.M. (1991). The hydraulic architecture of tree and other woody plants, *New Phytologist*, 119: 345–360.
- UN-ECE/FAO. (1985). *Forest resources of the ECE region (Europe, the USSR, North America)*. United Nations Economic Commission for Europe; Food and Agriculture Organization, Geneva, CH, Rome, IT.
- UN-ECE/FAO. (1992). *Forest resources of the temperate zones, the UN-ECE/FAO 1990 Forest Resource Assessment*. United Nations Economic Commission for Europe; Food and Agriculture Organization, Geneva, CH, Rome, IT.
- UN-ECE/FAO. (2000). *Temperate and Boreal Forest Resource Assessment (2000)*. United Nations Economic Commission for Europe; Food and Agriculture Organization, Geneva, CH, Rome, IT.
- UNFCCC. (1992). United Framework Convention on Climate Change.
- UNFCCC. (1998). Kyoto Protocol to the United Nations Framework Convention on Climate Change.
- Valentini, R., Matteucci, G., Dolman, A.J., Schulze, E.D., Rebmann, C., Moors, E.J., Granier, A., Gross, P., Jensen, N.O., Pilegaard, K., Lindroth, A., Grelle, A., Bernhofer, C., Grunwald, T., Aubinet, M., Ceulemans, R., Kowalski, A.S., Vesala, T., Rannik, U., Berbigier, P., Loustau, D., Guomundsson, J., Thorgeirsson, H., Ibrom, A., Morgenstern, K., Clement, R., Moncrieff, J., Montagnani, L., Minerbi, S., and Jarvis, P.G. (2000a). Respiration as the main determinant of carbon balance in European forests, *Nature*, 404 (6780): 861–865.
- Valentini, R., Matteucci, G., Granier, A., Berbigier, P., Loustau, D., Jensen, N.O., Pilegaard, K., Lindroth, A., Rebmann, C., Bernhofer, Ch., Dolman, A.J., Moors, E.J., Moncrieff, J., Jarvis, P., Aubinet, M., Ceulemans, R., Thorgeirsson, H., and Vesala, T. (2000b). The Euroflux dataset 2000. In: Valentini, R., editor, *Carbon, Water and Energy exchanges of European forests*, page 300pp. Springer Verlag, Heidelberg.
- Venevsky, S. (2001). *Broad-scale vegetation dynamics in north-eastern Eurasia - observations and simulations*. PhD thesis, Universität für Bodenkultur, Wien, AT.
- Venevsky, S., Thonicke, K., Sitch, S., and Cramer, W. (2002). Simulating fire regimes in human-dominated ecosystems: Iberian peninsula case study, *Global Change Biology*, 8: 984–998.
- Veroustraete, F., Sabbe, H., and Eerens, H. (2002). Estimation of carbon mass fluxes over Europe using the C-fix model and EUROFLUX data, *Remote Sensing of Environment*, 83 (3): 376–399.
- Vitousek, P.M., Aber, J.D., Howarth, R.W., Likens, G.E., Matson, P.A., Schindler, D.W., Schlesinger, W.H., and Tilman, D.G. (1997). Human alteration of the global nitrogen cycle: Sources and consequences, *Ecological Applications*, 7 (3): 737–750.
- Vogt, K.A., Vogt, D.J., Palmiotto, P.A., Boon, P., O'Hara, J., and Asbjornson, H. (1996). Review of root dynamics in forest ecosystems grouped by climate, climatic forest type and species, *Plant and Soil*, 187: 159–219.

- Walther, G.R., Post, E., Convey, P., Menzel, A., Parmesan, C., Beebee, T.J.C., Fromentin, J., Hoegh-Guldberg, O., and Bairlein, F. (2002). Ecological responses to recent climate change, *Nature*, 416: 389–395.
- Wang, Y.-P., Leuning, R., Cleugh, H.A., and Coppin, P.A. (2001). Parameter estimation in surface exchange models using nonlinear inversion: How many parameters can we estimate and which measurements are most useful?, *Global Change Biology*, 7: 495–510.
- Waring, R.H., Landsberg, J.J., and Williams, M. (1998). Net primary production of forests: A constant fraction of gross primary production?, *Tree Physiology*, 18: 129–134.
- Waring, R.H. and McDowell, N. (2002). Use of a physiological process model with forestry yield tables to set limits on annual carbon balances, *Tree Physiology*, 22: 197–188.
- Waring, R.H., Schroeder, P.E., and Oren, R. (1982). Application of the pipe model-theory to predict canopy leaf- area, *Canadian Journal of Forest Research*, 12 (3): 556–560.
- Washington, W.M., Weatherly, J.W., Meehl, G.A., Semtner Jr., A.J., Bettge, T.W., Craig, A.P., Strand Jr., W.G., Arblaster, J.M., Wayland, V.B., James, R., and Zhang, Y. (2000). Parallel climate model (PCM) control and transient simulations, *Climate Dynamics*, 16: 755–774.
- Watson, R.T., Dixon, J.A., Hanburg, S.P., Jenetos, A.C., and Moss, R.H., editors. (1998). *Protecting out planet, securing out future*. United Nations Environmental Program, NASA, and World Bank, Washington, DC, USA.
- Watson, R.T., Noble, I.R., Bolin, B., Ravindranath, N.H., Verardo, D.J., and Dokken, D.J., editors. (2000). *Land Use, Land-Use Change and Forestry*. Special report of the Intergovernmental Panel on Climate Change. Cambridge University Press, Cambridge, UK.
- Weatherly, P.E. (1982). Water uptake and flow in roots. In: Lange, O.L., Nobel, P.S., Osmond, D.B., and Ziegler, H., editors, *Encyclopedia of Plant Physiology*, volume 12 B, pages 79–109. Springer-Verlag, Berlin, DE.
- West, G.B., Brown, J.H., and Enquist, B.J. (1997). A general model for the origin of allometric scaling laws in biology, *Science*, 276 (5309): 122–126.
- West, G.B., Brown, J.H., and Enquist, B.J. (1999). A general model for the structure and allometry of plant vascular systems, *Nature*, 400 (6745): 664–667.
- White, A., Cannell, M.G.R., and Friend, A.D. (2000a). CO₂ stabilization, climate change and the terrestrial carbon sink, *Global Change Biology*, 6 (7): 817–833.
- White, M.A., Thornton, P.E., Running, S., and Nemani, R. (2000b). Parameterization and sensitivity analysis of the BIOME-BGC terrestrial ecosystem model: Net primary production controls, *Earth Interactions*, 4: 1–55.
- Whitehead, D., Edwards, W.R.N., and Jarvis, P.G. (1984). Conducting sapwood area, foliage area, and permeability in mature trees of *Picea sitchensis* and *Pinus cordata*, *Canadian Journal of Forest Research*, 14: 940–947.
- Whitehead, D. and Hinckley, T.M. (1991). Models of water flux through forest stands: Critical leaf and stand parameters, *Tree Physiology*, 9: 35–57.
- Whitehead, D., Kelliher, F.M., Lane, P.M., and Pollack, D.S. (1993). Seasonal partitioning of evaporation between trees and understory in a widely-spaced *Pinus radiata* stand, *Journal of Applied Ecology*, 31: 528–542.
- Wirth, C., Schumacher, J., and Schulze, E.D. (2004). Generic biomass function for Norway spruce in central Europe - a meta-analysis approach toward prediction and uncertainty estimation, *Tree Physiology*, 24: 121–139.

- Wofsy, S.C., Goulden, M.L., Munger, J.W., Fan, S., Bakwin, P., Daube, B.C., Bassow, S.L., and Bazzaz, F.A. (1993). Net exchange of CO₂ in a mid-latitude forest, *Science*, 260: 1314–1317.
- Woodruff, D.R., Bond, B.J., and Meinzer, F.C. (2004). Does turgor limit growth in tall trees?, *Plant, Cell and Environment*, 27 (2): 229–236.
- Woodward, F.I. (1996). Developing the potential for describing the terrestrial biosphere's response to a changing climate. In: Walker, B. and Steffen, W.L., editors, *Global Change and Terrestrial Ecosystems*, pages 511–529. University of Cambridge, Cambridge, UK.
- Woodward, F.I., Smith, T.M., and Emanuel, W.R. (1995). A global land primary productivity and phytogeography model, *Global Biogeochemical Cycles*, 9 (4): 471–490.
- Yang, S. and Tyree, M.T. (1993). Hydraulic resistance in *Acer saccharum* shoots and its influence on leaf water potential and transpiration, *Tree Physiology*, 12: 231–242.
- Yang, S. and Tyree, M.T. (1994). Hydraulic architecture of *Acer saccharum* and *Acer rubrum*: comparison of branches to whole trees and the contribution of leaves to hydraulic resistance, *Journal of Experimental Botany*, 45 (271): 179–186.
- Yoda, K., Shinozaki, K., Ogawa, H., Hozumi, K., and Kira, T. (1965). Estimation of total amount of respiration from woody organs of trees and forest communities, *Journal of Biology*, 16: 15–26.
- Yoder, B.J., Ryan, M.G., Waring, R.H., Schoettle, A.W., and Kaufmann, M.R. (1994). Evidence of reduced photosynthetic rates in old trees, *Forest Science*, 40 (3): 513–527.
- Zaehle, S. (2005). Effect of height on tree hydraulic conductance incompletely compensated by xylem tapering, *Functional Ecology*, 19: 359–364.
- Zaehle, S., Bondeau, A., Smith, P., Cramer, W., Erhard, M., Prentice, I.C., Sitch, S., Smith, B., and Sykes, M. (in prep.). Projected changes in terrestrial carbon storage in Europe under climate and land-use change, 2000–2100, *Regional Environmental Change*.
- Zaehle, S., Sitch, S., Smith, B., and Hattermann, F. (2005). Effects of parameter uncertainties on the modeling of terrestrial biosphere dynamics, *Global Biogeochemical Cycles*, in press.
- Zeide, B. (1993). Primary unit of the tree crown, *Ecology*, 74 (5): 1598–1602.
- Zimmermann, M.H. (1978). Hydraulic architecture of some diffuse-porous trees, *Canadian Journal of Forest Research*, 56: 2286–2295.
- Zobler, L. (1986). A world soil file for global climate modelling, *NASA Technical Memorandum*, 87802: 32.

APPENDIX

GLOSSARY

<i>Abbreviation</i>	<i>Description</i>
A	<i>GPP</i> minus leaf respiration
ANOVA	Analysis of Variance
ATEAM	Advanced Terrestrial Ecosystem Assessment and Modelling, EU research programme
atm. [CO ₂]	concentration of Carbon Dioxide in the atmosphere
BEF	Biomass Expansion Factor
C	Carbon
CCDAS	Carbon Cycle Data Assimilation System
CFT	Crop Functional Type, <i>e.g.</i> temperate cereals
CRU	Climate Research Unit, University of East Anglia, Norwich, UK
DGVM	Dynamic Global Vegetation Model
EEFR	Efiscen's European Forest Resource Database, Schelhaas <i>et al.</i> (1999)
EMDI	Ecosystem Model Data Intercomparison project, Olson <i>et al.</i> (2001)
EUROFLUX	EUROpean eddy covariance FLUX measurement programme, Valentini <i>et al.</i> (2000a)
FPC	Foliar Projective Cover of an individual PFT/CFT
GCM	General Circulation Model
<i>GPP</i>	terrestrial Gross Primary Production
IPCC	Intergovernmental Panel on Climate Change
LAI	Leaf Area Index
LHS	Latin Hypercube Sampling, see Appendix of Chapter 2
<i>NBE</i>	terrestrial Net Biome Exchange, see Box 1.1
<i>NEE</i>	terrestrial Net Ecosystem Exchange, see Box 1.1
<i>NEP</i>	The inverse of terrestrial Net Ecosystem Exchange, <i>i.e.</i> $-NEE$)
NMSD	Normalised Mean Square Deviation, see Appendix of Chapter 2
<i>NPP</i>	terrestrial Net Primary Production
PAR	Photosynthetically Active Radiation
PDF	Probability Density Function
PFT	Plant Functional Type, <i>e.g.</i> temperate broadleaved summer green trees
R_a	autotrophic Respiration
R_h	heterotrophic Respiration
RMSE	Root Mean Square Error, see Appendix of Chapter 2
(R)PCC	(Ranked) Partial Correlation Coefficient, see Appendix of Chapter 2
SRES	Special Report on Emission Scenarios of the IPCC, Nakicenovic <i>et al.</i> (2000)
SOM	Soil Organic Matter
TBM	Terrestrial Biogeochemical Model
TBFRA	Temperate and Boreal Forest Resource Assessment
WBE	West, Brown and Enquist model, West <i>et al.</i> (1999)

SCIENTIFIC PUBLICATIONS

Peer-reviewed articles:

- Zaehle, S. (2005). Effect of height on tree hydraulic conductance incompletely compensated by xylem tapering, *Functional Ecology*, **19**(2), 359-364.

accepted:

- Smith, P., Smith, J., Wattenbach, M., Meyer, J., Lindner, M., Zaehle, S., Hiederer, R., Jones, R., Montanarella, L., Rounsevell, M. and Reginster, I. Projected changes in mineral soil carbon of European forests, 1990-2100, *Canadian Journal of Soil Science*, in press.
- Zaehle, S., Sitch, S., Smith, B. and Hattermann, F. (2005). Effects of parameter uncertainties on the modelling of terrestrial biosphere dynamics, *Global Biogeochemical Cycles*, in press.

in review:

- Zaehle, S., Sitch, S., Prentice, I.C., Liski, J., Cramer, W., Erhard, M., Hickler, T., Smith, B. The hydraulic acclimation theory and implications for modelling terrestrial carbon balances, *Ecological Applications*, in review.
- Meyer, J., Lindner, M., Zudin, S., Liski, J., Zaehle, S. and Pussinen, A. Forest resource development in Europe under changing climate and land use, *Global Change Biology*, in review.
- Seguin, B., Arrouayas, D., Balesdent, C., Soussana, J.-F., Bondeau, A., Smith, P., Zaehle, S., de Noblet, N., Viovy, N. How to moderate the impact of agriculture of climate: The present limits of scientific knowledge in terms of integrated assessment, *Agricultural and Forest Meteorology*, in review.
- Smith, J., Smith, P., Wattenbach, M., Zaehle, S., Hiederer, R., Jones, R., Montanarella, L., Rounsevell, M., Reginster, I., and Ewert, F. Projected changes in mineral soil carbon of European croplands and grasslands, 1990-2080, *Global Change Biology*, in review.

Other publications and conference contributions:

- Zaehle, S., Bondeau, A., Smith, P., Sitch, S., Schröter, D., Erhard, M. and Cramer, W. (2004). Europe's terrestrial carbon sink may last until 2050 and then decline, *Geophysical Research Abstracts*, **6**: 3808.
- Zaehle, S., Bondeau, A., Smith, P., Sitch, S., and Cramer, W. (2004). Combining land use statistics with process-based ecosystem modelling to estimate the European carbon balance, *Regional Carbon Budgets: From methods to quantification*. Workshop of the Global Carbon Project 14.11-18.11.2004, Beijing, China. Poster.
- Lindner, M., Lucht, W., Bouriaud, O., Green, T., and Janssens, I. (ed., 2004). *Specific study on Forest Greenhouse Gas Budgets*. Discussion paper as contribution to the Concerted Action CarboEurope-GHG (incl. Zaehle, S. as contributing author).
- Schröter, D. and ATEAM members (incl. Zaehle, S., 2004). *The ATEAM final report 2004*. 139pp. available at www.pik-potsdam.de/ateam.

- Hickler, T., Prentice, I.C., Smith, B., Sykes, M. and Zaehle, S. (2004). *Using a global vegetation model to test a comprehensive hypothesis on the effect of plant hydraulic architecture on water uptake in different plant functional types*. In: Hicker, T. 2004. Towards an integrated ecology through mechanistic modelling of ecosystem structure and functioning. Meddelanden från Lunds Universitets Geografiska Institution. Avhandlingar, Lund, SE, 153pp.
- Lindner, M., Meyer, J., Pussinen, A., Liski, J., Zaehle, S., Lapveteläinen, T., Heikkinen, E. (2004). *Forest resource development under climate change*. In: Hasenauer, H. and Mäkelä, editors, *International Conference on Modelling Forest Production*, University of Natural Resources and Applied Life Sciences, Vienna, AU, pp. 244-251.
- Zaehle, S. (2001). *Assessing the impact of ENSO on agriculture - A northern Vietnam case study on rice production*. Master-Thesis, University of East Anglia, Norwich, UK, 65pp.

CURRICULUM VITAE

Name Sönke Zaehle
Date/Place of Birth 10.03.1977, Westerstede, DE
Nationality German
Address Potsdam Institute for Climate Impact Research, e.V.
PO Box, 60 12 03, D-14412 Potsdam, Germany

Education and Training

since 2001 Research assistant at the
Potsdam Institute for Climate Impact Research
– CarboEurope-IP (2004-2005)
– Advanced Terrestrial Ecosystem Assessment and Modelling
(2001-2004)

Aug. 2001 Master of Science in Environmental Sciences (with distinction)
2000-2001 Studies of Environmental Sciences at the
School of Environmental Sciences, University of East Anglia
–Master-Thesis: ‘Assessing the impact of ENSO on
agricultural productivity - A northern Vietnam case study.’
Supervisors: Dr. M. Kelly, Dr. K. Hiscock.

1997-2000 Studies in Geoecology at the Technische Universität Braunschweig
– Vordiplom (1.1) and 3rd year with focus on
Environmental Modelling, Eco-chemistry and GIS

1997-2004 Scholar of the German Merit Foundation

1996-1997 Civil Service at the Old-People’s Home in Westerstede, DE
May 1996 Graduation (Abitur)
1983-1996 Primary and Secondary Education in Westerstede, DE

If a tree falls in the forest, and
nobody is there to chew it –
Does it have a taste?